THERMODYNAMIC, ULTRASONIC AND TRANSPORT STUDIES OF NUCLEIC ACID BASES IN AQUEOUS SOLUTIONS OF SACCHARIDES

Thesis Submitted for the Award of the Degree of

DOCTOR OF PHILOSOPHY

in Chemistry

By

Asha Sharmhal Registration Number (42000447)

Supervised By

Dr. Praveen Kumar Sharma (14155) Department of Chemistry (Professor), School of Chemical Engineering and Physical Sciences, Lovely Professional University, Punjab, India

Co-Supervised by

Dr. Ashish Kumar Department of Chemistry (Professor), NCE, Bihar Engineering University, Department of Science Technology and Technical Education, Bihar, India



LOVELY PROFESSIONAL UNIVERSITY, PUNJAB 2025

DEDICATION

This thesis is dedicated to my beloved husband

Dr. Ashwani Kumar

and

Loving Family

Thank you God for the wisdom and perseverance that you have bestowed upon me during this research work and indeed, throughout my life...

Thank you...

DECLARATION

I, hereby declared that the presented work in the thesis entitled "Thermodynamic,

ultrasonic and transport studies of nucleic acid bases in aqueous solutions of saccharides"

in fulfillment of degree of **Doctor of Philosophy** (**Ph.D.**) is the outcome of research work

carried out by me under the supervision of Dr. Praveen Kumar Sharma, working as

Professor, in the Department of Chemistry, School of Chemical Engineering and Physical

Sciences, Lovely Professional University, Punjab, India and co-supervision of Dr. Ashish

Kumar, working as Professor, Department of Chemistry, NCE, Bihar Engineering

University, Department of Science Technology and Technical Education, Bihar, India. In

keeping with the general practice of reporting scientific observations, due

acknowledgements have been made whenever the work described here has been based on

the findings of other investigator. This work has not been submitted in part or full to any

other University or Institute for the award of any degree.

(Signature of Scholar)

Asha Sharmhal

Registration No.: 42000447

Department of Chemistry,

School of Chemical Engineering and Physical Sciences,

Lovely Professional University, Punjab, India

iii

CERTIFICATE

This is to certify that the work reported in the Ph.D. thesis entitled "Thermodynamic, ultrasonic and transport studies of nucleic acid bases in aqueous solutions of saccharides" submitted in fulfillment of the requirement for the reward of degree of **Doctor of Philosophy** (**Ph.D.**) in the Department of Chemistry, School of Chemical Engineering and Physical Sciences, Lovely Professional University, is a research work carried out by Asha Sharmhal, 42000447, is bonafide record of her original work carried out under my supervision and that no part of thesis has been submitted for any other degree, diploma or equivalent course.

(Signature of Supervisor)

Dr. Praveen Kumar Sharma Professor Department of Chemistry, School of Chemical Engineering and Physical Sciences, Lovely Professional University, Punjab India

(Signature of Co-Supervisor)

Dr. Ashish Kumar Professor Department of Chemistry, NCE, Bihar Engineering University, Department of Science Technology and Technical Education, Bihar, India

ABSTRACT

The whole thesis work has been divided into five chapters, namely Chapter 1 is Introduction, Chapter 2 is Review of Literature, Chapter 3 is Materials and Methods, Chapter 4 is Results and Discussion (includes Chapters 4.1, 4.2 and 4.3) and the last Chapter 5 is Summary and Conclusions.

Herein, conducted research work deals with the analysis of volumetric, thermodynamic, ultrasonic, rheological, spectroscopic properties and molecular interactions of several peculiar nitrogenous bases with distinct compositions of aqueous saccharide solvent systems at various temperatures. Properties analyzed include apparent molar volume (V_{ϕ}) , limiting apparent molar volume (V_{ϕ}) , hydration number (n_H) , limiting apparent molar expansivity (E^0_{ϕ}) , Hepler's constant $(\partial E^0_{\phi}/\partial T)_P$, apparent specific volume (ASV), apparent molar isentropic compression $(K_{\phi,s})$, limiting apparent molar isentropic compression $(K^0_{\phi,s})$, viscosity B-coefficients, transfer parameters and thermodynamic parameters of viscous flow $(\Delta \mu^0_I, \Delta \mu^0_2, T\Delta S^0_2)$ and ΔH^0_2 . These properties were processed to investigate various ionic and molecular interactions within the solution systems. To meet the objectives of the study, we initially measured several physicochemical quantities, viz sound velocity, density besides viscosity for different concentrations of peculiar nitrogenous bases in H_2O and H_2O + saccharide mixed systems.

Moreover, compounds utilized for experimentation were of analytical reagent category and are used as received. These compounds include thymine, adenine, cytosine, saccharides (sucrose, D-glucose, D-xylose, D-maltose and D-lactose). Before experimentation, the apparatus such as beakers, glass rods, volumetric flasks and watch glasses, etc. were thoroughly cleaned using freshly prepared chromic acid and triply distilled water. The weight of the chemical compounds was accurately measured using a Mettler Toledo balance (Model ML204), with a precision of ± 0.1 mg. The saccharide stock solutions, as well as aqueous solutions of nitrogenous bases, were prepared utilizing triply distilled degassed water. The uncertainties in the molal concentration of samples were examined to be $\pm 58 \times 10^{-4}$ mol/kg. Densities/ sound velocities of all mixtures were done through machine DSA, with exactness levels ± 0.005 kg/m³ for density and ± 0.5 m/s for

sound velocity. Also, the viscosity of samples was done through the micro viscometer attached to DSA. Further, the measured values of viscosity are correct upto ±0.5%. This experimental data of sound velocity, viscosity and density were undertaken to evaluate volumetric, ultrasonic and viscometric parameters to arrive at logical conclusion. Further, the absorption spectra of various nitrogenous bases in H₂O and in 0.15 mol/kg aqueous saccharide media were recorded on UV-visible spectrophotometer (LAMBDA 1050+). The prepared samples were examined via utilization of quartz cuvettes of 1 cm path length plus observance wavelength of 200 nm towards 400 nm. Also, the significant conclusions of the results obtained from chapters 4.1, 4.2 and 4.3 are discussed below:

In chapter 4.1, physicochemical analysis of thymine (nitrogenous base) has been carried out in water and aqueous glucose/sucrose solution media across five temperatures (293.15 to 313.15 K), while maintaining a standard pressure (0.1 MPa). The molality of thymine was kept in the range of (0.006 - 0.030) mol/kg in water and in aqueous solutions (0.05 – 0.15) mol/kg of glucose/sucrose. The experimentally determined physical properties such as density, velocity of sound, and viscosity have been utilized for the estimation of several volumetric, thermodynamic, ultrasonic, and rheological parameters. Results showed that the apparent molar volume, increased with solute concentration, while the apparent molar isentropic compression rose with both temperature and saccharide molality. Hepler's thermodynamic relation and dB/dT data confirmed thymine's chaotropic nature in both water and saccharide solutions. Additionally, the Co-sphere overlap model has been utilized for the analysis of assorted probable interactions operating in the prepared systems. The thermophysical property analysis suggested that solute-solvent interactions intensified with higher temperatures and saccharide concentrations in all solution systems. Lastly, UV spectral analysis verified the presence of effective dipole–dipole interactions in the studied systems.

In chapter 4.2, the volumetric, compressibility, and rheological properties for adenine in the peculiar composition ranges i.e. 0.002 to 0.010 mol/kg in water and in 0.05, 0.10, and 0.15 mol/kg D-glucose/D-maltose solutions were studied at temperatures from 293.15 K to 313.15 K under 0.1 MPa. The calculated $K_{\phi,s}$ was observed to boost with both rising temperature and saccharide molality, attributed to the increasing compressibility of

bulk water. In addition, the Co-sphere overlap model has been implicated for the analysis of assorted feasible interactions effective in the primed systems. The received outcomes forecast that in all solution systems, the solute-solvent interactions are progressing with rising temperatures and concentrations of saccharides. Furthermore, the structure breaking proclivity of adenine has been scrutinized via the abstraction of Hepler's constant data and positive values of dB/dT data for all the explored systems. Moreover, the inferred apparent specific volume data specify that adenine has a sweet taste in water and distinct concentrations of selected saccharides. Also, the UV absorption spectra of adenine in water and in 0.15 mol/kg D-glucose/D-maltose solvent revealed the subsistence of efficient hydrophilic-hydrophilic interactions amid adenine and D-glucose/D-maltose in the mixtures.

In chapter 4.3, the thermophysical properties of cytosine at varying compositions (0.005 to 0.030 mol/kg) in water and in aqueous D-xylose/D-lactose solutions (0.05, 0.10, and 0.15 mol/kg) are implicated at specific temperatures between 293.15 and 313.15 K plus P = 0.1 MPa. Apparent molar volume, $V_{\phi,s}$ increased with cytosine concentration, attributed to a rise in van der Waals volume. Similarly, $K_{\phi,s}$ grew with temperature and saccharide molal concentration due to increased compressibility of bulk water. Additionally, the Co-sphere overlap model has been utilized for the analysis of assorted probable interactions operating in the prepared systems. The results revealed that in all solution systems, the solute-solvent interactions are progressing with rising temperatures and concentrations of saccharides. Furthermore, the structure breaking tendency of cytosine has been examined via the sign of Hepler's constant and dB/dT data for all the investigational systems. Moreover, the interpretation of apparent specific volume data discerns that cytosine has sweet taste in water and sweet-bitter taste in peculiar concentrations of D-xylose/D-lactose media. Further, there is shifting in absorption band of cytosine from water to 0.15 mol/kg aqueous D-xylose/D-lactose media that reflected effective hydrophilic-hydrophilic interactions between cytosine and D-xylose/D-lactose, leading to greater stabilization of cytosine in these media compared to water. UV data findings were consistent with those from the physicochemical analysis.

ACKNOWLEDGEMENTS

Though words are seldom sufficient to express gratitude and feelings, it gives me an opportunity to acknowledge those who helped me during the course of my studies.

First and foremost, I would like to thank God, the Almighty for bestowing endless blessings upon me to carry out this work successfully, as no work is accomplished without his grace and guidance. The successful completion of any research work is a matter of great endeavourance but, the personal and practical support of numerous people makes the job entirely enjoyable and simple. It is a pleasant aspect that I have now the opportunity to express my gratitude to them.

I would like to express my sincere gratitude to my esteemed and learned Supervisor Dr. Praveen Kumar Sharma, Professor, Department of Chemistry, School of Chemical Engineering and Physical Sciences, Lovely Professional University, Punjab, India and Co-Supervisor Dr. Ashish Kumar, Professor, Department of Chemistry, NCE, Bihar Engineering University, Department of Science Technology and Technical Education, Bihar, India for their constant support, kind encouragement, immensely valuable ideas, suggestions and for having an unwavering attention. Their expertise, constructive feedback and encouragement played a pivotal role in shaping the direction of my research. I am truly thankful for the mentorship and inspiration provided by them, which significantly contributed to the successful completion of this academic endeavor. It has been a matter of great honour to work under their supervisions.

I feel privileged to my sincere regards and gratitude to **Dr. Sushma Sharma**, **Assistant Professor, Department of Chemistry, GCW Parade, Jammu** for her valuable guidance and constant encouragement throughout my research work. I am also thankful to all the faculty members of the G. G. M. Science College, Jammu for their generous support, encouragement, and valuable suggestions to improve the present work.

I gratefully acknowledge my sincere thanks to Dr. Kailash Chandra Juglan, HOS, School of Chemical Engineering and Physical Sciences, Lovely Professional University, Punjab for giving me an opportunity to become a scholar of this esteemed department and for providing necessary amenities required for my research work. Thanks are also due to

the CRDP Department of LPU for giving the timely information and helping me in the possible resolutions of all the administrative problems faced during the completion of the research work.

I am grateful to the **Higher Education Department**, **J&K Govt**. for their invaluable support, particularly for granting me permission to do research work.

I express my appreciation for valuable co-operation and help rendered to me by my research labmates; **Dr. Tanzeela Qadir, Dr. Ruchika Ganjoo, Dr. Humaira Assad, Dr. Shveta Sharma** and **Dr. Ishrat Fatma**. I pay my special heartfelt thanks to **Dr. Richu** and **Ms. Himani Singh** who helped me in completing this huge task. Without their immense support and help I would not have accomplished this work. I am also thankful to my fellow colleagues and friends.

I am profoundly grateful to my parents Sh. Mukhtiar Chand and Smt. Darshana Devi, my brother Mr. Vikram Sarmhal, my parents-in-law Sh. Tilak Raj and Smt. Sandhya Devi whose unwavering support has been the bedrock of my academic journey. In moments of doubt and challenge, their emotional support has been my guiding light. Their love, understanding, blessings and inspiration have transformed obstacles into opportunities and setbacks into stepping stones. I dedicate this achievement to them, recognizing that their sacrifice and support have been the driving force behind the realization of this work. I would also like to thank my son, Mr. Aashwik Kalsi and my lovely daughter Ms. Ayra Kalsi, my extended family and friends for always being a source of positivity and encouragement.

I must record my sincere thanks to my admired spouse, **Dr. Ashwani Kumar**, for his steady encouragement, timely support, unconditional love, and moral support, without whom I would never have enjoyed so many opportunities.

I also express my gratitude to all who knowingly and unknowingly contributed to the completion of this thesis. To all of them I say "THANKS" from the core of my heart.

Date: 27-09-2025 (Asha Sharmhal)

Place: Lovely Professional University, Punjab

TABLE OF CONTENTS

S.No.	CONTENT	Page No.
1	Title	i
2	Dedication	ii
3	Declaration	iii
4	Certificate	iv
5	Abstract	v-vii
6	Acknowledgements	viii-ix
7	Table of Contents	x-xiv
8	List of Tables	xv-xviii
9	List of Figures	xix-xxvi
10	List of Abbreviations	xxvii-xxviii
	CHAPTER-1 INTRODUCTION	1-27
1	Introduction	1-2
1.1	Nucleic Acids	2-3
1.1.1	Thymine	3-4
1.1.2	Adenine	4-5
1.1.3	Cytosine	5-6
1.2	Saccharides	6
1.2.1	Classification of Saccharides	6-7
1.2.2	D-(+)-glucose	7-8
1.2.3	D-(+)-xylose	8
1.2.4	D-(+)-maltose	9
1.2.5	D-(+)-lactose	9-10
1.2.6	Sucrose	10-11
1.3	Water	11-12
1.4	Organization of Aqueous Mixtures	12-14
1.5	Determination of Structure of Water by Various Models	14
1.5.1	Mixture Models	14-15

1.6	Intermolecular Interactions	15-19
	References	20-27
	CHAPTER-2 REVIEW OF LITERATURE	28-54
2	Review of Literature	28-33
2.1	Volumetric, Acoustic, Rheological and Thermodynamic Studies	33-34
	of Solution Samples	
2.1.1	Volumetric Studies	34
2.1.1.1	Apparent Molar Volume, (V_{ϕ})	34
2.1.1.2	Limiting Apparent Molar Volumes, (V^0_{ϕ})	34-35
2.1.1.3	Limiting Apparent Molar Volumes of Transfer, $(\Delta_{tr}V^0_{\phi})$	35-36
2.1.1.4	Co-spheres Overlap Model	36-37
2.1.1.5	Limiting Apparent Molar Expansibilities, (E^0_ϕ)	37
2.1.1.6	Temperature Derivative of Limiting Apparent Molar	38
	Expansibilities, $(\partial E^0_{\phi}/\partial T)_P$	
2.1.1.7	Apparent Specific Volume, (ASV)	38
2.1.2	Acoustic Studies	38-39
2.1.2.1	Apparent Molar Isentropic Compressions, $(K_{\phi,s})$	39
2.1.2.2	Limiting Apparent Molar Isentropic Compression, $(K^0_{\phi,s})$	39-40
2.1.2.3	Limiting Apparent Molar Isentropic Compression of Transfer,	40
	$(\Delta_{\operatorname{tr}} K^{\scriptscriptstyle O}{}_{\phi,s})$	
2.1.2.4	Hydration Number, (n_H)	40-41
2.1.3	Viscometric Studies	41
2.1.3.1	Jones-Dole Equation	41-42
2.1.3.2	Temperature Reliance of Procured <i>B</i> -coefficient, (dB/dT)	42
2.1.3.3	Viscosity <i>B</i> -coefficient of Transfer, $(\Delta_{tr}B)$	42
2.1.4	Thermodynamic Studies	42-43
2.2	Research Gap	43-44
2.3	Objectives	44
2.4	Research Methodology	45
	References	46-54

	CHAPTER-3 MATERIALS AND METHODS	55-69
3	Materials and Methods	55
3.1	Chemicals Used	55-56
3.2	Apparatus and Cleaning Protocols	56
3.3	Sample Preparation and Handling	57
3.4	Analysis of Density and Sound of Speed Using DSA 5000 M	57-59
3.4.1	Instrument Description and Specifications	59-60
3.4.2	Density Measurement Principle	60
3.4.3	Sound Speed Measurement Principle	60
3.4.4	Sample Injection and Air Bubble Detection	60-62
3.4.5	Cleaning and Drying of Measuring Cell	62-63
3.4.6	Characteristics and Benefits of DSA 5000 M	63-64
3.5	Measurement of Viscosity Using Lovis 2000 M/ME	64-65
3.5.1	Working Principle of Rolling-Ball Viscometer	65-66
3.6	UV-Vis Spectroscopy	66-67
	References	68-69
	CHAPTER-4 RESULTS AND DISCUSSION	70-213
	CHAPTER-4.1 Exploration of Volumetric, Viscometric, Compressibility and Spectroscopic properties of Thymine in Aqueous Saccharide (Glucose/Sucrose) Media at Discrete Compositions and Temperatures	70-113
4.1.1	Density Data	70-72
4.1.1.1	Apparent Molar Volume	73-74
4.1.1.2	Limiting Apparent Molar Volume	75-78
4.1.1.3	Limiting Apparent Molar Volume of Transfer	79-80
4.1.1.4	Limiting Apparent Molar Expansibility	80-82
4.1.1.5	Apparent Specific Volume	82-83
4.1.2	Speed of Sound Data	83-84
4.1.2.1	Apparent Molar Isentropic Compressions	84-87
4.1.2.2	Limiting Apparent Molar Isentropic Compression	88-91
4.1.2.3	Limiting Apparent Molar Isentropic Compression of Transfer	92-93

4.1.2.4	Hydration Number	93
4.1.3	Viscosity Data	93-97
4.1.3.1	Viscosity B-coefficient	97-102
4.1.3.2	Viscosity <i>B</i> -constraint of Transfer	102-103
4.1.4	Thermodynamic Properties of Viscous Motion	103-105
4.1.5	UV Absorption Studies	105-107
4.1.6	Summary	108
	References	109-113
	CHAPTER-4.2 Analysis of Volumetric, Compressibility and Viscometric Parameters of Adenine in Water + D-Maltose/D-Glucose Media at Varied Temperatures	114-168
4.2.1	Volumetric Properties	115-118
4.2.1.1	Apparent Molar Volume	118-122
4.2.1.2	Limiting Apparent Molar Volume	122-126
4.2.1.3	Limiting Apparent Molar Volume of Transfer	126-129
4.2.1.4	Temperature Dependent Limiting Apparent Molar Volume	129-130
4.2.1.5	Taste Behavior	131-134
4.2.2	Speed of Sound Data	135-137
4.2.2.1	Apparent Molar Isentropic Compression	137-141
4.2.2.2	Limiting Apparent Molar Isentropic Compression	141-145
4.2.2.3	Limiting Apparent Molar Isentropic Compression of Transfer	146-147
4.2.2.4	Hydration Number	147-148
4.2.3	Viscosity Data	148-154
4.2.3.1	Jones-Dole B-coefficient	155-158
4.2.3.2	Jones-Dole B-coefficient of Transfer	159-160
4.2.4	Thermodynamic Properties of Viscous Motion	160-162
4.2.5	UV Absorption Studies	162-164
	References	165-168
	CHAPTER-4.3 Studies on the Thermophysical Properties of Cytosine in Aqueous D-Xylose/D-Lactose Media at Distinct Temperatures	169-213
4.3.1	Volumetric Properties	169-172

4.3.1.1	Apparent Molar Volume	172-174
4.3.1.2	Limiting Apparent Molar Volume	174-178
4.3.1.3	Limiting Apparent Molar Volume of Transfer	178-181
4.3.1.4	Temperature Reliance of the Limiting Molar Volume	181-182
4.3.1.5	Taste Behavior	182-184
4.3.2	Speed of Sound Data	185
4.3.2.1	Apparent Molar Isentropic Compressions	185-187
4.3.2.2	Limiting Apparent Molar Isentropic Compressions	188-191
4.3.2.3	Limiting Apparent Molar Isentropic Compression of Transfer	192-193
4.3.2.4	Hydration Number	193-194
4.3.3	Viscosity Data	194-197
4.3.3.1	Viscosity coefficient	197-202
4.3.3.2	Viscosity B-coefficient of Transfer	202-203
4.3.4	Thermodynamic Properties of Viscous Motion	203-205
4.3.5	UV Absorption Studies	205-207
	References	208-213
	CHAPTER-5 SUMMARY AND CONCLUSIONS	214-221
5	Summary	214
5.1	Chapter 1	214-215
5.2	Chapter 2	216-217
5.3	Chapter 3	217
5.4	Chapter 4.1	217-218
5.5	Chapter 4.2	218-219
5.6	Chapter 4.3	219-220
5.7	Conclusions	220-221
	FUTURE OUTLOOKS	222-223
	LIST OF PUBLICATIONS	224-225
	LIST OF CONFERENCES	226

LIST OF TABLES

Table No.	Description	Page No.
3.1	The varied chemicals engaged in present work with allied CAS	55
	numbers, molecular formulas, purities and structures.	
3.2	Specifications of DSA 5000 M.	59
4.1.1	Densities, ρ and apparent molar volumes, V_{ϕ} of thymine in aqueous	73
	media and aqueous glucose/sucrose solutions at $T/K = 293.15$ –	
	313.15 and $P = 0.1$ MPa.	
4.1.2	Data of limiting molar volumes, V^0_{ϕ} along with slopes, S_v and	80
	analogous transfer values $\Delta_{tr}V^0_{\phi}$ for thymine in H ₂ O and aqueous	
	glucose/sucrose mixtures at $T/K = 293.15 - 313.15$ and $P =$	
	0.1 MPa.	
4.1.3	Deduced data of constants (a, b and c) for thymine in H ₂ O and	81
	aqueous saccharide (glucose/sucrose) solvent systems at $T/K =$	
	293.15 - 313.15 and $P = 0.1$ MPa.	
4.1.4	Deduced data of limiting molar expansibilities, E^0_ϕ as well as	82
	Hepler's constant, $(\partial E^0 \phi / \partial T)_P$ for thymine in H ₂ O along with H ₂ O +	
	saccharide solvent systems at discrete temperatures.	
4.1.5	Anticipated data of ASV for thymine in water and saccharide solvent	82
	systems at varied $Temp. = (293.15 - 313.15) \text{ K}.$	
4.1.6	Sound velocities, <i>u</i> and apparent molar isentropic compression,	86
	$K_{\phi,s}$ of thymine in aqueous media and aqueous	
	glucose/sucrose solutions at <i>Temp.</i> = (293.15 - 313.15) K	
	and Pressure = 0.1 MPa.	
4.1.7	Data of apparent molar isentropic compression at dilution (infinite),	92
	$K^0_{\phi,s}$ along with S_k slopes besides corresponding transfer values	
	$\Delta_{tr}K^0_{\phi,s}$ for thymine in water as well as aqueous glucose/sucrose	
	solutions $T/K = 293.15 - 313.15$ and $Pressure = 0.1$ MPa.	
4.1.8	Anticipated hydration numbers (n_H) for thymine in water and	93
	saccharide solvent systems at discrete temperatures.	
4.1.9	Experimentally acquired viscosities, η and calculated relative	96
	viscosities, η_r of thymine in several prepared solvent mixtures at	
	distinct temperatures.	

Table No.	Description	Page No.
4.1.10	Anticipated (d B /d T) data for thymine in in H ₂ O and H ₂ O +	102
	glucose/sucrose solutions at discrete temperatures.	
4.1.11	Deduced viscosity B coefficients and corresponding transfer values	102
	$\Delta_{tr}B$ for thymine in water and glucose/sucrose solvent systems.	
4.1.12	The estimated thermodynamic parameters for thymine in H ₂ O and	104
	aqueous glucose and sucrose media.	
4.2.1	Density values, $ ho$ and apparent molar volumes, V_{ϕ} for adenine in	118
	water and aqueous D-glucose/D-maltose solutions at $T/K =$	
	293.15 – 313.15.	
4.2.2	Data of limiting apparent molar volume, V^0_{ϕ} along with the S_{ν} slopes	127
	as well as analogous transfer volumes $\Delta_{tr}V^0_{\phi}$ for adenine in water and	
	aqueous D-glucose/D-maltose solutions at $T/K = 293.15 - 313.15$ and	
	P = 0.1 MPa.	
4.2.3	Deduced data of a, b and c constants corresponding to adenine in	130
	aqueous and H ₂ O + D-glucose/D-maltose mixtures.	
4.2.4	Deduced data of limiting apparent molar expansibility, E^0_{ϕ} and	130
	Hepler's constant, $(\partial E^0_{\phi}/\partial T)_p$ for adenine in water and aqueous D-	
	glucose/D-maltose solutions at $T/K = 293.15$ to 313.15 and $P = 0.1$	
	MPa.	
4.2.5	The deduced data of ASV for adenine in water and aqueous D-	131
	glucose/D-maltose solutions at $T/K = 293.15 - 313.15$ and $P = 0.1$	
	MPa.	
4.2.6	Experimentally acquired sound velocities, u and calculated apparent	138
	molar isentropic compressions, $K_{\phi,s}$ for adenine in water and aqueous	
	D-glucose/D-maltose solutions at $T/K = 293.15 - 313.15$ and $P = 0.1$	
	MPa.	
4.2.7	Data of apparent molar isentropic compression at very high dilution,	146
	$K^{0}_{\phi,s}$ along with S_{k} slopes, and corresponding transfer values $\Delta_{tr}K^{0}_{\phi,s}$	
	for adenine in water and aqueous D-glucose/D-maltose solutions	
	at $T/K = 293.15 - 313.15$ and $P = 0.1$ MPa.	
4.2.8	Data of hydration number (n_H) for adenine in water and aqueous D-	148
	glucose/D-maltose solutions at $T/K = 293.15$ to 313.15 and	
	P = 0.1 MPa.	

Table No.	Description	Page No.
4.2.9	Experimentally acquired viscosities, η and calculated relative	151
	viscosities, η_r for adenine in water and aqueous D-glucose/D-maltose	
	solutions at $T/K = 293.15 - 313.15$ and $P = 0.1$ MPa.	
4.2.10	Deduced data of viscosity B coefficients and corresponding transfer	159
	values $\Delta_{tr}B$ for adenine in water and aqueous D-glucose/D-maltose	
	solutions at $T/K = 293.15 - 313.15$ and $P = 0.1$ MPa.	
4.2.11	Deduced data of dB/dT for adenine in water and aqueous D-	160
	glucose/D-maltose solutions at $T/K = 293.15 - 313.15$ and $p = 0.1$	
	MPa.	
4.2.12	Data of chemical potential, entropy and enthalpy of activation for	161
	adenine in water and aqueous D-glucose/D-maltose solutions at $T/K =$	
	293.15 - 313.15 and $P = 0.1$ MPa.	
4.3.1	Experimentally acquired densities, ρ and calculated apparent	172
	molar volumes, V_{ϕ} for cytosine in water and aqueous D-xylose/D-	
	lactose solutions at $T/K = 293.15 - 313.15$ and $P = 0.1$ MPa.	
4.3.2	Data of limiting apparent molar volume, V^0_{ϕ} together with slopes, S_{ν}	179
	and associated transfer values $\Delta_{tr}V^0_{\phi}$ for cytosine in H ₂ O and aqueous	
	D-xylose/D-lactose media at $T/K = 293.15 - 313.15$ and $P =$	
	0.1 MPa.	
4.3.3	Deduced constraints (a, b, c) for cytosine in H ₂ O as well as aqueous	182
	D-xylose/D-lactose mixtures.	
4.3.4	Deduced data of apparent molar expansibility at dilution (infinite),	182
	E^0_{ϕ} besides Hepler's constant, $(\partial E^0_{\phi}/\partial T)_P$ for cytosine in H ₂ O and	
	H ₂ O + D-xylose/D-lactose mixtures.	
4.3.5	The deduced data of ASV for cytosine in water and aqueous D-	183
	xylose/D-lactose solutions at $T/K = 293.15 - 313.15$ and $P =$	
	0.1 MPa.	
4.3.6	Experimentally acquired sound velocities, u and calculated	186
	apparent molar isentropic compressions, $K_{\phi,s}$ for cytosine in	
	H ₂ O and H ₂ O + D-xylose/D-lactose mixtures at several	
	temperatures (K).	
4.3.7	Obtained partial molar isentropic compressions, $K^0_{\phi,s}$ together with	192
	slope, S_k besides calculated transfer partial molar isentropic	
	compression, $\Delta_{tr}K^0_{\phi,s}$ for cytosine in pure H ₂ O as well as aqueous D-	

Table No.	Description	Page No.
	xylose and D-lactose solutions.	
4.3.8	Hydration number (nH) for cytosine in H ₂ O and water +D-xylose/D-	194
	lactose implicated mixtures at assorted temperatures.	
4.3.9	Experimentally determined viscosities, η , and computed η_r values for	195
	cytosine in H ₂ O and H ₂ O + D-xylose/D-lactose media at diverse	
	temperatures (K).	
4.3.10	Deduced data of dB/dT for cytosine in H ₂ O and water + D-xylose/D-	201
	lactose mixtures at assorted temperatures.	
4.3.11	Deduced data of graphically manifested B coefficients as well as	202
	corresponding transfer values $\Delta_{tr}B$ for cytosine in H ₂ O and water + D-	
	xylose/D-lactose mixtures.	
4.3.12	Data of chemical potential, entropy and enthalpy of activation for	204
	cytosine in water and aqueous D-xylose/D-lactose media at $T =$	
	293.15 K – 313.15 K.	

LIST OF FIGURES

Figure No.	Description	Page No.
1.1	Structure of thymine	4
1.2	Structure of adenine	5
1.3	Structure of cytosine	5
1.4	Structure of D-(+)-glucose	7
1.5	Structure of D-(+)-xylose	8
1.6	Structure of D-(+)-maltose	9
1.7	Structure of D-(+)-lactose	10
1.8	Structure of sucrose	11
1.9	Arrangement of water in ionic hydration shells	13
1.10	(a) Structure maker ion showing effective interaction with water and (b) Structure breaker ion showing weak interaction with water	14
1.11	Structure of water according to Frank Cluster model	15
1.12	Ion-dipole interaction	16
1.13	Dipole-dipole interactions among the dipolar HCl molecules	17
1.14	Dipole-induced dipole interaction	17
1.15	Hydrogen bonding interaction	18
1.16	Dispersion force	18
2.1	Ion hydration co-spheres overlap adapted	37
3.1	Mettler Toledo (Model ML204)	57
3.2	Machine DSA 5000 M by Anton Paar	58
3.3	Operating elements of main screen	58
3.4	Filling of sample into sample inlet adapter	61
3.5	(i): Filling adapter at DSA5000M, (ii): Mounted injection adapter	61

Figure No.	Description	Page No.
3.6	Appearance of a gas bubble	62
3.7	Drying cartridge connected with the instrument	63
3.8	Lovis microviscometer 2000 M/ME, with DSA 5000 M	64
3.9	Lovis 2000 M/ME unit	65
3.10	Capillary with a ball	65
3.11	Measuring principle of Lovis 2000 M/ME	66
3.12	UV/vis spectrophotometer (LAMBDA 1050+)	67
4.1.1(a)	Comparison graph comprising density versus molality with literature for thymine in H_2O at discrete $T(K)$. \blacksquare : Conducted investigation on 293.15, \bullet : Conducted investigation on 298.15, \blacktriangle : Conducted investigation on 303.15, \blacktriangledown : Conducted investigation on 308.15, \bullet : Conducted investigation on 313.15, \bullet : Lit. [4] on 293.15, \blacktriangleright : Lit. [4] on 308.15, \bullet : Lit. [4] on 308.15, \bullet : Lit. [5] on 303.15, \star : Lit. [5] on 298.15, \star : Lit. [5] on 313.15.	72
4.1.1(b)	Comparison graph of density versus molality with literature for glucose in H_2O at diverse $T(K)$. \blacksquare : Conducted investigation on 293.15, \bullet : Conducted investigation on 298.15, \blacktriangle : Conducted investigation on 303.15, \blacktriangledown : Conducted investigation on 308.15, \bullet : Conducted investigation on 313.15, \blacktriangleleft : Lit. [6] on 293.15, \blacktriangleright : Lit. [6] on 308.15, \bullet : Lit. [6] on 313.15.	72
4.1.1(c)	Comparison graph of density versus molality with literature for sucrose in water at assorted $T(K)$. \blacksquare : Conducted investigation on 293.15, \blacksquare : Conducted investigation on 303.15, \blacktriangledown : Conducted investigation on 308.15, \blacktriangledown : Conducted investigation on 313.15, \blacktriangledown : Lit. [7] on 293.15, \blacktriangleright : Lit. [7] on 298.15, \spadesuit : Lit. [7] on 303.15, \bigstar : Lit. [7] on 313.15.	72
4.1.2	Graphs of $V_{\phi} \times 10^6 / (\text{m}^3 \text{ mol}^{-1})$ vs $m / (\text{mol kg}^{-1})$ for thymine in (a) water, (b) 0.05 mol kg ⁻¹ glucose, (c) 0.10 mol kg ⁻¹ glucose, (d) 0.15 mol kg ⁻¹ glucose, (e) 0.05 mol kg ⁻¹ sucrose, (f) 0.10 mol kg ⁻¹ sucrose and (g) 0.15 mol kg ⁻¹ sucrose at temperatures, ■ : 293.15 K, • : 303.15 K, • : 308.15 K, • : 313.15 K.	78

Figure No.	Description	Page No.
4.1.3(a)	Comparison graph of sound speed vs molality with literature for thymine in water at diverse $T(K)$. \blacksquare : Lit. [5] on 293.15, \blacksquare : Lit. [5] on 308.15, \blacksquare : Lit. [5] on 308.15, \blacksquare : Lit. [5] on 313.15, \blacksquare : Lit. [4] on 293.15, \blacksquare : Lit. [4] on 298.15, \blacksquare : Lit.	85
	[4] on 303.15, ★: Lit. [4] on 308.15, ♠: Lit. [4] on 313.15, ▶: Conducted investigation on 293.15, ♠: Conducted investigation on 303.15, ♠: Conducted investigation on 308.15, ♠: Conducted investigation on 313.15.	
4.1.3(b)	Comparison graph of sound speed vs molality with literature for glucose in water at diverse $T(K)$. \blacksquare : Conducted investigation on 293.15, \bullet : Conducted investigation on 298.15, \blacktriangle : Conducted investigation on 303.15, \blacktriangledown : Conducted investigation on 308.15, \blacktriangleright : Conducted investigation on 313.15, \blacktriangleleft : Lit. [6] on 293.15, \blacktriangleright : Lit. [6] on 298.15, \bullet : Lit. [6] on 308.15, \bullet :	86
	[6] on 298.15, • : Lit. [6] on 303.15, • : Lit. [6] on 308.15, • : Lit. [6] on 313.15.	
4.1.3(c)	Comparison graph of sound speed vs molality with literature for sucrose in water at diverse $T(K)$. \blacksquare : Conducted investigation on 293.15, \blacksquare : Conducted investigation on 298.15, \blacktriangle : Conducted investigation on 303.15, \blacktriangledown : Conducted investigation on 308.15, \clubsuit : Conducted investigation on 313.15, \blacktriangleleft : Lit. [7] on 293.15, \blacktriangleright : Lit. [7] on 298.15, \blacktriangleright : Lit. [7] on 303.15, \blacktriangleright : Lit. [7] on 313.15.	86
4.1.4	Graph of $K_{\phi,s}$ × 10 ¹⁵ /(m³ mol ⁻¹ Pa ⁻¹) vs m /(mol kg ⁻¹) for thymine in (a) water, (b) 0.05 mol kg ⁻¹ glucose, (c) 0.10 mol kg ⁻¹ glucose, (d) 0.15 mol kg ⁻¹ glucose, (e) 0.05 mol kg ⁻¹ sucrose, (f) 0.10 mol kg ⁻¹ sucrose and (g) 0.15 mol kg ⁻¹ sucrose at $T = \blacksquare$: 293.15 K, ●: 298.15 K, ▲: 303.15 K, ▼: 308.15 K, ◆: 313.15 K.	91
4.1.5(a)	Comparison graph of viscosity vs molality with literature for thymine in H_2O at discrete $T(K)$. \blacksquare : Conducted investigation on 293.15, \bullet : Conducted investigation on 298.15, \wedge : Conducted investigation on 303.15, \vee : Conducted investigation on 308.15, \circ : Conducted investigation on 313.15, \circ : Lit. [4] on 293.15, \circ : Lit. [4] on 298.15, \circ : Lit. [4] on 303.15, \star : Lit. [5] on 308.15, \star : Lit. [5] on 298.15, \star : Lit. [5] on 303.15, \star : Lit. [5] on 313.15.	95
4.1.5(b)	Comparison graph of viscosity vs molality with literature for glucose in H_2O at discrete $T(K)$. \blacksquare : Conducted investigation on 293.15, \bullet :	95

Figure No.	Description	Page No.
	Conducted investigation on 298.15, ▲: Conducted investigation on 303.15, ▼: Conducted investigation on 308.15, ◆: Conducted investigation on 313.15, ◄: Lit. [6] on 293.15, ►: Lit. [6] on 298.15, ♠: Lit. [6] on 303.15, ★: Lit. [6] on 308.15, ♠: Lit. [6] on 313.15.	
4.1.5(c)	Comparison graph of viscosity vs molality with literature for sucrose in H_2O at discrete $T(K)$. \blacksquare : Conducted investigation on 293.15, \bullet : Conducted investigation on 303.15, \checkmark : Conducted investigation on 308.15, \checkmark : Conducted investigation on 313.15, \checkmark : Lit. [7] on 293.15, \checkmark : Lit. [7] on 298.15, \bullet : Lit. [7] on 303.15, \checkmark : Lit. [7] on 313.15.	95
4.1.6	Graph of η_r vs molaity, $C/(\text{mol L}^{-1})$ for thymine in (a) water, (b) 0.05 mol kg ⁻¹ glucose, (c) 0.10 mol kg ⁻¹ glucose, (d) 0.15 mol kg ⁻¹ glucose, (e) 0.05 mol kg ⁻¹ sucrose, (f) 0.10 mol kg ⁻¹ sucrose and (g) 0.15 mol kg ⁻¹ sucrose at $T = \blacksquare : 293.15 \text{ K}, $	101
4.1.7	Plots of absorbance versus wavelength for thymine in (a) water, (b) 0.15 mol kg ⁻¹ glucose + water media, (c) 0.15 mol kg ⁻¹ sucrose + water media.	107
4.2.1(a)	Graphs representing contrast of measured density data with the accessible reports at discrete temperatures for adenine + water at $T(K) = \blacksquare$: Conducted investigation on 293.15, •: Conducted investigation on 298.15, •: Conducted investigation on 303.15, • Conducted investigation on 308.15, • Conducted investigation on 313.15, •: Lit. [1] on 293.15, •: Lit. [1] on 298.15, •: Lit. [1] on 303.15, •: Lit. [1] on 313.15.	117
4.2.1(b)	D-Glucose + water at $T(K) = \blacksquare$: Conducted investigation on 293.15, • : Conducted investigation on 298.15, • : Conducted investigation on 303.15, • : Conducted investigation on 308.15, • : Lit. [3] on 308.15, • : Lit. [3] on 293.15, • : Lit. [3] on 298.15, • : Lit. [2] on 303.15, • : Lit. [2] on 293.15, • : Lit. [2] on 298.15, • : Lit. [2] on 303.15, • : Lit. [2] on 313.15, • : Lit. [5] on 293.15, • : Lit. [6] on 293.15, • : Lit. [6] on 308.15, • : Lit. [6] on 308.15, • : Lit. [6] on 313.15.	117

Figure No.	Description	Page No.
4.2.1(c)	D-Maltose + water at $T(K) = \blacksquare$: Conducted investigation on 293.15, • : Conducted investigation on 298.15, ▲ : Conducted investigation on 303.15, ▼ : Conducted investigation on 308.15, ▼ : Conducted investigation on 313.15,	117
4.2.2	The graphs depicting change in $V_{\phi} \times 10^6/\text{m}^3$ mol ⁻¹ against m/mol kg ⁻¹ for adenine in (a) water, (b) 0.04994 mol kg ⁻¹ D-glucose, (c) 0.09939 mol kg ⁻¹ D-glucose, (d) 0.15003 mol kg ⁻¹ D-glucose, (e) 0.04992 mol kg ⁻¹ D-maltose, (f) 0.09947 mol kg ⁻¹ D-maltose, (g) 0.14947 mol kg ⁻¹ D-maltose at discrete temperatures, ■ : 293.15 K, • : 298.15 K, • : 303.15 K, • : 308.15 K, • : 313.15 K.	126
4.2.3(a)	Graphs representing deviation in measured sound velocity data with the accessible reports at discrete temperatures for adenine + water at $T(K) = \blacksquare$: Conducted investigation on 293.15, •: Conducted dataon 298.15, •: Conducted investigation on 303.15, • Conducted investigation on 303.15, • Conducted investigation on 313.15, •: Lit. [1] on 293.15, •: Lit. [1] on 298.15, •: Lit. [1] on 303.15, •: Lit. [1] on 313.15.	137
4.2.3(b)	D-Glucose + water at $T(K) = \blacksquare$: Conducted investigation on 293.15, • : Conducted investigation on 298.15, • : Conducted investigation on 303.15, ▼ : Conducted investigation on 308.15, • : Lit. [2] on 293.15, • : Lit. [2] on 298.15, • : Lit. [2] on 303.15, • : Lit. [2] on 308.15, • : Lit. [3] on 298.15, • : Lit. [3] on 298.15, • : Lit. [3] on 298.15, • : Lit. [3] on 303.15, • : Lit. [3] on 308.15, • : Lit. [17] on 293.15, • : Lit. [17] on 303.15, • : Lit. [17] on 308.15, • : Lit. [18] on 303.15, • : Lit. [19] on	137
4.2.3(c)	D-Maltose + water at $T(K) = \blacksquare$: Conducted investigation on 293.15, • : Conducted investigation on 298.15, • : Conducted investigation on 303.15, \blacktriangledown : Conducted investigation on 308.15, •	137

Figure No.	Description	Page No.
	: Conducted investigation on 313.15,	
4.2.4	The graph depicting change in $K_{\phi,s} \times 10^{15}/\text{m}^3 \text{ mol}^{-1} \text{ Pa}^{-1}$ against $m/\text{mol kg}^{-1}$ for adenine in (a) water, (b) 0.04994 mol kg ⁻¹ D-glucose, (c) 0.09939 mol kg ⁻¹ D-glucose, (d) 0.15003 mol kg ⁻¹ D-glucose, (e) 0.04992 mol kg ⁻¹ D-maltose, (f) 0.09947 mol kg ⁻¹ D-maltose, (g) 0.14947 mol kg ⁻¹ D-maltose at discrete temperatures, \blacksquare : 293.15 K, \blacksquare : 303.15 K, \blacksquare : 308.15 K, \blacksquare : 313.15 K.	145
4.2.5(a)	Graphs representing comparison of measured viscosity data with the accessible reports at discrete temperatures for adenine + water at $T(K) = \blacksquare$: Conducted investigation on 293.15, • : Conducted investigation on 298.15, • : Conducted investigation on 303.15, • Conducted investigation on 303.15, • Conducted investigation on 313.15, • : Lit. [1] on 293.15, • : Lit. [1] on 298.15, • : Lit. [1] on 303.15, • : Lit. [1] on 313.15.	150
4.2.5(b)	D-Glucose + water at $T(K) = \blacksquare$: Conducted investigation on 293.15, • : Conducted investigation on 298.15, ▲ : Conducted investigation on 303.15, ▼ : Conducted investigation on 303.15, ▼ : Lit. [2] on 293.15, ▶ : Lit. [2] on 298.15, • : Lit. [2] on 303.15, ★ : Lit. [2] on 308.15, ★ : Lit. [2] on 308.15, ★ : Lit. [3] on 298.15, × : Lit. [3] on 303.15, ♦ : Lit. [3] on 308.15, ★ : Lit. [3] on 313.15, □ : Lit. [20] on 293.15, □ : Lit. [20] on 303.15, ♠ : Lit. [20] on 303.15, ♠ : Lit. [20] on 308.15, ▼ : Lit. [21] on 298.15, □ : Lit. [21] on 308.15, □ : Lit. [21] on	150
4.2.5(c)	D-Maltose + water at $T(K) = \blacksquare$: Conducted investigation on 293.15, • : Conducted investigation on 298.15, • : Conducted investigation on 303.15, • : Conducted investigation on 303.15, • : Lit. [13] on 293.15, • : Lit. [13] on 298.15, • : Lit. [13] on 303.15, • : Lit. [13] on 313.15, • : Lit. [21] on 298.15, + : Lit. [21] on	150

Figure No.	Description	Page No.
	308.15, × : Lit. [7] on 293.15, ★: Lit. [7] on 298.15, —: Lit. [7] on 303.15, : Lit. [7] on 308.15, ■ : Lit. [7] on 313.15 K, ● : Lit. [22] on 298.15, ▲ : Lit. [22] on 308.15, ▼ : Lit. [23] on 298.15, ◇: Lit. [23] on 308.15.	
4.2.6	The graph depicting change in η_r against $C(\text{mol/L})$ for adenine in (a) water, (b) 0.04994 mol/kg D-glucose, (c) 0.09939 mol/kg D-glucose, (d) 0.15003 mol/kg D-glucose, (e) 0.04992 mol/kg D-maltose, (f) 0.09947 mol/kg D-maltose, (g) 0.14947 mol/kg D-maltose at discrete temperatures, \blacksquare : 293.15 K, \bullet : 303.15 K, \triangleright : 308.15 K, \bullet : 313.15 K.	158
4.2.7	Plots of absorbance versus wavelength for discrete systems of implication: (a) adenine $+$ H ₂ O; (b) adenine $+$ 0.15 mol/kg D-glucose; (c) adenine $+$ 0.15 mol/kg D-maltose.	164
4.3.1(a)	Graphs insinuating contrast of measured density data with the accessible reports at discrete temperatures for cytosine in water at T/K , \blacksquare : Conducted investigation on 298.15, \bullet : Conducted investigation on 308.15, \blacktriangle : Lit. [2] on 308.15.	171
4.3.1(b)	D-Xylose in water at T/K , \blacksquare : Conducted investigation on 293.15, \bullet : Conducted investigation on 303.15, \checkmark Conducted investigation on 308.15, \checkmark Conducted investigation on 313.15, \checkmark : Lit. [3] on 293.15, \checkmark : Lit. [3] on 298.15, \bullet : Lit. [3] on 303.15, \checkmark : Lit. [3] on 308.15, \bullet : Lit. [4] on 308.15, \bullet : Lit. [4] on 298.15, \bullet : Lit. [4] on 308.15, \bullet : Lit. [4] on 313.15.	172
4.3.1(c)	D-Lactose in water at T/K , \blacksquare : Conducted investigation on 293.15, \bullet : Conducted investigation on 303.15, \blacktriangledown : Conducted investigation on 303.15, \blacktriangledown : Conducted investigation on 308.15, \bullet : Conducted investigation on 313.15, \blacktriangleleft : Lit. [5] on 293.15, \bullet : Lit. [5] on 308.15, \bullet : Lit. [5] on 313.15, \bullet : Lit. [6] on 293.15, \bullet : Lit. [6] on 298.15, \bullet : Lit. [6] on 308.15, \bullet : Lit. [6] on 308.15.	172
4.3.2	The analysed graphs depicting change in $V_{\phi} \times 10^6 (\text{m}^3/\text{mol})$ against $m(\text{mol/kg})$ for diverse systems (a) cytosine + H ₂ O, (b) cytosine + 0.05 mol/kg D-xylose, (c) cytosine + 0.10 mol/kg D-xylose, (d) cytosine + 0.15 mol/kg D-xylose, (e) cytosine + 0.05 mol/kg D-lactose, (f) cytosine + 0.10 mol/kg D-lactose, (g) cytosine + 0.15	178

Figure No.	Description	Page No.
	mol/kg D-lactose at several $T(K)$. ■ : 293.15, • : 298.15, • : 303.15, • : 313.15.	
4.3.3	Graph representing deviation in measured sound velocity data with the accessible reports at discrete temperatures for D-lactose in water. ■ : Conducted investigation on 293.15 K, ● : Conducted investigation on 298.15 K, ▲ : Conducted investigation on 303.15 K, ▼: Conducted investigation on 313.15 K, ▼: Lit. [5] on 293.15 K, ▷ : Lit. [5] on 298.15 K, ● : Lit. [5] on 303.15 K, ★ : Lit. [5] on 308.15 K, ● : Lit. [5] on 313.15 K.	185
4.3.4	Graphs of $K_{\phi,s} \times 10^{15} (\text{m}^3 / \text{mol/ Pa})$ against $m(\text{mol/kg})$ for several systems (a) cytosine + H ₂ O, (b) cytosine + 0.05 mol/kg D-xylose, (c) cytosine + 0.10 mol/kg D-xylose, (d) cytosine + 0.15 mol/kg D-xylose, (e) cytosine + 0.05 mol/kg D-lactose, (f) cytosine + 0.10 mol/kg D-lactose, (g) cytosine + 0.15 mol/kg D-lactose at varying $T/(K)$, \blacksquare : 293.15, \bullet : 303.15, \checkmark : 308.15, \bullet : 313.15.	191
4.3.5	Graph representing comparison of measured viscosity data with the accessible reports at discrete $T(K)$ for D-lactose in water. \blacksquare : Conducted investigation on 293.15, \bullet : Conducted investigation on 298.15, \wedge : Conducted investigation on 303.15, \vee : Conducted investigation on 308.15, \vee : Conducted investigation on 313.15, \vee : Lit. [5] on 293.15, \vee : Lit. [5] on 303.15, \vee : Lit. [5] on 308.15, \circ : Lit. [5] on 313.15.	195
4.3.6	Graphs of η_r against concentration, $C/(\text{mol L}^{-1})$ for diverse mixtures (a) cytosine + H ₂ O, (b) cytosine + 0.05 mol/kg D-xylose, (c) cytosine + 0.10 mol/kg D-xylose, (d) cytosine + 0.15 mol/kg D-xylose, (e) cytosine + 0.05 mol/kg D-lactose, (f) cytosine + 0.10 mol/kg D-lactose, (g) cytosine + 0.15 mol/kg D-lactose at discrete temperatures, \blacksquare : 293.15 K, \bullet : 303.15 K, \triangleright : 308.15 K, \bullet : 313.15 K.	201
4.3.7	Plots of absorbance versus wavelength for peculiar systems (a) cytosine + H ₂ O, (b) cytosine + 0.15 mol/kg D-xylose and (c) cytosine + 0.15 mol/kg D-lactose.	206

LIST OF ABBREVIATIONS

ABBREVIATIONS DESCRIPTION

 $K_{\phi,s}$ Apparent Molar Isentropic Compressibility

 V_{ϕ} Apparent Molar Volume

Cm Centimeter a, b, c Coefficients

°C Degree Celsius

ρ Density of Solution

 ρ_0 Density of Solvent

DSA Density and Speed of Sound Analyzer

DNA Deoxyribose Nucleic Acid

 $V^0_{\phi}(elect.)$ Electrostriction Partial Molar Volume

 S_{ν}, S_k Experimental Slopes

A Falkenhagen Coefficient

T Flow Time

R Gas Constant

 $\Delta \mu_2$ Gibbs Free Energy of Activation for Solution $\Delta \mu_1$ Gibbs Free Energy of Activation for Solvent

Hz Hertz

n_H Hydration Number

 V^0_{ϕ} (int.) Intrinsic Partial Molar Volume

 $K^{0}_{\phi,s,b}$ Isentropic Compressibility of Bulk Water

 k_s Isentropic Compressibility of Solution k_s^0 Isentropic Compressibility of Solvent

B Jones-Dole Coefficient

K Kelvin

Kcal KilocalorieKg KilogramkJ Kilojoule

 $K^0_{\phi,s}$ Limiting Apparent Molar Compressibility

 E^{θ}_{ϕ} Limiting Apparent Molar Expansibility

 V_{ϕ}^{0} Limiting Apparent Molar Volume

Mg Milligram

M Molality of the Solute

M Molar Mass

 $V^0_{\phi,b}$ Molar Volume of Bulk Water

Mole Pa Pascal

 η_r Relative Viscosity

RNA Ribonucleic Acid

 $V_{shrinkage}$ Shrinkage Volume

U Speed of Sound

Temperature

dB/dT Temperature Coefficient $\Delta_{tr}K^0_{\phi,s}$ Transfer Compressibility

 $\Delta_{\rm tr} V^{\theta}_{\phi}$ Transfer Volume

UV Ultraviolet

 V_{vw} Van der Waals Volume

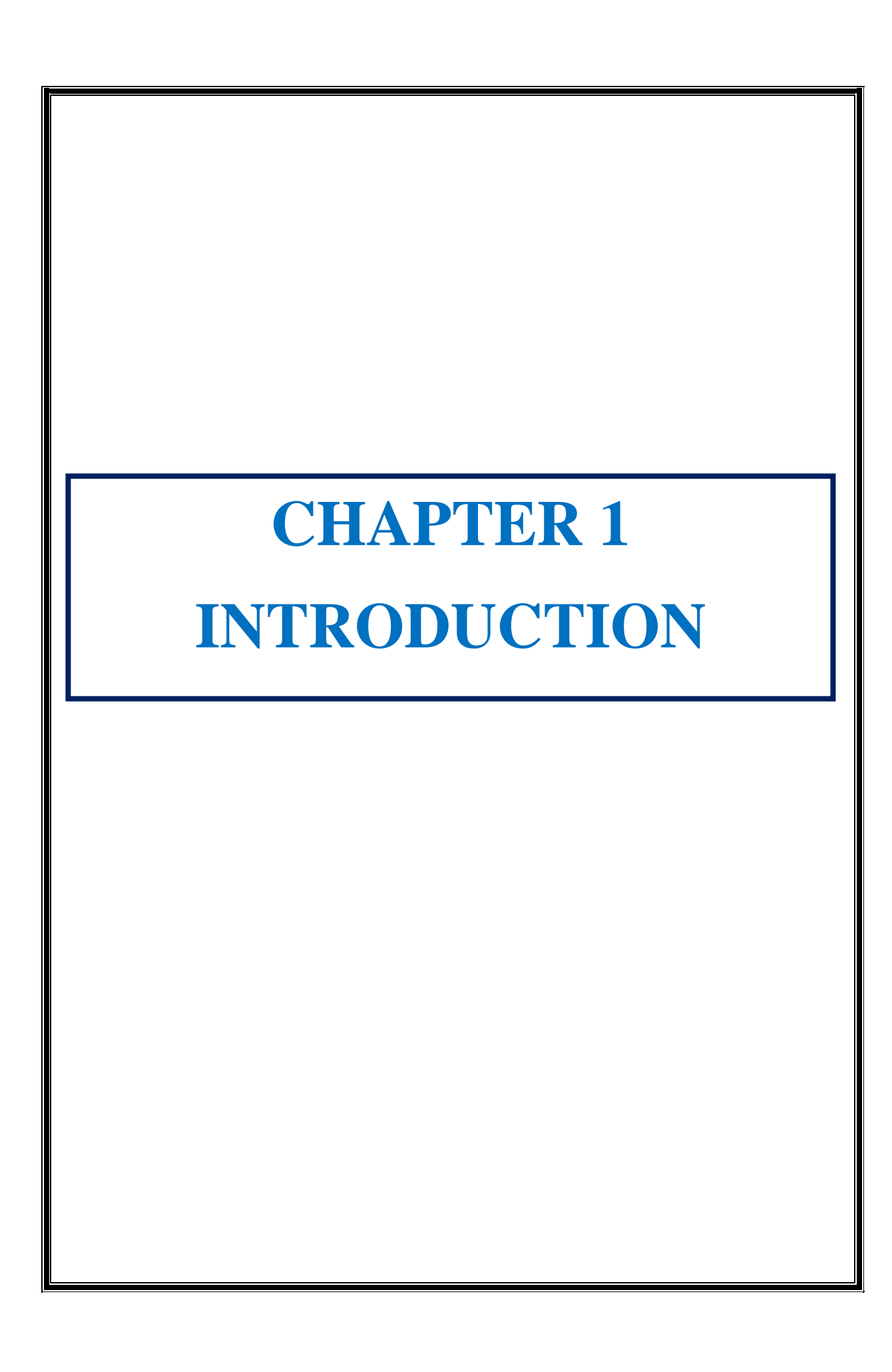
 $\Delta_{tr}B$ Viscosity *B*-coefficients of Transfer

H Viscosity of Solution

 η_0 Viscosity of Solvent

V Volume

 V_{void} Volume of Void



1 Introduction

All the biological systems in this world are comprised of several lifeless substances that are existing in their cells in a very obscure but highly organized form; these are called biomolecules [1]. Biomolecules include both large macromolecules as well as small molecules examples include proteins, nucleic acids, lipids, carbohydrates, as macromolecules and primary metabolites, natural products, secondary metabolites, as microbiomolecules [2]. Biomolecules created within the organism are endogenous, solely organisms usually need exogenous biomolecules in the form of nutrients for survival [3,4]. Most of the biological molecules are organic composites and only four elements: C, O, H and N make up 96% of the living body's weight [5]. Various processes like morphogenesis, energy creation, hormonal activity, synthesis of plasma membranes, the transmission of biogenetic material etc. in the living systems are brought out by the biomolecules [6]. Regardless of the basic biological role, these are having enormous prospects on industrial level [7]. Additionally, these compounds have fascinating peculiar prominence in ecological sectors and biotechnology like in the manufacturing of ingenious hybrid materials, photonics, sensors, etc [9-11]. The examination of chemistry operating between biomolecules has gained huge interest in the fields of food industries, biochemistry, environment, etc [12-14]. So, it is necessary to analyze the consequence of diverse compositions and temperatures on the structural heterogeneity of biomolecules.

A mixed system is termed as a harmonized blend of having 2 or else more chemically inert stuffs having uniform properties like density, refractive index etc throughout and whose composition can be altered within certain limits [15]. The substances used to make up solutions are known as components of a solution. That component of the solution which is present in a larger amount and has the same physical state as that of the solution is referred to as a solvent. A solute is the substance in a solution that exists in a smaller amount. The research on solutions has gained comprehensive importance due to the accessibility of an ample range of solvents as reaction media [16]. Dissolution of a substance in a solvent is accompanied by electrostriction of the solvent under the action of electrostatic fields of ions in solutions [17]. There are numerous types of inter-molecular

interactions which are found in solution state. Of these, solute and solute along with solvent and solute interactions are of ample importance [18].

Various physical properties for instance ultrasonic velocity, density, surface tension, refractive index, viscosity etc, find enormous applications in characterizing the physicochemical behavior and molecular interactions [19]. Thermodynamic, acoustic and transport studies have a considerable part in studying the nature along with concentration variation and molecular arrangement of the components [20]. Further, these properties have gained comprehensive role in important areas such as designing of various pharmaceutical drugs, operations of batteries, metal refining, petrochemical and chemical industries [21,22]. These properties include partial molar isentropic compressibilities, partial molar expansivities, apparent molar volumes, transfer volumes and transfer values of isentropic compression, various viscometric coefficients, apparent molar isentropic compressibility, etc [23]. To analyze assorted interactions prevailing in binary/ternary mixtures, water is a comprehensively used component because of its high dielectric constant, high dipole moment and economical nature [24]. Sound velocities, viscosities and densities are important properties of the solutions that can be used to enumerate the physicochemical properties of solutions. Thus these properties help in reporting the inter-molecular interactions existing among the mixture moieties [25].

This thesis employs volumetric, compressibility, and viscometric methods to investigate the intermolecular interactions in systems consisting of nucleic acid bases and H_2O + saccharides. In the first series, thymine is chosen as solute and aqueous glucose/sucrose is solvent. In the second series, the physicochemical effects of adenine (solute) are studied in D-glucose as well as D-maltose aqueous solutions. The third series deals with the investigation of plausible intermolecular interactions present in cytosine and aqueous xylose and lactose solutions at varied temperatures.

1.1 Nucleic Acids

Nucleic acids are vital biomolecules accountable for storing and passing on genetic information in all living beings [26]. The RNA plus DNA comprise two foremost kinds of nucleic acids. These are composed of repeating units known as nucleotides, with each

nucleotide consisting of a nitrogenous base, a phosphate group, and a pentose sugar [27] i.e. each nucleotide in a nucleic acid consists of three components:

- (i) Nitrogenous Base: These organic molecules are categorized into purines as well as pyrimidines. Pyrimidines contain cytosine, thymine (originate in DNA), plus uracil (originate in RNA) on contrary purines contain adenine and guanine.
- (ii) **Pentose Sugar:** The sugar present in RNA includes ribose in contrast DNA contains deoxyribose. The disparity lies in the existence or nonexistence of oxygen atom at the 2' position.
- (iii) **Phosphate Group:** The phosphate moiety unites the 5' C of first sugar with the 3' C of second, forming the nucleic acid's sugar-phosphate backbone.

Nucleotides are linked together through phosphodiester bonds, which outline amid the phosphate group (nucleotide) and OH group (sugar) of the adjacent nucleotides [28]. This linkage creates a sugar-phosphate backbone with protruding nitrogenous bases. Further, in DNA, bases pair specifically (A with T and G with C) through hydrogen bonds, stabilizing the double helix structure [29].

In RNA, while it's usually single-stranded, intramolecular base pairing can occur, leading to complex structures essential for its function. DNA's stability makes it suitable for long-term genetic storage, while RNA's flexibility allows it to participate in various cellular functions. Mutations or changes in nucleotide sequences can alter genetic information, leading to variations in traits or diseases. Nucleic acids are the molecular foundation of life, encoding and managing the information necessary for biological functions and heredity [30]. Understanding their structure and composition is essential for studying genetics, molecular biology, and biochemistry.

1.1.1 Thymine

Thymine is chemically known as 5-methyluracil having molecular formula C₅H₆N₂O₂. Thymine pairs with adenine (A) through two hydrogen bonds and helps to stabilize the nucleic acid structures. Thymine is a pyrimidine derivative, having a single-

ring structure, unlike purines, which have a double-ring structure. In RNA, thymine is replaced by uracil (U).

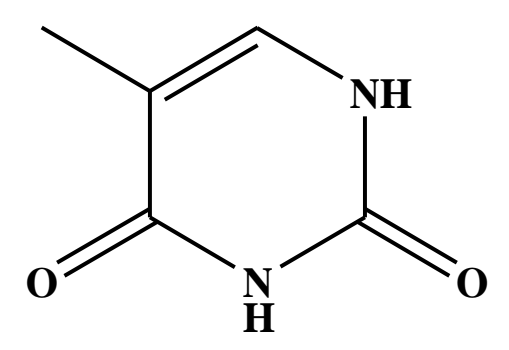


Figure 1.1: Structure of thymine

It is crucial in maintaining the genetic code and ensuring accurate DNA replication. It can undergo chemical changes, such as methylation, which plays a role in gene regulation. In the presence of UV light, it gets damaged thereby leading to the formation of thymine dimers, which can cause mutations if not repaired by cellular mechanisms [31]. The synthesis of thymidine nucleotides requires energy, which is often derived from carbohydrate metabolism. Its derivatives are used in antiviral and anticancer therapies, where they can inhibit DNA synthesis in rapidly dividing cells [32].

1.1.2 Adenine

Adenine belongs to the purine group of nucleobases which is characterized by a double-ring structure. It's molecular formula is $C_5H_5N_5$. It consists of a fused double-ring system comprising a 6-membered ring (pyrimidine) fused with a 5-membered ring (imidazole).

It is a key component of ATP, the primary energy carrier in cells. ATP comprises of adenine linked to a ribose sugar along with three phosphate groups [33].

ATP hydrolysis liberates energy which is used in various cellular phenoms, together with muscle contraction, protein creation, and dynamic transport across plasma lemma. It is also a part of other important nucleotides like AMP i.e. adenosine monophosphate, ADP i.e. adenosine diphosphate and NAD⁺ i.e. nicotinamide adenine

dinucleotide, all of which are involved in energy metabolism and redox reactions [34]. It is a component of mRNA i.e. messenger RNA, which transmits genetic instructions from DNA to ribosome for protein synthesis. Additionally, it is part of coenzymes like FAD (flavin adenine dinucleotide), as well as CoA (coenzyme A), which are involved in essential biochemical phenoms such as the citric acid cycle, glycolysis, fatty acid metabolism, etc [35].

Figure 1.2: Structure of adenine

1.1.3 Cytosine

It is a pyrimidine base, having molecular formula as C₄H₅N₃O. In the constitution of nucleic acids, cytosine pairs with guanine through three hydrogen bonds, contributing to the strength of the DNA double helix. Cytosine is often methylated to form 5-methylcytosine, which plays a role in regulating gene expression and epigenetic modifications [36]. Abnormal cytosine methylation patterns are linked to various cancers. Aberrant cytosine methylation patterns have been implicated in neurodegenerative contagion like Alzheimer's and Parkinson's [37]. Cytosine derivatives are used in the development of antiviral drugs, for instance, zidovudine is used to treat HIV.

Figure 1.3: Structure of cytosine

Its analogs, such as 5-azacytidine and decitabine, are used as chemotherapeutic agents. Cytosine-modified DNA is employed in the development of biosensors that identifies environmental pollutants, pathogens, and other analytes [38]. In synthetic biology, cytosine is used in the design and synthesis of artificial nucleic acids and genetic circuits. These innovations have applications in creating synthetic organisms that can produce valuable compounds, such as biofuels, pharmaceuticals, and industrial enzymes [39].

1.2 Saccharides

Saccharides are one of the primary classes of biomolecules, also referred as the compounds comprising polyhydroxy aldehydes/ketones [40]. This class of compounds contains only C, H and O; the H and O being present in the similar ratio as in H₂O. Carbohydrates are referred to as hydrates of carbon that are sparingly solvable in organic solvents (except certain polysaccharides) and solvable in water [41].

1.2.1 Classification of Saccharides

Depending upon the behavior of saccharides towards hydrolysis, they are categorized into the following three classes [42]-

(i) Monosaccharides

These are the simplest and most uncomplicated carbohydrates which cannot be more hydrolyzed to minor units. Their common formula is $(CH_2O)_n$ where n = 3-8.

(ii) Oligosaccharides

These carbohydrates upon their hydrolysis furnish 2-10 molecules of the equivalent or different monosaccharides. Depending upon numeral figure of monosaccharide molecules attained upon hydrolysis, they are auxiliary divided as di, tri, tetrasaccharides etc.

a) Disaccharides

These upon hydrolysis produce two molecules of the identical or distinct monosaccharides. For example, maltose, lactose, sucrose etc. Their general formula is $C_{12}H_{22}O_{11}$.

b) Trisaccharides

These upon hydrolysis produce three molecules of the identical or distinct monosaccharides. For example, raffinose upon hydrolysis produces one molecule each of glucose, fructose and galactose. Their general formula is $C_{18}H_{32}O_{16}$.

c) Tetrasaccharides

These upon hydrolysis produce four molecules of the equivalent or distinct monosaccharides. For example, stachyrose upon hydrolysis produces one each molecule of glucose and fructose and two galactose molecules. Their general formula is $C_{24}H_{42}O_{21}$.

(iii) Polysaccharides

These upon hydrolysis produce a huge number of monosaccharide moieties. The most usually occurring polysaccharides are starch, glycogen and cellulose. Their molecular formula is $(C_6H_{10}O_5)_n$ where n = 100-3000.

1.2.2 D-(+)-glucose

D-glucose is a monosaccharide, exists in cyclic form which is a six-membered ring known as pyranose in its aqueous solution. Its molecular formula is $C_6H_{12}O_6$ and is a crucial energy supply for living cells. It is metabolized through glycolysis [43], where it is wrecked down to create ATP- the cell's primary energy source.

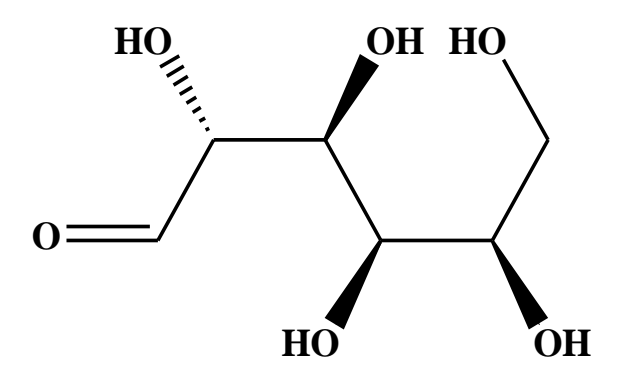


Figure 1.4: Structure of D-(+)-glucose

In animals, surplus glucose is accumulated in the liver as well as muscles in the form of glycogen while in plants, it has been stored as starch. Its concentration is tightly regulated by hormones such as insulin and glucagon. Abnormal levels of glucose in the

blood can escort to hyperglycemia or hypoglycemia. In fermentation processes, it is a key substrate for the creation of ethanol, antibiotics, amino acids, as well as other valuable compounds [44]. Further, it is used in the formulation of skincare products due to its moisturizing properties.

1.2.3 **D-(+)-xylose**

D-xylose is a monosaccharide, also known as wood sugar that is found in the hemicellulose constituent of plant cell walls. It is a five-carbon sugar (pentose) with molecular formula $C_5H_{10}O_5$. It can exist as both linear and cyclic forms, where the cyclic form is more stable in solution.

It is metabolized in certain bacteria and fungi through specific pathways to produce xylulose-5-phosphate, that enters the pentose phosphate phenom, an imperative metabolic route for generating nucleotides and other biomolecules [45]. One of the most significant uses of D-xylose is in the production of xylitol, a sugar alcohol used as a low-calorie sweetener. Xylitol is popular in sugar-free gum, candies, and oral care products due to its dental benefits, as it does not cause tooth decay.

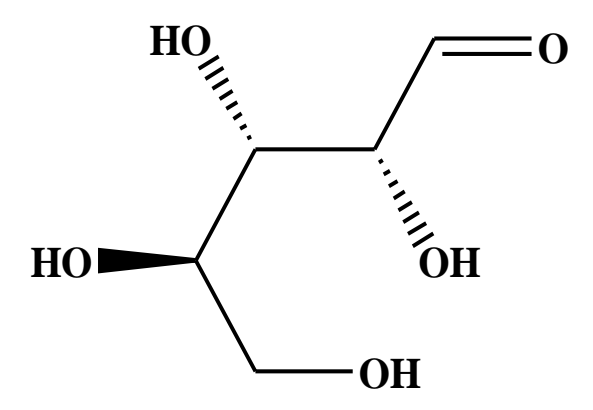


Figure 1.5: Structure of D-(+)-xylose

D-xylose and its derivatives are used in the production of biodegradable plastics and other materials, offering a sustainable alternative to petroleum-based products [46]. Also, its derivatives are sometimes used in agricultural applications to promote plant growth or as part of biostimulants that improve soil health. Its role in metabolic pathways and research makes it a valuable compound in both industrial and scientific contexts [47].

1.2.4 D-(+)-maltose

D-maltose having molecular formula $C_{12}H_{22}O_{11}$ is a disaccharide and is chiefly present in cereals and malted milk products [48]. It comprises two D-glucose moieties allied by an $\alpha(1\rightarrow 4)$ glycosidic linkage. The $\alpha(1\rightarrow 4)$ bond connects C-1 i.e. anomeric carbon of a glucose molecule to OH group on C-4 on other glucose. In an open-chain, it behaves as reducing sugar due to a free aldehydic part in one of the glucose moieties. This allows it to participate in reduction reactions, such as reducing copper in Benedict's or Fehling's tests. During fermentation, yeast breaks down D-maltose into glucose, which is then fermented to produce alcohol and carbon dioxide [49].

Figure 1.6: Structure of D-(+)-maltose

Additionally, implicated a sweetener in different processed foods, including candies, cereals, and beverages. It also serves as a preservative and flavoring agent. It serves as an intermediate in the metabolic conversion of complex carbohydrates to glucose, which is used as a primary energy source by the cells.

1.2.5 D-(+)-lactose

It is a disaccharide sugar primarily found in milk as well as dairy products [50]. It is comprised of two monosaccharides: D-galactose & D-glucose, allied via $\beta(1\rightarrow 4)$ glycosidic link. It's molecular formula is $C_{12}H_{22}O_{11}$. It is a reducing sugar for the reason that it comprises complimentary anomeric carbon that participates in redox reactions. It serves as a significant source of energy, especially for infants, who rely on it as their primary carbohydrate during early development. Through the action of the enzyme lactase,

located in the small intestine [51], it is broken down into galactose and glucose. It serves as a filler or binder in tablets and capsules due to its stability, non-reactivity, and ease of processing [52]. Lactobacillus bacteria can ferment lactose to produce lactic acid, which is essential in production of yogurt, cheese, as well as other fermented dairy foodstuffs.

Figure 1.7: Structure of D-(+)-lactose

It has been observed to be less sweet than sucrose. It is important for calcium and magnesium, absorption in the intestines, as it enhances the solubility and absorption of calcium, which is crucial for bone health. Thus, it is a versatile disaccharide with an extensive array of applications in the food, pharmaceutical, as well as biotechnological industries [53].

1.2.6 Sucrose

It is frequently recognized as table sugar and it is a disaccharide comprised of glucose as well as fructose units allied via $\alpha(1\rightarrow 2)$ glycosidic bond [54]. It's molecular formula is $C_{12}H_{22}O_{11}$. It is widely used as a sweetener in victuals and beverages and plays a significant role in various industries. It is naturally found in many plants, particularly in sugarcane and sugar beets, which are the primary sources for commercial sugar production. It is also present in fruits, vegetables, and honey.

Figure 1.8: Structure of sucrose

Unlike some other disaccharides like maltose and lactose, sucrose is a non-reducing sugar having no free aldehydic/ketonic group, which makes it less reactive in certain chemical reactions. It is used as a preservative in jams, jellies, and other food products. In the production of ethanol and other alcohols, sucrose is a key substrate for fermentation by yeast, converting the sugar into alcohol and carbon dioxide.

High utilization of sucrose is linked with an enlarged risk of dental caries (cavities). High intake of sucrose, particularly from processed foods and sugary beverages, has been linked to metabolic disorders, including diabetes and fatty liver disease [55].

1.3 Water

Water is the most versatile of all the solvents because of its plentiful existence in nature. Its molecular formula is H₂O, comprising of two H atoms which are linked covalently to an oxygen. It is regarded as an 'anomalous' solvent because its characteristics vary considerably from the other solvents [56]. It is a polar compound that is flavorless, transparent and scentless at room temperature. Water can dissolve multiple compounds in it and thus it can be utilized as a solvent for conducting out different chemical reactions in industries and also in mining.

The various characteristics of the liquid water [57] are:

- i) Boiling point = 373.15 K.
- ii) Viscosity = 1002 Pa s.
- iii) Molecular shape = Bent
- iv) Melting point =273.15 K
- v) Density = $999.8396 \text{ g L}^{-1} \text{ at } 273.15 \text{ K}.$
- vi) Molecular mass = $18015 \text{ kg mol}^{-1}$.
- vii) Vapor pressure =3169 Pa.
- viii) Refractive index = 1.3330 (293.15 K).
- ix) Heat capacity = 0.07538 kJ mol⁻¹K⁻¹.
- x) Gibbs free energy = $-237.240 \text{ kJ mol}^{-1}$.
- xi) Dielectric constant = 80.10 at 293.15 K.
- xii) Surface tension = 72 milli Nm⁻¹at 298.15 K.

Also, water has the highest dielectric constant. When cooled from 4°C to its freezing point; it shows expansion. Due to its miniature bent structure, it possesses a high heat of vaporization and specific heat. This triatomic molecule has a bond angle and O-H bond-length of 104.5° and 0.096 nm, respectively [58]. Amongst three states of water (gas, liquid and solid), liquid state is the most prominent as various biological processes operate in this medium. A hydrogen bond is merely 2-5% as burly as a typical covalent bond [59].

The polar moieties comprising H's linked directly to small electronegative atoms such as nitrogen, oxygen and fluorine manifests the strong intermolecular force depicted as H-bond. The H-bonding is a polar bond between hydrogen atom and the electronegative atom and is a specialized category of dipole-dipole force. H-bonds strength between the two atoms in their vapour state is about 22.7 kJ mol⁻¹.

1.4 Organization of Aqueous Mixtures

Water is designated as the universal liquid and hydrates distinct solutes like ions, biomolecules, charged species etc and displays main role in biomolecular binding

interactions. Ionic compound such as NaCl (table salt) once dissolved in water, furnishes hydrated Na⁺ and Cl⁻ ions. Due to the highly polar nature of NaCl and H₂O, strong interaction occurs amid oppositely charged ions leading to the formation of primary hydration shell (or inner shell) as depicted in Figure 1.9.

The ordered arrangement within the primary hydration shell generates a region in which the nearby water molecules are also somewhat arranged in partially ordered pattern through hydrogen bonding known as cybotactic region or outer hydration shell.

Further, solutes can be categorized as structure-makers or breakers depending upon the ability to reduce or improve the local tetrahedral order of adjacent water molecules [60,61].

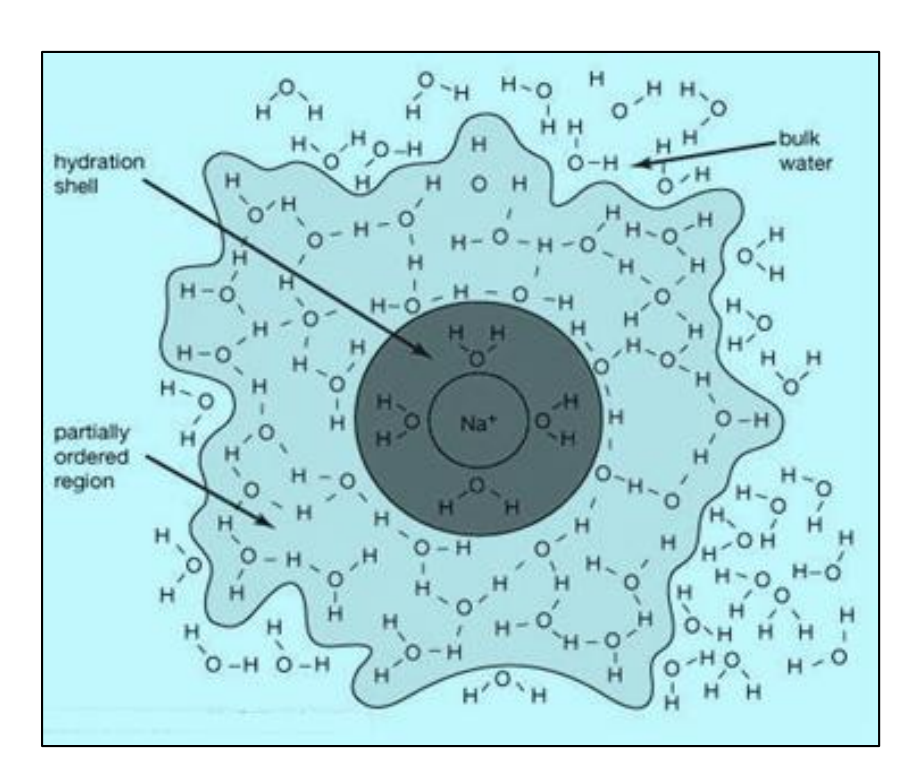


Figure 1.9: Arrangement of water in ionic hydration shells

The structure breaking or structure making nature for solute has been used for the perception on the structure of water by solute [62,63]. Also, studies have shown that structure makers [Figure 1.10 (a)] strongly attract H₂O molecules and develop a larger hydration/solvation sphere, in which H₂O molecules are highly ordered compared to those present in the bulk.

Besides, structure breakers [Figure 1.10 (b)] interact weakly with the neighboring H₂O molecules, thus making them less structured than the bulk water [64]. These characteristics can be experimentally detected by the modifications brought by solutes in kinetic properties of H₂O such as viscosities, conductance, fluidity etc. For example, structure makers decrease the fluidity of water by elevating reorientation time and viscosity of water. However, structure breakers show opposite trend.

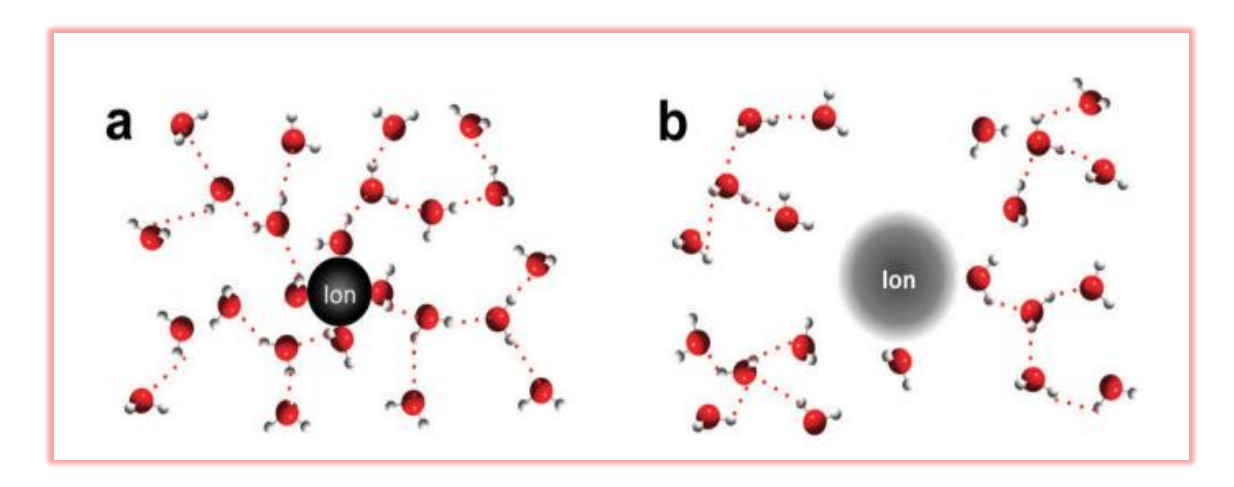


Figure 1.10: (a) Structure maker ion showing effective interaction with water and (b) Structure breaker ion showing weak interaction with water

1.5 Determination of Structure of Water by Various Models

To know about various interactions prevailing in the solvent water, it is vital to apprehend characteristics of water. Water plays noteworthy role in biochemical reactions and this makes it essential to have an extensive perception of the water molecules structure for the interpretation of alterations that happen in the water due to the addition of other substances to it [65]. The characteristics of water have been reported by different models:

1.5.1 Mixture Models

According to certain models, in the liquid water, there is equilibrium between the H-bonded and non H-bonded clusters of water. These mixture models [66-68] reports that with the ascend in temperature, the level of H-bonding among the molecules decreases and creation of clusters of water molecules is also affected by the fluctuation in temperature.

The flickering cluster model of Frank and Wen insinuated that there exists a dynamic equilibrium between the clumps of H-bonded as well as non H-bonded aqua molecules. In other words, the dense water particles (non H-bonded molecules) are swiftly transforming into hydrogen-bonded clumps (bulky water). This inter conversion is initiated by the variation in energy of molecules.

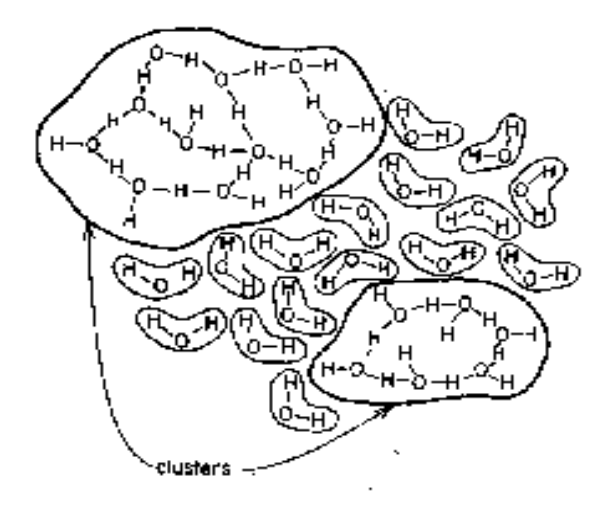


Figure 1.11: Structure of water according to Frank Cluster model

The creation and rupturing of hydrogen bonds in water is a collaborative phenomenon [69]. This model was further modified by Nemethy and Scherage and their model gained immense importance in physical chemistry [70,71]. Those solutes which enhance the half-life of hydrogen-bonded clusters will behave as kosmotropes and those solutes which lead to lessening in H-bonding amid molecules of water will behave as structure breaker in aqueous solutions [72].

The continuum models [73,74] of ion solvation have usually considered that the water molecules around each solute ion forms the hydration spheres and that each water molecule in the hydration sphere has the same physical properties like dielectric constant, refractive index etc.

1.6 Intermolecular Interact1ions

The numerous interactions that happen in an aqueous phase linking solute-solvent, solute-solute in addition to solvent-solvent molecules provide us erudition about the

physicochemical properties of the solution [75,76]. From the thermodynamic treatment, we can examine the solute-solvent interactions by the extrapolation of property (dependent upon concentration) to the limit of zero concentration. The distinct types of hydration phenomenons/interactions that occur in aqueous solutions are addressed as underneath:

(i) Ion-Dipole Interactions

It is a force of attraction between an ion and the partial charge on a polar molecule. These are comparable to ion-ion interactions except that the potential energy pertaining to the ion-dipole forces relies on the charge on the ion, dipole moment of the dipolar moiety as well as the distance amid ion and dipole.

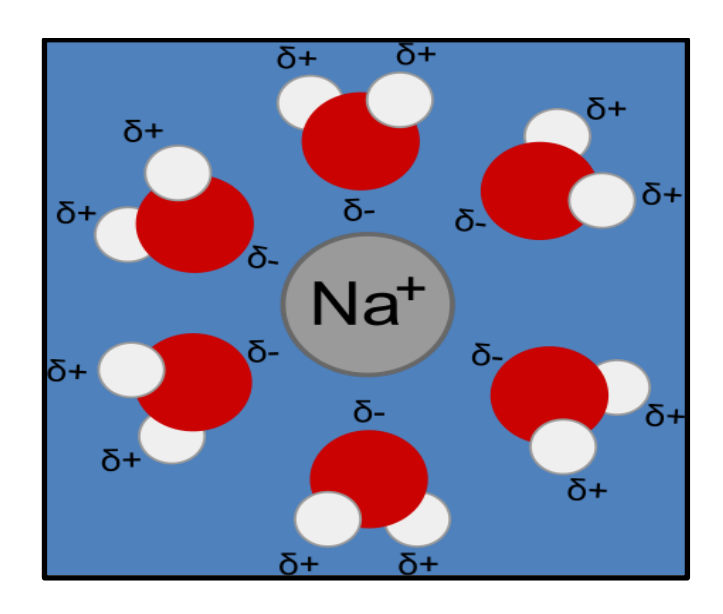


Figure 1.12: Ion-dipole interaction

Figure 1.12 shows ion-dipole interaction between sodium ion (Na⁺) and negative end of polar water molecules. Similarly, ion-dipole interactions persist among the positive end of water molecules and negatively charged chloride ions.

(ii) Dipole-Dipole Interactions

In these, the attraction takes place between oppositely charged moieties of the polar molecules. The better the dipole moment (i.e. higher polarity of the polar molecule), the greater is the strength of these interactions.

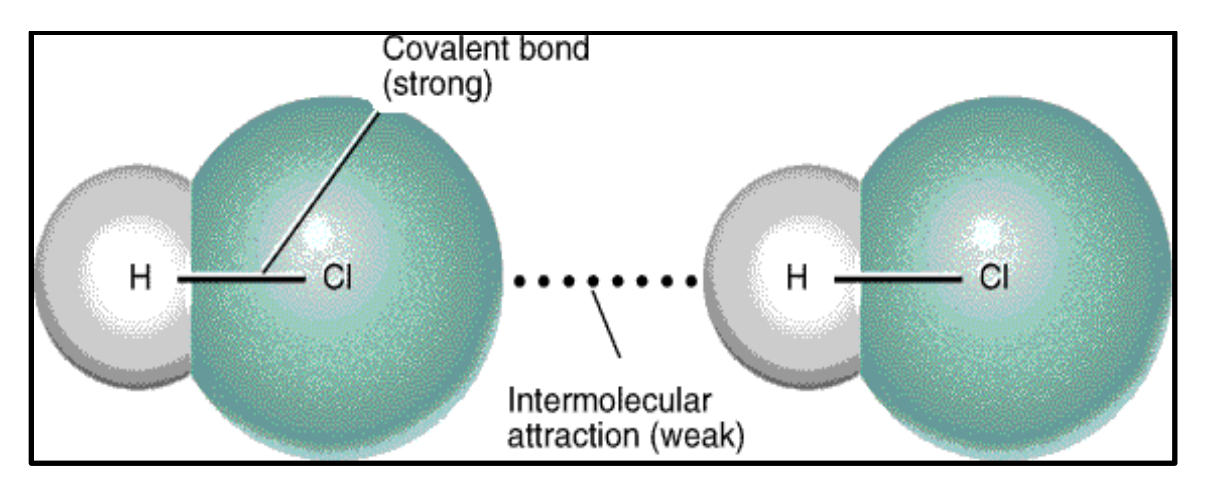


Figure 1.13: Dipole-dipole interactions among the dipolar HCl molecules

Dipole-Induced Dipole Interactions: When the non-polar molecules/hydrophobic species possessing spherical charge distribution come near a polar molecule, charge severance is tempted in the non-polar molecule. This kind of interaction amid polar as well as non-polar substances is known as dipole-induced dipole interaction. Larger is the polarizability of the non-polar substance, better will be the potency of the dipole-induced dipole interactions. Figure 1.14 shows the presence of dipole-induced dipole interactions amid polar ammonia molecules and benzene molecules.

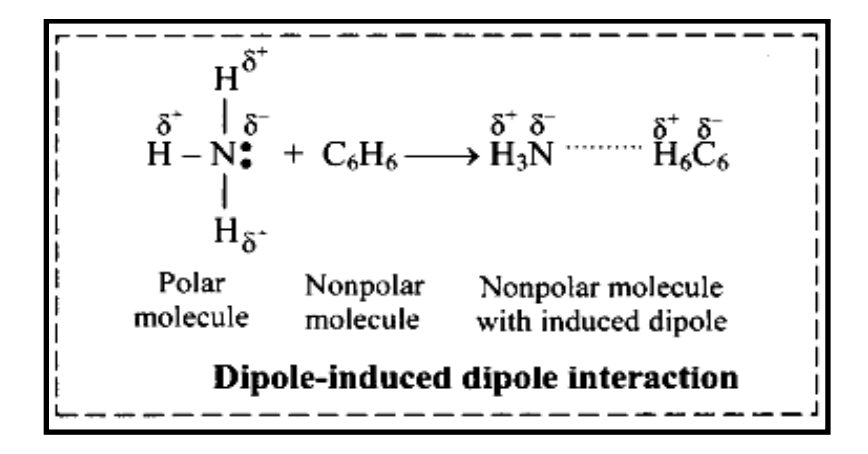


Figure 1.14: Dipole-induced dipole interaction

(iii) Hydrogen Bonding Interactions

Mentioned interactions are detected amongst polar molecules possessing an electronegative atom like fluorine/nitrogen/oxygen and hydrogen atom. Such attractive forces are known as hydrogen bond. Further, the potency of H-bonds is lesser than normal

covalent bonds. However, the strength of these H-bonds is stronger than dispersion forces/London forces. The hydrogen bonding is of two types- intermolecular H-bonding and intramolecular H-bonding. In general, intermolecular H-bonding occurs amid two neighbouring molecules of same or different substance. It results in high melting point/boiling point, greater stability and low vapor pressure of the substance.

Figure 1.15: Hydrogen bonding interaction

It is found to exist between the molecules of water, alcohols, amines, carboxylic acids, etc. On the other hand, intramolecular H-bonding is found to occur within a molecule like in o-nitrophenol, salicylic acid, salicylamide, etc.

(iv) Dispersion Forces/London Forces/Hydrophobic Interactions

In contrast to polar substances which exemplify hydrophilic interactions, the non-polar substances demonstrate London forces of attraction. These interactions are established in those compounds which possesses extensive hydrocarbon chains and doesn't interact with polar substances.

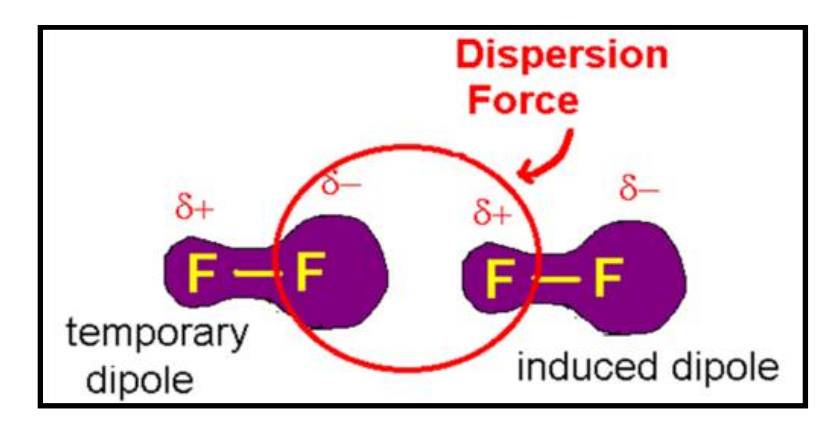


Figure 1.16: Dispersion force

Figure 1.16 demonstrates the presence of London forces between two non-polar F_2 molecules. These forces are due to generation of induced dipoles between two non-polar molecules, thereby generating force of attraction between them.

Thus, by assessing numerous transport and thermodynamic parameters, we can get decent acquaintance of the interactions happening between various components of the solution [77]. Addition of solute into the solvent leads to an alteration in the organization of solvent and also changes in various properties of solvent such as change in viscosity etc [78].

REFERENCES

- 1. Bao, G. (2002). Mechanics of biomolecules. *Journal of the Mechanics and Physics of Solids*, 50, 2237-2274.
- 2. Flitsch, S. L., & Ulijn, R. V. (2003). Sugars tied to the spot. *Nature*, 421, 219-220.
- 3. Yeung, E. S. (2004). Dynamics of single biomolecules in free solution. *Annual Reviews of Physical Chemistry*, *55*, 97-126.
- 4. Kostova, I. (2023). The role of complexes of biogenic metals in living organisms. *Inorganics*, 11, 56.
- 5. Wu, D., Lei, J., Zhang, Z., Huang, F., Buljan, M., & Yu, G. (2023). Polymerization in living organisms. *Chemical Society Reviews*, 52, 2911-2945.
- 6. Richu, Kumar, A. (2020). Apparent molar volume, isentropic compressibilities, viscosity B-coefficients and activation parameters of thiamine hydrochloride in aqueous solutions of saccharides at different temperatures. *The Journal of Chemical Thermodynamics*, 150, 106228.
- 7. Rifna, E. J., Misra, N. N., & Dwivedi, M. (2023). Recent advances in extraction technologies for recovery of bioactive compounds derived from fruit and vegetable waste peels: A review. *Critical Reviews in Food Science and Nutrition*, 63, 719-752.
- 8. Manzoor, M. F., Siddique, R., Hussain, A., Ahmad, N., Rehman, A., Siddeeg, A., ... & Yahya, M. A. (2021). Thermosonication effect on bioactive compounds, enzymes activity, particle size, microbial load, and sensory properties of almond (Prunus dulcis) milk. *Ultrasonics Sonochemistry*, 78, 105705.
- 9. Zuliska, S., Zakiyyah, S. N., Hartati, Y. W., Einaga, Y., & Maksum, I. P. (2025). Electrochemical aptasensor for ultrasensitive detection of glycated hemoglobin (HbA1c) using gold-modified SPCE. *Sensing and Bio-Sensing Research*, 47, 100765.

- 10. Choudhary, D., Mossa, A., Jadhav, M., & Cecconi, C. (2019). Bio-molecular applications of recent developments in optical tweezers. *Biomolecules*, *9*, 23.
- Karra-Chaabouni, M., Trigui, M., Yust, M. M., Awad, M. K., & Moreno, P. J. G. (2018). Biochemistry: Production of high-added value biomolecules for industrial uses. *Journal of Biomedicine and Biotechnology*, 2018, 4012145.
- Santos, D. K. F., Rufino, R. D., Luna, J. M., Santos, V. A., & Sarubbo, L. A. (2016).
 Biosurfactants: multifunctional biomolecules of the 21st century. *International Journal of Molecular Sciences*, 17, 401.
- 13. Richu, Sharmhal, A., Kumar, A., & Kumar, A. (2022). Insights into the applications and prospects of ionic liquids towards the chemistry of biomolecules. *Journal of Molecular Liquids*, *368*, 120580.
- 14. Erfani, A., Seaberg, J., Aichele, C. P., & Ramsey, J. D. (2020). Interactions between biomolecules and zwitterionic moieties: A review. *Biomacromolecules*, 21, 2557-2573.
- 15. Çalýk, M., Ayas, A., & Ebenezer, J. V. (2005). A review of solution chemistry studies: Insights into students' conceptions. *Journal of Science Education and Technology*, 14, 29-50.
- 16. Clarke, C. J., Tu, W. C., Levers, O., Brohl, A., & Hallett, J. P. (2018). Green and sustainable solvents in chemical processes. *Chemical Reviews*, *118*, 747-800.
- 17. Marcus, Y. (2011). Electrostriction in electrolyte solutions. *Chemical Reviews*, 111, 2761-2783.
- Kozlowska, M., Rodziewicz, P., Utesch, T., Mroginski, M. A., & Kaczmarek-Kedziera, A. (2018). Solvation of diclofenac in water from atomistic molecular dynamics simulations—interplay between solute—solute and solute—solvent interactions. *Physical Chemistry Chemical Physics*, 20, 8629-8639.

- 19. Qiu, L., Zhu, N., Feng, Y., Michaelides, E. E., Żyła, G., Jing, D., & Mahian, O. (2020). A review of recent advances in thermophysical properties at the nanoscale: From solid state to colloids. *Physics Reports*, 843, 1-81.
- 20. Saxena, I., Kumar, V., & Gupta, A. (2024). An overview of molecular interaction studies of binary/ternary liquid mixtures with R₄NI salts using ultrasonic velocity, transport, apparent molar volume, and dielectric constant properties. *Journal of Solution Chemistry*, 53, 182-202.
- Kontogeorgis, G. M., Dohrn, R., Economou, I. G., de Hemptinne, J. C., Ten Kate, A., Kuitunen, S., & Vesovic, V. (2021). Industrial requirements for thermodynamic and transport properties: 2020. *Industrial & Engineering Chemistry Research*, 60, 4987-5013.
- 22. Ijardar, S. P., Singh, V., & Gardas, R. L. (2022). Revisiting the physicochemical properties and applications of deep eutectic solvents. *Molecules*, 27, 1368.
- 23. Bandral, A., Richu, & Kumar, A. (2021). Investigations on thermophysical properties of glycine and glycylglycine in aqueous betaine hydrochloride solutions at different temperatures. *Journal of Molecular Liquids*, *348*, 118081.
- 24. Karimi, S., Shekaari, H., & Ahadzadeh, I. (2020). The sweetness response and thermophysical properties of glucose and fructose in the aqueous solution of some deep eutectic solvents at T = (288.15–318.15) K. *Carbohydrate Research*, 495, 108083.
- 25. Singh, M., Singh, J., Sharma, S., Sharma, S., & Sharma, M. (2023). Molecular interaction studies of an antidepressant drug with imidazolium-based ionic liquids in an aqueous system: A volumetric, acoustic, and viscometric approach. *Journal of Chemical & Engineering Data*, 68, 1834-1855.
- 26. Dux, T. (2023). Fundamental use of nucleic acids in biological processes. *Advanced Techniques in Biology & Medicine*, 11(4), 425.
- 27. Orgel, L. (2000). A simpler nucleic acid. Science, 290, 1306-1307.

- 28. Minchin, S., & Lodge, J. (2019). Understanding biochemistry: Structure and function of nucleic acids. *Essays in Biochemistry*, *63*, 433-456.
- 29. Wachowius, F., Attwater, J., & Holliger, P. (2017). Nucleic acids: Function and potential for abiogenesis. *Quarterly Reviews of Biophysics*, 50, 4.
- 30. Samanta, D., Ebrahimi, S. B., & Mirkin, C. A. (2020). Nucleic-acid structures as intracellular probes for live cells. *Advanced Materials*, *32*, 1901743.
- 31. Fraikin, G. Y., Belenikina, N. S., & Rubin, A. B. (2024). Photochemical processes of cell DNA damage by UV radiation of various wavelengths: Biological consequences. *Molecular Biology*, 58, 1-16.
- 32. Guinan, M., Benckendorff, C., Smith, M., & Miller, G. J. (2020). Recent advances in the chemical synthesis and evaluation of anticancer nucleoside analogues. *Molecules*, 25, 2050.
- 33. Fillion, A., Vichier-Guerre, S., & Arimondo, P. B. (2024). Adenine, a key player in biology and medicinal chemistry. *Comptes Rendus Chimie*, 27, 1-18.
- 34. Zhang, Y., Krahnert, I., Bolze, A., Gibon, Y., & Fernie, A. R. (2020). Adenine nucleotide and nicotinamide adenine dinucleotide measurements in plants. *Conducted Protocols in Plant Biology*, *5*, 20115.
- 35. Dashty, M. (2013). A quick look at biochemistry: Carbohydrate metabolism. *Clinical Biochemistry*, 46, 1339-1352.
- 36. Breiling, A., & Lyko, F. (2015). Epigenetic regulatory functions of DNA modifications: 5-Methylcytosine and beyond. *Epigenetics & Chromatin*, 8, 1-9.
- 37. Blanch, M., Mosquera, J. L., Ansoleaga, B., Ferrer, I., & Barrachina, M. (2016). Altered mitochondrial DNA methylation pattern in Alzheimer disease–related pathology and in Parkinson disease. *The American Journal of Pathology*, 186, 385-397.

- 38. Porfireva, A., Subjakova, V., Evtugyn, G., & Hianik, T. (2023). Electrochemical DNA sensors based on nanomaterials for pharmaceutical determination. In *Nanosensors* (pp. 23-68). CRC Press.
- 39. Saltepe, B., Kehribar, E. S., Su Yirmibeşoğlu, S. S., & Şafak Şeker, U. O. (2018). Cellular biosensors with engineered genetic circuits. *ACS Sensors*, *3*, 13-26.
- 40. Brouns, F. (2020). Saccharide characteristics and their potential health effects in perspective. *Frontiers in Nutrition*, *7*, 541167.
- 41. Baur, D. A., & Saunders, M. J. (2021). Carbohydrate supplementation: a critical review of recent innovations. *European Journal of Applied Physiology*, *121*, 23-66.
- 42. Rodriguez, J., O'Neill, S., & Walczak, M. A. (2018). Constrained saccharides: a review of structure, biology, and synthesis. *Natural Product Reports*, *35*, 220-229.
- 43. Leung, S. W. S., & Shi, Y. (2022). The glycolytic process in endothelial cells and its implications. *Acta Pharmacologica Sinica*, *43*, 251-259.
- 44. Tse, T. J., Wiens, D. J., & Reaney, M. J. (2021). Production of bioethanol—A review of factors affecting ethanol yield. *Fermentation*, 7, 268.
- 45. Stincone, A., Prigione, A., Cramer, T., Wamelink, M. M., Campbell, K., Cheung, E., ... & Ralser, M. (2015). The return of metabolism: Biochemistry and physiology of the pentose phosphate pathway. *Biological Reviews*, *90*, 927-963.
- 46. Jagtap, S. S., & Rao, C. V. (2018). Microbial conversion of xylose into useful bioproducts. *Applied Microbiology and Biotechnology*, *102*, 9015-9036.
- 47. Neta, M. D. R. A. V., Azevedo, M. A., Delforno, T. P., & Duarte, I. C. S. (2021). Xylose a carbon source for the production of biosurfactant: Mini review. *Research, Society and Development*, *10*, 17810615573-17810615573.
- 48. Kharat, S. J., & Patil, M. D. (2021). Density study of (D-(+)-mannose + water), (D-(+)-mannose + water + sodium cyclamate), (D-(+)-maltose monohydrate + water)

- and (D-(+)-maltose monohydrate + water + sodium cyclamate) systems at T = 298.15 K. Oriental Journal of Chemistry, 37, 1317.
- Yabaci Karaoglan, S., Jung, R., Gauthier, M., Kinčl, T., & Dostálek, P. (2022).
 Maltose-negative yeast in non-alcoholic and low-alcoholic beer production.
 Fermentation, 8, 273.
- 50. Anguita-Ruiz, A., Vatanparast, H., Walsh, C., Barbara, G., Natoli, S., Eisenhauer, B., ... & Gil, A. (2025). Alternative biological functions of lactose: A narrative review. *Critical Reviews in Food Science and Nutrition*, 27, 1-14.
- 51. Portnoy, M., & Barbano, D. M. (2021). Lactose: Use, measurement, and expression of results. *Journal of Dairy Science*, *104*, 8314-8325.
- 52. Hassan, L. K., Abd-Wahhab, K. G., & El-Aziz, A. (2022). Lactose derivatives: Properties, preparation and their applications in food and pharmaceutical industries. *Egyptian Journal of Chemistry*, 65, 339-356.
- 53. Sarkar, A., & Sinha, B. (2016). Solution properties and taste behavior of lactose monohydrate in aqueous ascorbic acid solutions at different temperatures: Volumetric and rheological approach. *Food Chemistry*, 211, 590-597.
- 54. Queneau, Y., Jarosz, S., Lewandowski, B., & Fitremann, J. (2007). Sucrose chemistry and applications of sucrochemicals. *Advances in Carbohydrate Chemistry and Biochemistry*, 61, 217-292.
- 55. Qi, X., & Tester, R. F. (2020). Lactose, maltose, and sucrose in health and disease. *Molecular Nutrition & Food Research*, 64, 1901082.
- 56. Lynden-Bell, R. M., Morris, S. C., Barrow, J. D., Finney, J. L., & Harper, C. L. (2010). Water and life. *Water Life Unique Prop*, 2, 69.
- 57. Amiri, M., & Bélanger, D. (2021). Physicochemical and electrochemical properties of water-in-salt electrolytes. *ChemSusChem*, *14*, 2487-2500.

- 58. Drewitt, J. W. (2021). Liquid structure under extreme conditions: high-pressure x-ray diffraction studies. *Journal of Physics: Condensed Matter*, *33*, 503004.
- 59. Renati, P., & Madl, P. (2024). What is the "hydrogen bond"? A QFT-QED perspective. *International Journal of Molecular Sciences*, 25, 3846.
- 60. Mancinelli, R., Botti, A., Bruni, F., Ricci, M. A., & Soper, A. K. (2007). Hydration of sodium, potassium, and chloride ions in solution and the concept of structure maker/breaker. *The Journal of Physical Chemistry B*, *111*, 13570-13577.
- 61. Duboué-Dijon, E., & Laage, D. (2015). Characterization of the local structure in liquid water by various order parameters. *The Journal of Physical Chemistry B*, *119*, 8406-8418.
- 62. Marcus, Y. (2009). Effect of ions on the structure of water: structure making and breaking. *Chemical Reviews*, *109*, 1346-1370.
- 63. Singh, V., & Kasaudhan, V. (2024). Volumetric and taste behavior of D-(+)-glucose and D-(-)-fructose in aqueous solutions of ethanolammoium acetate. *Food Chemistry*, 446, 138864.
- 64. Huang, B., Muy, S., Feng, S., Katayama, Y., Lu, Y. C., Chen, G., & Shao-Horn, Y. (2018). Non-covalent interactions in electrochemical reactions and implications in clean energy applications. *Physical Chemistry Chemical Physics*, 20, 15680-15686.
- 65. Mokshin, A. V., & Vlasov, R. V. (2024). Liquid–liquid crossover in water model: Local structure vs kinetics of hydrogen bonds. *The Journal of Physical Chemistry B*, 128, 2337-2346.
- 66. Rahman, A., Stillings, F. H., & Lainberg, H. L. (1975). Molecular dynamics and monte carlo calculations on water. *The Journal of Chemical Physics*, 69, 5223.
- 67. Frank, H. S., & Wen, W. Y. (1957). Ion-solvent interaction. Structural aspects of ion-solvent interaction in aqueous solutions: a suggested picture of water structure. *Discussions of the Faraday Society*, 24, 133-140.

- 68. Benesi, H. A., & Hildebrand, J. H. (1949). A spectrophotometric investigation of the interaction of iodine with aromatic hydrocarbons. *Journal of the American Chemical Society*, 71, 2703-2707.
- 69. Fuhrhop, J. H., & Koning, J. (2007). *Membranes and molecular assemblies: The synkinetic approach*. Royal Society of Chemistry.
- 70. Clementi, E. (1976). Lecture notes in chemistry and References therein, 19.
- 71. Gurney, R. W. (1953). Ionic processes in solution.
- 72. Israelachvili, J. N. (2011). *Intermolecular and surface forces*. Academic press.
- 73. Barnes, P., Finney, J. L., Nicholas, J. D., & Quinn, J. E. (1979). Cooperative effects in simulated water. *Nature*, 282, 459-464.
- 74. Nomoto, O. (1958). Empirical formula for sound velocity in liquid mixtures. Journal of the Physical Society of Japan, 13, 1528-1532.
- 75. Sharma, S., Saini, M., & Pal, A. (2023). Solute–solvent interactions of glycine, L–alanine, and L–valine in aqueous 1–butyl–3–methylimidazolium methylsulfate ionic liquid solutions at different temperatures. *Journal of Ionic Liquids*, *3*, 100064.
- 76. Lomesh, S. K., Bala, M., Kumar, D., & Kumar, I. (2019). Investigation of molecular interactions of the drug diclofenac sodium salt in water and aqueous sorbitol systems at different temperatures (305.15 K–315.15 K). *Journal of Molecular Liquids*, 289, 109479.
- 77. Nain, A. K. (2016). Physicochemical study of solute–solute and solute–solvent interactions of glycine, L-alanine, L-valine and L-isoleucine in aqueous D-mannose solutions at temperatures from 293.15 K to 318.15 K. *The Journal of Chemical Thermodynamics*, 98, 338-352.
- 78. Rajagopal, K., & Johnson, J. (2015). Thermodynamic interactions of L-histidine in aqueous fructose solutions at different temperatures. *International Journal of Scientific and Research Publications*, 5, 66-69.

CHAPTER 2 REVIEW OF LITERATURE

2 Review of Literature

For discovering the behavior of biomolecules in diverse types of solvent systems, a vast array of work has been reported by the canvassers. This scrutiny is an important aspect for indulging the applications of biomolecules in various living processes, in the designing of diverse drugs, medicines etc. Densimetric, rheological and compressibility properties of basic factors of nucleic acids in solutions of aqueous media offer in sequence for the explanation of solute and solute along with solute and solvent interactions which is liable for the structure modification of water and destabilization/stabilization of helices. Hence, a brief evaluation of literature about the representative physicochemical properties of such systems is being provided in this section carried out by various workers. Moreover, to improve coherence and structure, we reorganized the literature review into clearer subgroups based on solute/solvent classes and experimental focus, such as:

(i) Nucleic acid bases and nucleosides

Banipal *et al.* [1] studied the volumetric behavior of various nucleic acid components in aqueous guanidine hydrochloride and found significant temperature-dependent variations in solute-solvent interactions, as evidenced by changes in apparent molar volumes.

Høiland *et al.* [2] determined velocity of sound for the aqueous mixtures of nucleosides: adenosine, uridine as well as cytidine at ambient pressure and *Temp.* = 298.15 K. The compressibility parameters were derived as well as reorganized in stipulations of diverse solute-solvent interactions.

Ahluwalia *et al.* [3] evaluated partial molar heat capacities together with partial molar volume for model components of nucleic acids in the mixtures of calcium chloride as well as sodium chloride. Positive transfer values corresponding to partial molar heat capacity and molar volumes were obtained; and the higher transfer values were observed in case of calcium chloride which clearly revealed the existence of strong interactions with calcium chloride as compared to sodium chloride.

In another paper, Banipal *et al.* [4] evaluated the transport properties of nucleosides as well as nucleobases in guanidine hydrochloride + H₂O solutions. The estimated properties were evaluated in the stipulations of different physicochemical interactions and then construed in provisos of the structure breaking/making abilities of studied solute systems.

Khan *et al.* [5] investigated the thermophysical behavior of montelukast sodium and its interaction with DNA using surface tension, density, and viscosity measurements. The study revealed that temperature, concentration, and co-solvents (ethanol and sodium chloride) significantly influenced the drug's properties. Spectroscopic analysis confirmed hydrogen bonding between montelukast sodium and DNA.

Rajput *et al.* [6] evaluated the thermophysical parameters pertaining to some of nitrogenous base pairs like uracil (U) and thymine (T) in L-histidine + water mixtures at discrete temperatures ranging between 293.15 and 313.15 K. Thus inferred outcomes were elaborated in terms of interactions present within.

Moreover, Rajput *et al.* [7] investigated physicochemical studies of adenine, thymine/uracil in H₂O as well as in binary H₂O + inositol media at varied temperatures (293.15, 298.15, 303.15, 308.15, 313.15, 318.15) K. Various volumetric, viscometric and compressibility parameters were estimated. By the cosphere overlap model, varied synergies established in the ternary mixtures were analyzed and the kosmotropic/chaotropic capability of solutes was interpreted.

Banipal *et al.* [8] measured the density, enthalpy of dilution, viscosity as well as sound speed for uridine, uracil, thymidine, and thymine in H₂O and in H₂O + ciprofloxacin hydrochloride at different temperatures. Furthermore, the gathered information has also been frenzied to assess standard molar enthalpies, partial molar isentropic compressions, *B*-coefficients, of dilution, partial molar volumes etc. Moreover, the UV–visible studies expressed the existence of well-built interactions linking pyrimidine molecules along with drug.

Maksudov *et al.* [9] performed the rheological measurements, circular dichroism, and molecular dynamics simulations of phosphorodiamidate morpholino oligonucleotides

(PMOs). The obtained results emphasize the significance of the conformational band outlook of PMO solution constitution, thermodynamic constancy of their non-canonical composition, and concentration reliant viscous properties.

(ii) Carbohydrates and saccharides

Kumar *et al.* [10] explored the interactions of monosaccharides like D-glucose and D-fructose interact in aqueous DAP (diammonium hydrogen phosphate) mixtures, observing temperature-dependent solute-solvent dynamics. Their findings suggest that sugar structure significantly influences hydration behavior, aligning with previous studies on saccharide-based ternary systems.

Sharma *et al.* [11] studied D-maltose and D-lactose in trisodium citrate solutions across various temperatures, using density and sound speed data to evaluate volumetric and compressibility parameters. Their findings, interpreted through the co-sphere overlap model, highlighted significant intermolecular interactions and structural effects in the systems.

Karimi *et al.* [12] evaluated the thermophysical properties pertaining to glucose as well as its structural isomer fructose in aqueous and mixed aqueous deep eutectic solvent media. They deliberated density, refractive index, sound speed as well as viscosity data at 288.15 – 318.15 K. The consequences of the study specified that the glucose in aqueous mixtures of ChCl and urea has effective synergies which come better with escalation in temperature along with the concentration of DES.

Nain *et al.* [13] precised the densities, speeds of ultrasonic waves and viscosities corresponding to the aqueous mixture for sodium salicylate and its mixtures in the aqueous D-glucose/D-sucrose solutions. Also, free energy of activation of viscous motion parameters were determined to find different solute-solvent interaction studies. The investigational data was employed to determine apparent/limiting molar volumes, apparent/limiting molar compressibilities, transfer volumes, transfer compressibilities, *B* coefficients and thermodynamic parameters. The co-sphere model has been escorted to construe the different types of solute/solute in addition to the solute/solvent connections prevailing among mixtures.

Zafarani-Moattar *et al.* [14] studied the assorted thermophysical properties along with taste deeds of sucrose in water + 1-octyl-3-methyl imidazolium chloride or1-octyl-3-methyl imidazolium bromide solution mixtures at T = (288.15 to 318.15) K. Deduced data of positive $\Delta_{tr}V^0_{\phi}/\Delta_{tr}K^0_{\phi}$ were investigated that revealed the predominance of ion–dipole interactions in these systems.

Ali and coworkers [15] examined impact of glycine on molecular interactions of glucose, sucrose, and raffinose through different viscometric as well as volumetric properties. Further, refractive indices were determined for the sugars in solutions of glycine (aqueous). The resulting data was operated to demonstrate the solute-solvent interactions prevailing in considered systems.

Aggarwal *et al.* [16] studied the effect of phosphate salts on the isentropic compressibility of various saccharides and their derivatives. Their analysis revealed strong solute–cosolute interactions, with transfer parameters and hydration numbers confirming the dominance of hydrophilic and ionic interactions over hydrophobic ones.

Ankita *et al.* [17] obtained the viscosities, ultrasonic speeds and densities of isoniazid drug in H_2O and aqueous saccharides like D-glucose/D-sucrose over distinct temperatures. The premeditated parameters were conferred in provisions of diverse solute-solvent synergies widespread in the mixtures. In addition, the structure breaking/making affinity of isoniazid drug was analyzed via sign using Hepler's constant along with the dB/dT data. Besides, Gibbs free energy, enthalpy as well as entropy of activation values, were inferred and analyzed via the Eyring's theory.

Rani *et al.* [18] examined thiamine HCl in aqueous lactose and glucose solutions at various temperatures using viscosity, density, and sound speed data. Their analysis revealed that hydrophilic and ion—ion interactions predominated over hydrophobic interactions.

Zhuo *et al.* [19] computed the volumetric and rheological properties like apparent molar volumes together with their allied transfer volumes for some imperative aqueous monosaccharides + amino acid solution systems at 298.15 K and in addition established that the positive transfer values of monosaccharides increases with increasing amino acid

concentration. The results clearly revealed the subsistence of influential interactions flanked by saccharides and amino acids in aqueous media.

Banipal *et al.* [20] have determined the solvation characteristics of sugar alcohols, disaccharides, monosaccharides and their deoxy, methoxy derivatives in different compositions of pyridoxine hydrochloride and vitamin B1. They evaluated the massive volumes, transport parameters etc. in a series of temperature range commencing from 288.15 to 318.15 K.

Chandrasekaran *et al.* [21] investigated the solvation behavior, thermochemical and viscometric parameters of sweeteners such as fructose and sorbitol in water and non-aqueous medium through experimentally obtained physical parameters, volumetric, ultrasonic and viscometric measurements. The results of their study confirmed that the intact assortment of selected solutes emerge as structure breakers in the chosen solvent media.

Malik *et al.* [22] have examined various physicochemical parameters like for sucrose, maltose and D-glucose, in aqueous mixtures of L-lysine/L-arginine over a series of temperatures. They concluded the doable molecular links for instance solute/solute in addition to solute/solvent; ultimately conferred about behavior of saccharides in specified systems.

Sirbu *et al.* reported the performance of *N*-methylglycine in glucose + water solutions at various temperatures by computing various acoustic and thermodynamic parameters like partial molar compressibility, partial molar volume and transfer volumes etc. At last, for the ternary mixtures, the molar refractivity was inferred via Lorentz-Lorenz expression [23].

Zhuo *et al.* [24] analyzed the viscosities plus densities of aqueous arginine + glucose, L-ascorbic acid, sucrose media at Temp. (K) = 298.15. Further, the deduced transfer volumes from aqua to assorted aqueous liquids is being measured and inspected in provisos of the organizational solvation model.

Chen *et al.* [25] estimated the density and viscosity data for aqueous nicotinic acid and carbohydrates media such as aq. xylose and L-arabinose at distinct temperature values. The experimental data was employed towards calculation of different physicochemical parameters. Consequences revealed that the nicotinic acid behaves as kosmotropic in water + carbohydrates solutions.

Sharma *et al.* [26] probed interactions established amid lactose monohydrate and tributylmethylammonium chloride via amalgamation of volumetric, acoustic and viscometric approaches. The results inferred via viscometric and thermodynamic properties have been interpreted and discussed. Further, it was concluded that lactose monohydrate reveals structure making capability in aqueous tributylmethylammonium chloride solutions.

Zafarani-Moattar *et al.* [27] scrutinized the interactions customary amid fruit sugar + [Bmim][Br]/[Omim][Br]/[Omim][Cl] + H₂O mixtures at assorted temperatures. Commencing the premeditated viscometric, acoustic, along with volumetric properties, they accomplished the preponderance of ion–hydrophilic type interactions in deliberated mixtures.

Singh *et al.* [28] computed the volumetric and taste behavior of sugars like glucose and fructose in aqueous ethanolammonium acetate solution systems. The results clearly revealed the predominance of hydrophilic interactions between saccharides and ethanolammonium acetate. Also, monosaccharides are sweet in aqueous ethanolammonium acetate media.

Alalaw *et al.* [29] investigated the solubility of uracil and guanine in aqueous sugar (xylose, glucose, sucrose) solutions.

2.1 Volumetric, Acoustic, Rheological and Thermodynamic Studies of Solution Samples

To understand molecular as well as ionic interactions in the solutions, it is important to consider thermodynamic/compressibility quantities like the apparent molar isentropic compressions, their limiting apparent molar values, apparent molar volumes, and viscometric coefficients [30].

The values at immeasurable dilution offer insight into concentration dependency and solute/solvent relations, reflecting both solute/solute along with solute/solvent interactions. Below is a summary of theoretical foundation for the various physicochemical properties computed in this research work.

2.1.1 Volumetric Studies

The investigation of the volumetric characteristics of solutions is a vital tool for providing gainful information about interactions amongst the solutes/solvents. The following parameters were established using experimentally determined density values:

2.1.1.1 Apparent Molar Volume, (V_{ϕ})

Contribution that a constituent in the solution makes to the mixture's non-ideality is known as its apparent molar volume, or V_{ϕ} . Assuming that the properties of every other mixture component stay constant upon addition; it represents the molar property of a component in solution. Succeeding equation can be applied in acquiring apparent molar volume of various solutions from their given density values [31,32]:

$$V_{\phi} = (M/\rho) - [(\rho - \rho_0)1000/m\rho\rho_0] \tag{2.1}$$

Here, M has been defined as molecular mass of solute molecules, ρ represents density (expressed in kg m⁻³) for produced solutions while ρ_0 is the density for solvent system and m is the molal concentrations (expressed in mol kg⁻¹) for a solute in a solution. For densities demonstrated in g cm⁻³, the factor 1000 is applied.

2.1.1.2 Limiting Apparent Molar Volumes, (V_{ϕ}^0)

The partial molar volumes or in other words limiting apparent molar volumes (V^0_ϕ) for a solute is the apparent molar (volume) at immeasurable dilution. It offers gainful knowledge towards solute or solvent interactions present in solution systems since the adhesive forces between solute constituents are nearly insignificant at an indefinite dilution.

Furthermore, V_{ϕ}^{0} and V_{ϕ} values at infinite dilution become comparable. By using Masson's expression [33] to evaluate the linear regression of apparent molar volumes, the

 V^{0}_{ϕ} values are obtained. This provides the correlation between V_{ϕ} and molality, m, as discussed below.

$$V_{\phi} = V^{0}_{\phi} + S_{\nu} m \tag{2.2}$$

In this expression, intercept, V^0_{ϕ} denotes the subsistence of solute or solvent interactions whilst S_{ν} slope demonstrates the type of interactions amongst solute moieties. The V^0_{ϕ} trend towards increase or decrease can be explained using an easy model [34].

$$V^{0}_{\phi} = V_{\phi (int.)} + V_{\phi (solv.)} \tag{2.3}$$

Here, the terms $V_{\phi (int.)}$ and $V_{\phi (solv.)}$ refer to solute molecules' intrinsic volume and solvent's solvation volume, correspondingly. Intrinsic volume is the same at all the molal concentrations. Since the solvation volumes are negatively influenced by the weaker contacts amid solute and cosolute molecules in a mixture, thus values of V_{ϕ}^{0} are lowered as a result.

2.1.1.3 Limiting Apparent Molar Volumes of Transfer, $(\Delta_{tr}V^0_{\phi})$

 $\Delta_{tr}V^0_{\phi}$ parameter bestow valuable insight into interactions among solute as well as cosolute molecules in solutions being studied [35,36]. The transfer parameter is calculated by applying the following equation and is defined as a variance between partial molar volumes in the solution and pure water.

$$\Delta_{tr}V^{0}_{\phi} = V^{0}_{\phi \text{ (in mixed aqueous solutions)}} - V^{0}_{\phi \text{ (in water)}}$$
(2.4)

where, $V^0_{\phi \, (in \, mixed \, aqueous \, solutions)}$ denotes apparent molar volumes at infinite dilution for solute in solvent system while $V^0_{\phi \, (in \, water)}$ characterizes apparent molar volumes of a solute in water at infinite dilution.

A typical partial molar volume for non-electrolytic system is determined by intrinsic volume for particles of solute, while volume alterations on account of interactions amongst the solute and solvent, according to Franks *et al.* [37], but Tarasawa *et al.* [38] found that intrinsic volume is made up of two factors as well:

$$V_{(int.)} = V_{vw} + V_{void} \tag{2.5}$$

where, V_{void} represents the volume due to spaces contained in solute and V_{vw} refers to solute's van der Waals volume [39,40]. Shahidi and Farrell [41] adjusted Equation (2.5) to determine partial molar volumes for solute as these particles also contribute towards standard partial volumes. It can be illustrated as:

$$V^{0}_{\phi} = V_{vw} + V_{void} - V_{shrinkage} \tag{2.6}$$

Here, $V_{shrinkage}$ signifies volume shrinkage created through interactions of solute's H-bonding sites with H₂O moieties. Both in ternary as well as binary solutions, V_{void} and V_{vw} values are almost identical. Thus, the description of $\Delta_{tr}V^0_{\phi}$ or its involvement can be based on changes in the volume of solute molecule shrinkage when solvent molecules are present in aqueous solutions.

2.1.1.4 Co-spheres Overlap Model

In addition to ion concentrations, the solute's surroundings or the structure of the ions affects how hydration co-spheres overlap and release water molecules. Figure 2.1 shows overlap of ion-hydration cospheres. When two solute particles are close on each other, their spheres of influence overlap, leading to changes in their thermodynamic properties. This happens when there is a shift in the materials surrounding the solutes. According to the co-sphere model, the reason for the decrease in volume when two hydrophobic hydration cospheres meet is the liberation of a small number of H₂O molecules from hydration spheres into the surrounding solution. This results into a reduction in volume of water moieties surrounding polar species due to electrostriction and decline in the network of H-bonding, causing these aqua moieties to transfer to the bulk solution. As a result, interactions between hydrophobic and hydrophobic ions lead to negative values, while interactions between hydrophilic and charged ions result in positive values [42-44].

The observed volume changes are a direct result of the interactions amongst solute/solvent, since there are no interactions amidst solute particles in an infinitely diluted solution. Dehydration is caused by highly hydrated ions, which interact more strongly with polar groups compared to weakly hydrated ions in terms of solute/co-solute interactions.

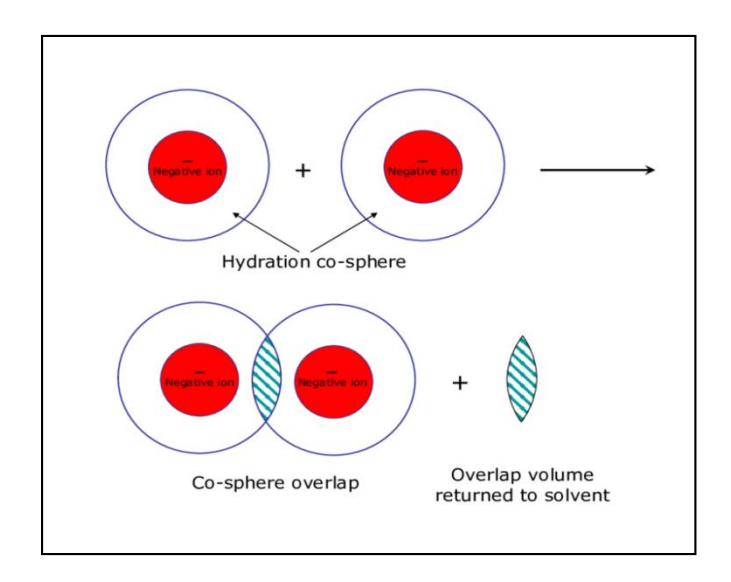


Figure 2.1: Ion hydration co-spheres overlap adapted

2.1.1.5 Limiting Apparent Molar Expansibilities, (E^0_{ϕ})

For investigating the relationship of temperature to V^0_{ϕ} , the following standard polynomial equation has been utilized:

$$V^{0}_{\phi} = a + b (T - T_{r}) + c (T - T_{r})^{2}$$
(2.7)

Shown temperature T in the equation above is in the units of Kelvin (K), T_r is midpoint of taken temperature range, and T_r (K) = 303.15. Empirical constants a, b, c represent the results of least square-fitting mode [45].

Further, the limiting or partial molar expansibility values [46] might be computed using the equation shown below since they aid in measuring the interactions that exist in solutions:

$$E^{0}_{\phi} = (\partial V^{0}_{\phi}/\partial T)_{P} = b + 2c (T-T_{r})$$

$$\tag{2.8}$$

Partial molar expansibility is a fusion of two terms [47] as shown below:

$$E^{0}_{\phi} = E^{0}_{\phi (elect.)} + E^{0}_{\phi (str.)} \tag{2.9}$$

In the above Eqn., $E^0_{\phi \ (elect.)}$ and $E^0_{\phi \ (str.)}$ represent the expansibility due to electrostriction and structural changes, respectively. Moreover, $E^0_{\phi \ (elect.)}$ is dominant at high temperatures, while $E^0_{\phi \ (str.)}$ is dominant at low temperatures [48].

2.1.1.6 Temperature Derivative of Limiting Apparent Molar Expansibilities, $(\partial E^0_{\phi}/\partial T)_P$

Hepler introduced a term that provides qualitative in sequence about the solute's capacity to create or ruin structures when it dissolves in binary/ternary solvent systems [49]. By using the general equation, one can create the Hepler relation, which represents the second derivative of partial molar volumes concerning temperatures.

$$(\partial E^0 / \partial T)_P = (\partial^2 V^0 / \partial T^2)_P = 2c \tag{2.10}$$

Hepler [50,51] stated that sign of $(\partial E^0_{\phi}/\partial T)_P$ indicates whether the systems under study are capable of making or breaking structures.

2.1.1.7 Apparent Specific Volume, (ASV)

The hydrological packaging of solute particles in the media (aqueous) can be demonstrated by the critical parameter called as *ASV* (apparent specific volume). It is interrelated with the standard volumes of solute particles in a medium. *ASV* has been a useful measure to determine the taste or smell of a solutes at different compositions and in different solvent media. This parameter has been calculated using the equation that is provided as [52]:

$$ASV = V_{\phi}/M \tag{2.11}$$

 V_{ϕ} in the above expression is apparent molar volumes of solute particles whilst M is solute's molecular mass. ASV values for varied flavour ranges have been mentioned as follows, according to the literature [53]:

<0.00033 m³/kg/mol: taste is salty,

 $(0.00033 \text{ to } 0.00053) \text{ m}^3/\text{kg/mol}$: taste is sour,

 $(0.00053 \text{ to } 0.00071) \text{ m}^3/\text{kg/mol}$: taste is sweet,

 $(0.00071 \text{ to } 0.00093) \text{ m}^3/\text{kg/mol}$: taste is bitter.

2.1.2 Acoustic Studies

When studying nucleic acid bases in different liquid solutions and adding various substances, using ultrasonic investigations provides valuable insights into the interactions

among molecules as well as the formation of complexes and related structural changes. Although this is a complex topic, it is of great importance due to the practical applications of mixed solvent systems for predicting intermolecular interactions. Density and sound speed are key factors for predicting these interactions. Ultrasonic techniques are highly beneficial and versatile as they can effectively analyze residual stress, hardness, microstructure, and other properties.

Parameters acquired from speed of sound, such as compressibility, are sensitive indicators that can quickly provide information about molecular interactions when partial molar volume is unable to yield conclusive results [54,55]. The following is a brief overview of the several parameters that were identified using sound speed data:

2.1.2.1 Apparent Molar Isentropic Compressions, $(K_{\phi,s})$

 $K_{\phi,s}$ or isentropic compressions of one mol solute can be obtained by utilising experimentally obtained density and sound speed data in the below-mentioned equation:

$$K_{\phi,s} = Mk_s/\rho + (k_s\rho_0 - k^0_s\rho)/m\rho_0\rho$$
 (2.12)

Herein, m signifies the molal concentration of solute in a solution system (mol/kg), M characterizes the molar weight for a solute (kg mol⁻¹), k^0_s , k_s , symbolizes the compressibilities (isentropic) of ultrapure solvent together with solution system, correspondingly while ρ_0 characterizes the density of pure solvent and ρ indicates the density of prepared solution.

The k_s values i.e. the isentropic compressibilities of the solutions can be determined by utilising the equation called Newton-Laplace equation [56] as:

$$k_s = 1/(u^2 \rho) \tag{2.13}$$

$$k^0_s = 1/(u_0^2 \rho_0) \tag{2.14}$$

2.1.2.2 Limiting Apparent Molar Isentropic Compression, $(K^0_{\phi,s})$

The interactions amongst solute as well as the solvent moieties in attendance inside solutions are indicated by limiting apparent or partial molar isentropic compression, that is being determined through the equation that follows:

$$K_{\phi,s} = K^0_{\phi,s} + S_k m \tag{2.15}$$

In the above relation, the values of both $K^0_{\phi,s}$ and S_k are being attained from intercept and the slope in the plots containing $K_{\phi,s}$ vs m in the course of linear regression. Here, $K^0_{\phi,s}$ is devoid of solute interactions with other solute and, thus offers in sequence of solute together with solvent communications while S_k i.e. slope (experimental), denotes solute/solute interactions.

2.1.2.3 Limiting Apparent Molar Isentropic Compression of Transfer, $(\Delta_{tr}K^0_{\phi,s})$

The parameter $\Delta_{tr}K^0_{\phi,s}$ is defined as difference between $K^0_{\phi,s}$ in the solution and that in the pure water, is another characteristic utilize to acquire solute /solvent interactions existing among prepared sample mixtures. It can be symbolized by the following expression:

$$\Delta_{tr} K^{0}_{\phi,s} = K^{0}_{\phi,s} \text{ (in mixed aqueous solution)} - K^{0}_{\phi,s} \text{ (in pure water)}$$
(2.16)

Here, $K^0_{\phi,s~(in~pure~water)}$ corresponds to limiting or partial apparent molar isentropic compressions for a solute within pure water while $K^0_{\phi,s~(in~mixed~aqueous~solutions)}$ stand for the apparent molar isentropic compressions at indefinite dilution for a solute in mixed aqueous solutions.

2.1.2.4 Hydration Number, (n_H)

 n_H , (hydration number) shows how many water molecules are typically present around the solute particles in an aqueous medium at a given concentration. Millero *et al.* [57] approach, Eqn. (2.17) has been applied in the conducted investigation to determine the hydration number of solutes.

$$n_{H} = -K^{0}_{\phi,s \,(elect,)}/(V^{0}_{\phi,b} * K^{0}_{\phi,s,b})$$
(2.17)

The analytical value of $V^0_{\phi,b}*K^0_{\phi,s,b}$ in the preceding equation is 8.1×10^{-15} (m⁵/N/mol). Here, $K^0_{\phi,s,b}$ symbolize isothermal compressibilities in the bulk water, and calculated $K^0_{\phi,s}$ values have been used to calculate $K^0_{\phi,s}$ (elect.) using the relation given below:

$$K^{0}_{\phi,s \,(elect.)} = K^{0}_{\phi,s \,(int.)}$$
 (2.18)

In the above Eqn., $K^0_{\phi,s}$ (elect.) denotes solute's electrostriction apparent molar isentropic compression at unlimited dilution where as $K^0_{\phi,s}$ (int.) denotes its intrinsic $K^0_{\phi,s}$. Since, the

expected values for $K^0_{\phi,s}$ (int.) of organic solutes are assumed to be zero [58]. Thus, the aforementioned relation (2.18) becomes:

$$K^{0}_{\phi,s \,(elect.)} = K^{0}_{\phi,s}$$
 (2.19)

Therefore, Equation (2.17) gets modified like:

$$n_H = -K^0_{\phi,s}/8.1 \times 10^{-15} \,(\text{m}^5/\text{N/mol})$$
 (2.20)

2.1.3 Viscometric Studies

Studying the viscous behavior of molecules in a solution is crucial for understanding transport processes. Research suggests that the viscometric property is a delicate measure to identify diverse type of molecular interactions prevalent in solutions [59]. Viscosity, which is observed in the liquid and gaseous states of matter, reveals the underlying microscopic interactions among the material's molecules.

2.1.3.1 Jones-Dole Equation

The relationship between the electrolytic solution's viscosity and solute concentration has shed light on important interactions taking place in the solution and its structure. According to the theory of inter-electronic interaction, when a salt's concentration approaches zero,

$$\eta/\eta_0 - 1 = AC^{1/2} \tag{2.21}$$

In this case, the solvent's viscosity is denoted by η_0 and the solution's viscosity by η . Values for the dielectric constant, valency, solvent viscosity, and limiting conductance of ions can be used to analyse the constant A.

In addition, the Jones-Dole eqn. is applied by the side of greater concentrations. The relationship between a solution's viscosity at a given temperature and pressure and its solute content is illustrated empirically by the Jones-Dole equation [60]. Nucleic acid base aqueous solutions can also be utilised with Jones-Dole equation as:

$$\eta_r = 1 + BC + AC^{1/2} \tag{2.22}$$

Herein, C be the solute concentration on molarity basis (derived from the molality), η and η_0 corresponds to viscosities for solution as well as pure solvent, and $\eta_r = \eta/\eta_0$ stands for relative viscosity for solution. Solute-solute molecule interaction is represented by the Falkenhagen coefficient, A, and the structural alterations caused by solute-solvent interactions are determined by Jones-Dole viscosity B-coefficient [61–63].

By employing a plot between η_r and C utilizing least square fitting analysis, one may obtain the values of coefficients A as well as B. Here, the slope yields the values for the Jones-Dole coefficient (B), while the intercept yields the values of A.

The readjustment of Equation (2.22) yields the following relation:

$$\eta_r = \eta/\eta_0 = 1 + BC \tag{2.23}$$

2.1.3.2 Temperature Reliance of Procured B-coefficient, (dB/dT)

Besides magnitude or sign of Jones Dole coefficient (B), sign of temperature derivative for B-coefficient can provide more reliable information about the capability of solute to create or break structures. Hence, the solute's properties as chaotropic (structure breaking) and kosmotropic (structure making) are shown by positive or negative signs of (dB/dT), correspondingly [64].

2.1.3.3 Viscosity B-coefficient of Transfer, $(\Delta_{tr}B)$

To analyse solute-solvent interaction present in solutions one may determine the transfer values of viscosity B-coefficient, represented as $\Delta_{tr}B$. It is computed using the following equation and is defined as the disparity between B-coefficient for a solute in pure water as well as that in a mixture:

$$\Delta_{tr}B = B \text{ (in mixed aq. solutions)} - B \text{ (in pure water)}$$
(2.24)

2.1.4 Thermodynamic Studies

Chemical potential or the free energy of activation, for a solute inside media (water) in addition to in mixed aq. solution can be computed using transition state theory [65].

Therefore, the following expression can be utilised to get the values for chemical potential $(\Delta \mu^0_I)$ per mole for the solvent:

$$\Delta \mu^0_I = RT \ln(\eta_0 \overline{V}^0_I / h N_A) \tag{2.25}$$

Here, \overline{V}_{I}^{0} is defined as average molar volumes and may be evaluated via succeeding expression:

$$\overline{V}_I^0 = \sum X_i M_i / \rho_0 \tag{2.26}$$

Where, T is the temperature, N_A and h define the Avogadro's number and Planck's constant, correspondingly while R is Molar gas constant. In addition, ρ_0 , X_i and M_i stand for density of the pure solvent, mole fraction as well as molar mass for i^{th} component in the sample mixture.

Additionally, Feakins *et al.* [66] hypothesized the following relationship amid the viscosity *B*-coefficient as well as the Gibbs free energy:

$$\Delta \mu^{0}_{2} = \Delta \mu^{0}_{1} + (RT/\bar{V}^{0}_{1}). \left[1000B - (\bar{V}^{0}_{1} - \bar{V}^{0}_{2})\right] \tag{2.27}$$

Here, $\overline{V}^0{}_2$ represents solute's partial molar volume. Additionally, implication of the equations below has been utilized to deduce the enthalpy $(\Delta H^0{}_2)$ and entropy $(\Delta S^0{}_2)$ of activation for each of the selected mixtures.

$$\Delta S^{0}_{2} = -\left(\mathrm{d}\Delta\mu^{0}_{2}/\mathrm{d}T\right) \tag{2.28}$$

$$\Delta H^0{}_2 = \Delta \mu^0{}_2 + T\Delta S^0{}_2 \tag{2.29}$$

2.2 Research Gap

The research work mentioned above is wholly justified as the interactions between bioactive solutes in aqueous and non-aqueous medium are of ample importance. Thermodynamic and physiochemical parameters of bioactive solutes like carbohydrates, amino acids, vitamins in addition to nucleic acids in aq. and mixed aqueous solution systems has utilization in food and biopharmaceutical industries for the preparation of medicines, for enhancing the permeation, solubility and absorption of drugs, in production of food and nutritional supplements, electrochemical sensors, cosmetics and various skin

care products etc. Besides, vitamin-based solutes have been affirmed to have antifungal, antibacterial, and antioxidant properties and so are employed as vital nutrients in the pharmaceutical industries and for sustainable control of collected and stored crop products. An apprehension into the forces employing in the liquid mixtures can be gained through the investigation of molecular interactions via the acquired physicochemical properties. In this research, our approach will be to investigate the physicochemical properties via volumetric, acoustic and viscometric methods. Taste behaviour study can be done for saccharides as they are sweet in taste whereas solvation number and activation parameters can be determined for all the systems.

2.3 Objectives

The chief endeavor of conducted work is to learn the plausible molecular synergies in diverse binary and ternary systems at erratic temperatures and compositions consequently that the accurate comprehension about the behavior of the molecules in amalgamation can be established. Outcome of one experimental practice frequently rebuff the consequences obtained from some additional practices; therefore, endeavor has been made through implication of further techniques to craft the nature of interaction, as a result that specific correlation flanked by microscopic constitution and macroscopic properties can be completed. The main objectives of the present research work are presented below:

- (i) To determine experimentally different physical properties like density, sound speed and viscosity for nucleic acid bases in aqueous solutions of saccharides at different temperatures and concentrations.
- (ii) To assess different volumetric and compressibility characteristics from the experimentally measured density and sound speed data.
- (iii) To estimate the viscosity coefficients by using the Jones-Dole equation.
- (iv) To study the activation parameters of viscous flow and solvation characteristics of the systems under consideration at different temperatures.
- (v) To interpret various sorts of intermolecular interactions operating in the studied systems.

2.4 Research Methodology

The sample solutions will be prepared on molality basis by measuring the required quantity of chemicals on an electrical balance (Mettler Toledo, ML 204), having an uncertainty of ± 0.1 mg. Subsequently, prepared stock solutions will be stored in airtight flasks in order to prevent moisture absorption. Further, the physical properties like density, speed of sound and viscosity of each prepared sample solution will be acquired from a vibrating tube digital densimeter (Density and sound velocity analyzer, DSA 5000M), along with Lovis 2000 M/ME microviscometer allied to densimeter. Prior to usage of the instrument, a density test on water/air adjustment will be done at 293 K by using triply distilled water pursued by dry air at ambient pressure.

The experimentally obtained data of physical characteristics (density, sound speed and viscosity) will be employed to calculate the various densimetric, acoustic and rheological parameters like apparent molar volume (V_{ϕ}) , partial molar volume (V^{0}_{ϕ}) , limiting apparent molar expansibility (E^{0}_{ϕ}) , apparent molar isentropic compression $(K_{\phi,s})$, partial molar isentropic compression $(K^{0}_{\phi,s})$, viscosity *B*-coefficients, transfer properties, hydration number (n_{H}) , etc. In addition, the Hepler's thermodynamic relation will be utilized to determine the chaotropic/kosmotropic nature of nucleic acid bases in aqua and aqueous saccharides solutions. Further, viscosity data will be used to calculate Falkenhagen coefficient alongside viscosity *B*-coefficient by applying equation allocated by Jones and Dole. Lastly, the co-sphere overlap model will be applied to assess the various intermolecular interactions occurring in the examined systems.

REFERENCES

- 1. Banipal, T. S., Kaur, N., & Banipal, P. K. (2015). Volumetric studies on nucleic acid bases and nucleosides in aqueous guanidine hydrochloride solutions at *T* = (288.15 to 318.15) K and at atmospheric pressure. *The Journal of Chemical Thermodynamics*, 82, 12-24.
- 2. Hedwig, G. R., & Høiland, H. (2011). Partial molar isentropic and isothermal compressions of the nucleosides adenosine, cytidine, and uridine in aqueous solution at 298.15 K. *Journal of Chemical & Engineering Data*, 56, 2266-2272.
- 3. Kishore, N., & Ahluwalia, J. C. (1990). Partial molar heat capacities and volumes of transfer of nucleic acid bases, nucleosides and nucleotides from water to aqueous solutions of sodium and calcium chloride at 25° C. *Journal of Solution Chemistry*, 19, 51-64.
- 4. Banipal, T. S., Kaur, N., & Banipal, P. K. (2016). Solvation behavior of some nucleic acid bases and nucleosides in water and in aqueous guanidine hydrochloride solutions: Viscometric, calorimetric and spectroscopic approach. *The Journal of Chemical Thermodynamics*, 95, 149-158.
- 5. Khan, A., Shahid, K., Khan, S., Humayun, M., Bououdina, M., Rehman, N., ... & Munawar, K. S. (2023). Effect of ethanol and sodium chloride on the physiochemical properties of Montelukast sodium and its interaction with DNA. *Zeitschrift für Physikalische Chemie*, 237, 1361-1380.
- 6. Rajput, P., Singh, H., Bandral, A., Richu, Majid, Q., & Kumar, A. (2022). Explorations on thermophysical properties of nitrogenous bases (uracil/thymine) in aqueous L-histidine solutions at various temperatures. *Journal of Molecular Liquids*, 367, 120548.
- 7. Rajput, P., Richu, Sharma, T., & Kumar, A. (2021). Temperature dependent physicochemical investigations of some nucleic acid bases (uracil, thymine and adenine) in aqueous inositol solutions. *Journal of Molecular Liquids*, 326, 115210.

- 8. Banipal, T. S., Kaur, S., Beri, A., & Banipal, P. K. (2022). Elucidation of interactions between ciprofloxacin hydrochloride monohydrate and constituents of nucleic acids in aqueous solutions at different temperatures. *Journal of Chemical & Engineering Data*, 67, 1335-1349.
- Maksudov, F., Kliuchnikov, E., Pierson, D., Ujwal, M. L., Marx, K. A., Chanda, A., & Barsegov, V. (2023). Therapeutic phosphorodiamidate morpholino oligonucleotides: Physical properties, solution structures, and folding thermodynamics. *Molecular Therapy-Nucleic Acids*, 31, 631-647.
- 10. Kumar, H., Kaur, S., Kumar, V., Ghfar, A. A., Katal, A., Sharma, M., & Singla, M. (2022). Study of the interactions of monosaccharides D-(+)-glucose and D-(-)-fructose in aqueous diammonium hydrogen phosphate over the temperature range T = (288.15–318.15) K. *The Journal of Chemical Thermodynamics*, 172, 106793.
- 11. Sharma, P., Sharma, S., & Sharma, M. (2022). Effect of trisodium citrate dihydrate on thermophysical properties of saccharides in aqueous media at different temperatures: Volumetric and acoustic properties. *Chemical Thermodynamics and Thermal Analysis*, 6, 100051.
- 12. Karimi, S., Shekaari, H., & Ahadzadeh, I. (2020). The sweetness response and thermophysical properties of glucose and fructose in the aqueous solution of some deep eutectic solvents at T = (288.15–318.15) K. *Carbohydrate Research*, 495, 108083.
- 13. Nain, A. K. (2020). Solute-solute and solute-solvent interactions of drug sodium salicylate in aqueous-glucose/sucrose solutions at temperatures from 293.15 to 318.15 K: A physicochemical study. *Journal of Molecular Liquids*, 298, 112006.
- 14. Zafarani-Moattar, M. T., Shekaari, H., & Agha, E. M. H. (2019). Effect of ionic liquids 1-octyl-3-methyl imidazolium bromide or 1-octyl-3-methyl imidazolium chloride on thermophysical properties and taste behavior of sucrose in aqueous media at different temperatures: Volumetric, compressibility and viscometric properties. Food Chemistry, 295, 662-670.

- 15. Ali, A., Bidhuri, P., Malik, N. A., & Uzair, S. (2019). Density, viscosity, and refractive index of mono-, di-, and tri-saccharides in aqueous glycine solutions at different temperatures. *Arabian Journal of Chemistry*, *12*, 1684-1694.
- 16. Aggarwal, N., Sharma, M., Banipal, T. S., & Banipal, P. K. (2019). Influence of phosphate-based salts on enthalpy of dilution and isentropic compressibility properties of saccharides and their derivatives in aqueous solutions. *Journal of Chemical & Engineering Data*, 64, 517-528.
- 17. Ankita, Nain, A. K. (2019). Volumetric, acoustic and viscometric studies of solute-solute and solute-solvent interactions of isoniazid in aqueous-glucose/sucrose solutions at temperatures from 293.15 K to 318.15 K. *The Journal of Chemical Thermodynamics*, 133, 123-134.
- 18. Rani, R., Kumar, A., & Bamezai, R. K. (2017). Effect of glucose/lactose on the solution thermodynamics of thiamine hydrochloride in aqueous solutions at different temperatures. *Journal of Molecular Liquids*, 240, 642-655.
- Zhuo, K., Liu, Q., Wang, Y., Ren, Q., & Wang, J. (2006). Volumetric and viscosity properties of monosaccharides in aqueous amino acid solutions at 298.15
 K. Journal of Chemical & Engineering Data, 51, 919-927.
- 20. Banipal, P. K., Sharma, M., & Banipal, T. S. (2017). Solvation behavior and sweetness response of carbohydrates, their derivatives and sugar alcohols in thiamine HCl (vitamin B1) and pyridoxine HCl (vitamin B6) at different temperatures. *Food chemistry*, 237, 181-190.
- 21. Chandrasekaran, J. R., & Nithiyanantham, S. (2023). Solvation number, thermochemical parameter, and viscosity study of sweeteners in aqueous and non-aqueous media through ultrasonic measurements. *ChemPhysMater*, 2, 303-314.
- 22. Malik, N., Khan, A. U., Naqvi, S., & Arfin, T. (2016). Ultrasonic studies of different saccharides in α-amino acids at various temperatures and concentrations. *Journal of Molecular Liquids*, 221, 12-18.

- 23. Sirbu, F., & Gheorghe, I. L. (2018). Study on thermophysical properties in the ternary mixture of N-methylglycine solute with (D-glucose + water) binary solvent at temperatures of 298.15, 308.15, and 318.15 K. *Journal of Molecular Liquids*, 253, 149-159.
- 24. Zhao, C., Ma, P., & Li, J. (2005). Partial molar volumes and viscosity B-coefficients of arginine in aqueous glucose, sucrose and L-ascorbic acid solutions at T = 298.15 K. *The Journal of Chemical Thermodynamics*, *37*, 37-42.
- 25. Chen, B., Liu, K., Wang, D., Kong, Y., Qu, K., Zhang, X., & Liu, M. (2022). Volumetric, viscometric, and refractive index studies of drug nicotinic acid in aqueous D-xylose/L-arabinose solutions from 293.15 to 313.15 K: Insights into solute—solute and solute—solvent interactions. *Journal of Chemical & Engineering Data*, 67, 1089-1100.
- 26. Sharma, T., Singh, H., Bamezai, R. K., & Kumar, A. (2022). Analysing the molecular interactions of ternary (lactose + water + tributylmethylammonium chloride) solutions at different temperatures via physicochemical methods. *Journal of Molecular Liquids*, 349, 118412.
- 27. Zafarani-Moattar, M. T., Shekaari, H., & Mazaher Haji Agha, E. (2019). Investigation of the thermodynamic properties in aqueous solutions containing D-fructose and some imidazolium-based ionic liquids at different temperatures. Journal of Chemical & Engineering Data, 64, 1385-1398.
- 28. Singh, V., & Kasaudhan, V. (2024). Volumetric and taste behavior of D-(+)-glucose and D-(-)-fructose in aqueous solutions of ethanolammoium acetate. *Food Chemistry*, 446, 138864.
- 29. Alalaw, N. K., Hamooshy, E. A., & Hussein, H. H. (2022). Thermodynamic study of the solubility of guanine and uracil in deferent aqueous sugar solution. *Egyptian Journal of Chemistry*, 65, 371-376.
- 30. Singh, H., Richu, Bandral, A., Majid, Q., & Kumar, A. (2023). Investigation of molecular interactions of streptomycin sulphate with aqueous L-aspartic acid

- through volumetric, ultrasonic and viscometric approach. *Journal of Molecular Liquids*, 382, 121885.
- 31. Romero, C. M., Rodríguez, D. M., Ribeiro, A. C., & Esteso, M. A. (2017). Effect of temperature on the partial molar volume, isentropic compressibility and viscosity of DL-2-aminobutyric acid in water and in aqueous sodium chloride solutions. *The Journal of Chemical Thermodynamics*, 104, 274-280.
- Dhondge, S. S., Dahasahasra, P. N., Paliwal, L. J., Tangde, V. M., & Deshmukh,
 D. W. (2017). Volumetric and viscometric study of thiamine hydrochloride,
 pyridoxine hydrochloride and sodium ascorbate at T = (275.15, 277.15 and 279.15)
 K in dilute aqueous solutions. *The Journal of Chemical Thermodynamics*, 107, 189-200.
- 33. Masson, D. O. (1929). XXVIII. Solute molecular volumes in relation to solvation and ionization. *The London, Edinburgh, and Dublin Philosophical Magazine and Journal of Science*, 8, 218-235.
- 34. Shekaari, H., & Kazempour, A. (2011). Solution properties of ternary D-glucose + 1-ethyl-3-methylimidazolium ethyl sulfate + water solutions at 298.15 K. *Journal of solution chemistry*, 40, 1582-1595.
- 35. Belibaĝli, K. B., & Ayranci, E. (1990). Viscosities and apparent molar volumes of some amino acids in water and in 6M guanidine hydrochloride at 25 °C. *Journal of Solution Chemistry*, *19*, 867-882.
- 36. Wadi, R. K., & Ramasami, P. (1997). Partial molal volumes and adiabatic compressibilities of transfer of glycine and DL-alanine from water to aqueous sodium sulfate at 288.15, 298.15 and 308.15 K. *Journal of the Chemical Society, Faraday Transactions*, 93, 243-247.
- 37. Franks, F., Quickenden, M. A. J., Reid, D. S., & Watson, B. (1970). Calorimetric and volumetric studies of dilute aqueous solutions of cyclic ether derivatives. *Transactions of the Faraday Society*, 66, 582-589.

- 38. Terasawa, S., Itsuki, H., & Arakawa, S. (1975). Contribution of hydrogen bonds to the partial molar volumes of nonionic solutes in water. *The Journal of Physical Chemistry*, 79, 2345-2351.
- 39. Bondi, A. V. (1964). van der Waals volumes and radii. *The Journal of Physical Chemistry*, 68, 441-451.
- 40. Bondi, A. (1954). Free volumes and free rotation in simple liquids and liquid saturated hydrocarbons. *The Journal of Physical Chemistry*, *58*, 929-939.
- 41. Shahidi, F., & Farrell, P. G. (1978). Partial molar volumes of organic compounds in water. Part 4.—Aminocarboxylic acids. *Journal of the Chemical Society, Faraday Transactions 1: Physical Chemistry in Condensed Phases*, 74, 858-868.
- 42. Krishnan, C. V., Garnett, M., & Chu, B. (2007). Solute-solvent interactions from admittance measurements: Potential induced and water structure-enforced ion-pair formation. *International Journal of Electrochemical Science*, 2, 958-972.
- 43. Streng, W. H., & Wen, W. Y. (1974). Calculation of Gurney parameters for aqueous tetraalkylammonium halides based on Friedman's cosphere-overlap model. *Journal of Solution Chemistry*, *3*, 865-880.
- 44. Lin, G., Bian, P., & Lin, R. (2006). The limiting partial molar volume and transfer partial molar volume of glycylglycine in aqueous sodium halide solutions at 298.15 K and 308.15 K. *The Journal of Chemical Thermodynamics*, *38*, 144-151.
- 45. Pal, A., & Chauhan, N. (2012). Interactions of amino acids and peptides with the drug pentoxifylline in aqueous solution at various temperatures: A volumetric approach. *The Journal of Chemical Thermodynamics*, *54*, 288-292.
- 46. Krishnan, C. V., & Friedman, H. L. (1973). Enthalpies of alkyl sulfonates in water, heavy water, and water-alcohol mixtures and the interaction of water with methylene groups. *Journal of Solution Chemistry*, 2, 37-51.
- 47. Jamkhande, K. M., Khaty, N. T., Pandhurnekar, C. P., & Tangde, V. M. (2025). Thermodynamic studies of binary and ternary mixtures of duloxetine hydrochloride

- and myo-inositol: A volumetric, acoustic and viscometric approach. *Journal of Chemical & Engineering Data*, 70, 890-907.
- 48. Dhondge, S. S., Zodape, S. P., & Parwate, D. V. (2012). Volumetric and viscometric studies of some drugs in aqueous solutions at different temperatures. *The Journal of Chemical Thermodynamics*, 48, 207-212.
- 49. Sharmhal, A., Richu, Singh, H., Sharma, P. K., Kumar, A., & Kumar, A. (2024). Physicochemical investigations on molecular interactions of adenine with aqueous D-glucose/D-maltose solvent media at varying temperatures and compositions. *The Journal of Chemical Thermodynamics*, 201, 107399.
- 50. Hepler, L. G. (1969). Thermal expansion and structure in water and aqueous solutions. *Canadian Journal of Chemistry*, 47, 4613-4617.
- 51. Singh, H., Majid, Q., Richu, Singh, M., Kang, T. S., & Kumar, A. (2023). Explorations on solute–solvent interactions of tripotassium citrate and sodium benzoate in aqueous 1-ethyl-3-methylimidazolium ethyl sulfate solutions: Physicochemical, spectroscopic, and computational approaches. *Journal of Chemical & Engineering Data*, 68, 2563-2584.
- 52. Parke, S. A., Birch, G. G., & Dijk, R. (1999). Some taste molecules and their solution properties. *Chemical Senses*, *24*, 271-279.
- 53. Shamil, S., Birch, G. G., Mathlouthi, M., & Clifford, M. N. (1987). Apparent molar volumes and tastes of molecules with more than one sapophore. *Chemical Senses*, 12, 397-409.
- 54. Bahadur, I., & Deenadayalu, N. (2011). Apparent molar volume and isentropic compressibility at T = 298.15, 303.15, 308.15 and 313.15 K and atmospheric pressure. *Journal of Solution Chemistry*, 40, 1528-1543.
- 55. Thakur, A., Juglan, K. C., Kumar, H., & Kaur, K. (2019). Investigation on molecular interaction of glycols in methanol solutions of methylparaben (methyl 4–hydroxybenzoate) at different temperatures through thermo-acoustical

- analysis. Journal of Molecular Liquids, 288, 111014.
- 56. Bandral, A., Singh, H., Richu, Majid, Q., Rajput, P., & Kumar, A. (2024). Effect of semicarbazide hydrochloride on the physicochemical properties of L-leucine and glycylglycine at varied temperatures and compositions. *The Journal of Chemical Thermodynamics*, 188, 107176.
- 57. Millero, F. J., Lo Surdo, A., & Shin, C. (1978). The apparent molal volumes and adiabatic compressibilities of aqueous amino acids at 25 degree C. *The Journal of Physical Chemistry*, 82(7), 784-792.
- 58. Rajput, P., Singh, H., & Kumar, A. (2022). Volumetric, ultrasonic and viscometric behavior of nucleosides (uridine and cytidine) in aqueous L-ascorbic acid solutions at different temperatures. *The Journal of Chemical Thermodynamics*, *171*, 106805.
- 59. Sharmhal, A., Singh, H., Richu, Fatma, I., Sharma, P. K., Sharma, S., Kumar, A., & Kumar, A. (2023). Influence of carbohydrates on the volumetric, acoustic and viscometric properties of thymine in aqueous solutions at different temperatures. *Journal of Molecular Liquids*, 385, 122264.
- 60. Jones, G., & Dole, M. (1929). The viscosity of aqueous solutions of strong electrolytes with special reference to barium chloride. *Journal of the American Chemical Society*, *51*, 2950-2964.
- 61. Chandra, A., Patidar, V., Singh, M., & Kale, R. K. (2013). Physicochemical and friccohesity study of glycine, L-alanine and L-phenylalanine with aqueous methyltrioctylammonium and cetylpyridinium chloride from T = (293.15 to 308.15) K. *The Journal of Chemical Thermodynamics*, 65, 18-28.
- 62. Falkenhagen, H., & Vernon, E. L. (1932). LXII. The viscosity of strong electrolyte solutions according to electrostatic theory. *The London, Edinburgh, and Dublin Philosophical Magazine and Journal of Science*, *14*, 537-565.
- 63. Feakins, D., Freemantle, D. J., & Lawrence, K. G. (1974). Transition state treatment of the relative viscosity of electrolytic solutions. Applications to aqueous, non-

- aqueous and methanol+ water systems. *Journal of the Chemical Society, Faraday Transactions 1: Physical Chemistry in Condensed Phases*, 70, 795-806.
- 64. Sarma, T. S., & Ahluwalia, J. C. (1973). Experimental studies on the structures of aqueous solutions of hydrophobic solutes. *Chemical Society Reviews*, 2, 203-232.
- 65. Glasstone, S., Laidler, K. J., & Eyring, H. (1941). The theory of rate processes: the kinetics of chemical reactions, viscosity, diffusion and electrochemical phenomena. *McGraw-Hill Book Company*.
- 66. Feakins, D., Waghorne, W. E., & Lawrence, K. G. (1986). The viscosity and structure of solutions. Part 1.—A new theory of the Jones–Dole *B*-coefficient and the related activation parameters: application to aqueous solutions. *Journal of the Chemical Society, Faraday Transactions 1: Physical Chemistry in Condensed Phases*, 82, 563-568.

CHAPTER 3 MATERIALS AND METHODS

3 Materials and Methods

In this chapter, a brief overview of chemicals, instrumental characteristics, their working principle for the precise assessment of physical effects (density, sound speed and viscosity), and the exploration approach are outlined.

3.1 Chemicals Used

All chemicals used were of analytical grade and used without further purification. The complete list of chemicals, along with their molecular details and purities, is presented in Table 3.1. To ensure experimental precision, all reagents were carefully selected and properly handled as outlined below:

Table 3.1: The varied chemicals engaged in present work with allied CAS numbers, molecular formulas, purities and structures.

Chemical used	CAS number	Molecular formula with Molecular weight (g mol ⁻¹)	Supplier and Mass Fraction Purity ^a	Structure
Thymine	CAS- 65-71-4	$C_5H_6N_2O_2$ (126.12)	HiMedia, India ≥0.980	O N O
D-(+)- glucose	CAS- 50-99-7	C ₆ H ₁₂ O ₆ (180.16)	Sigma Aldrich, India ≥0.995	OH OH OH
Sucrose	CAS- 57-50-1	C ₁₂ H ₂₂ O ₁₁ (342.30)	Sigma Aldrich, India ≥0.995	CH ₂ OH CH ₂ OH H OH OH H OH OH OH OH H OH OH H

Adenine	CAS-	$C_5H_5N_5$	Sigma	// NH
Adellific	73-24-5	(135.13)	Aldrich,	
	, 5 2 . 5	(133.13)	India	NH ₂
			≥0.990	
				N N
D- (+)-	CAS-	$C_{12}H_{22}O_{11}.H_2$	Sigma	он он Т
maltose	6363-	O	Aldrich,	OH HO _{IIIII}
monohydrat	53-7	(360.31)	India	H H
e			≥0.990	
				HO O OH
				E OH
				НО
Cytosine	CAS	$C_4H_5N_3O$	TCI,	N
	RN 71-	(111.10)	India	
	30-7		≥ 0.980	
				H_2N N O
D-(+)-xylose	CAS-	$C_5H_{10}O_5$	Sigma	HOO
	58-86-6	(150.13)	Aldrich,	³ /
			India	
			≥0.990	НО
				ОН
Lactose	CAS-	$C_{12}H_{22}O_{11}.H_2$	Sigma	НО
monohydrat		O	Aldrich,	
e	81-1	(360.31)	India	, o
			≥0.990	но
				но он о
				—
				ОН
				ОН

^aAs declared by purveyor

3.2 Apparatus and Cleaning Protocols

Prior to use, all glassware (beakers, flasks, etc.) was thoroughly cleaned using chromic acid and triple-distilled water, then dried at $70-80^{\circ}$ C. Solutions were stored in foil-covered containers to prevent contamination and evaporation [1]. With preparation conditions ensured, the following steps describe sample preparation.

3.3 Sample Preparation and Handling

All chemicals employed in this study were employed as received without any further refinement, vacuum dried, then stowed over P_2O_5 in desiccator for around 48 hours before being used. Further, all the sample mixtures were formulated via weighing the obligatory amount of substance on electrical balance (ML204, Mettler Toledo) having a vagueness of ± 0.1 mg as displayed in Figure 3.1.



Figure 3.1: Mettler Toledo (ML204)

Deionized triply distilled water, Millipore SAS-67120, possessing a specific conductance $<1 \times 10^{-6}$ S/cm attained from Molsheim-France has been deployed for solution processing. Moreover, solutes with varying concentrations were dissolved in water to prepare binary solutions and in mixed aqueous solvent systems to prepare ternary systems [2-4]. Once samples were ready, physicochemical measurements were carried out using highly sensitive instruments, as described in the following sections.

3.4 Analysis of Density and Sound of Sound Using DSA 5000 M

Extremely meticulous oscillating tube density (ρ) as well as sound speed (u) analyser ie. DSA 5000 M (Anton Paar, Austria) is being exercised towards empirical evaluation of density along with speed of sound of various sample solutions (Figure 3.2). The operating elements of main screen for the DSA 5000 M and its specifications are displayed in Figure 3.3 and Table 3.2, respectively. Also, the apparatus was calibrated using ethyl alcohol and arid air at room pressure prior to each cycle of experimental

research. It produces precise density and sound speed data and accomplishes it accurately with only a small sample volume. Additionally, there should be no air bubbles in the introduced sample, which can be detected by the built-in camera or a filling warning. In commercial and research chemical laboratories, the DSA 5000 M is widely implicated to assess density as well as sound velocity of various samples at the required temperature and conditions. [5-7]. To facilitate clarity, the operation of this instrument is explained in the following subsections.



Figure 3.2: Machine DSA 5000 M by Anton Paar



Figure 3.3: Operating elements of main screen

Table 3.2: Specifications of DSA 5000 M.

Density assessing range (g cm ⁻³)	0 to 3			
Measuring range ultrasonic speed (m s ⁻¹)	1000 to 2000			
Measuring range temperature (K)	273.15 to 343.15			
Repeatability in density (g cm ⁻³)	0.000001			
Repeatability in sound's velocity (m s ⁻¹)	0.1			
Repeatability temperature (K)	273.15			
Pressure range (bar)	0 to 3			
Sample volume (mL)	3 (approx.)			
Measuring time per sample (min.)	1 to 4			
Visual check of the density measuring cell	Camera			
Reference oscillator	Yes			
Automatic bubble detection	Yes			
Ambient air pressure sensor	Yes			

3.4.1 Instrument Description and Specifications

The device has a cell for density assessment and a cell for estimation of sound speed, both of which have built-in Peltier thermostats to control their respective temperatures. The density along with sound speed measurements lie in range 0-3 g/cm³ and 1000-2000 m/s, correspondingly. Also, the reproducibility in density and ultrasonic velocity of this instrument is 0.5 g/cm^3 as well as $5 \times 10^{-6} \text{ m/s}$, correspondingly.

The sample is loaded into a U-shaped borosilicate tube that vibrates; its frequency change is then used to calculate density by applying the following equation:

Density
$$(\rho) = k_1 \times Q^2 \times f_1 - k_2 \times f_2$$
 (3.1)

Where, k_1 and k_2 denotes the equipment constraints, Q refers to proportion of vibration phase of U-shaped tube alienated by the vibration time phase of orientation oscillator, f_1 and f_2 symbolize the rectification stipulations for non-linearity, viscosity, temperature etc.

A reference oscillator amplifies the irregular signal of the instrument. The thermal balance tests specific data over the entire temperature range, providing fault corrections at designated temperatures and minor adjustments at 293.15 K.

3.4.2 Density Measurement Principle

The density (ρ) of any sample is determined via following relation:

Density
$$(\rho) = \text{Mass/Volume}$$
 (3.2)

The specific gravity is defined as the density for a substance per unit density for pure water at 20°C, given as:

Specific gravity (SG) = Density of sample
$$(\rho_{sample})$$
/Density of water (ρ_{water}) (3.3)

3.4.3 Sound Speed Measurement Principle

This instrument consists of a velocity measurement cell where the sample is inserted to estimate the speed for sound. The cell has sound speed transmitter on one side, which sends ultrasonic waves of specific frequency throughout the prepared sample solution. Since the solution is crammed in a cell having recognized length, the distance travelled by the waves is also identified. On another end, there is a receiver that receives these waves so the adopted time by ultrasonic rays to pass over the solutions could be determined. It can be determined through the relation:

$$V = [Path \ length \times (1 + 1.6E - 5 \times \Delta T)]/[(P_r/Divisor) - TAU \times f_a]$$
(3.4)

Where, ΔT is temperature variation to 293.15 K, P_r is oscillating phase of customary ultrasonic waves, TAU refers to instrumental/apparatus constraint, Divisor has the value of 512, f_a is alteration constant for temperature.

3.4.4 Sample Injection and Air Bubble Detection

For the recognition of sound velocity as well as density of a sample, the DSA 5000M requires two adapters and a conjunction tube. The first adapter, DSA, connects to the sound velocity calculating cell and provides a sample inlet adapter. The sample then travels through the pre-assembled conjunction tube to the density measuring cell. Finally,

the sample is directed from the density measuring cell to the waste using the injection adapter, Luer. In order to acquire accurate measurement results, it is important to uniformly introduce the specimen into the cell without any gas bubbles.

Gas bubbles can cause errors in the measurement of sound speed and density. DSA 5000 M is highly sensitive and can detect the presence of bubbles in the measuring unit.



Figure 3.4: Filling of sample into sample inlet adapter

It does this by approximating its oscillation sequence and displaying a warning. Additionally, the instrument has a real-time camera with a zoom effect to visually inspect any gas bubbles in density measuring unit.

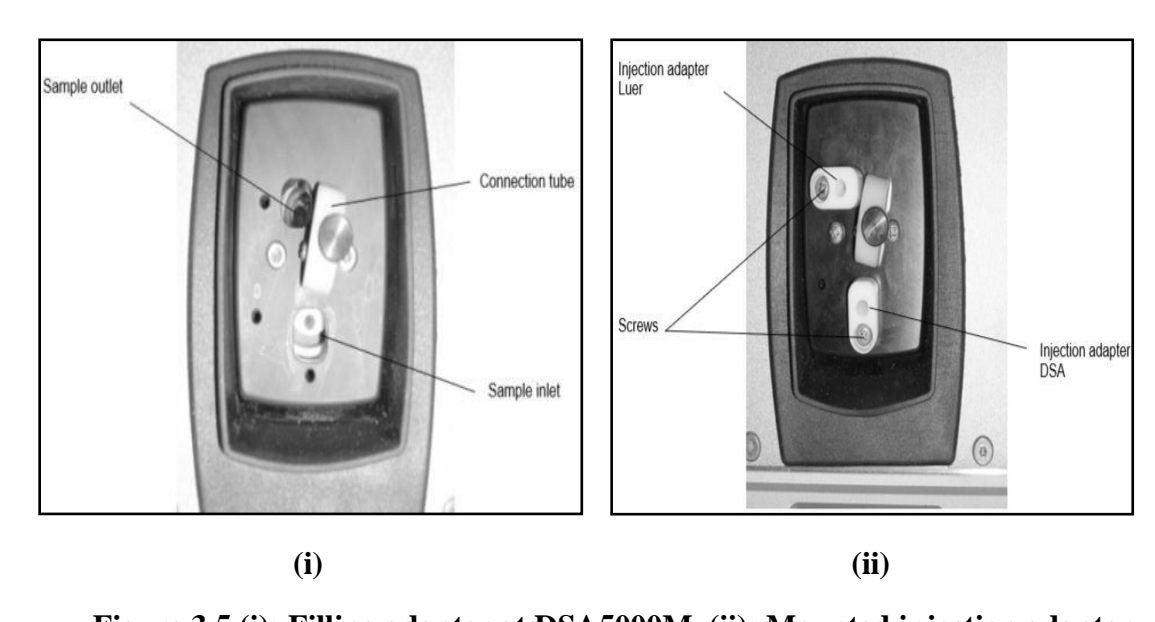


Figure 3.5 (i): Filling adapter at DSA5000M, (ii): Mounted injection adapter

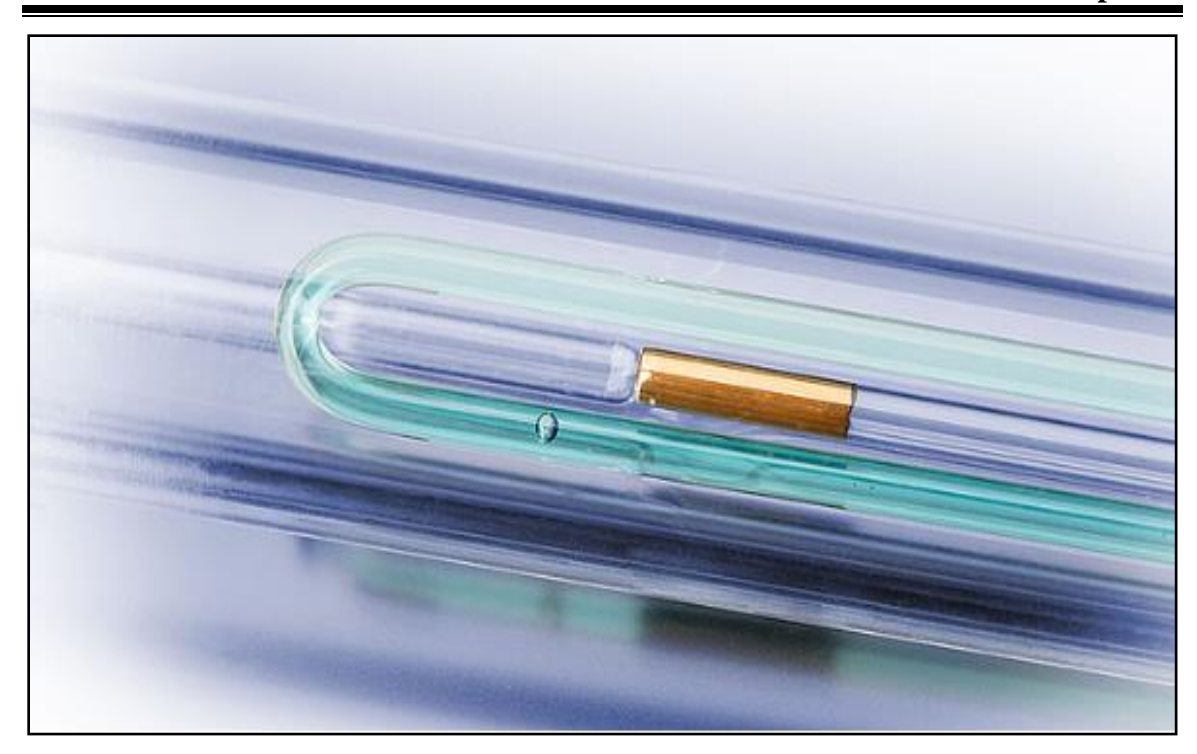


Figure 3.6: Appearance of a gas bubble

3.4.5 Cleaning and Drying of Measuring Cell

After taking the basic measurements of the selected samples, the cell is cleaned using two solutions named as Solution 1 and Solution 2. Solution 1 is used to clean the measuring cell as it dissolves and removes sample deposits, and it works well as a solvent for all sample components. Solution 2 is used to remove Solution 1 from the cell and then evaporated by dry air, to speed up cell drying process. In order to do so, Solution 2 should be a good solvent for Solution 1.

- i. Water and non-denatured ethanol for testing aqueous samples and beverages.
- ii. Acetone and petroleum naphtha for petrochemical mixtures.

If the temperature inside the measuring cell is lower than the outside temperature and the air has high humidity, then condensation may form in the measuring cell and measuring cell block. In order to prevent this condensation from forming, we need to connect a dry air supply to the dry air block connector located at the back of DSA 5000 M and make sure to use a hose that is made of appropriate material such as silicone.

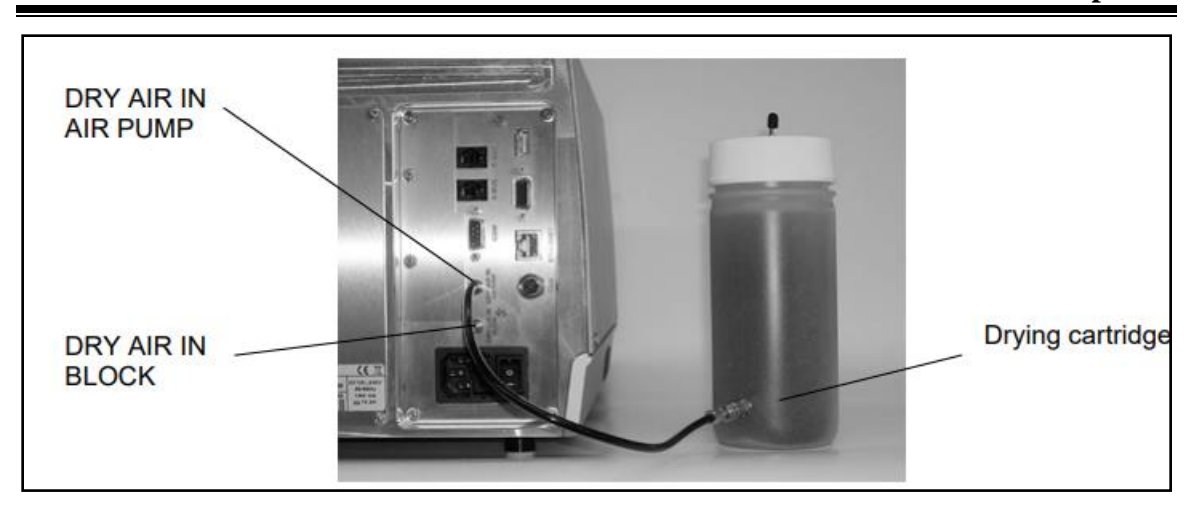


Figure 3.7: Drying cartridge connected with the instrument

3.4.6 Characteristics and Benefits of DSA 5000 M

- Accuracy, Reproducibility and Repeatability: DSA 5000 M offers high reproducibility as 0.000005 g/cm³ in density together with 0.5 m/sin sound velocity. It also provides high repeatability of up to the 7th digit for densimetric while 0.1 (m/s) for sound velocity values.
- Filling CheckTM: By analysing the oscillation pattern, the DSA can detect irregularities and air bubbles across the entire density cell and display a warning for each measurement.
- ➤ **U-View**TM **Camera:** Visual inspection of the density cell is performed in real-time using a camera with zoom application.
- Thermo BalanceTM: An additional reference oscillator accurately measures data over the entire temperature range in one setting at 20°C to provide long-term stability and eliminate temperature-related fluctuations.
- Automatic Viscosity Related Error Rectification: To estimate the ultrasonic speeds of high viscosity substances, we first determine their dampening effect. The density values are then corrected using mathematical calculations. This instrument offers special settings to accurately measure high viscosity and density of solutions. For even more precision, it offers an additional stainless steel measuring unit with high-resolution electronics.

Following the measurement of density and sound speed, viscosity was assessed using a complementary technique, detailed below:

3.5 Measurement of Viscosity Using Lovis 2000 M/ME

There are various types of viscometers available commercially to measure viscosity, including rotational, capillary, and moving body viscometers. The selection of viscometer depends on several factors, such as whether sample solution is elastic, whether it is transparent or opaque, the magnitude of viscosity to be measured, the temperature dependence of viscosity etc. In this research work, Lovis 2000 M/ME (rolling-ball microviscometer) has been chosen to analyse the viscosity of prepared samples [8,9]. This viscometer can provide dynamic viscosity as well as intrinsic viscosity of the sample. It is a versatile, time-saving and specific viscometer that procedures the rolling movements of a ball in crystal clear as well as opaque fluids. A small volume of sample, as low as 100 μL, can be utilised for the complete assessment of results. The material to be examined is inserted into a thin capillary tube that is placed in a block with temperature control. The capillary block can be angled in various ways. Moreover, the potential measurement range can be increased by thermoelectric temperature regulation and configurable inclination angles. The smaller volume capillaries used for the measurements are made of borosilicate glass, enabling the testing of corrosive as well as hazardous fluids. This viscometer can be linked to several Anton Paar evaluating modules and an automatic sample changer. The working principle of the instrument is described next.



Figure 3.8: Lovis microviscometer 2000 M/ME, with DSA 5000 M

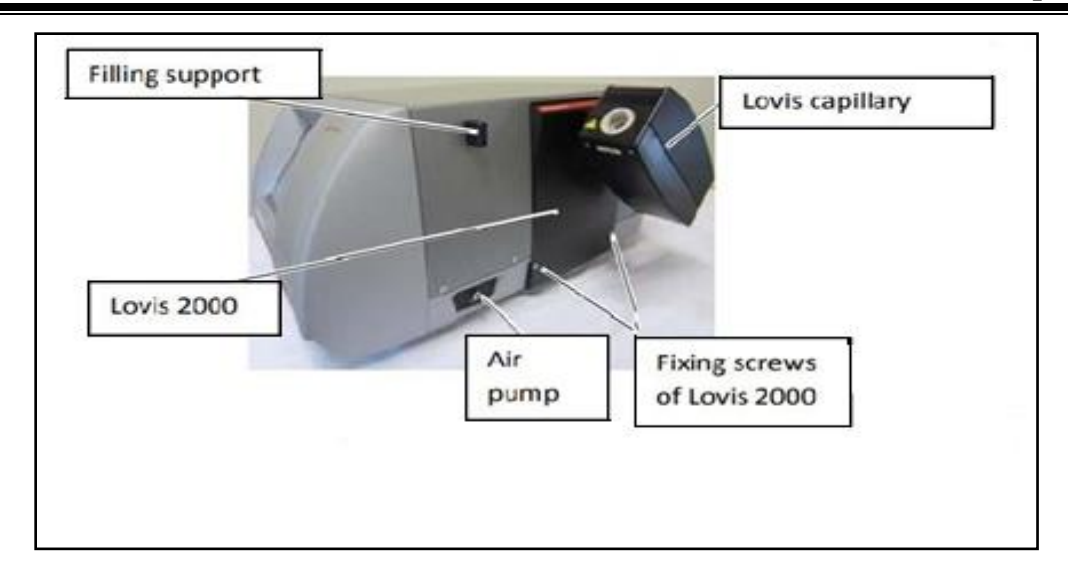


Figure 3.9: Lovis 2000 M/ME unit



Figure 3.10: Capillary with a ball

3.5.1 Working Principle of Rolling-Ball Viscometer

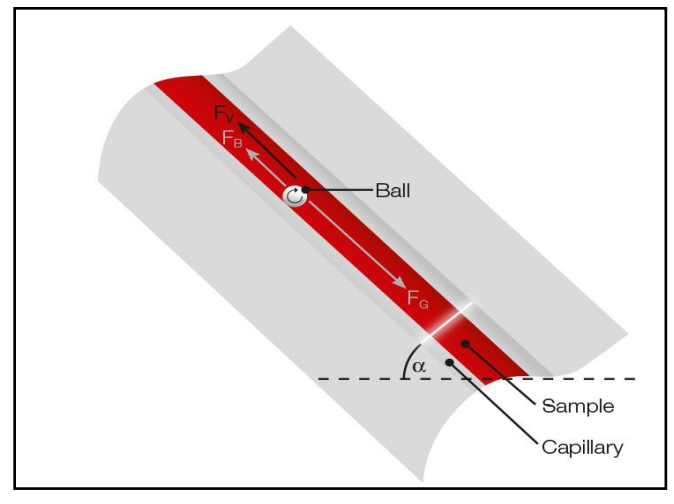
Similar to the conventional falling-ball viscometer, the rolling-ball microviscometer operates on the Höppler principle. This hypothesis states that the ball takes longer to roll very viscous samples and less time to roll moderately viscous materials. Thus, the seconds it takes a ball to roll a specific distance is correlated to viscosity. The ball's rolling and lowering motion through the sample placed inside a cylindrical measurement tube with a modest inclination is defined by the fall time. The capillary's slanting angle allows the driving force to be fixed. Gravitational force, which is

proportional to the inclination angle, causes the ball to roll downhill. These forces define the viscosity equation that follows.

$$\eta = -K(d_{sample} - d_{ball})t \tag{3.5}$$

Where, t is the ball's rolling duration, d_{ball} and d_{sample} are densities of ball and sample, K refers to the proportionality constraint while η signify the dynamic viscosity.

There are two sections to the range of a rolling-ball viscometer: a shorter section and a longer section. When the experiment first begins, the ball crosses the shorter distance, and how long it takes it to do so indicate how viscous the sample was chosen. Therefore, by calculating the ball's rolling time during the shorter section, we may examine the characteristics of the sample [10].



FB: Effectual fraction of buoyancy force, FG: Effectual fraction of gravitational force,

FV: Viscous force

Figure 3.11: Measuring principle of Lovis 2000 M/ME

3.6 UV-Vis Spectroscopy

Spectrophotometry, another name for UV-vis spectroscopy, is a quantitative method for figuring out how much light a chemical substance absorbs. The foundation of UV-visible spectroscopy is the way that chemicals absorb ultraviolet or visible light, resulting in the creation of distinct spectra. By contrasting the intensity of light flowing through a sample with that of a blank or reference sample, this is achieved. Spectroscopy

involves examining the interaction between light waves and matter. A continuum is formed when matter particles undergo absorption of light and undergoes excitation as well as de-excitation. The absorption spectrum of the substances under study was captured using a UV-visible spectrophotometer (LAMBDA 1050+) for the conducted study.

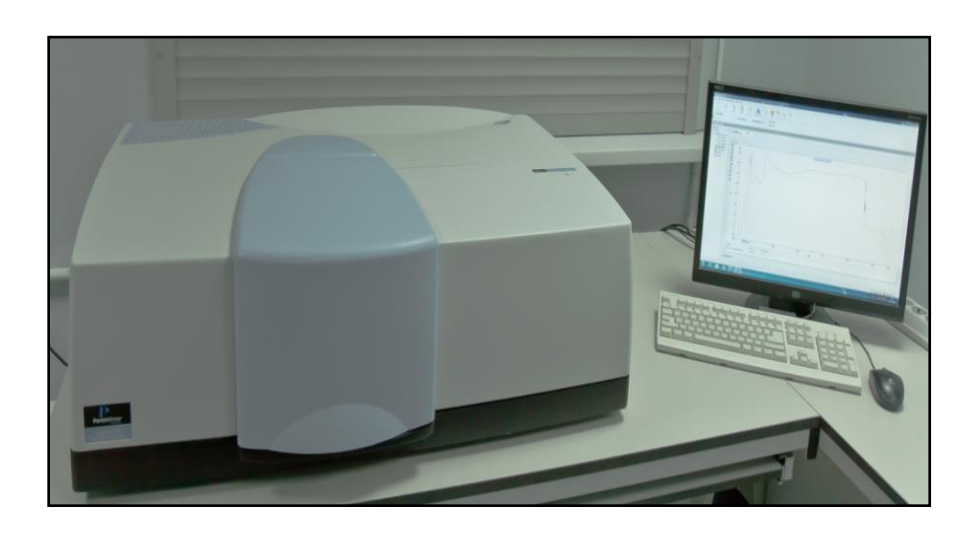


Figure 3.12: UV/vis spectrophotometer (LAMBDA 1050+)

Perkin Elmer's line of extremely-recital UV/Vis/NIR spectrophotometers was recently expanded with the LAMBDA 1050+. With its full wavelength range triple detector technology, which offers utmost sensitivity transversely with the accessible wavelengths (190 nm to 3300 nm) or (7.1 eV to 0.4 eV), an extreme resolution, elevated energy visual scheme with little drifts beam holographic strident, and Indium Gallium Arsenide sampling sections for superior NIR recital, the appliance includes numerous recent hi-tech advancements in ocular devise. Its UV/vis resolution (spectral bandwidth) is specified to be <0.05 nm. High resolution spectroscopy can therefore be used to analyse the chemical bonds of tiny molecules by revealing their precise vibrational structure. It can introspect a variety of mixture types, including solutions, fluids, powders, crystal clear solids, and bony coatings on surfaces. The optical system's theoretical limiting resolution is less than or equal to 0.03 nm. It works within the temperature interval of 15-35 °C. This spectroscopic method complemented the physical measurements by revealing molecular-level interactions.

REFERENCES

- 1. Sharma, T., Singh, H., Bamezai, R. K., & Kumar, A. (2022). Analysing the molecular interactions of ternary (lactose + water + tributylmethylammonium chloride) solutions at different temperatures via physicochemical methods. *Journal of Molecular Liquids*, 349, 118412.
- 2. Rajput, P., Richu, Sharma, T., & Kumar, A. (2021). Temperature dependent physicochemical investigations of some nucleic acid bases (uracil, thymine and adenine) in aqueous inositol solutions. *Journal of Molecular Liquids*, 326, 115210.
- 3. Sharma, R., & Thakur, R. C. (2018). Molecular interactions of pyridoxine hydrochloride in aqueous mixed solutions of D-glucose, D-fructose, and D-lactose at different temperatures. *Russian Journal of Physical Chemistry A*, 92, 2685-2692.
- 4. Singh, H., Richu, Bandral, A., Majid, Q., & Kumar, A. (2023). Investigation of molecular interactions of streptomycin sulphate with aqueous L-aspartic acid through volumetric, ultrasonic and viscometric approach. *Journal of Molecular Liquids*, 382, 121885.
- 5. Xing, G., Liu, X., Wu, J., Wang, W., Wu, Z., & Zhang, J. (2023). Density and viscosity of polyethylene glycol 400 + 1, 2-propanediamine binary mixtures at T = (293.15–318.15) K and spectral analysis. *Journal of Solution Chemistry*, 52(3), 263-287.
- 6. Mohapatra, P., Panda, S., Mishra, D., Singh, S., & Talukdar, M. (2025). Interference of potassium chloride and diammonium hydrogen phosphate on volumetric, viscometric and spectroscopic properties of aqueous nicotinamide. *RSC Advances*, *15*(3), 1813-1830.
- 7. Singh, H., Richu, Bandral, A., Majid, Q., & Kumar, A. (2023). Investigation of molecular interactions of streptomycin sulphate with aqueous L-aspartic acid through volumetric, ultrasonic and viscometric approach. *Journal of Molecular Liquids*, 382, 121885.

- 8. Majid, Q., Richu, Singh, H., Bandral, A., & Kumar, A. (2022). Thermophysical studies on molecular interactions of semicarbazide hydrochloride/domiphen bromide in aqueous deep eutectic solvent media at various temperatures. *Journal of Chemical & Engineering Data*, 67, 2974-2985.
- 9. Jamal, M. A., Shahazidy, U., Al-Saeed, F. A., Al Syaad, K. M., Muneer, M., Ahmed, I., & Ahmed, A. E. (2022). Investigations to explore molecular interactions and sweetness response of polyhydroxy compounds with amino acids in aqueous systems. *ACS omega*, 7, 40950-40962.
- 10. Richu, Bandral, A., Singh, H., & Kumar, A. (2022). Effect of [Bmim][Br] and [Emim][HSO4] on the solution properties of pyridoxine HCl at various temperatures: A physicochemical, thermodynamic and spectroscopic approach. *Journal of Molecular Liquids*, 364, 120024.

CHAPTER 4 RESULTS AND DISCUSSION

CHAPTER 4.1

Exploration of Volumetric, Viscometric, Compressibility and Spectroscopic Properties of Thymine in Aqueous Saccharide (Glucose/Sucrose) Media at Discrete Compositions and Temperatures

Journal of Molecular Liquids, 2023, 385, 122264

(Impact factor: 5.2)

Exploration of Volumetric, Viscometric, Compressibility and Spectroscopic properties of Thymine in Aqueous Saccharide (Glucose/Sucrose) Media at Discrete Compositions and Temperatures

This chapter, volumetric, compressibility and viscometric properties of thymine have been investigated in aqueous and mixed aqueous (0.05, 0.10 and 0.15) mol kg⁻¹ Dglucose/sucrose solvent media at discrete temperatures (293.15 to 313.15) K and experimental pressure (0.1 MPa). The properties like ρ , u, η that were obtained through experimentation were used to calculate a number of densimetric, compressibility, as well as viscometric parameters, mainly apparent molar volume (V_{ϕ}) , limiting apparent molar volume (V_{ϕ}^{0}) , hydration number (n_{H}) , limiting apparent molar expansivity (E_{ϕ}^{0}) , Hepler's constant $(\partial E^0 \phi / \partial T)_P$, apparent specific volume (ASV), apparent molar isentropic compression $(K_{\phi,s})$, limiting apparent molar isentropic compression $(K^0_{\phi,s})$, viscosity Bcoefficients, transfer parameters and thermodynamic parameters of viscous flow $(\Delta \mu^0)$, $\Delta \mu^{0}_{2}$, $T\Delta S^{0}_{2}$ and ΔH^{0}_{2}). Additionally, the Co-sphere overlap model has been utilized for the analysis of assorted probable interactions operating in the prepared systems. The received outcomes forecast that in all solution systems, the solute-solvent interactions are progressing with rising temperatures and concentrations of saccharides. Furthermore, the chaotropic character of thymine in H₂O and aqueous saccharide solution media has been ascertained by applying the Hepler's thermodynamic relation. Finally, UV spectral analysis verified that effective dipole-dipole interactions continue to exist in the systems under consideration.

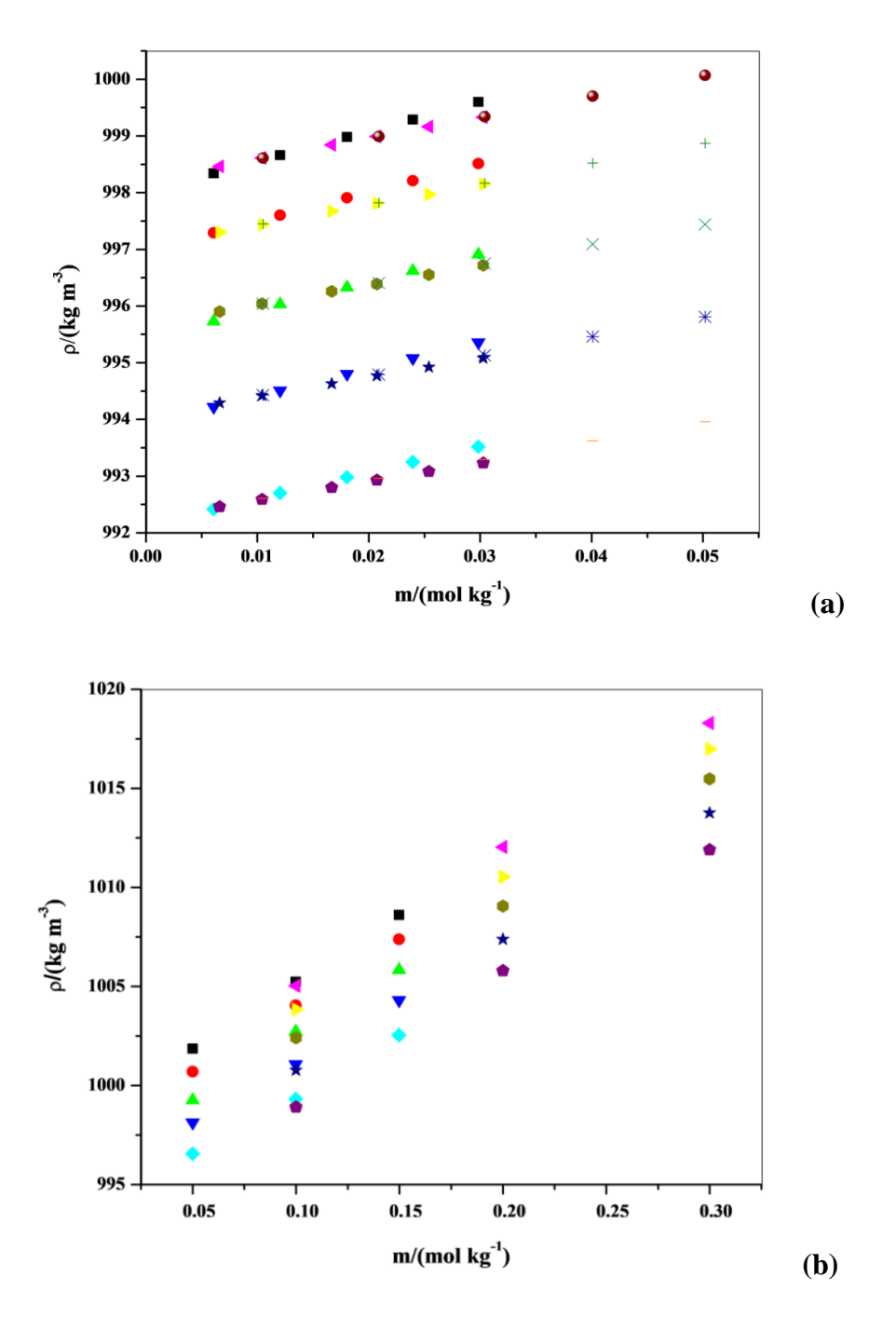
4.1.1 Density Data

Through the usage of Density and Speed of sound Analyzer (DSA 5000 M), the physical properties like density and speed of sound have been acquired at five dissimilar temperatures (293.15 K to 313.15 K) for (0.006, 0.012, 0.018, 0.024, and 0.030) mol kg⁻¹ of thymine in water and in (0.05, 0.10 and 0.15) mol kg⁻¹ water + sucrose/glucose solvent. Table 4.1.1 lists the experimentally specified values of density.

This table also shows that the densities drop with the temperature augmentation and the density values (ρ) escalates with increasing thymine, glucose, and sucrose concentrations. Increased mass/volume of the solution mixtures results from increased

concentration, which raises density. Conversely, as temperature rises, density decreases, this may be attributed to an increase in solution particles' kinetic energy as well as an expansion in the volume [3].

The empirically obtained ρ (density) values for thymine [4,5], glucose [6], as well as sucrose [7] in H₂O medium are contrasted with the available reports at various temperatures and are manifested in Figure's 4.1.1 (a), (b) as well as (c).



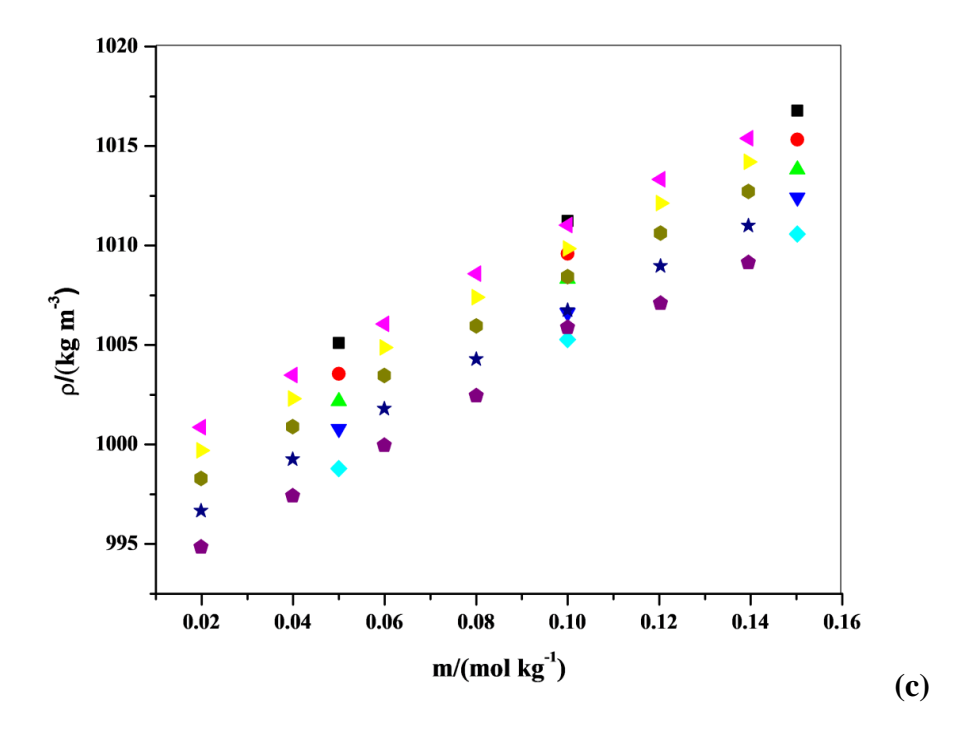


Figure 4.1.1(a): Comparison graph comprising density versus molality with literature for thymine in H_2O at discrete T(K). ■ : Conducted investigation on 293.15, • : Conducted investigation on 298.15, • : Conducted investigation on 303.15, • : Conducted investigation on 308.15, • : Lit. [4] on 293.15, • : Lit. [4] on 298.15, • : Lit. [4] on 303.15, • : Lit. [4] on 313.15, • : Lit. [5] on 293.15, + : Lit. [5] on 298.15, × : Lit. [5] on 303.15, * : Lit. [5] on 308.15, - : Lit. [5] on 313.15.

- **(b)** Comparison graph of density versus molality with literature for glucose in H₂O at diverse T(K). : Conducted investigation on 293.15, : Conducted investigation on 298.15, : Conducted investigation on 303.15, : Conducted investigation on 308.15, : Lit. [6] on 293.15, : Lit. [6] on 298.15, : Lit. [6] on 303.15, : Lit. [6] on 308.15, : Lit. [6] on 313.15.
- (c) Comparison graph of density versus molality with literature for sucrose in water at assorted *T*(K). : Conducted investigation on 293.15, : Conducted investigation on 298.15, ▲ : Conducted investigation on 303.15, ▼ : Conducted investigation on 308.15, : Lit. [7] on 293.15, ▷ : Lit. [7] on 298.15, : Lit. [7] on 303.15, ★ : Lit. [7] on 308.15, : Lit. [7] on 313.15.

This figure suggests that there has been a better agreement amid experimental and published data; nonetheless, at higher concentrations and temperatures, a very small variation has been noted for sucrose and thymine. Moreover, analysis of these graphs shows that densities increase as molality rises and decrease as temperature rises.

4.1.1.1 Apparent Molar Volume

Contribution that a constituent in a mixture formulates to non-ideality of the solution is known as its apparent molar volume, or V_{ϕ} . Furthermore, Eqn. (2.1) had been utilised to determine V_{ϕ} values or apparent molar volumes, based on the experimental densities. Table 4.1.1 presents the V_{ϕ} values that have been assessed. In both solvent systems, it is seen that these values rise as temperature and molality rise. The rise in V_{ϕ} with molal concentrations may be accredited to strong molecular interactions prevalent among solute (thymine) and cosolute particles that cause the release of aqueous particles present in 1° and 2° hydration layers of the nitrogenous base. This results in expansion of solution mixture volume and thus rises in apparent molar volumes. In addition, rising temperatures increase the kinetic energy of water molecules, which further releases water around solute into the bulk mixture and increases volume [8].

Table 4.1.1: Densities, ρ and apparent molar volumes, V_{ϕ} of thymine in aqueous media and aqueous glucose/sucrose solutions at T/K = 293.15 - 313.15 and P = 0.1 MPa.

		$V_{\phi} imes 10^6 (ext{m}^3/ ext{mol})$									
m(mol/kg)	T(K)										
	293.15	298.15	303.15	308.15	313.15	293.15	298.15	303.15	308.15	313.15	
				Thym	ine + wa	ter					
0.0000	998.01	996.97	995.42	993.92	992.13						
0.0061	998.34	997.29	995.73	994.22	992.42	71.84	73.52	75.21	76.91	78.63	
0.0120	998.66	997.60	996.03	994.51	992.70	72.16	73.85	75.55	77.27	79.01	
0.0181	998.98	997.91	996.33	994.80	992.98	72.37	74.06	75.77	77.49	79.23	
0.0239	999.29	998.21	996.62	995.08	993.25	72.61	74.31	76.03	77.76	79.51	
0.0298	999.60	998.51	996.91	995.36	993.52	72.69	74.40	76.13	77.87	79.63	
			Thy	mine + 0.0	0501 mol	/kg gluco	se				
0.0000	1001.86	1000.69	999.26	998.13	996.56						
0.0060	1002.19	1001.01	999.57	998.43	996.85	72.39	74.04	75.70	77.36	79.04	
0.0119	1002.50	1001.31	999.86	998.71	997.12	72.78	74.47	76.17	77.87	79.59	
0.0179	1002.81	1001.61	1000.15	998.99	997.39	73.11	74.80	76.51	78.21	79.94	
0.0240	1003.12	1001.91	1000.44	999.27	997.66	73.43	75.13	76.83	78.54	80.27	
0.0300	1003.42	1002.20	1000.72	999.54	997.92	73.71	75.41	77.12	78.84	80.57	
Thymine + 0.0999 mol/kg glucose											
0.0000	1005.23	1004.04	1002.72	1001.07	999.32						

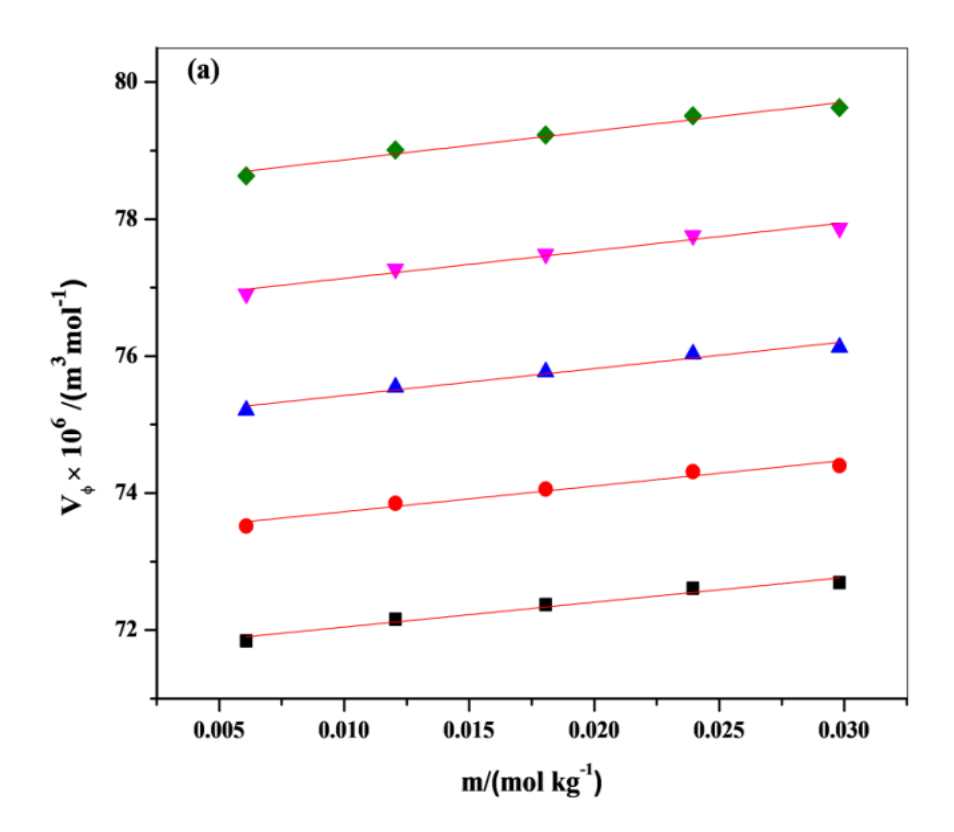
0.0060	1005.55	1004.35	1003.02	1001.36	999.60	73.43	75.08	76.75	78.43	80.13
0.0121	1005.85	1004.64	1003.30	1001.63	999.86	73.93	75.63	77.33	79.05	80.79
0.0180	1006.16	1004.94	1003.59	1001.91	1000.13	74.45	76.13	77.81	79.52	81.24
0.0239	1006.46	1005.23	1003.87	1002.18	1000.39	74.73	76.41	78.10	79.81	81.54
0.0299	1006.76	1005.52	1004.15	1002.45	1000.64	74.94	76.62	78.31	80.02	82.09
			Thy	mine + 0.1	1498 mol/	kg gluce	ose			
0.0000	1008.60	1007.38	1005.84	1004.31	1002.54					
0.0060	1008.91	1007.68	1006.13	1004.59	1002.81	75.30	76.94	78.59	80.26	81.95
0.0119	1009.20	1007.96	1006.40	1004.85	1003.06	75.76	77.43	79.13	80.84	82.56
0.0180	1009.50	1008.25	1006.68	1005.12	1003.32	75.98	77.65	79.34	81.04	82.75
0.0240	1009.79	1008.53	1006.95	1005.38	1003.57	76.18	77.86	79.56	81.26	82.99
0.0300	1010.08	1008.81	1007.22	1005.64	1003.82	76.41	78.09	79.79	81.49	83.22
Thymine + 0.0500 mol/kg sucrose										
0.0000	1005.10	1003.55	1002.17	1000.79	998.79					
0.0060	1005.40	1003.84	1002.45	1001.06	999.05	76.12	77.81	79.50	81.21	82.95
0.0119	1005.69	1004.12	1002.72	1001.32	999.30	76.35	78.06	79.77	81.50	83.26
0.0179	1005.98	1004.40	1002.99	001.58	999.55	76.82	78.53	80.24	81.95	83.71
0.0240	1006.27	1004.68	1003.26	1001.84	999.80	77.10	78.86	80.57	82.28	84.03
0.0300	1006.56	1004.95	1003.52	1002.09	1000.04	77.22	79.25	80.95	82.67	84.42
			Thy	mine + 0.1	1000 mol/	kg sucr	ose			
0.0000	1011.23	1009.58	1008.33	1006.62	1005.28					
0.0060	1011.52	1009.86	1008.60		1005.53		79.03	80.71	82.42	84.13
0.0121	1011.81	1010.14	1008.87	1007.14	1005.78	77.63	79.31	80.98	82.68	84.38
0.0180					1006.02		79.71	81.39	83.09	84.79
0.0239					1006.26		80.17	81.45	83.17	84.87
0.0299	1012.63	1010.93	1009.64	1007.88	1006.50	78.80	80.49	81.86	83.57	84.96
Thymine + 0.1502 mol/kg sucrose										
0.0000		1015.32								
0.0060					1010.80		80.61	82.28	83.96	85.67
0.0119					1011.03		81.00	82.69	84.38	86.11
0.0180					1011.26		81.55	83.23	84.91	86.63
0.0240	1017.87	1016.37	1014.83	1013.38	1011.49	80.10	81.77	83.45	85.13	86.85
0.0300	1018.13	1016.62	1015.07	1013.61	1011.71	80.42	82.09	83.78	85.46	87.18

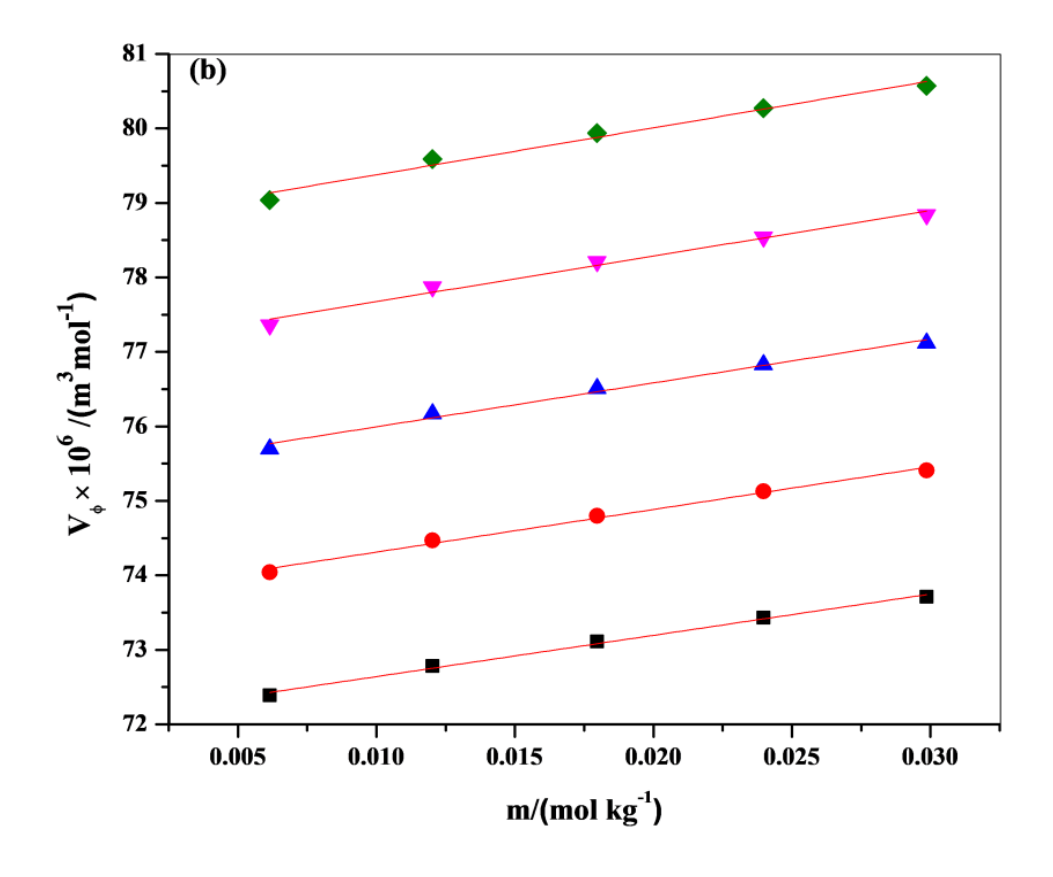
m (mol/kg) symbolizes molality composition of thymine in (water + glucose/sucrose) solutions.

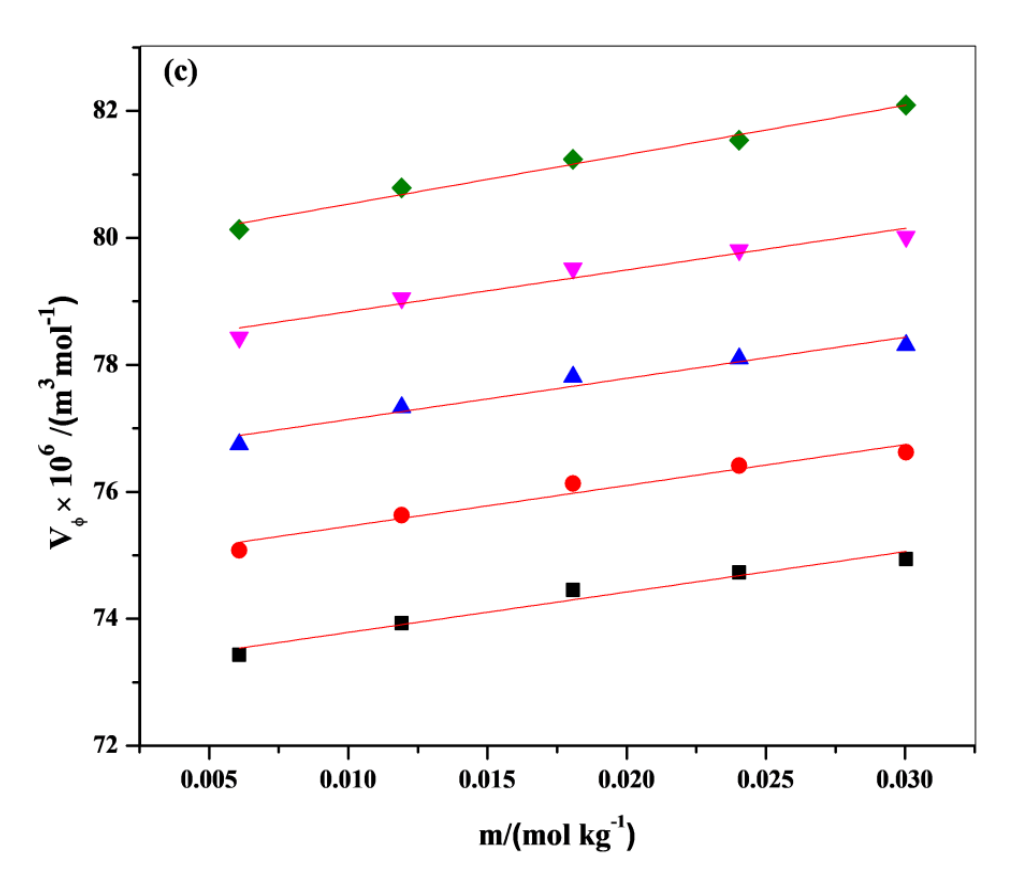
4.1.1.2 Limiting Apparent Molar Volume

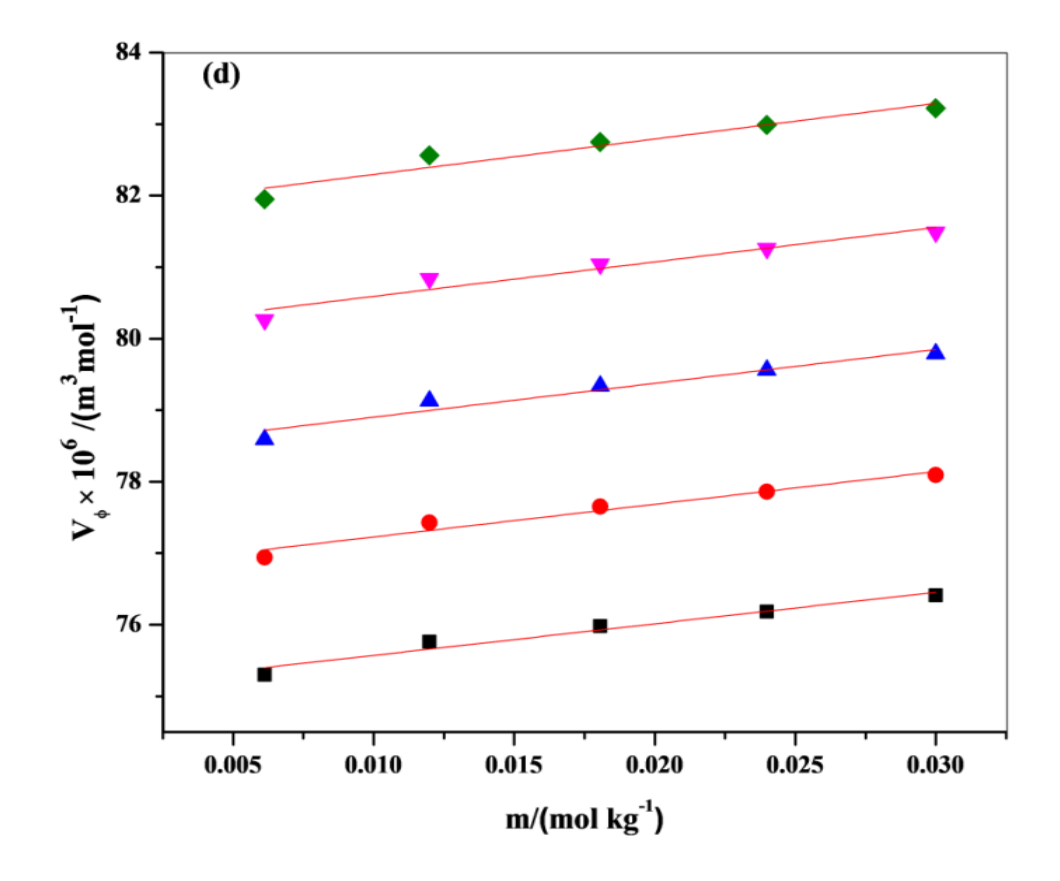
Most common application of apparent molar volume at infinite dilution is for acquiring information concerning the numerous communications that arise amongst the solute and cosolute in binary/ternary mixtures. To assess the V^0_{ϕ} values, the Masson equation [9], or Eqn. (2.2), was used.

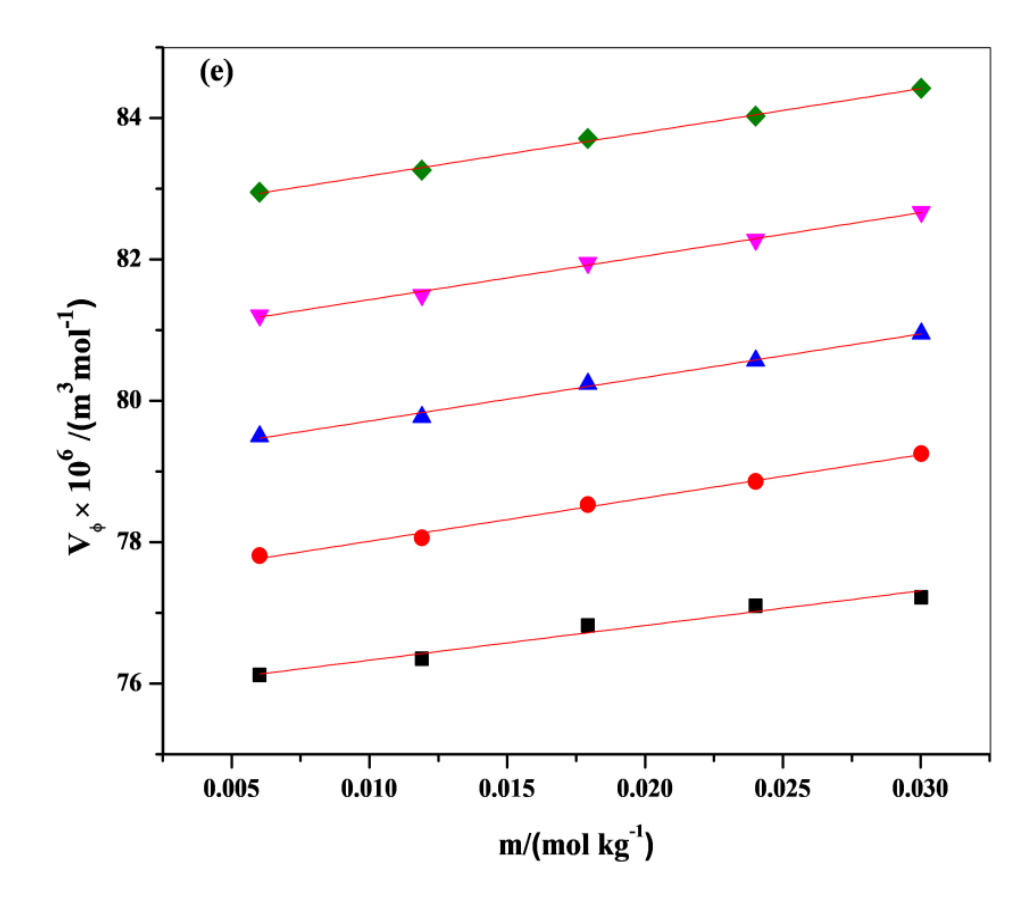
Additionally, Figure 4.1.2 [(a)-(g)] displays the graphs of V_{ϕ} verses molality, m for thymine in H₂O and aqueous mixtures for glucose and sucrose at five temperatures. Additionally, Table 4.1.2 provides the computed values for V_{ϕ}^{0} and S_{v} with their standard deviations. According to this table, there are more solute-solvent synergies when the V_{ϕ}^{0} values escalate as temperature rises and are positive. The size of the solvation shells neighboring the solute moieties may account for an enhancement in V_{ϕ}^{0} values with increasing temp. This observable fact can be interpreted as a result of solvent moieties commencing slack secondary covers of solvation pertaining solute moieties becoming unbound to interior of solution relatively than attaching to the moieties, which causes the mixture volume to expand as temperature rises [10,11].











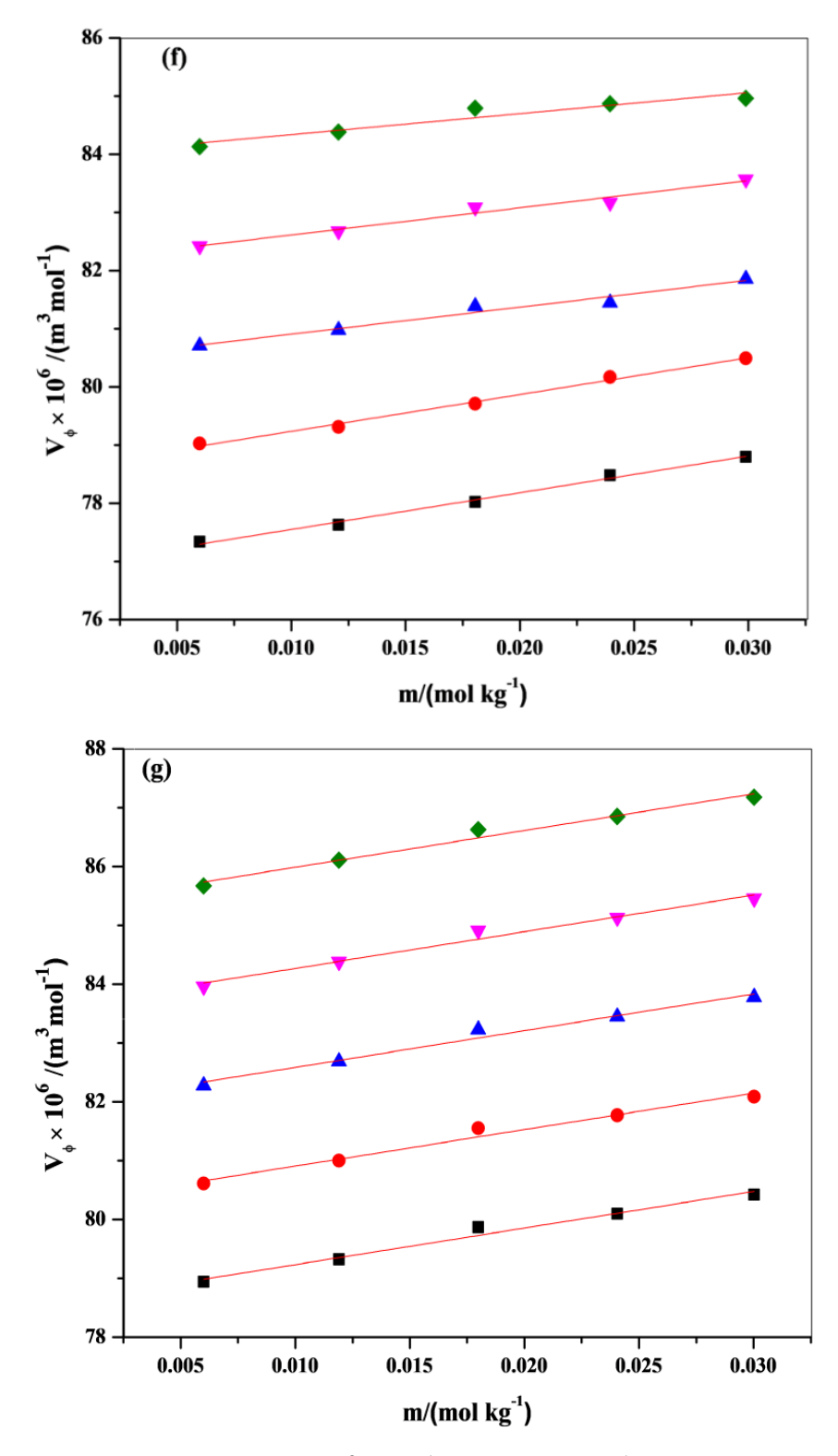


Figure 4.1.2: Graphs of $V_{\phi} \times 10^6 / (\text{m}^3 \text{ mol}^{-1})$ vs $m / (\text{mol kg}^{-1})$ for thymine in (a) water, (b) 0.05 mol kg⁻¹ glucose, (c) 0.10 mol kg⁻¹ glucose, (d) 0.15 mol kg⁻¹ glucose, (e) 0.05 mol kg⁻¹ sucrose, (f) 0.10 mol kg⁻¹ sucrose and (g) 0.15 mol kg⁻¹ sucrose at temperatures, ■ : 293.15 K, ●: 298.15 K, ▲ : 303.15 K, ▼ : 308.15 K, ◆ : 313.15 K.

4.1.1.3 Limiting Apparent Molar Volume of Transfer

Furthermore, transfer attributes that is, $\Delta_{tr}V^0_{\phi}$ provide valuable insights into a variety of solute-cosolute intermolecular interactions. This transfer attribute is free from the solute and solute interaction because the interactions amongst individual solute molecules are insignificant at infinite dilution. Relation (2.4) has been implicated to estimate the transfer volume values of thymine from H₂O to H₂O + glucose/sucrose mixtures.

The deduced values for $\Delta_{tr}V^0_{\phi}$ have been reported in Table 4.1.2 which suggests that the transfer volumes are assessed to be positive at a piece investigational temperature and progresses with progression in molal concentrations of saccharidesin the ternary systems. This might be portrayed through cosphere overlap model put forth by the scientists Friedman and Krishnan, [12,13]. In this study, the interactions amongst hydrophilic groups predominate over those between ion-hydrophobic and hydrophobic and hydrophobic groups which are responsible for the attained positive transfer volume values. Additionally, the following forms of interactions between the solute moieties as well as cosolute moieties have been discussed:

- i. The hydrophilic-hydrophilic synergies amid polar clusters of saccharides molecules and the polar moieties of nitrogenous base i.e. >C-N<, >C=O.
- ii. The hydrophilic type interactions among the polar parts and hydrophobic sites of thymine and glucose/sucrose molecules.
- iii. The hydrophobic type interactions linking the non-polar moieties in solute and sugars.

Typically, interactions of type (i) contribute positively to $\Delta_{tr}V^0_{\phi}$ values, whereas interactions of type (ii) and (iii) contribute negatively. It is clear from Table 4.1.2, type (i) interactions leads in the mixtures under investigation. Furthermore, attendance of more hydroxyl clusters in sucrose than in glucose results in better hydrophilic-hydrophilic connections amid thymine and sucrose contrasted to glucose, resulting to larger transfer values.

Table 4.1.2: Data of limiting molar volumes, V^0_{ϕ} along with slopes, S_{ν} and analogous transfer values $\Delta_{tr}V^0_{\phi}$ for thymine in H₂O and aqueous glucose/sucrose mixtures at T/K = 293.15 - 313.15 and P = 0.1 MPa.

Duonoutu	$T(\mathbf{K})$									
Property	293.15	298.15	303.15	308.15	313.15					
		Thymine in	water							
$V^0_{\phi} \times 10^6 / (\text{m}^3 \text{ mol}^{-1})$	71.68(±0.08)	73.35(±0.07)	75.03(±0.07)	76.73(±0.08)	78.44(±0.08)					
$S_{\nu} \times 10^6 / (\text{m}^3 \text{ mol}^{-2} \text{ kg})$	$36.25(\pm 3.83)$	37.42(±3.78)	39.11(±3.78)	40.63(±3.89)	42.14(±4.02)					
	Thymir	ne in 0.0501 m	ol kg ⁻¹ glucose							
$V^{0}_{\phi} \times 10^{6} / (\mathrm{m}^{3} \; \mathrm{mol}^{-1})$	72.09(±0.04)	73.74(±0.05)	75.41(±0.07)	77.06(±0.08)	78.75(±0.09)					
$S_{\nu} \times 10^6 / (\text{m}^3 \text{ mol}^{-2} \text{ kg})$	55.40(±1.97)	57.25(±2.63)	58.93(±3.38)	61.11(±3.93)	62.96(±4.72)					
$\Delta_{tr}V^0_{\phi} \times 10^6/(\mathrm{m}^3 \mathrm{mol}^{-1})$	0.41	0.39	0.38	0.33	0.31					
Thymine in 0.0999 mol kg ⁻¹ glucose										
$V^{0}_{\phi} \times 10^{6}/(\mathrm{m}^{3} \mathrm{mol}^{-1})$	73.15(±0.14)	74.81(±0.15)	76.49(±0.15)	78.18(±0.16)	79.75(±0.11)					
$S_{\nu} \times 10^6 / (\text{m}^3 \text{ mol}^{-2} \text{ kg})$	63.64(±6.93)	64.29(±7.47)	64.78(±7.67)	65.61(±8.26)	77.76(±5.68)					
$\Delta_{tr}V^0_{\phi}\times 10^6/(\mathrm{m}^3\ \mathrm{mol}^{-1})$	1.47	1.46	1.46	1.45	1.32					
	Thymin	ne in 0.1498 m	ol kg ⁻¹ glucose							
$V^0_{\phi} \times 10^6 / (\mathrm{m}^3 \ \mathrm{mol}^{-1})$	75.13(±0.10)	76.77(±0.11)	78.43(±0.12)	80.11(±0.14)	81.80(±0.15)					
$S_{\nu} \times 10^6 / (\text{m}^3 \text{ mol}^{-2} \text{ kg})$	44.17(±4.85)	45.67(±5.33)	47.34(±6.21)	48.17(±6.99)	49.67(±7.41)					
$\Delta_{tr}V^0_{\phi}\times 10^6/(\mathrm{m}^3\ \mathrm{mol}^{-1})$	3.45	3.42	3.40	3.38	3.36					
	Thymin	e in 0.0500 m	ol kg ⁻¹ sucrose							
$V^0_{\phi} \times 10^6 / (\mathrm{m}^3 \ \mathrm{mol}^{-1})$	75.84(±0.11)	77.40(±0.05)	79.10(±0.05)	80.81(±0.04)	82.56(±0.04)					
$S_{\nu} \times 10^6/(\mathrm{m}^3 \mathrm{mol}^{-2} \mathrm{kg})$	49.07(±5.35)	61.23(±2.67)	61.55(±2.38)	61.56(±1.94)	61.71(±1.80)					
$\Delta_{tr}V^0_{\phi} \times 10^6/(\mathrm{m}^3\ \mathrm{mol}^{-1})$	4.16	4.05	4.07	4.08	4.12					
	Thymin	e in 0.1000 m	ol kg ⁻¹ sucrose							
$V^{\theta_{\phi}} \times 10^6/(\mathrm{m}^3 \mathrm{mol}^{-1})$	76.92(±0.05)	78.60(±0.06)	80.44(±0.09)	82.14(±0.09)	83.98(±0.12)					
$S_v \times 10^6/(\mathrm{m}^3 \mathrm{mol}^{-2} \mathrm{kg})$	63.14(±2.78)	63.31(±2.95)	46.42(±4.79)	46.75(±4.42)	36.06(±6.21)					
$\Delta_{tr}V^0_{\phi}\times 10^6/(\mathrm{m}^3\ \mathrm{mol}^{-1})$	5.24	5.25	5.41	5.42	5.54					
	Thymin	ne in 0.1502 m	ol kg ⁻¹ sucrose							
$V^0_{\phi} imes 10^6 / ({ m m}^3 \ { m mol}^{-1})$	78.61(±0.10)	80.29(±0.10)	81.96(±0.10)	83.65(±0.10)	85.36(±0.10)					
$S_{\nu} \times 10^6/(\mathrm{m}^3 \mathrm{mol}^{-2} \mathrm{kg})$	62.17(±4.90)	62.00(±5.11)	62.49(±5.06)	62.32(±5.04)	62.49(±5.15)					
$\Delta_{tr}V^0_{\phi}\times 10^6/(\mathrm{m}^3\ \mathrm{mol}^{-1})$	6.93	6.94	6.93	6.92	6.92					

4.1.1.4 Limiting Apparent Molar Expansibility

The limiting apparent molar volume relies on temperature as per the polynomial equation (2.7). In the Conducted case, 303.15 K is taken as reference temperature.

Table 4.1.3: Deduced data of constants (a, b and c) for thymine in H₂O and aqueous saccharide (glucose/sucrose) solvent systems at T/K = 293.15 - 313.15 and P = 0.1 MPa.

System	$a \times 10^6 (\text{m}^3/\text{mol})$	$b \times 10^6 (\mathrm{m}^3/\mathrm{mol}/\mathrm{K})$	$c \times 10^6 (\mathrm{m}^3/\mathrm{mol}/\mathrm{K}^2)$
Thymine + water	75.03(±0.01)	0.3380(±0.0001)	-0.0003(±0.00002)
Thymine + 0.0501 mol/kg glucose	75.40(±0.01)	0.3328(±0.0006)	-0.0002(±0.00010)
Thymine + 0.0999 mol/kg glucose	76.49(±0.02)	0.3318(±0.0019)	-0.0004(±0.00030)
Thymine + 0.1498 mol/kg glucose	78.43(±0.01)	0.3340(±0.0001)	-0.0003(±0.00003)
Thymine + 0.0500 mol/kg sucrose	79.08(±0.02)	0.3370(±0.0015)	-0.0012(±0.00030)
Thymine + 0.1000 mol/kg sucrose	80.39(±0.03)	0.3532(±0.0031)	-0.0005(±0.00052)
Thymine + 0.1502 mol/kg sucrose	81.96(±0.01)	0.3372(±0.0004)	-0.0002(±0.00008)

Table 4.1.3 provides the inferred values of the aforementioned constants. Additionally, limiting apparent molar expansibility (E^0_ϕ) has been considered as a qualitative criterion for analysis of the various solute-cosolute interactions in the solution samples. It has been assessed using the expression (2.8). The E^0_ϕ values are displayed in Table 4.1.4 which indicates that the evaluated E^0_ϕ are positive at all studies temperature as well as concentrations. This might be due to packing or caging effect [14-16]. On changing the solvent media from H₂O to saccharides, volume of hydration shells for thymine increases; which in turn results to increase in expansibility of solutions.

Further, to determine structure breaking/making ability of specific compound, Hepler [17] gave the general thermodynamic relation (2.10).

Hepler states that sign of first derivative of E^0_{ϕ} or partial molar expansibilities that is, $(\partial E^0_{\phi}/\partial T)_P$, provides significant details on whether the solute in consideration is chaotropic, or a structure breaker or kosmotropic, or a structure maker. The negative sign of deduced Hepler's constant (as displayed in the Table 4.1.4) denotes thymine's capacity to break down structural bonds in water, together with the aqueous glucose/sucrose samples.

Table 4.1.4: Deduced data of limiting molar expansibilities, E^0_{ϕ} as well as Hepler's constant, $(\partial E^0_{\phi}/\partial T)_P$ for thymine in H₂O along with H₂O + saccharide solvent systems at discrete temperatures.

System		$\frac{(\partial E^0_{\phi}/\partial T)_P}{(\mathbf{m}^3/\mathbf{mol/K}^2)}$				
	293.15	298.15	303.15	308.15	313.15	_(// /
Thymine + water	0.344	0341	0.338	0.335	0.332	-0.0006
Thymine + 0.0501 mol/kg glucose	0.337	0.335	0.333	0.331	0.329	-0.0004
Thymine + 0.0999 mol/kg glucose	0.339	0.336	0.332	0.328	0.324	-0.0008
Thymine + 0.1498 mol/kg glucose	0.340	0.337	0.334	0.331	0.328	-0.0006
Thymine + 0.0500 mol/kg sucrose	0.361	0.349	0.337	0.325	0.313	-0.0024
Thymine + 0.1000 mol/kg sucrose	0.363	0.358	0.353	0.348	0.343	-0.0010
Thymine + 0.1502 mol/kg sucrose	0.341	0.339	0.337	0.335	0.333	-0.0004

4.1.1.5 Apparent Specific Volume

A hydrological packaging of the solute particles in hydrated media can be represented by the critical parameter defined as apparent specific volumes (ASV), and it is associated with volumes of solute moieties inside the solution. It has been a useful measure to determine how a solute tastes or smells at diverse concentrations or solvent mediums.

Table 4.1.5: Anticipated data of *ASV* for thymine in water and saccharide solvent systems at varied Temp. = (293.15 - 313.15) K.

m(mol/kg)			$T(\mathbf{K})$			
	293.15	298.15	303.15	308.15	313.15	
	Th	ymine + water				
0.0000						
0.0061	0.57	0.58	0.60	0.61	0.62	
0.0120	0.57	0.59	0.60	0.61	0.63	
0.0181	0.57	0.59	0.60	0.61	0.63	
0.0239	0.58	0.59	0.60	0.62	0.63	
0.0298	0.58	0.59	0.60	0.62	0.63	
	Thymine +	0.0501 mol/kg s	glucose			
0.0000	-					
0.0060	0.57	0.59	0.60	0.61	0.63	
0.0119	0.58	0.59	0.60	0.62	0.63	
0.0179	0.58	0.59	0.61	0.62	0.63	
0.0240	0.58	0.59	0.61	0.62	0.64	
0.0300	0.58	0.60	0.61	0.62	0.64	
	Thymine +	0.0999 mol/kg	glucose			
0.0000						
0.0060	0.58	0.59	0.61	0.62	0.63	

0.0121	0.59	0.60	0.61	0.63	0.64
0.0180	0.59	0.60	0.62	0.63	0.64
0.0239	0.59	0.61	0.62	0.63	0.65
0.0299	0.59	0.61	0.62	0.63	0.65
	Thymine+	0.1498 mol/kg	glucose		
0.0000					
0.0060	0.59	0.61	0.62	0.64	0.65
0.0119	0.60	0.61	0.63	0.64	0.65
0.0180	0.60	0.62	0.63	0.64	0.66
0.0240	0.60	0.62	0.63	0.64	0.66
0.0300	0.61	0.62	0.63	0.65	0.66
	Thymine +	0.0500 mol/kg	sucrose		
0.0000					
0.0060	0.60	0.62	0.63	0.64	0.66
0.0119	0.60	0.62	0.63	0.65	0.66
0.0179	0.61	0.62	0.64	0.65	0.66
0.0240	0.61	0.62	0.64	0.65	0.67
0.0300	0.61	0.63	0.64	0.66	0.67
	Thymine +	0.1000 mol/kg	sucrose		
0.0000					
0.0060	0.61	0.63	0.64	0.65	0.67
0.0121	0.62	0.63	0.64	0.66	0.67
0.0180	0.62	0.63	0.64	0.66	0.67
0.0239	0.62	0.63	0.65	0.66	0.67
0.0299	0.62	0.64	0.65	0.66	0.67
	Thymine +	0.1502 mol/kg	sucrose		
0.0000					
0.0060	0.62	0.64	0.65	0.67	0.68
0.0119	0.63	0.64	0.66	0.67	0.68
0.0180	0.63	0.65	0.66	0.67	0.69
0.0240	0.63	0.65	0.66	0.67	0.69
0.0300	0.64	0.65	0.66	0.68	0.69

In conducted research work, the *ASV* parameter is evaluated by using the Eqn. (2.11). The estimated *ASV* for thymine is displayed in Table 4.1.5 that ranges from 0.57×10^{-3} m³ kg⁻¹ mol⁻¹ to 0.69×10^{-3} m³ kg⁻¹ mol⁻¹, indicating clear sweet taste in water or aqueous glucose and sucrose media.

4.1.2 Speed of Sound Data

Table 4.1.6 enlists the empirical estimates of the solute's or thymine's ultrasonic velocity, in both aqueous and binary aqueous sucrose/glucose medium at T = 293.15 K - 313.15 K. It can be deduced from the table that sound speed increase with increasing temperature or molal concentration.

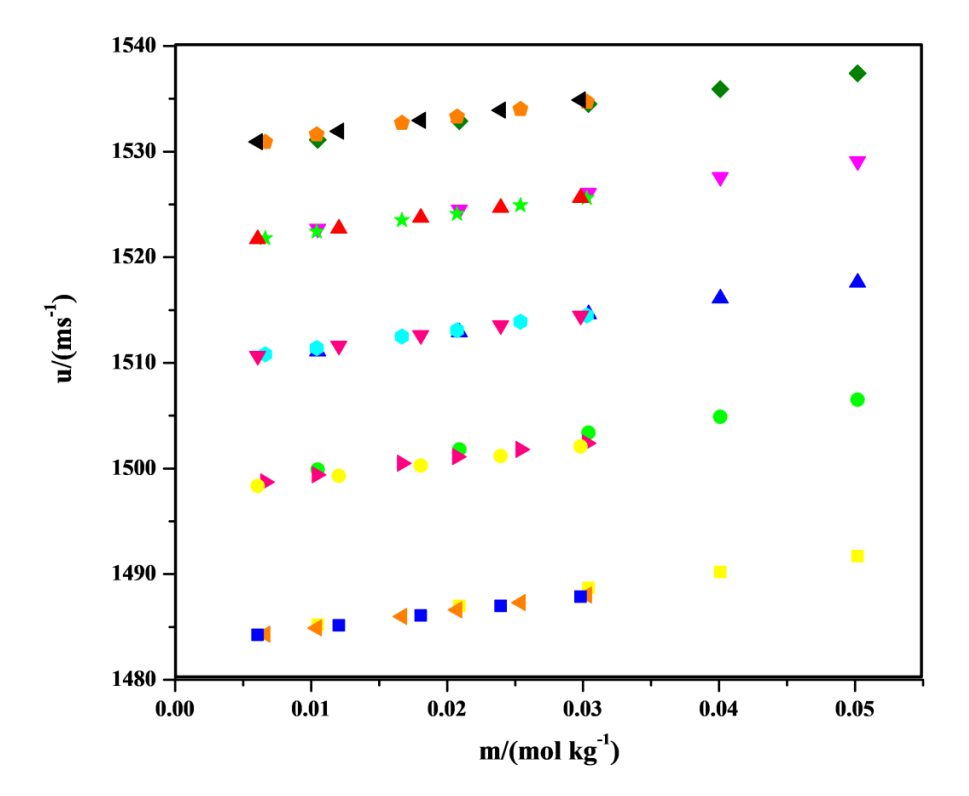
The experimentally obtained sound velocity for thymine [4,5], glucose [6] as well as sucrose [7] in aqueous media have been contrasted with literature reports and portrayed in Figure 4.1.3 (a, b and c). These Figures further demonstrate the strong concordance between published data and empirically determined sound velocities.

4.1.2.1 Apparent Molar Isentropic Compressions

The exploratory density and velocity of sound data were utilized for the estimation of apparent molar isentropic compression as per the equation (2.12). By the use of the Newton-Laplace relation, the adiabatic compressibilities have been inferred, as per the relations (2.13) and (2.14).

Further, the figured data of $K_{\phi,s}$ has been itemized in Table 4.1.6. Moreover, $K_{\phi,s}$ is recognized to have negative sign at all molalities and temperatures, also their magnitude decreases as glucose/sucrose concentration rises.

The compressibility of H₂O molecules is indicated by negative sign of $K_{\phi,s}$, and this also suggest that presence of solute molecules have a strong ordering influence on the solvent particles [18,19].



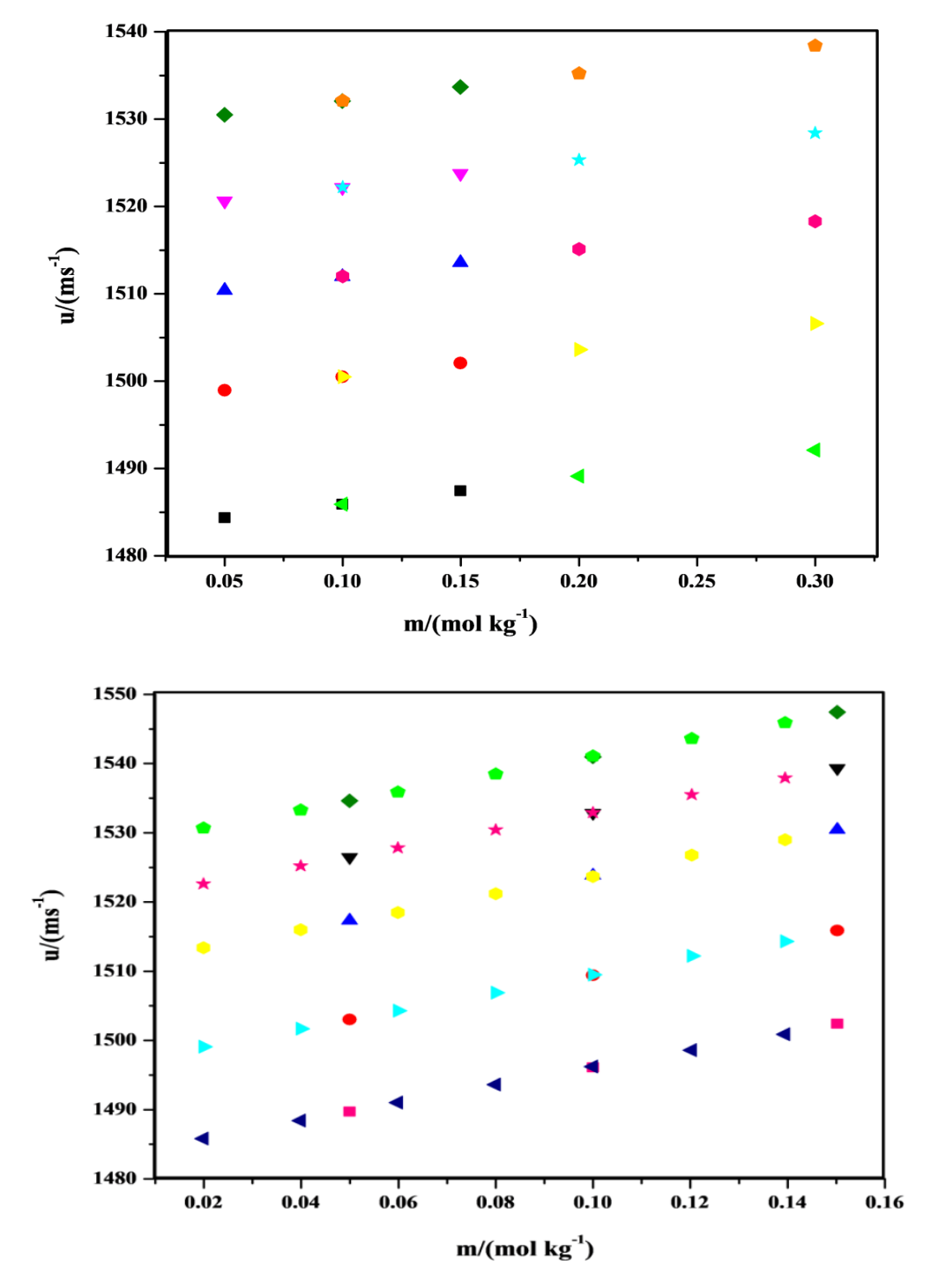


Figure 4.1.3(a): Comparison graph of sound speed vs molality with literature for thymine in water at diverse T(K). □: Lit. [5] on 293.15, •: Lit. [5] on 298.15, •: Lit. [5] on 303.15, •: Lit. [5] on 313.15, •: Lit. [4] on 293.15, •: Lit. [4] on 293.15, •: Lit. [4] on 303.15, •: Lit. [4] on 308.15, •: Lit. [4] on 313.15, •: Conducted investigation on 293.15, •: Conducted investigation on 303.15, •: Conducted investigation on 308.15, •: Conducted investigation on 313.15.

- (b) Comparison graph of sound speed vs molality with literature for glucose in water at diverse *T*(K). : Conducted investigation on 293.15, : Conducted investigation on 298.15, ▲ : Conducted investigation on 303.15, ▼ : Conducted investigation on 308.15, : Conducted investigation on 313.15, : Lit. [6] on 293.15, ▷ : Lit. [6] on 298.15, : Lit. [6] on 303.15, ★ : Lit. [6] on 308.15, : Lit. [6] on 313.15.
- (c) Comparison graph of sound speed vs molality with literature for sucrose in water at diverse *T*(K). : Conducted investigation on 293.15, : Conducted investigation on 298.15, ▲ : Conducted investigation on 303.15, ▼ : Conducted investigation on 308.15, : Conducted investigation on 313.15, : Lit. [7] on 293.15, ▷ : Lit. [7] on 298.15, : Lit. [7] on 303.15, ★ : Lit. [7] on 308.15, : Lit. [7] on 313.15.

Table 4.1.6: Sound velocities, u and apparent molar isentropic compression, $K_{\phi,s}$ of thymine in aqueous media and aqueous glucose/sucrose solutions at Temp. = (293.15 – 313.15) K and Pressure = 0.1 MPa.

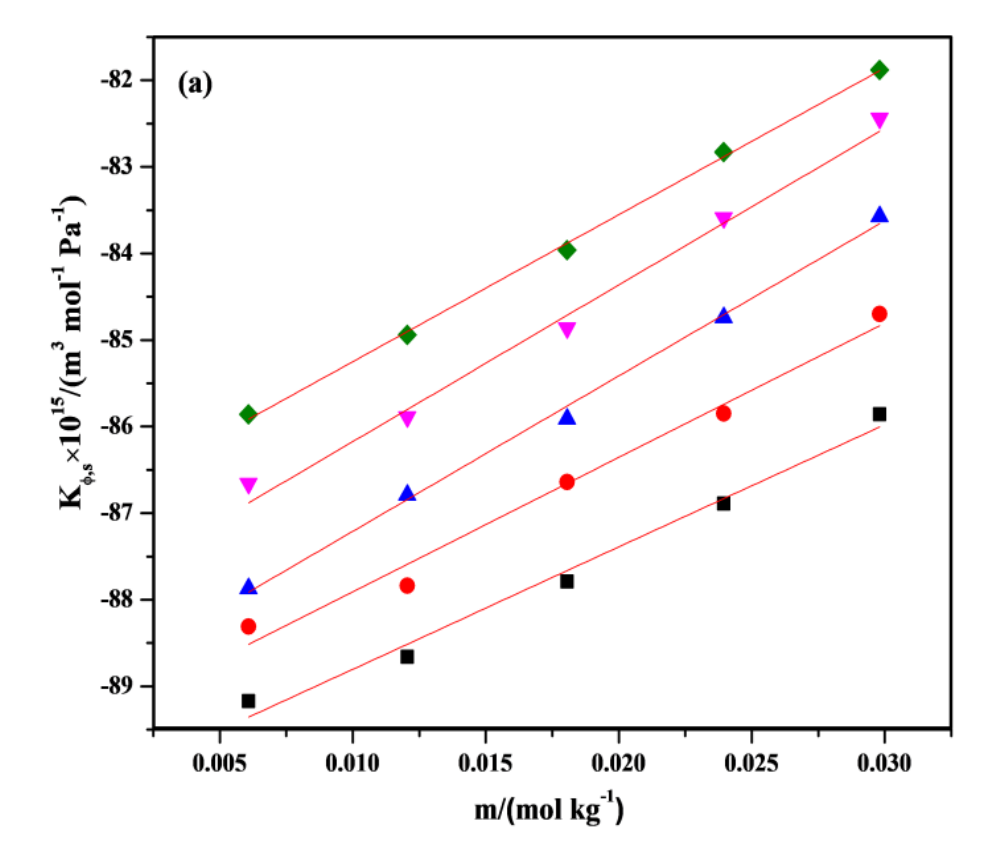
			<i>u</i> (m/s)		$K_{\phi,s} \times 10^{15} \text{ (m}^3\text{/mol/Pa)}$					
m(mol/kg)					T(K)					
	293.15	298.15	303.15	308.15	313.15	293.15	298.15	303.15	308.15	313.15
				Thymir	ne + water					
0.0000	1483.26	1497.34	1509.62	1520.69	1529.84					
0.0061	1484.22	1498.33	1510.64	1521.73	1530.90	-89.17	-88.31	-87.87	-86.66	-85.86
0.0120	1485.16	1499.30	1511.63	1522.74	1531.93	-88.66	-86.84	-85.95	-85.25	-84.94
0.0181	1486.09	1500.25	1512.61	1523.74	1532.95	-87.79	-86.64	-85.91	-85.06	-83.96
0.0239	1486.99	1501.18	1513.55	1524.70	1533.93	-86.89	-85.85	-84.74	-83.59	-82.83
0.0298	1487.86	1502.07	1514.46	1525.63	1534.89	-85.86	-84.7	-83.57	-82.44	-81.88
			Thy	mine+ 0.05	01 mol/kg	glucose				
0.0000	1484.36	1498.96	1510.39	1520.63	1530.48					
0.0060	1485.33	1499.96	1511.41	1521.67	1531.54	-87.44	-86.52	-86.21	-85.09	-84.13
0.0119	1486.25	1500.90	1512.38	1522.66	1532.54	-86.70	-85.35	-84.60	-83.99	-83.06
0.0179	1487.16	1501.84	1513.33	1523.64	1533.53	-85.51	-84.35	-83.79	-83.66	-81.80
0.0240	1488.07	1502.77	1514.29	1524.63	1534.52	-84.41	-83.11	-82.65	-82.54	-80.69
0.0300	1488.94	1503.67	1515.22	1525.58	1535.48	-83.28	-82.11	-81.90	-81.43	-79.78
			Thyr	nine + 0.09	99 mol/kg	glucose				
0.0000	1485.91	1500.48	1511.97	1522.16	1532.06					
0.0060	1486.87	1501.47	1512.98	1523.19	1533.11	-85.37	-84.51	-83.26	-82.30	-81.41
0.0121	1487.79	1502.41	1513.94	1524.17	1534.12	-84.88	-83.57	-82.34	-81.41	-81.01

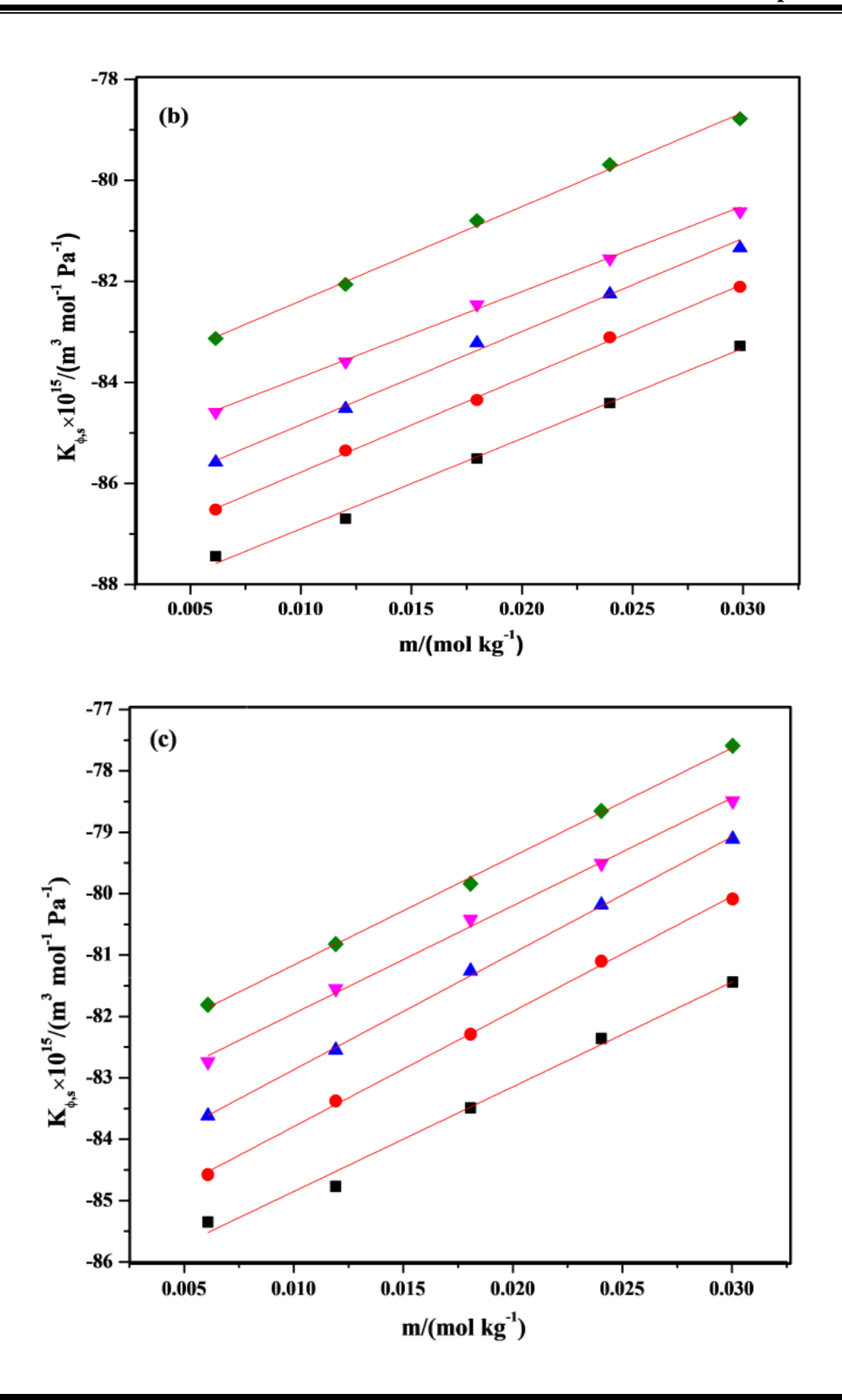
0.0180	1488.73	1503.38	1514.94	1525.19	1535.16	-83.33	-82.21	-81.32	-80.39	-79.83			
0.0239	1489.64	1504.31	1515.89	1526.17	1536.15	-82.46	-81.20	-80.25	-79.57	-78.71			
0.0299	1490.53	1505.22	1516.82	1527.13	1537.14	-81.38	-80.05	-79.07	-78.54	-77.61			
			Thy	nine + 0.14	198 mol/kg	glucose							
0.0000	1502.4	1515.2	1526.8	1536.6	1544.7								
0.0060	1503.9	1516.8	1528.4	1538.3	1546.4	-82.99	-81.21	-80.05	-79.10	-78.25			
0.0119	1505.4	1518.3	1529.9	1539.8	1547.9	-81.72	-80.47	-79.33	-78.40	-77.10			
0.0180	1506.9	1519.8	1531.6	1541.5	1549.6	-80.32	-79.26	-78.44	-77.22	-76.09			
0.0240	1508.6	1521.5	1533.3	1543.3	1551.4	-79.33	-78.38	-77.27	-76.14	-75.10			
0.0300	1509.9	1522.9	1534.8	1544.7	1552.9	-78.21	-77.13	-76.23	-75.16	-74.00			
Thymine + 0.0500 mol/kg sucrose													
0.0000	1489.73	1503.04	1517.32	1526.47	1534.63								
0.0060	1490.73	1504.05	1518.36	1527.51	1535.68	-87.38	-84.82	-84.02	-81.29	-79.82			
0.0119	1491.71	1505.03	1519.35	1528.51	1536.68	-86.75	-84.20	-82.47	-80.22	-78.29			
0.0179	1492.68	1506.02	1520.37	1529.53	1537.71	-85.63	-83.11	-81.71	-79.32	-77.56			
0.0240	1493.66	1507.01	1521.37	1530.53	1538.72	-84.69	-82.19	-80.51	-78.05	-76.39			
0.0300	1494.61	1507.96	1522.34	1531.52	1539.70	-83.74	-80.97	-79.31	-77.20	-75.22			
			Thyı	nine + 0.10	000 mol/kg	sucrose							
0.0000	1496.11	1509.42	1523.85	1532.85	1540.96								
0.0060	1497.12	1510.45	1524.91	1533.90	1542.02	-88.41	-86.74	-84.92	-82.32	-80.82			
0.0121	1498.09	1511.44	1525.91	1534.91	1543.07	-88.03	-86.37	-84.57	-81.94	-81.81			
0.0180	1499.12	1512.48	1526.97	1535.98	1544.11	-87.75	-85.77	-83.97	-81.67	-79.57			
0.0239	1500.09	1513.45	1527.94	1536.97	1545.08	-86.82	-84.46	-82.23	-80.33	-77.95			
0.0299	1501.04	1514.44	1528.92	1537.97	1546.07	-85.71	-83.9	-81.21	-79.56	-76.72			
			Thyı	mine + 0.15	502 mol/kg	sucrose							
0.0000	1502.42	1515.88	1530.45	1539.33	1547.42								
0.0060	1503.46	1516.93	1531.52	1540.41	1548.50		-81.36	-79.64	-77.98	-75.67			
0.0119	1504.46	1517.95	1532.56	1541.45	1549.54	-82.46	-80.44	-78.75	-76.64	-74.34			
0.0180	1505.49	1518.99	1533.63	1542.51	1550.61	-81.53	-79.38	-78.10	-75.47	-73.47			
0.0240	1506.48	1520.01	1534.65	1543.55	1551.66	-80.21	-78.47	-76.59	-74.52	-72.69			
0.0300	1507.45	1520.99	1535.66	1544.58	1552.67	-79.14	-77.28	-75.65	-73.86	-71.60			

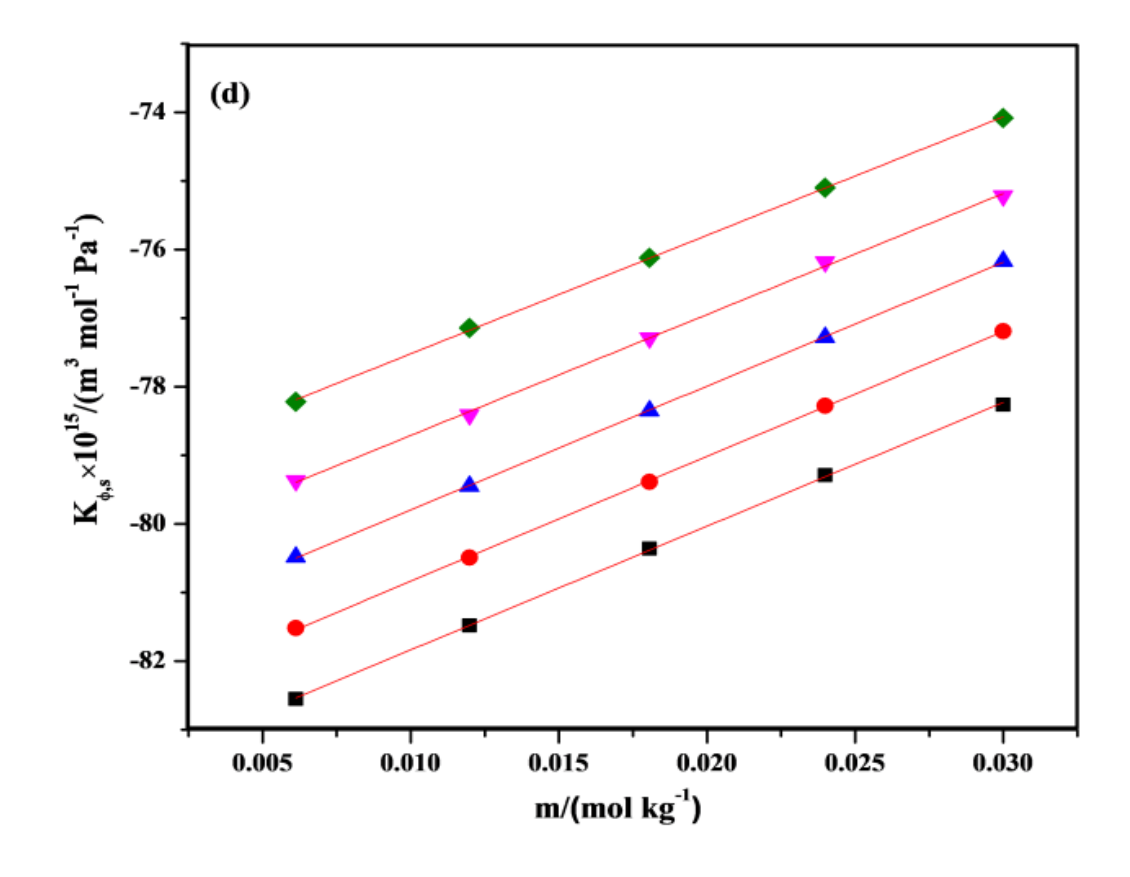
m(mol/kg) stands for molality of thymine in H_2O and varied (water + glucose/sucrose) mixtures.

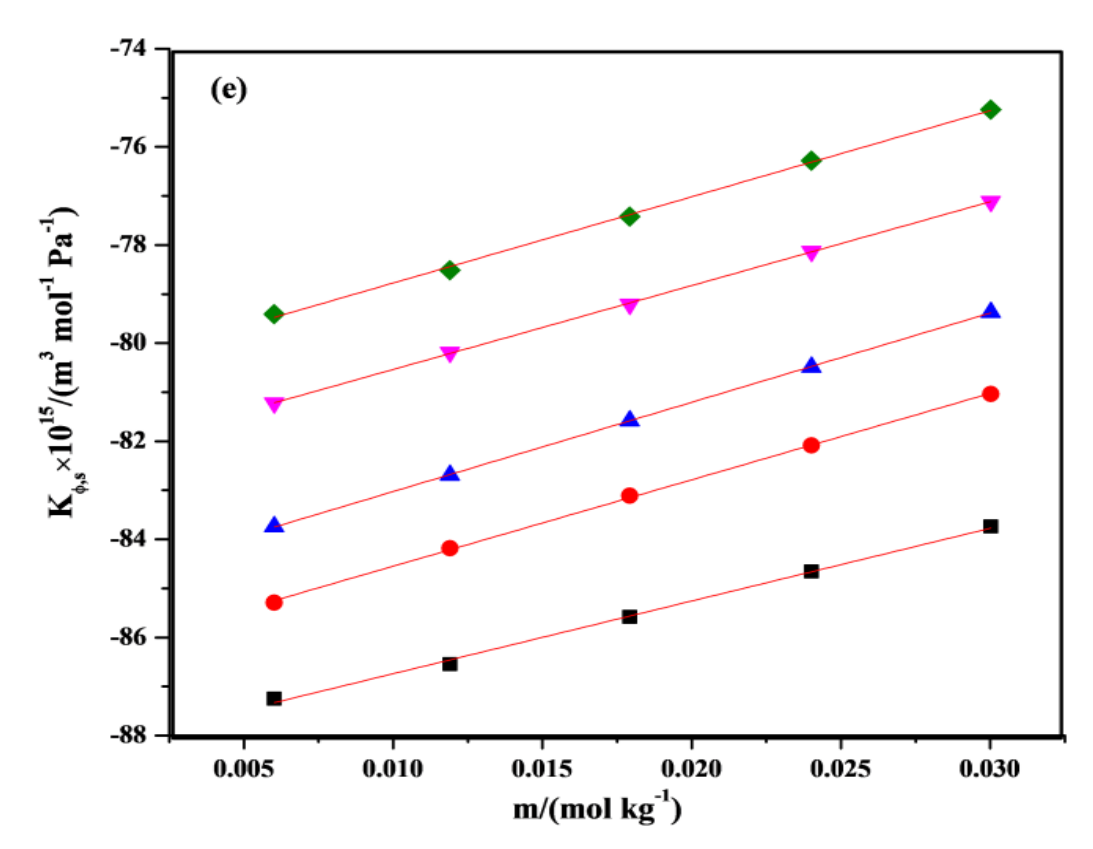
4.1.2.2 Limiting Apparent Molar Isentropic Compression

The limiting apparent molar isentropic compression ($K^0_{\phi,s}$) furnishes commendable data related to the extent of interactions acting in the explored systems. By creating the plots of $K_{\phi,s}$ against m, we obtain the intercept ($K^0_{\phi,s}$) and slope (S_k) as illustrated by equation (2.15). Furthermore, it can be deduced from Table 4.1.7 that as temperature rises, the $K^0_{\phi,s}$ values of thymine grow less negative, which can be explained by considering various models [20,21]. These simulations suggest that water undergoes electrostriction around solute molecules, rendering the molecules more compressible than bulk water with an open structure. Also, the suppression in electrostriction of water happens with the addition of cosolute (glucose/sucrose) possibly due to better interactions among thymine and saccharides. Additionally, plots of $K_{\phi,s}$ of thymine in H₂O as well as aqueous glucose and sucrose mixtures against molal concentration, m are shown in Figure 4.1.4 (a) to (g).









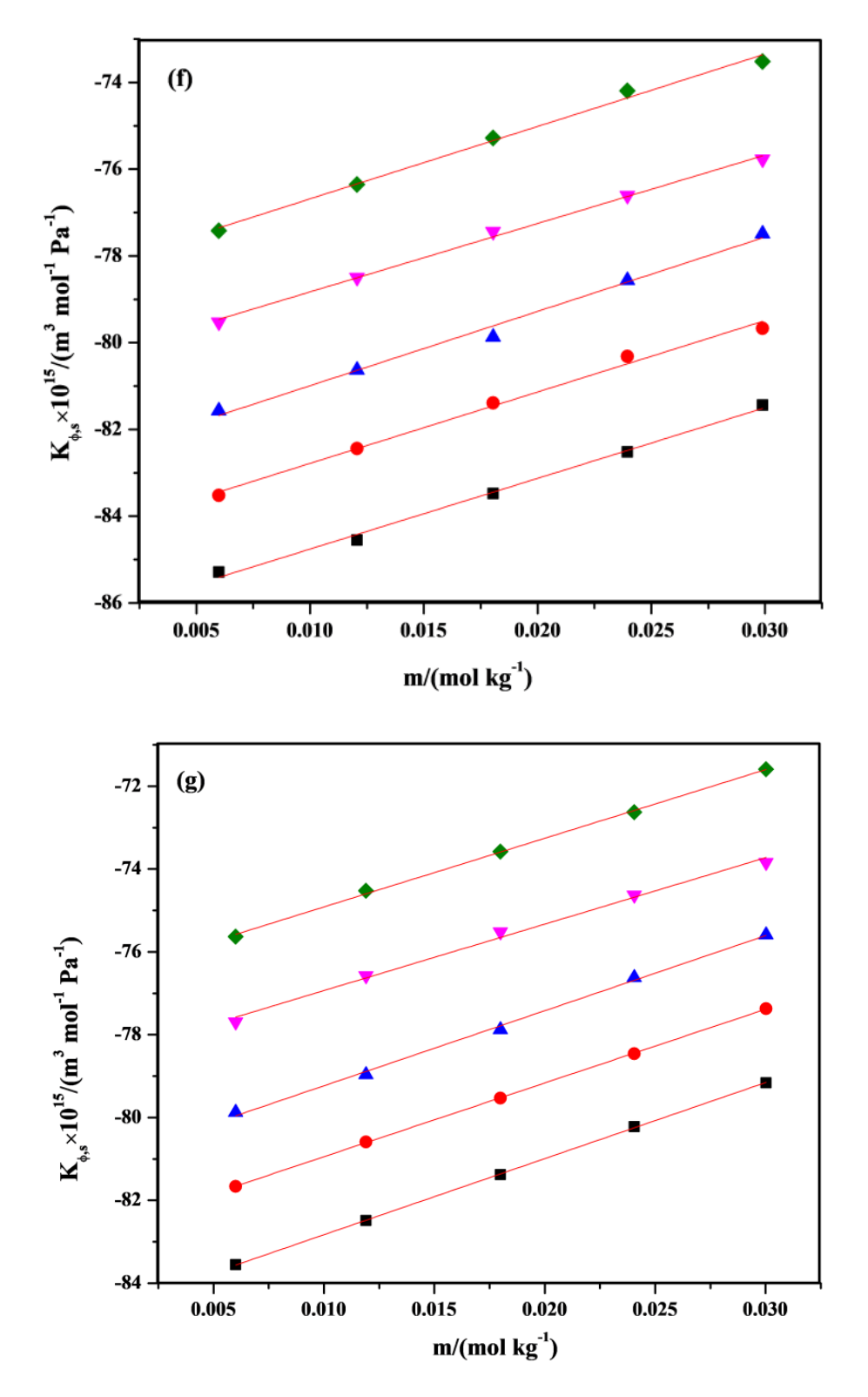


Figure 4.1.4: Graph of $K_{\phi,s} \times 10^{15} / (\text{m}^3 \, \text{mol}^{-1} \, \text{Pa}^{-1})$ vs $m / (\text{mol kg}^{-1})$ for thymine in (a) water, (b) 0.05 mol kg⁻¹ glucose, (c) 0.10 mol kg⁻¹ glucose, (d) 0.15 mol kg⁻¹ glucose, (e) 0.05 mol kg⁻¹ sucrose, (f) 0.10 mol kg⁻¹ sucrose and (g) 0.15 mol kg⁻¹ sucrose at $T = \blacksquare$: 293.15 K, ●: 298.15 K, ▲: 303.15 K, ▼: 308.15 K,

4.1.2.3 Limiting Apparent Molar Isentropic Compression of Transfer

For thymine, the limiting apparent molar isentropic compression of transfer from water to aqueous glucose/sucrose media has been fetched by the use of equation (2.16). Table 4.1.7 gives the values for $\Delta_{tr}K^0_{\phi,s}$. The positive transfer results show that interactions of the hydrophilic kind are preferred over those of the hydrophobic type. Additionally, the positive transfer values become stronger as the cosolute concentration rises. As such, the outcomes of acoustic analyses are more consistent with the findings of volumetric studies.

Table 4.1.7: Data of apparent molar isentropic compression at dilution (infinite), $K^0_{\phi,s}$ along with S_k slopes besides corresponding transfer values $\Delta_{tr}K^0_{\phi,s}$ for thymine in water as well as aqueous glucose/sucrose solutions T/K = 293.15 - 313.15 and Pressure = 0.1 MPa.

Duomontes			T(K)		
Property	293.15	298.15	303.15	308.15	313.15
		Thymine + v	vater		
$\overline{K^0_{\phi,s} \times 10^{15} \text{ (m}^3 /\text{mol/ Pa)}}$	-90.21(±0.19)	-89.46(±0.22)	-89.00(±0.11)	-87.98(±0.27)	-86.95(±0.07)
$S_k \times 10^{15} (\mathrm{m}^3 \mathrm{kg} / \mathrm{mol}^2 / \mathrm{Pa})$	a) 141.27(±9.54) 155.11(±11.29) 179.36(±5.70)		180.82(±13.82)	169.62(±3.56)	
	Thy	mine + 0.0501 m	ol/kg glucose		
$\overline{K^0_{\phi,s} \times 10^{15} \text{ (m}^3 /\text{mol/ Pa)}}$	-88.68(±0.14)	-87.64(±0.06)	-86.68(±0.32)	-85.59(±0.23)	-84.25(±0.11)
$S_k \times 10^{15} (\mathrm{m}^3 \mathrm{kg /mol^2 /Pa})$	$178.71(\pm 7.14)$	186.26(±3.28)	184.33(±16.25)	169.69(±11.67)	186.43(±5.41)
$\Delta_{tr} K^0_{\phi,s} \times 10^{15} (\text{m}^3 / \text{mol/ Pa})$	1.53	1.82	2.32	2.39	2.70
	Thy	mine + 0.0999 m	ol/kg glucose		
$\overline{K^0_{\phi,s} \times 10^{15} \text{ (m}^3 /\text{mol/ Pa)}}$	-86.56(±0.19)	-85.67(±0.07)	-84.77(±0.06)	-83.71(±0.11)	-82.93(±0.07)
$S_k \times 10^{15} (\mathrm{m}^3 \mathrm{kg /mol^2 /Pa})$	$170.55(\pm 9.55)$	187.58(±3.39)	189.79(±16.25)	175.58(±5.39)	176.77(±3.67)
$\Delta_{tr} K^0_{\phi,s} \times 10^{15} (\text{m}^3 / \text{mol/ Pa})$	3.65	3.79 4.23		4.27	4.02
	Thy	mine + 0.1498 m	ol/kg glucose		
$\overline{K^0_{\phi,s} \times 10^{15} \text{ (m}^3 /\text{mol/ Pa)}}$	-83.64(±0.03)	-82.66(±0.02)	-81.60(±0.02)	-80.47(±0.06)	-79.25(±0.03)
$S_k \times 10^{15} (\mathrm{m}^3 \mathrm{kg /mol^2 /Pa})$	$180.31(\pm 1.41)$	181.99(±1.06)	$180.65(\pm0.87)$	176.30(±2.75)	$172.76(\pm 1.58)$
$\Delta_{tr} K^0_{\phi,s} \times 10^{15} (\text{m}^3 / \text{mol/ Pa})$	6.57	6.80	7.40	7.51	7.70
	Thy	mine + 0.0500 m	ol/kg sucrose		
$\overline{K^0_{\phi,s} \times 10^{15} \text{ (m}^3 /\text{mol/ Pa)}}$	-88.22(±0.08)	-86.31(±0.04)	-84.84(±0.01)	-82.25(±0.02)	-80.53(±0.06)
$S_k \times 10^{15} (\mathrm{m}^3 \mathrm{kg /mol^2 /Pa})$	148.24(±3.85)	176.13(±2.14)	181.97(±0.75)	170.99(±1.15)	175.85(±3.27)
$\Delta_{tr} K^0_{\phi,s} \times 10^{15} (\text{m}^3 / \text{mol/ Pa})$	1.99	3.15	4.16	5.73	6.42
	Thy	mine + 0.1000 m	ol/kg sucrose		
$\overline{K^0_{\phi,s} \times 10^{15} \text{ (m}^3 / \text{mol/ Pa)}}$	-86.39(±0.12)	-84.43(±0.15)	-82.70(±0.18)	-80.41(±0.09)	-78.35(±0.06)

$S_k \times 10^{15} (\text{m}^3 \text{ kg /mol}^2 /\text{Pa})$	162.96(±6.06)	164.55(±7.77)	171.32(±9.07)	157.68(±4.91)	$166.89(\pm 7.49)$				
$\Delta_{tr} K^0_{\phi,s} \times 10^{15} (\text{m}^3/\text{mol/Pa})$	3.82	5.03	6.30	7.57	8.60				
Thymine + 0.1502 mol/kg sucrose									
$K^0_{\phi,s} \times 10^{15} (\text{m}^3 / \text{mol} / \text{Pa})$	-84.66(±0.02)	-82.73(±0.02)	-81.05(±0.09)	-78.54(±0.13)	-76.57(±0.06)				
$S_k \times 10^{15} (\text{m}^3 \text{ kg /mol}^2 /\text{Pa})$	183.68(±1.17)	178.02(±0.79)	181.22(±4.94)	160.39(±6.75)	165.69(±3.19)				
$\Delta_{tr} K^0_{\phi,s} \times 10^{15} (\text{m}^3/\text{mol/Pa})$	5.55	6.73	7.95	9.44	10.38				

4.1.2.4 Hydration Number

The capability of solute and solvent molecules to link to one another determines the quality of their interaction. In order to determine the extent of hydration of thymine molecules with sugar moieties, the hydration number, (n_H) is computed. Many techniques can be used to determine it.

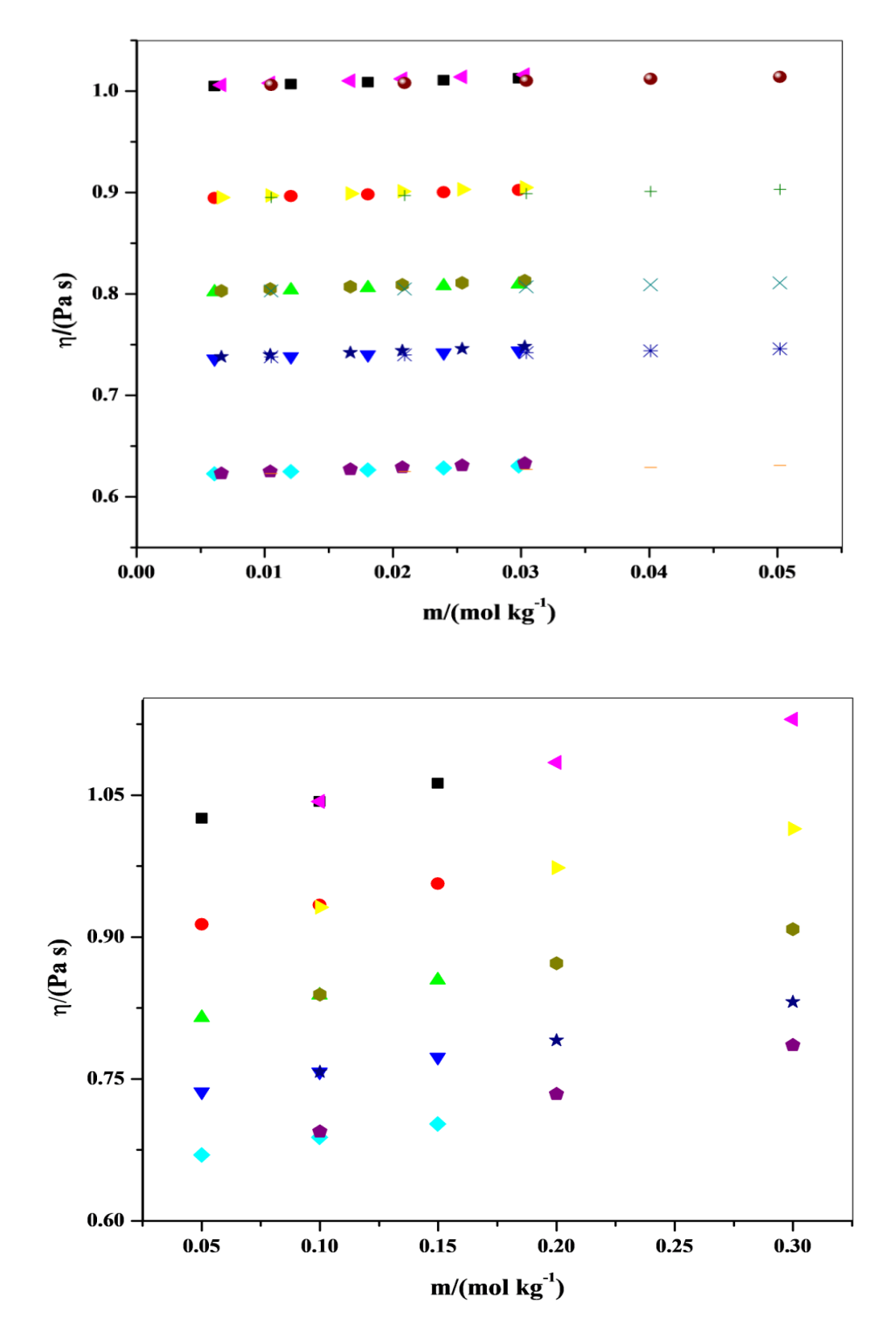
Table 4.1.8: Anticipated hydration numbers (n_H) for thymine in water and saccharide solvent systems at discrete temperatures.

			η_H						
System	$T(\mathbf{K})$								
	293.15	298.15	303.15	308.15	313.15				
Thymine in water	11.14	11.04	10.99	10.86	10.73				
Thymine in 0.0501 mol kg ⁻¹ glucose	10.95	10.82	10.70	10.57	10.40				
Thymine in 0.0999 mol kg ⁻¹ glucose	10.69	10.58	10.47	10.33	10.24				
Thymine in 0.1498 mol kg ⁻¹ glucose	10.33	10.20	10.07	9.93	9.78				
Thymine in 0.0500 mol kg ⁻¹ sucrose	10.89	10.66	10.47	10.15	9.94				
Thymine in 0.1000 mol kg ⁻¹ sucrose	10.67	10.42	10.21	9.93	9.67				
Thymine in 0.1502 mol kg ⁻¹ sucrose	10.45	10.21	10.01	9.70	9.45				

4.1.3 Viscosity Data

Viscosity is an essential measure in explaining the interactions amongst solutes and solvents since it is dependent on the bonding amid solute and solvent particles. The viscosity η , of different solution samples for thymine in H₂O and in H₂O + glucose/sucrose mixtures are deduced by considering time of surge of these solution mixtures.

Table 4.1.9 illustrates the viscosities for thymine in aqua or in aqueous glucose/sucrose. Given that viscosity and molar mass are co-related, the cosolute having more molecular mass will move slowly, increasing the viscosity value; in this regard, sucrose moieties have a higher viscosity values than the glucose molecules.



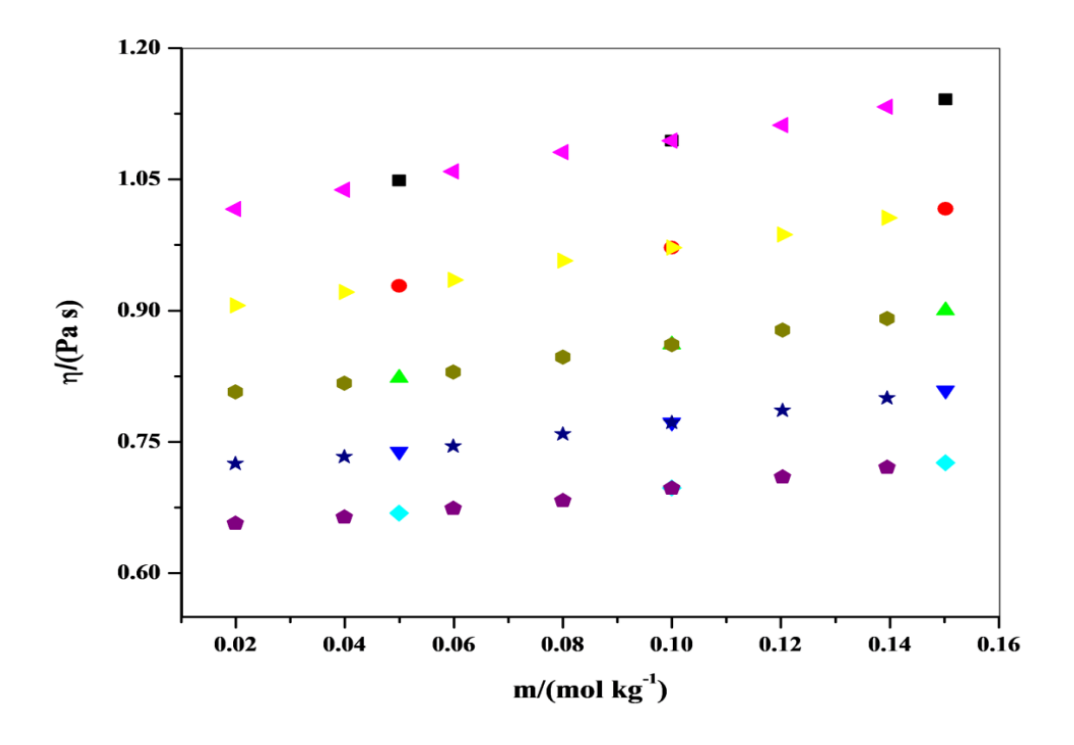


Figure 4.1.5(a): Comparison graph of viscosity vs molality with literature for thymine in H_2O at discrete T(K). ■ : Conducted investigation on 293.15, • : Conducted investigation on 298.15, • : Conducted investigation on 303.15, • : Conducted investigation on 308.15, • : Conducted investigation on 313.15, • : Lit. [4] on 293.15, • : Lit. [4] on 298.15, • : Lit. [4] on 303.15, • : Lit. [5] on 308.15, • : Lit. [5] on 308.15, • : Lit. [5] on 313.15.

(b) Comparison graph of viscosity vs molality with literature for glucose in H_2O at discrete T(K). ■ : Conducted investigation on 293.15, ● : Conducted investigation on 298.15, ▲ : Conducted investigation on 303.15, ▼ : Conducted investigation on 308.15, ○ : Conducted investigation on 313.15, < : Lit. [6] on 293.15, ▷ : Lit. [6] on 298.15, ○ : Lit. [6] on 303.15, ★ : Lit. [6] on 308.15, ○ : Lit. [6] on 313.15.

(c) Comparison graph of viscosity vs molality with literature for sucrose in H_2O at discrete T(K). \blacksquare : Conducted investigation on 293.15, \bullet : Conducted investigation on 303.15, \checkmark : Conducted investigation on 308.15, \checkmark : Conducted investigation on 313.15, \checkmark : Lit. [7] on 293.15, \checkmark : Lit. [7] on 298.15, \bullet : Lit. [7] on 303.15, \star : Lit. [7] on 313.15.

Additionally, comparison graphs of the dynamic viscosity values of thymine [4,5], glucose [6], as well as sucrose [7] in an aqueous media with the available literature are publicized in Figure's 4.1.5 (a, b, as well as c). These figures demonstrate the improved congruence between data obtained through experiments and data from the literature.

Nonetheless, changes in the experimental mode of performance and variances in the instruments themselves could be the cause of observed variations in thymine comparison plots.

Table 4.1.9: Experimentally acquired viscosities, η and calculated relative viscosities, η_r of thymine in several prepared solvent mixtures at distinct temperatures.

		η	$\times 10^3 (Pc)$	a s)				η_r		
<i>m</i> /(mol /kg)						T(K)				
/ II S)	293.15	298.15	303.15	308.15	313.15	293.15	298.15	303.15	308.15	313.15
				Т	hymine -	+ water				
0.0000	1.002	0.891	0.799	0.733	0.620					
0.0061	1.005	0.894	0.802	0.736	0.623	1.0029	1.0034	1.0038	1.0042	1.0047
0.0120	1.007	0.896	0.804	0.738	0.625	1.0049	1.0056	1.0061	1.0071	1.0081
0.0181	1.009	0.898	0.806	0.740	0.626	1.0068	1.0075	1.0088	1.0095	1.0108
0.0239	1.011	0.900	0.808	0.742	0.628	1.0087	1.0099	1.0111	1.0124	1.0137
0.0298	1.013	0.902	0.810	0.744	0.630	1.0108	1.0122	1.0134	1.0150	1.0168
Thymine + 0.0501 mol /kg glucose										
0.0000	1.026	0.913	0.815	0.736	0.670					
0.0060	1.029	0.916	0.818	0.739	0.673	1.0030	1.0034	1.0037	1.0041	1.0045
0.0119	1.031	0.918	0.820	0.741	0.675	1.0050	1.0055	1.0059	1.0066	1.0073
0.0179	1.033	0.920	0.822	0.743	0.677	1.0070	1.0078	1.0085	1.0092	1.0104
0.0240	1.035	0.923	0.824	0.745	0.679	0.0090	1.0101	1.0110	1.0121	1.0136
0.0300	1.037	0.925	0.826	0.747	0.681	1.0011	1.0123	1.0134	1.0149	1.0164
]	Γhymine⊣	- 0.0999	mol /kg g	glucose			
0.0000	1.043	0.934	0.839	0.757	0.688					
0.0060	1.046	0.937	0.842	0.760	0.691	1.0031	1.0034	1.0037	1.0041	1.0045
0.0121	1.049	0.939	0.844	0.762	0.694	1.0051	1.0056	1.0061	1.0067	1.0075
0.0180	1.051	0.941	0.846	0.764	0.696	1.0071	1.0079	1.0087	1.0094	1.0106
0.0239	1.053	0.943	0.848	0.767	0.698	1.0091	1.0103	1.0114	1.0124	1.0138
0.0299	1.055	0.946	0.850	0.769	0.700	1.0111	1.0125	1.0138	1.0152	1.0168
			1	Thymine -	+ 0.1498	mol /kg	glucose			
0.0000	1.063	0.956	0.855	0.773	0.703					
0.0060	1.066	0.960	0.858	0.776	0.706	1.0031	1.0034	1.0037	1.0041	1.0045
0.0119	1.068	0.962	0.860	0.778	0.708	1.0052	1.0056	1.0062	1.0068	1.0077
0.0180	1.070	0.964	0.862	0.780	0.710	1.0071	1.0079	1.0088	1.0094	1.0107
0.0240	1.072	0.966	0.864	0.783	0.712	1.0091	1.0103	1.0115	1.0125	1.0139
0.0300	1.075	0.968	0.866	0.785	0.714	1.0113	1.0126	1.0139	1.0153	1.0169

-				Γhymine	+ 0.0500	mol /kg	sucrose			
0.0000	1.049	0.928	0.823	0.739	0.671					
0.0060	1.052	0.932	0.827	0.742	0.674	1.0034	1.0038	1.0040	1.0042	1.0046
0.0119	1.054	0.934	0.828	0.744	0.676	1.0054	1.0059	1.0063	1.0070	1.0076
0.0179	1.056	0.936	0.831	0.746	0.678	1.0073	1.0082	1.0089	1.0097	1.0107
0.0240	1.058	0.938	0.833	0.748	0.680	1.0094	1.0106	1.0114	1.0124	1.0139
0.0300	1.061	0.940	0.835	0.750	0.682	1.0115	1.0128	1.0140	1.0154	1.0168
			7	Thymine	+ 0.1000	mol /kg	sucrose			
0.0000	1.094	0.972	0.861	0.772	0.697					
0.0060	1.098	0.975	0.865	0.776	0.701	1.0035	1.0038	1.0042	1.0043	1.0047
0.0121	1.100	0.978	0.867	0.778	0.703	1.0055	1.0060	1.0064	1.0071	1.0077
0.0180	1.102	0.980	0.869	0.780	0.705	1.0074	1.0082	1.0089	1.0098	1.0109
0.0239	1.105	0.982	0.871	0.782	0.707	1.0095	1.0106	1.0118	1.0127	1.0140
0.0299	1.107	0.984	0.873	0.784	0.709	1.0116	1.0130	1.0143	1.0155	1.0171
			,	Thymine-	+ 0.1502	mol /kg s	sucrose			
0.0000	1.141	1.016	0.900	0.809	0.726					
0.0060	1.145	1.020	0.904	0.812	0.730	1.0035	1.0038	1.0042	1.0043	1.0048
0.0119	1.148	1.022	0.906	0.815	0.732	1.0055	1.0060	1.0064	1.0072	1.0078
0.0180	1.150	1.025	0.908	0.817	0.734	1.0075	1.0084	1.0091	1.0099	1.0111
0.0240	1.152	1.027	0.911	0.819	0.737	1.0096	1.0108	1.0121	1.0129	1.0143
0.0300	1.155	1.029	0.913	0.823	0.739	1.0118	1.0132	1.0144	1.0158	1.0173

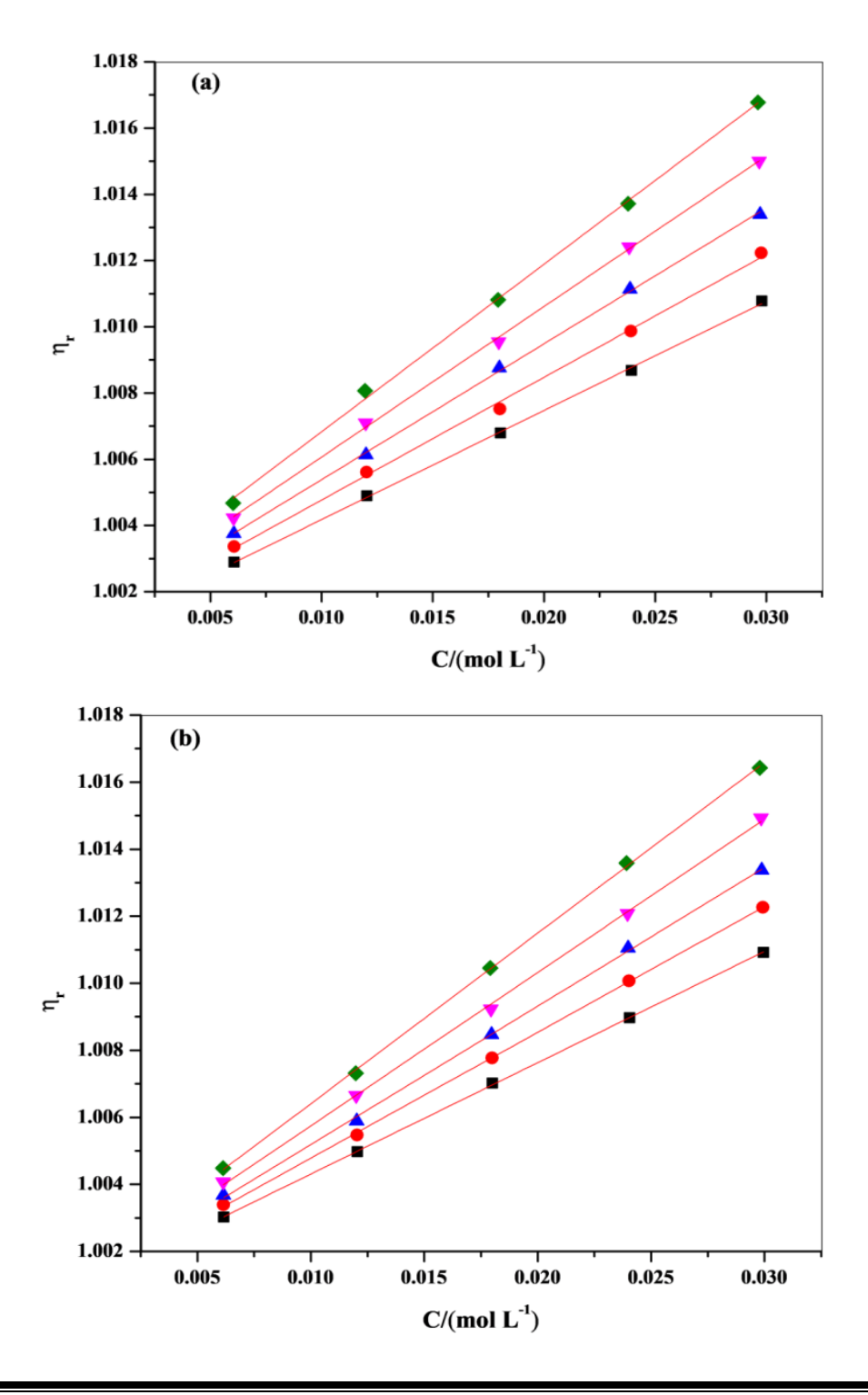
m(mol/kg) stands for molality of thymine in H_2O and varied (water + glucose/sucrose) mixtures.

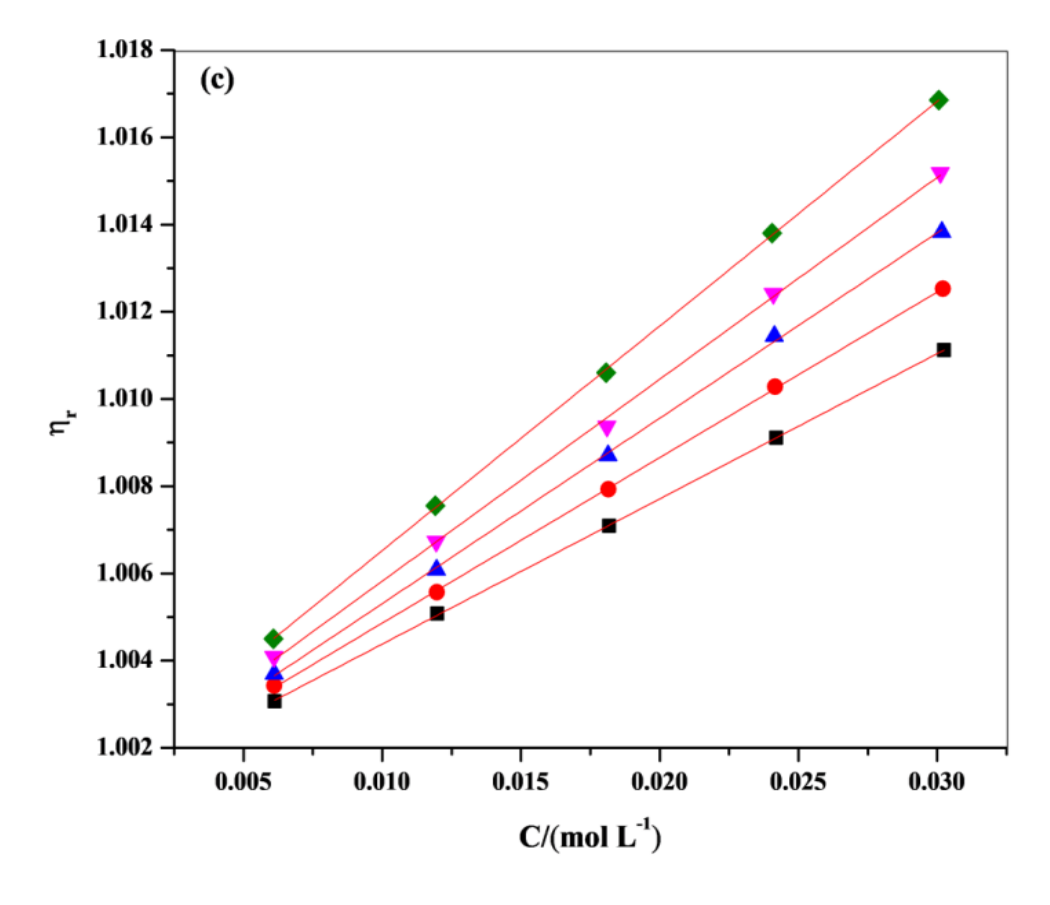
Moreover, Table 4.1.9 demonstrates that although solution viscosity reduces with temp. but increases with molal concentration of thymine. The trend might be owed to stronger synergies amongst the solute-cosolute moieties that result in an increase in the frictional forbearance towards the molecular motions. Additionally, as temperature rises, the solution mixture's enlarged molecular movements cause the viscosity to decrease.

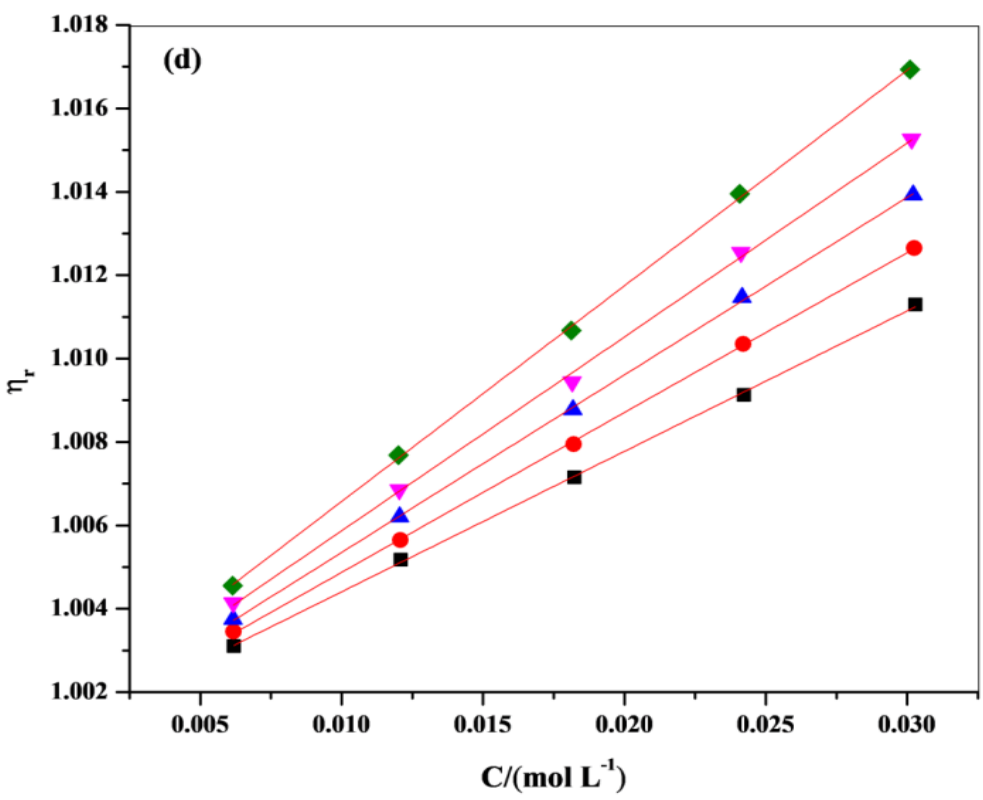
4.1.3.1 Viscosity B-coefficient

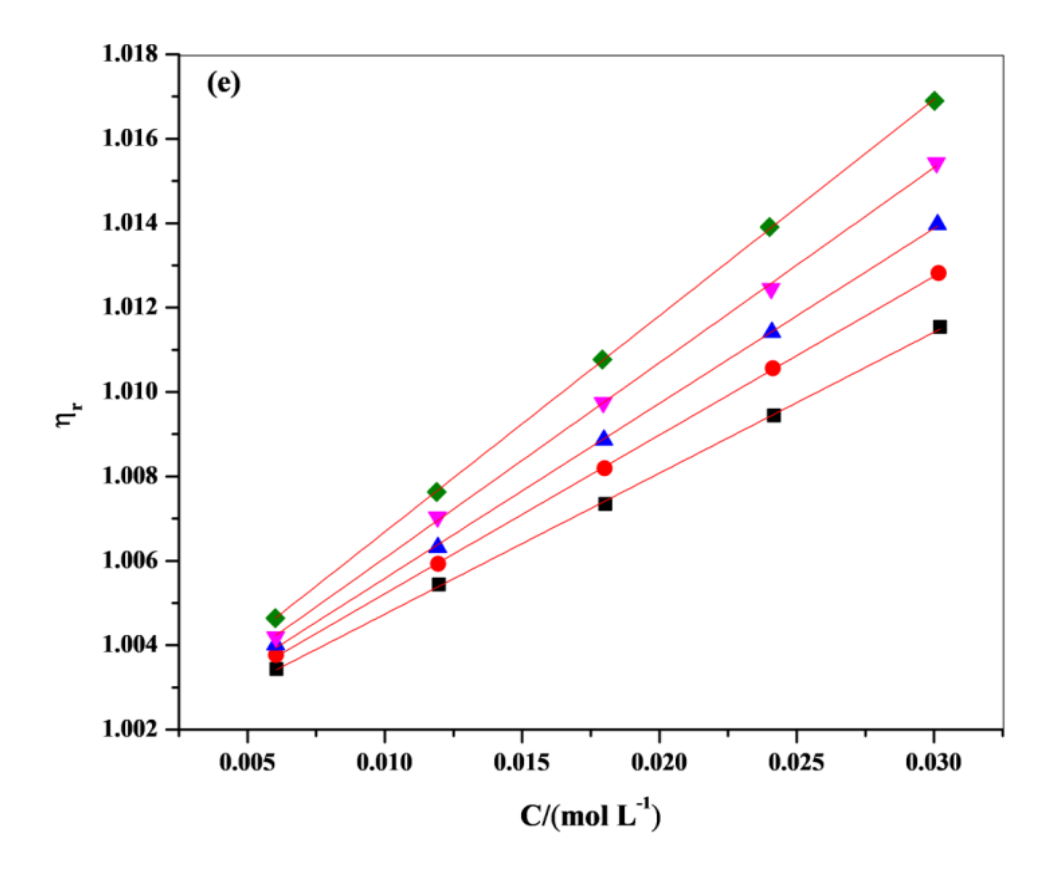
Further, the viscosities of all the prepared sample solutions are related to the consequent molalities in harmony with Jones-Dole Equation (2.23) [24,25]. Figure 4.1.6 [(a)-(g)] signifies the graphs of η_r (relative viscosity) versus C(molarity) of thymine in binary and ternary systems. Furthermore, Table 4.1.10 displays the stated values of B-coefficients together with corresponding standard deviation. This table indicates that B-coefficient data for thymine is all having positive sign and get higher with temperature and

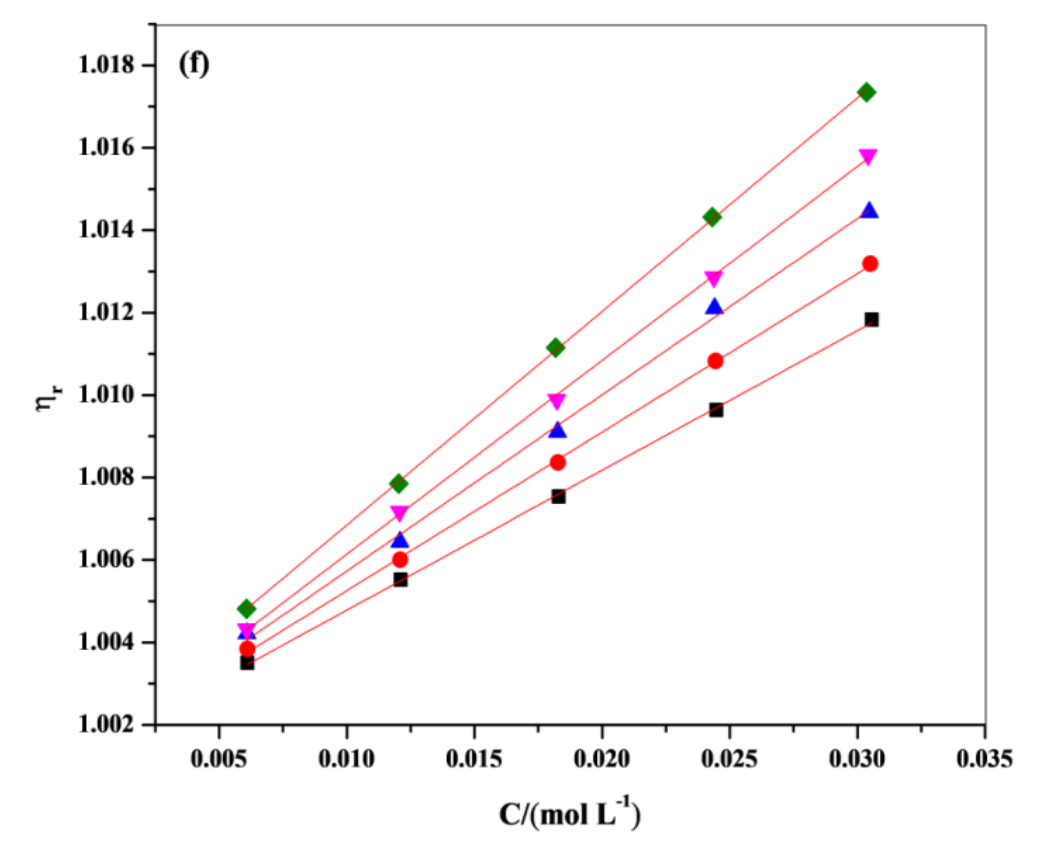
concentrations of solvent system. In the selected systems, this increase in the *B*-coefficient indicates the intensification of solute-cosolute interactions with temperature. Also, a greater number of hydrophilic sites in sucrose molecules may be responsible for of the higher *B*-coefficients for thymine in sucrose solutions compared to the aqueous glucose solutions.











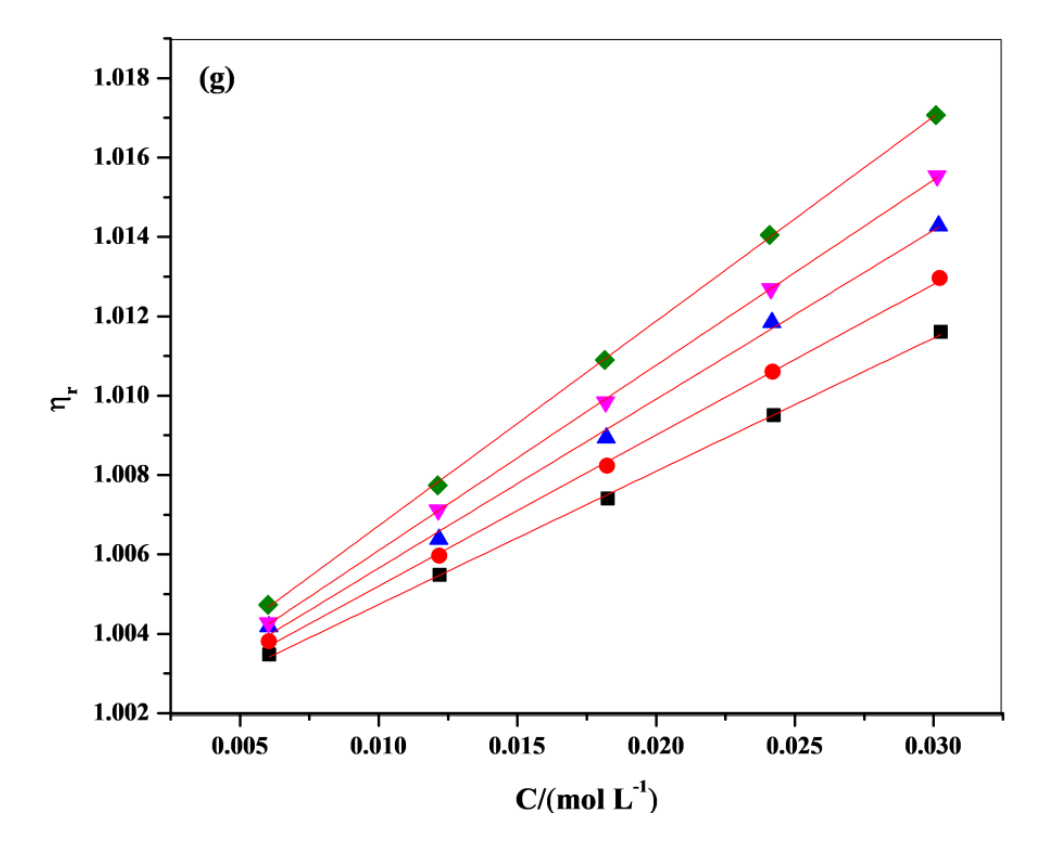


Figure 4.1.6: Graph of $η_r$ vs molaity, $C/(\text{mol L}^{-1})$ for thymine in (a) water, (b) 0.05 mol kg⁻¹ glucose, (c) 0.10 mol kg⁻¹ glucose, (d) 0.15 mol kg⁻¹ glucose, (e) 0.05 mol kg⁻¹ sucrose, (f) 0.10 mol kg⁻¹ sucrose and (g) 0.15 mol kg⁻¹ sucrose at $T = \blacksquare$: 293.15 K, ●: 298.15 K, ▲: 303.15 K, ▼: 308.15 K, ★: 313.15 K.

Furthermore, via the sign of dB/dT, we can categorize the solutes as structure breakers/makers. Those solutes which have positive sign of dB/dT values are exemplified as structure breakers whereas the solutes harboring negative sign of dB/dT values are embodied as structure makers [26,27]. Table 4.1.11 represents the evaluated dB/dT values in which the positive signfor thymine in H_2O and H_2O + glucose/sucrose solutions reveal its structure-breaking ability. As a result, dB/dT results are supporting the information haggard from the Hepler's constant analysis, presented in Table 4.1.4.

Table 4.1.10: Anticipated (dB/dT) data for thymine in in H₂O and H₂O + glucose/sucrose solutions at discrete temperatures.

m/(mol/kg)	dB/dT values
Thymine + water	0.00872 (±0.00027)
Thymine + 0.0501 mol/kg glucose	0.00873 (±0.00028)
Thymine + 0.0999 mol/kg glucose	0.00896 (±0.00021)
Thymine + 0.1498 mol/kg glucose	0.00884 (±0.00021)
Thymine + 0.0500 mol/kg sucrose	0.00880 (±0.00023)
Thymine + 0.1000 mol/kg sucrose	0.00898 (±0.00012)
Thymine + 0.1502 mol/kg sucrose	0.00888 (±0.00010)

4.1.3.2 Viscosity B-constraint of Transfer

Applying the Eqn. (2.24), one may derive the $\Delta_{tr}B$ values. The record of *B*-coefficient transfer for thymine has been accredited in Table 4.1.10.

Table 4.1.11: Deduced viscosity *B* coefficients and corresponding transfer values $\Delta_{tr}B$ for thymine in water and glucose/sucrose solvent systems.

Deduced	T(K)					
Parameters	293.15	298.15	303.15	308.15	313.15	
Thymine + water						
$B \times 10^3 (\text{m}^3/\text{mol})$	0.330(±0.004)	0.371(±0.009)	0.410(±0.005)	0.455(±0.006)	0.506(±0.009)	
	Thymine+ 0.0501 mol/kg glucose					
$B \times 10^3 (\text{m}^3/\text{mol})$	0.332(±0.002)	0.375(±0.003)	0.413(±0.005)	0.457(±0.006)	0.509(±0.005)	
$\Delta_{tr}B \times 10^3 (\text{m}^3/\text{mol})$	0.002	0.004	0.003	0.003	0.003	
Thymine + 0.0999 mol/kg glucose						
$B \times 10^3 (\text{m}^3/\text{mol})$	0.333(±0.001)	0.379(±0.002)	0.425(±0.005)	0.463(±0.007)	0.515(±0.003)	
$\Delta_{tr}B \times 10^3 (\mathrm{m}^3/\mathrm{mol})$	0.003	0.009	0.015	0.008	0.009	
Thymine + 0.1498 mol/kg glucose						
$B \times 10^3 (\text{m}^3/\text{mol})$	0.337(±0.003)	0.383(±0.003)	0.426(±0.003)	0.465(±0.008)	0.517(±0.005)	

$\Delta_{tr}B \times 10^3 (\text{m}^3/\text{mol})$	0.007	0.013	0.016	0.010	0.011	
	Thymine + 0.0500 mol/kg sucrose					
$B \times 10^3 (\text{m}^3/\text{mol})$	0.334(±0.003)	0.376(±0.002)	0.415(±0.003)	0.462(±0.005)	0.511(±0.004)	
$\Delta_{tr}B \times 10^3 (\text{m}^3/\text{mol})$	0.004	0.005	0.004	0.008	0.005	
Thymine + 0.1000 mol/kg sucrose						
$B \times 10^3 (\text{m}^3/\text{mol})$	0.335(±0.004)	0.380(±0.004)	0.426(±0.010)	0.467(±0.005)	0.516(±0.003)	
$\Delta_{tr}B \times 10^3 (\text{m}^3/\text{mol})$	0.006	0.009	0.015	0.012	0.009	
Thymine + 0.1502 mol/kg sucrose						
$B \times 10^3 (\text{m}^3/\text{mol})$	0.339(±0.004)	0.384(±0.005)	0.427(±0.012)	0.470(±0.003)	0.518(±0.004)	
$\Delta_{tr}B\times10^3(\mathrm{m}^3/\mathrm{mol})$	0.009	0.014	0.017	0.016	0.012	

It can be predicted from the study of these values that the transfer values rise as the concentrations of sucrose and glucose rise. This illustrates the progress in hydrophilic interactions [28-30]. As a result, the results for $\Delta_{tr}B$ agree with the results from the analysis of $\Delta_{tr}V^0_{\phi}$ as well as $\Delta_{tr}K^0_{\phi,s}$.

4.1.4 Thermodynamic Properties of Viscous Motion

By the usage of activated complex theory presented by Eyring *et al.* [31]. the Gibb's free energy of activation per mole of solute (chemical potential) has been demarcated for the inspected solute (thymine) in water and assorted concentrations of glucose/sucrose media. As per this theory, in one molar solution, the solvent molecules are escorted by a shift, as an influence of which they either incorporate strongly or weakly with solute molecules in the solution. Hence, the chemical potential of the solvent has been figured at eclectic temperatures via the relation (2.25). Likewise, the chemical potential of solute (thymine) has been summed utilizing a thermodynamic relation (2.27) given by Feakin's *et al.* [32]. Essentially, $\Delta\mu^0_2$ is a criterion of divergence in chemical potential of solute in the immediacy of selected solvent system as well as additional free energy differences appearing as a consequence of vibrations of solute molecules.

Table 4.1.12: The estimated thermodynamic parameters for thymine in H_2O and aqueous glucose and sucrose media.

Inferred		T(K)				
Characteristic	293.15	298.15	303.15	308.15	313.15	
		Thymin	e + water			
$\Delta \mu^{\theta_I}$ (kJ/mol)	9.29	9.16	9.05	8.98	8.69	
$\Delta\mu^{\theta_2}$ (kJ/mol)	53.83	60.07	66.24	73.31	81.31	
$T\Delta S^{\theta}_{2}$ (kJ/mol)	399.74	406.56	413.38	420.20	427.01	
ΔH^{0}_{2} (kJ/mol)	453.58	466.63	479.62	493.50	508.32	
	T	hymine +0.050	1 mol/kg gluco	ose		
$\Delta\mu^{0}_{1}$ (kJ/mol)	9.36	9.24	9.11	9.00	8.90	
$\Delta\mu^{0}_{2}$ (kJ/mol)	54.06	60.53	66.44	73.47	81.67	
$T\Delta S^{\theta_2}$ (kJ/mol)	399.63	406.44	413.26	420.08	426.89	
ΔH^{0}_{2} (kJ/mol)	453.68	466.98	479.70	493.55	508.56	
	T	hymine + 0.099	9 mol/kg gluco	ose		
$\Delta \mu^{\theta_I}$ (kJ/mol)	9.41	9.30	9.19	9.08	8.99	
$\Delta \mu^{\theta_2}$ (kJ/mol)	54.02	60.96	67.95	73.99	82.26	
$T\Delta S^{\theta}_{2}$ (kJ/mol)	407.48	414.43	421.38	428.33	435.28	
ΔH^{0}_{2} (kJ/mol)	461.50	475.39	489.33	502.33	517.53	
	T	hymine + 0.149	8 mol/kg gluco	ose		
$\Delta \mu^{\theta_I}$ (kJ/mol)	9.47	9.37	9.25	9.15	9.05	
$\Delta \mu^{\theta_2}$ (kJ/mol)	54.39	61.31	67.81	74.05	82.30	
$T\Delta S^{\theta_2}$ (kJ/mol)	402.01	408.86	415.72	422.58	429.43	
ΔH^{0}_{2} (kJ/mol)	456.40	470.18	483.54	496.63	511.74	
Thymine + 0.0500 mol/kg sucrose						
$\Delta \mu^{\theta_1}$ (kJ/mol)	9.43	9.29	9.14	9.02	8.91	
$\Delta\mu^{\theta_2}$ (kJ/mol)	54.17	60.45	66.41	73.88	81.76	
$T\Delta S^{\theta}_{2}$ (kJ/mol)	348.17	354.11	360.05	365.99	371.93	
ΔH^{0}_{2} (kJ/mol)	402.34	141.559	426.47	439.87	453.69	
Thymine + 0.1000 mol/kg sucrose						
$\Delta \mu^{\theta_I}$ (kJ/mol)	9.55	9.43	9.28	9.16	9.05	

$\Delta\mu^{\theta_2}$ (kJ/mol)	54.07	60.64	67.51	73.91	81.66
$T\Delta S^{\theta_2}$ (kJ/mol)	347.57	353.50	359.42	365.35	371.28
ΔH^{θ_2} (kJ/mol)	401.64	414.13	426.93	439.32	452.94
Thymine + 0.1502 mol/kg sucrose					
$\Delta\mu^{\theta_I}(\text{kJ/mol})$	9.68	9.56	9.42	9.30	9.18
$\Delta\mu^{\theta_2}$ (kJ/mol)	54.19	60.86	67.31	73.95	81.41
$T\Delta S^{\theta}_{2}$ (kJ/mol)	341.58	347.40	353.23	359.06	364.88
ΔH^{θ_2} (kJ/mol)	395.77	408.26	420.54	433.01	446.29
-					

In present research work, the expected $\Delta\mu^0_1$ and $\Delta\mu^0_2$ show positive values for all premediated thymine systems shown in Table 4.1.12. Also, the $\Delta\mu^0_2$ values for all thymine systems are increasing with rising temperatures. These positive and increasing values of $\Delta\mu^0_2$, according to the Feakin *et al.* [32] model, indicate that the thymine's ability to form a transition state in the selected solvent systems is weak for all investigated temperatures.

Additionally, equations (2.28) and (2.29) have been utilized for the assessment of the entropy of activation (ΔS^0_2) as well as enthalpy of activation (ΔH^0_2) of the selected solution mixtures. Table 4.1.12 displays the calculated values for ΔH^0_2 and $T\Delta S^0_2$. Furthermore, it is seen that ΔH^0_2 values are larger than the $T\Delta S^0_2$, signifying the attendance of well-built interactions linking thymine and prepared saccharides solutions in the ground state.

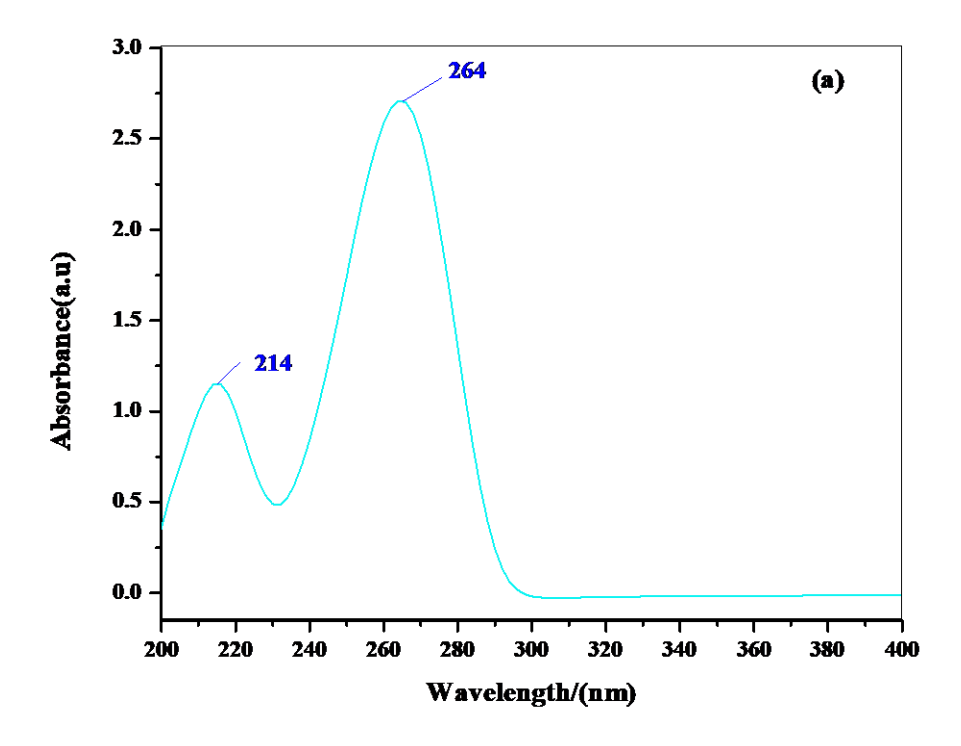
4.1.5 UV Absorption Studies

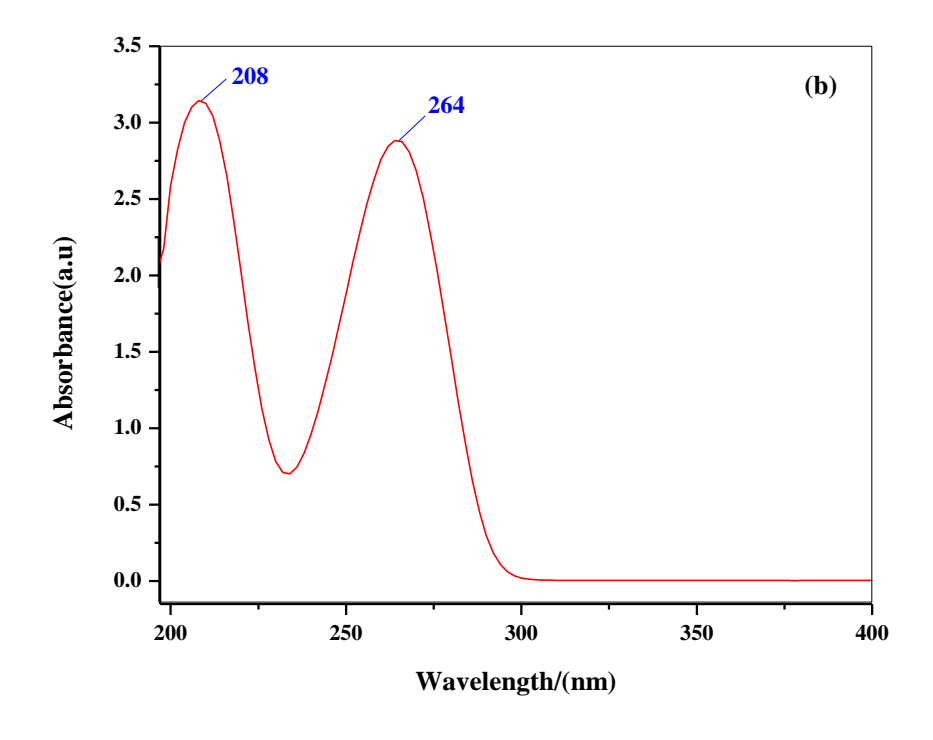
The absorption spectrum of thymine in aqueous solutions, as well as in aqueous glucose and sucrose (0.15 mol kg⁻¹) solutions, was observed using the UV-visible spectrophotometer (LAMBDA 1050+). Using quartz cuvettes with a path length of one centimeter, UV spectra of the solution samples were prepared while keeping the wavelength within 200–400 (nm) range. The resulting absorbance vs wavelength charts are displayed in Figure 4.1.7 [(a)-(c)]. The n $\rightarrow \pi^*$ as well as $\pi \rightarrow \pi^*$ transitions for thymine in H₂O are seen at 214 (nm) and 264 (nm), correspondingly, as shown in Figure 4.1.7(a).

Additionally, we can observe from Figure 4.1.7(b) that absorption bands for thymine in aqueous glucose solution (0.15 mol kg⁻¹) appear at 264 (nm) and 208 (nm), whereas the thymine absorption bands in water + sucrose solution (0.15 mol kg⁻¹) emerge at 264 (nm) and 206 (nm) in Figure 4.1.7(b). As a result, there is a hypsochromic shift in the absorption maxima, which are found at 214 (nm), in water and at 206 (nm) and 208 (nm), in aqueous sucrose and glucose, respectively.

Greater polarity of thymine in its ground state than in its excited state, this can justify this trend. Thus, effective interaction occurs between thymine and polar saccharides solutions in the G.S (ground state) as it escorts to a decrease in thymine's ground state energy, an increase in energy gap amid G.S and E.S, also a decrease in absorption maxima.

Furthermore, it can be accredited that the thymine moieties interact efficiently with the sucrose moieties than the glucose moieties, resulting in the appearance of the absorption band for $n \to \pi *$ transition at 206 (nm), for aqueous sucrose and 208 nm, for aqueous glucose. Hence, efficient hydrophilic-hydrophilic type interactions among thymine and sugar molecules result in the shifting of the absorption bands in samples under exploration.





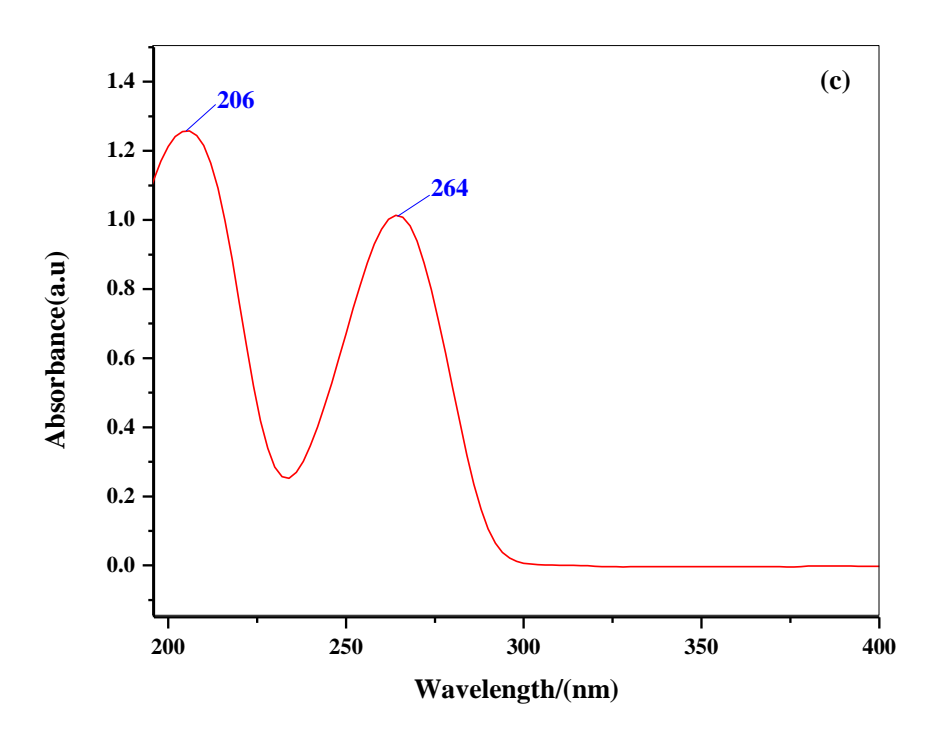


Figure 4.1.7: Plots of absorbance versus wavelength for thymine in (a) water, (b) 0.15 mol kg⁻¹ glucose + water media, (c) 0.15 mol kg⁻¹ sucrose + water media.

4.1.6 *Summary*

Here is a more visual summary of trends across temperature and concentration, aiding quick comprehension.

Property	Effect of Increasing Concentration	Effect of Increasing Temperature
Density	Increases	Decreases
Apparent Molar Volume	Increases	Increases
Limiting Apparent Molar Volume	Increases	Increases
Speed of Sound	Increases	Increases
Apparent molar isentropic compression	Increases	Increases
Limitimg apparent molar isentropic compression	Increases	Increases
Hydration number	Decreases	Decreases
Viscosity	Increases	Decreases
Viscosity B-coefficient	Increases	Increases

REFERENCES

- 1. Nielsen, P. E. (1995). DNA analogues with non-phosphodiester backbones. *Annual Review of Biophysics and Biomolecular Structure*, 24, 167-183.
- 2. Hedwig, G. R., & Høiland, H. (2011). Partial molar isentropic and isothermal compressions of the nucleosides adenosine, cytidine, and uridine in aqueous solution at 298.15 K. *Journal of Chemical & Engineering Data*, 56, 2266-2272.
- 3. Bandral, A., Singh, H., Richu, Majid, Q., Rajput, P., & Kumar, A. (2024). Effect of semicarbazide hydrochloride on the physicochemical properties of L-leucine and glycylglycine at varied temperatures and compositions. *The Journal of Chemical Thermodynamics*, 188, 107176.
- 4. Rajput, P., Richu, Sharma, T., & Kumar, A. (2021). Temperature dependent physicochemical investigations of some nucleic acid bases (uracil, thymine and adenine) in aqueous inositol solutions. *Journal of Molecular Liquids*, 326, 115210.
- 5. Rajput, P., Singh, H., Bandral, A., Richu, Majid, Q., & Kumar, A. (2022). Explorations on thermophysical properties of nitrogenous bases (uracil/thymine) in aqueous L-histidine solutions at various temperatures. *Journal of Molecular Liquids*, 367, 120548.
- 6. Rani, R., Kumar, A., & Bamezai, R. K. (2017). Effect of glucose/lactose on the solution thermodynamics of thiamine hydrochloride in aqueous solutions at different temperatures. *Journal of Molecular Liquids*, 240, 642-655.
- 7. Sharma, T., Bandral, A., Bamezai, R. K., & Kumar, A. (2022). Interaction behavior of sucrose in aqueous tributylmethylammonium chloride solutions at various temperatures: a volumetric, ultrasonic and viscometric study. *Chemical Thermodynamics and Thermal Analysis*, 6, 100043.
- 8. Richu, Bandral, A., Singh, H., & Kumar, A. (2022). Effect of [Bmim][Br] and [Emim][HSO4] on the solution properties of pyridoxine HCl at various

- temperatures: A physicochemical, thermodynamic and spectroscopic approach. *Journal of Molecular Liquids*, *364*, 120024.
- 9. Masson, D. O. (1929). XXVIII. Solute molecular volumes in relation to solvation and ionization. *The London, Edinburgh, and Dublin Philosophical Magazine and Journal of Science*, 8, 218-235.
- Richu, & Kumar, A. (2021). A comprehensive study on molecular interactions of L-ascorbic acid/nicotinic acid in aqueous [BMIm] Br at varying temperatures and compositions: spectroscopic and thermodynamic insights. *Journal of Chemical & Engineering Data*, 66, 3859-3880.
- 11. Jamal, M. A., Naseem, B., Khan, J. H., & Arif, I. (2019). Temperature dependent solution properties of amino acids in colloidal solutions. *Journal of Molecular Liquids*, 275, 105-115.
- 12. Iqbal, M. J., & Chaudhry, M. A. (2010). Effect of temperature on volumetric and viscometric properties of some non-steroidal anti-inflammatory drugs in aprotic solvents. *The Journal of Chemical Thermodynamics*, 42, 951-956.
- 13. Mishra, A. K., & Ahluwalia, J. C. (1984). Apparent molal volumes of amino acids, N-acetylamino acids, and peptides in aqueous solutions. *The Journal of Physical Chemistry*, 88, 86-92.
- Singh, H., Richu, Bandral, A., Majid, Q., & Kumar, A. (2023). Investigation of molecular interactions of streptomycin sulphate with aqueous L-aspartic acid through volumetric, ultrasonic and viscometric approach. *Journal of Molecular Liquids*, 382, 121885.
- 15. Parmar, M. L., & Banyal, D. S. (2009). Effect of temperature on the partial molar volumes of some bivalent transition metal nitrates and magnesium nitrate in the water-rich region of binary aqueous mixtures of dimethyl acetamide. *Indian Journal of Chemistry*, 48A(12), 1667-1672.

- 16. Kaur, A., Bansal, S., Chauhan, D., Bhasin, K. K., & Chaudhary, G. R. (2019). The study of molecular interactions of aqueous solutions of Choline Acetate at different temperatures. *Journal of Molecular Liquids*, 286, 110878.
- 17. Hepler, L. G. (1969). Thermal expansion and structure in water and aqueous solutions. *Canadian Journal of Chemistry*, 47, 4613-4617.
- 18. Kaur, H., Chakraborty, N., Juglan, K. C., & Upmanyu, A. (2025). Study of thermodynamic and acoustic properties of DEGMME/DEGMEE in aqueous erythritol solutions at different temperatures. *The Journal of Chemical Thermodynamics*, 204, 107446.
- 19. Kumar, H., Singla, M., & Jindal, R. (2014). Investigations on solute—solvent interactions of amino acids in aqueous solutions of sodium dihydrogen phosphate at different temperatures. *Monatshefte für Chemie-Chemical Monthly*, 145, 1063-1082.
- 20. Frank, H. S., & Evans, M. W. (1945). Free volume and entropy in condensed systems III. Entropy in binary liquid mixtures; partial molal entropy in dilute solutions; structure and thermodynamics in aqueous electrolytes. *The Journal of Chemical Physics*, *13*, 507-532.
- 21. Kirkwood, J. G. (1939). Theoretical Studies upon Dipolar Ions. *Chemical Reviews*, 24, 233-251.
- 22. Millero, F. J., Lo Surdo, A., & Shin, C. (1978). The apparent molal volumes and adiabatic compressibilities of aqueous amino acids at 25. degree. C. *The Journal of Physical Chemistry*, 82, 784-792.
- 23. Sharma, S. K., Singh, G., Kumar, H., & Kataria, R. (2016). Effect of N-acetylglycine on volumetric and acoustic behaviour of aqueous tetrabutylammonium iodide solutions at different temperatures. *The Journal of Chemical Thermodynamics*, 96, 143-152.

- 24. Lan, W., Liu, C. F., Yue, F. X., Sun, R. C., & Kennedy, J. F. (2011). Ultrasound-assisted dissolution of cellulose in ionic liquid. *Carbohydrate Polymers*, 86, 672-677.
- 25. Jones, G., & Dole, M. (1929). The viscosity of aqueous solutions of strong electrolytes with special reference to barium chloride. *Journal of the American Chemical Society*, *51*, 2950-2964.
- 26. Chialvo, A. A. (2024). On the solute-induced structure-making/breaking phenomena: Myths, verities, and misuses in solvation thermodynamics. *Liquids*, 4, 592-623.
- 27. Sawhney, N., Kumar, M., Sharma, A. K., & Sharma, M. (2020). molecular interactions of non-steroid anti-inflammatory drug dolonex in aqueous solutions of L-alanine/L-valine at different temperatures: viscometric approach. *Russian Journal of Physical Chemistry A*, *94*, 756-761.
- 28. Richu, Majid, Q., Singh, H., Bandral, A., Singh, M., Kang, T. S., & Kumar, A. (2024). Solution properties of folic acid/nicotinic acid in aqueous 1-butyl-3-methylimidazolium-chloride media at discrete concentrations and temperatures: A thermodynamic, computational, and spectroscopic study. *Journal of Chemical & Engineering Data*, 69, 2503-2527.
- 29. Dhal, K., Singh, S., & Talukdar, M. (2022). Elucidation of molecular interactions of aspartic acid with aqueous potassium sorbate and sodium benzoate: Volumetric, viscometric and FTIR spectroscopic investigation. *Journal of Molecular Liquids*, 352, 118659.
- 30. Rajput, P., Singh, H., & Kumar, A. (2022). Volumetric, ultrasonic and viscometric behavior of nucleosides (uridine and cytidine) in aqueous L-ascorbic acid solutions at different temperatures. *The Journal of Chemical Thermodynamics*, *171*, 106805.
- 31. Glasstone, S., Laidler, K. J., & Eyring, H. (1941). The theory of rate processes: the kinetics of chemical reactions, viscosity, diffusion and electrochemical phenomena. *McGraw-Hill Book Company*.

32. Feakins, D., Waghorne, W. E., & Lawrence, K. G. (1986). The viscosity and structure of solutions. Part 1.—A new theory of the Jones–Dole *B*-coefficient and the related activation parameters: application to aqueous solutions. *Journal of the Chemical Society, Faraday Transactions 1: Physical Chemistry in Condensed Phases*, 82, 563-568.

CHAPTER 4.2

Analysis of Volumetric, Compressibility and Viscometric Properties of Adenine in Water + D-Maltose/D-Glucose Media at Varied Temperatures

The Journal of Chemical Thermodynamics, 2024, 201, 107399 (Impact factor: 2.2)

Analysis of Volumetric, Compressibility and Viscometric Parameters of Adenine in Water + D-Maltose/D-Glucose Media at Varied Temperatures

In this chapter, volumetric, compressibility and viscometric properties of adenine have been investigated in aqueous and mixed aqueous (0.05, 0.10 and 0.15) mol kg⁻¹ Dglucose/D-maltose solvent media at discrete temperatures (293.15 to 313.15) K and experimental pressure (0.1 MPa). The experimentally determined physical properties such as density, velocity of sound, and viscosity have been utilized for the estimation of several parameters such as apparent molar volume (V_{ϕ}) , limiting apparent molar volume (V_{ϕ}) , hydration number (n_H) , limiting apparent molar expansivity (E^0_{ϕ}) , Hepler's constant $(\partial E^0_{\phi}/\partial T)_P$, apparent specific volume (ASV), apparent molar isentropic compression $(K_{\phi,s})$, limiting apparent molar isentropic compression $(K^0_{\phi,s})$, viscosity B-coefficients, transfer parameters and thermodynamic parameters of viscous flow $(\Delta \mu^0_1, \Delta \mu^0_2, T\Delta S^0_2)$ and ΔH^0_2 . Additionally, the Co-sphere overlap model has been utilized for the analysis of assorted probable interactions operating in the prepared systems. The received outcomes forecast that in all solution systems, the solute-solvent interactions are progressing with rising temperatures and concentrations of saccharides. Furthermore, the structure breaking proclivity of adenine has been scrutinized via the abstraction of Hepler's constant data and positive values of dB/dT data for all the explored systems. Moreover, the inferred apparent specific volume data specify that adenine has a sweet taste in water and distinct concentrations of selected saccharides. These findings suggest that saccharides notably influence the solvation behavior and structural stability of adenine. This is particularly relevant because adenine is a fundamental component of DNA, RNA, ATP, and various coenzymes. To strengthen the broader impact of this work, it is important to emphasize its biochemical and pharmaceutical implications.

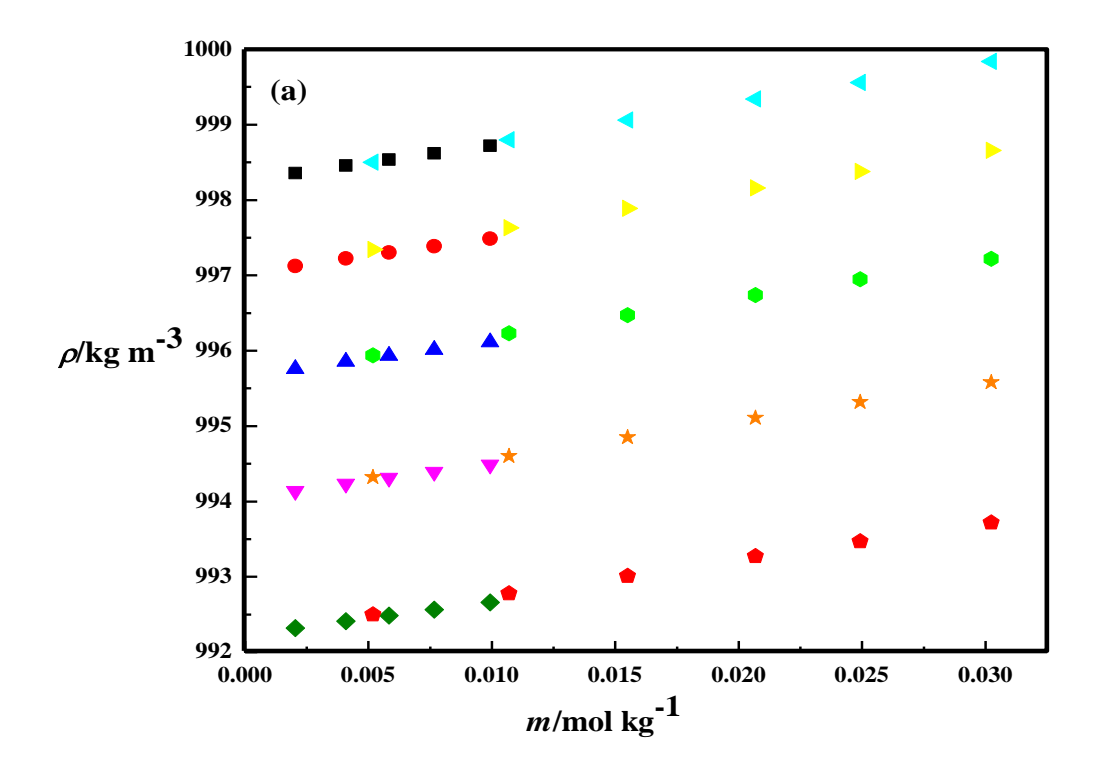
From a biochemical perspective, these interactions are essential for understanding how nucleobases like adenine behave in crowded, sugar-rich biological environments. In vivo, nucleobases exist in proximity to carbohydrates, proteins, and salts, all of which influence their solvation and association behavior. The impact of sugars on adenine's physicochemical properties can directly affect nucleic acid structure, base pairing efficiency, and enzymatic processing especially under temperature fluctuations or osmotic stress. The findings thus contribute to our understanding of how environmental conditions

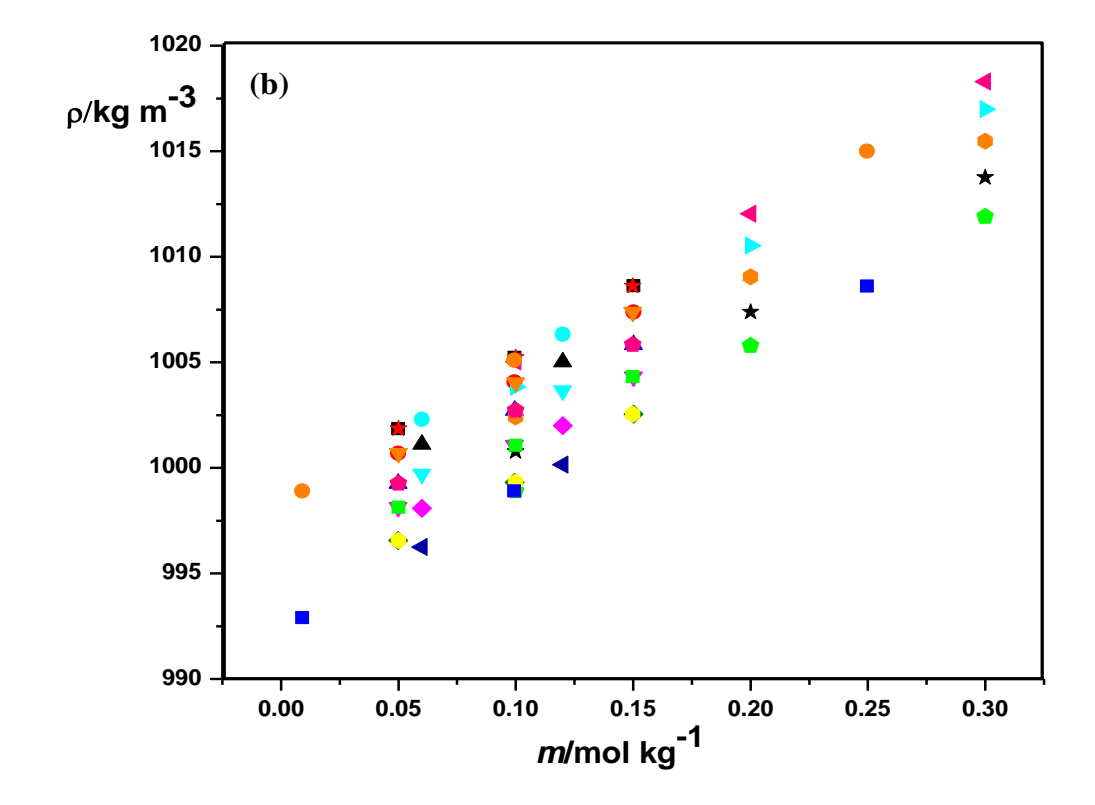
and cellular metabolites modulate DNA/RNA behavior and stability, with implications for genetic regulation, molecular recognition, and metabolic balance.

In the pharmaceutical domain, the results of this chapter are valuable for designing sugar-based formulations and delivery systems for nucleobase analogs and gene-based therapeutics. Glucose and maltose are widely used as stabilizers, cryoprotectants, and excipients in drug formulations. Knowledge of how these sugars influence adenine's solvation, viscosity, and compressibility enables the formulation of more stable, effective solutions for storing and delivering nucleic acid-based drugs. This research supports the development of biocompatible buffers, injectable carriers, and long-term preservation media for vaccines, gene therapies, and diagnostic reagents. It also lays a foundation for extending such studies to other nucleobases and co-solvents, advancing the fields of pharmaceutical chemistry, biophysics, and molecular biotechnology.

4.2.1 Volumetric Properties

Through the usage of Density and Speed of sound Analyzer (DSA 5000 M), the physical properties like density and speed of sound have been acquired at five dissimilar temperatures (293.15 K to 313.15 K) for (0.002 to 0.010) mol kg⁻¹ of adenine in water and in (0.05, 0.10 and 0.15) mol kg⁻¹ D-glucose/D-maltose solvent. The density data has been exemplified in Table 4.2.1. A contemplation of Table 4.2.1 signifies an increase in density with advancement in molality of adenine as well as the D-glucose/D-maltose solvent system, while with ascending temperature, there is a decline in density values. The enhancement in concentration directs to an upsurge in mass per unit volume of the solutions, so the density proliferates while the drop in density with rising temperature can be owed to an increase in kinetic energy of the particles of solution which renders an elaboration in volume of solution.





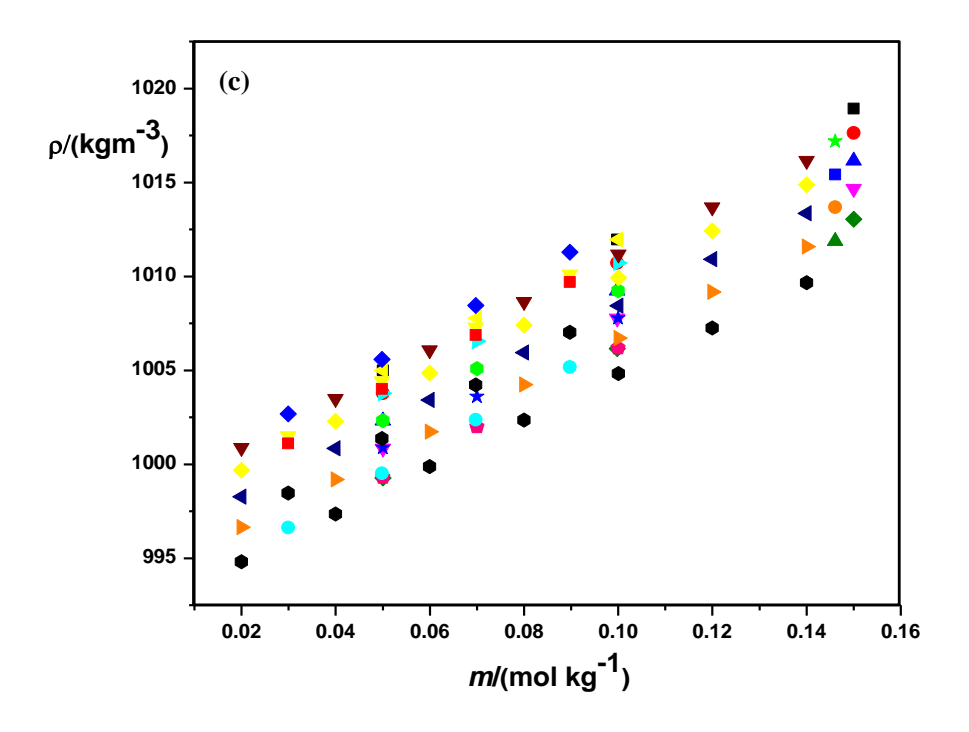


Figure 4.2.1: Graphs representing contrast of measured density data with the accessible reports at discrete temperatures.

(a) For adenine + water at $T(K) = \blacksquare$: Conducted investigation on 293.15, \blacksquare : Conducted investigation on 298.15, \blacktriangle : Conducted investigation on 303.15, \blacktriangledown Conducted investigation on 308.15, \spadesuit Conducted investigation on 313.15, \blacktriangleleft : Lit. [1] on 293.15, \blacktriangleright : Lit. [1] on 303.15, \bigstar : Lit. [1] on 313.15.

(b) D-Glucose + water at $T(K) = \blacksquare$: Conducted investigation on 293.15, ● : Conducted investigation on 298.15, ▲ : Conducted investigation on 303.15, ▼ : Conducted investigation on 308.15, ◆ : Conducted data on 313.15, ◀ : Lit. [3] on 293.15, ▶ : Lit. [3] on 298.15, ● : Lit. [3] on 303.15, ★ : Lit. [3] on 308.15, ● : Lit. [2] on 313.15, ▼ : Lit. [2] on 303.15, ■ : Lit. [2] on 308.15, ● : Lit. [6] on 293.15, ● : Lit. [6] on 303.15, ■ : Lit. [6] on 313.15, ■ : Lit. [6] on 313.15. ■ : Lit. [6] on 313.15.

Furthermore, the acquired density data complementary to adenine, D-glucose, and D-maltose in water has been analogized with the available publications [1,2-9,10] and the comparison plots are being shown in Figures 4.2.1 (a), (b) and (c). From the comparison plots, it can be gathered that there is a fine concurrence between the obtained data and available publications. Nevertheless, the subtle divagations in the plots might be due to instrumental deviations, dissimilarity in rendition of the experiment, and variations in the uncertainties being briefed.

4.2.1.1 Apparent Molar Volume

By substituting acquired density data in equation (2.1), the apparent molar volume has been summed and illustrated in Table 4.2.1. A contemplation of V_{ϕ} data demonstrates that there is a progression in apparent molar volume with expanding molality of adenine as well as with temperature. The increase in V_{ϕ} with ascending concentration of adenine is attributed to an increase in the van der Waals volume of adenine in the formulated solutions. Likewise, a cliff in temperature guides to the migration of H_2O from the hydration shells of solute to the bulk causing an expansion in the volume of solution. Besides, for a satisfactory interpretation of intermolecular interactions amid adenine and D-glucose/D-maltose solvent system, the limiting apparent molar volumes were assessed.

Table 4.2.1: Density values, ρ and apparent molar volumes, V_{ϕ} for adenine in water and aqueous D-glucose/D-maltose solutions at T/K = 293.15 - 313.15.

T/K	am/mol/kg	$\rho/\text{kg/m}^3$	$V_{\phi} \times 10^6/\mathrm{m}^3/\mathrm{mol}$	T/K	am/mol kg-1	$ ho/{ m kg~m}^{-3}$	$V_{\phi} imes 10^6 / \mathrm{m}^3 \ \mathrm{mol}^{-1}$
			Adenin	e in wate	er		
293.15	0.00000	998.26		308.15	0.00000	994.04	
293.15	0.00202	998.36	86.42	308.15	0.00202	994.14	88.17
293.15	0.00408	998.45	87.01	308.15	0.00408	994.23	88.86
293.15	0.00582	998.54	87.49	308.15	0.00582	994.31	89.39
293.15	0.00765	998.62	88.04	308.15	0.00765	994.39	89.93
293.15	0.00992	998.72	88.54	308.15	0.00992	994.49	90.55
298.15	0.00000	997.03		313.15	0.00000	992.22	
298.15	0.00202	997.12	86.96	313.15	0.00202	992.32	89.15
298.15	0.00408	997.22	87.55	313.15	0.00408	992.41	89.73
298.15	0.00582	997.30	88.06	313.15	0.00582	992.49	90.17

298.15	0.00765	997.38	88.49	313.15	0.00765	992.56	90.81
298.15	0.00992	997.48	89.09	313.15	0.00992	992.66	91.35
303.15	0.00000	995.66					
303.15	0.00202	995.76	87.51				
303.15	0.00408	995.86	88.10				
303.15	0.00582	995.93	88.63				
303.15	0.00765	996.01	89.20				
303.15	0.00992	996.12	89.66				
		Ad	lenine in 0.0	4994 mol kg	¹ D-glucose		
293.15	0.00000	1001.86		308.15	0.00000	998.13	
293.15	0.00193	1001.95	87.11	308.15	0.00193	998.22	89.84
293.15	0.00413	1002.05	87.69	308.15	0.00413	998.32	90.27
293.15	0.00650	1002.16	88.18	308.15	0.00650	998.42	90.64
293.15	0.00797	1002.23	88.65	308.15	0.00797	998.48	91.08
293.15	0.01000	1002.32	89.05	308.15	0.01000	998.57	91.42
298.15	0.00000	1000.69		313.15	0.00000	996.56	
298.15	0.00193	1000.78	87.67	313.15	0.00193	996.65	90.43
298.15	0.00413	1000.88	88.47	313.15	0.00413	996.75	90.83
298.15	0.00650	1000.99	88.99	313.15	0.00650	996.85	91.33
298.15	0.00797	1001.05	89.33	313.15	0.00797	996.91	91.65
298.15	0.01000	1001.14	89.80	313.15	0.01000	996.99	92.10
303.15	0.00000	999.26					
303.15	0.00193	999.35	88.76				
303.15	0.00413	999.45	89.25				
303.15	0.00650	999.56	89.82				
303.15	0.00797	999.62	90.02				
303.15	0.01000	999.71	90.47				
		Ad	lenine in 0.0	9939 mol kg	¹ D-glucose		
293.15	0.00000	1005.23		308.15	0.00000	1001.07	
293.15	0.00191	1005.32	87.52	308.15	0.00191	1001.16	90.05
293.15	0.00427	1005.43	88.17	308.15	0.00427	1001.26	90.49
293.15	0.00597	1005.50	88.89	308.15	0.00597	1001.33	91.08
293.15	0.00812	1005.59	89.48	308.15	0.00812	1001.42	91.75
293.15	0.01009	1005.68	90.00	308.15	0.01009	1001.51	92.17

298.15	0.00000	1004.06		313.15	0.00000	999.32	
298.15	0.00191	1004.15	88.08	313.15	0.00191	999.40	90.88
298.15	0.00427	1004.26	88.91	313.15	0.00427	999.50	91.45
298.15	0.00597	1004.33	89.44	313.15	0.00597	999.57	92.00
298.15	0.00812	1004.43	90.02	313.15	0.00812	999.66	92.57
298.15	0.01009	1004.51	90.64	313.15	0.01009	999.74	92.95
303.15	0.00000	1002.72					
303.15	0.00191	1002.81	89.17				
303.15	0.00427	1002.92	89.66				
303.15	0.00597	1002.99	90.17				
303.15	0.00812	1003.08	90.81				
303.15	0.01009	1003.16	91.30				
		Ad	lenine in 0.1	15003 mol kg	¹ D-glucose		
293.15	0.00000	1008.62		308.15	0.00000	1004.31	
293.15	0.00216	1008.72	88.21	308.15	0.00216	1004.41	90.22
293.15	0.00411	1008.81	88.63	308.15	0.00411	1004.49	90.74
293.15	0.00605	1008.89	89.18	308.15	0.00605	1004.58	91.17
293.15	0.00804	1008.98	89.62	308.15	0.00804	1004.66	91.78
293.15	0.01027	1009.08	90.24	308.15	0.01027	1004.75	92.36
298.15	0.00000	1007.38		313.15	0.00000	1002.54	
298.15	0.00216	1007.48	88.72	313.15	0.00216	1002.64	91.22
298.15	0.00411	1007.57	89.16	313.15	0.00411	1002.72	91.54
298.15	0.00605	1007.65	89.72	313.15	0.00605	1002.80	92.24
298.15	0.00804	1007.74	90.16	313.15	0.00804	1002.88	92.73
298.15	0.01027	1007.83	90.58	313.15	0.01027	1002.97	93.42
303.15	0.00000	1005.84					
303.15	0.00216	1005.94	89.34				
303.15	0.00411	1006.03	89.95				
303.15	0.00605	1006.11	90.45				
303.15	0.00804	1006.19	90.97				
303.15	0.01027	1006.29	91.52				
		Ad	enine in 0.0	4992 mol kg ⁻	¹ D-maltose		
293.15	0.00000	1004.99		308.15	0.00000	1000.85	
293.15	0.00217	1005.09	89.28	308.15	0.00217	1000.95	91.09

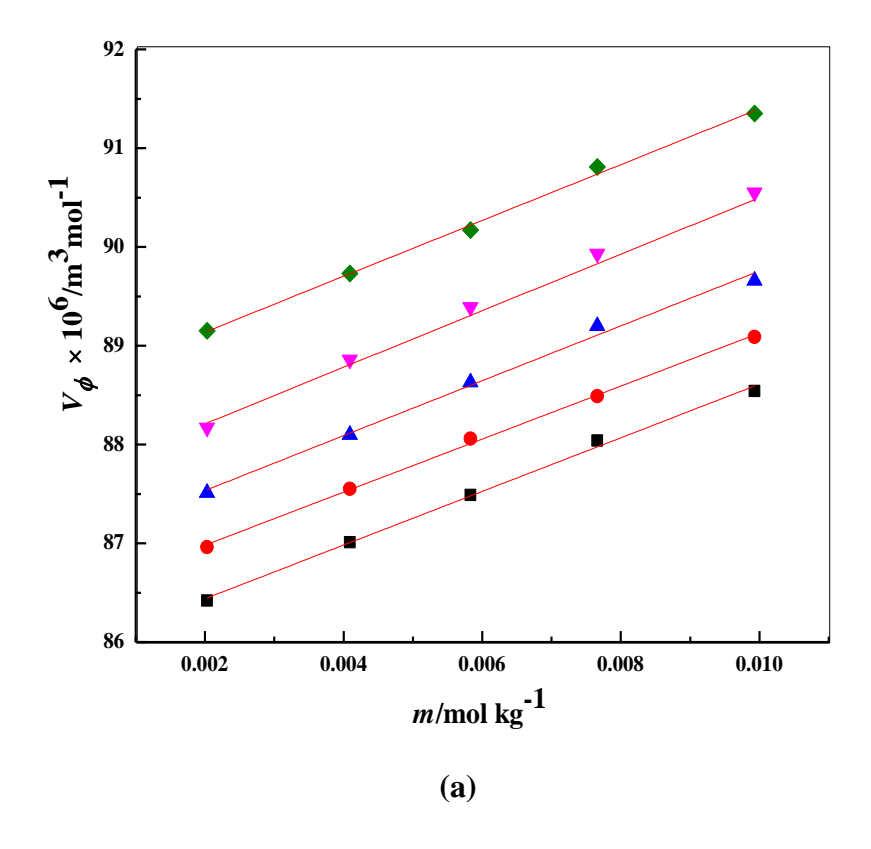
293.15	0.00411	1005.18	89.74	308.15	0.00411	1001.03	91.39
293.15	0.00606	1005.26	90.32	308.15	0.00606	1001.11	91.99
293.15	0.00805	1005.35	90.89	308.15	0.00805	1001.19	92.32
293.15	0.01028	1005.44	91.46	308.15	0.01028	1001.28	92.93
298.15	0.00000	1003.78		313.15	0.00000	999.27	
298.15	0.00217	1003.88	89.79	313.15	0.00217	999.36	91.38
298.15	0.00411	1003.97	90.28	313.15	0.00411	999.45	91.95
298.15	0.00606	1004.05	90.87	313.15	0.00606	999.53	92.40
298.15	0.00805	1004.14	91.31	313.15	0.00805	999.61	93.02
298.15	0.01028	1004.23	91.81	313.15	0.01028	999.69	93.59
303.15	0.00000	1002.32					
303.15	0.00217	1002.41	90.41				
303.15	0.00411	1002.49	90.83				
303.15	0.00606	1002.58	91.27				
303.15	0.00805	1002.66	91.76				
303.15	0.01028	1002.76	92.37				
		Ad	enine in 0.0	09947 mol kg ⁻	¹ D-maltose		
293.15	0.00000	1011.95		308.15	0.00000	1007.75	
293.15	0.00200	1012.04	89.80	308.15	0.00200	1007.84	91.82
293.15	0.00400	1012.13	90.41	308.15	0.00400	1007.93	92.08
293.15	0.00633	1012.23	90.84	308.15	0.00633	1008.02	92.60
293.15	0.00788	1012.29	91.30	308.15	0.00788	1008.08	93.13
293.15	0.01019	1012.39	91.85	308.15	0.01019	1008.17	93.70
298.15	0.00000	1010.71		313.15	0.00000	1006.16	
298.15	0.00200	1010.80	90.34	313.15	0.00200	1006.24	92.15
298.15	0.00400	1010.89	90.72	313.15	0.00400	1006.32	92.66
298.15	0.00633	1010.98	91.37	313.15	0.00633	1006.42	93.30
298.15	0.00788	1011.05	91.73	313.15	0.00788	1006.48	93.83
298.15	0.01019	1011.14	92.39	313.15	0.01019	1006.57	94.27
303.15	0.00000	1009.23					
303.15	0.00200	1009.32	91.11				
303.15	0.00400	1009.41	91.38				
303.15	0.00633	1009.50	92.06				
303.15	0.00788	1009.57	92.43				

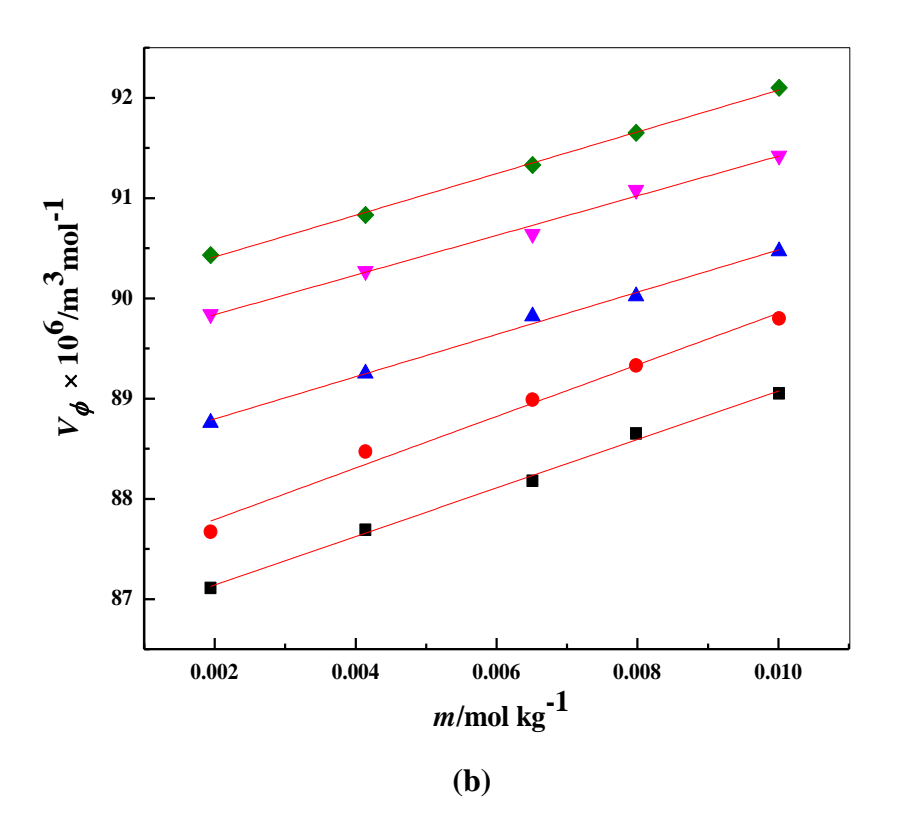
303.15	0.01019	1009.66	92.95						
Adenine in 0.14947 mol kg ⁻¹ D-maltose									
293.15	0.00000	1018.93		308.15	0.00000	1014.66			
293.15	0.00199	1019.01	90.23	308.15	0.00199	1014.74	92.35		
293.15	0.00409	1019.10	90.79	308.15	0.00409	1014.83	92.81		
293.15	0.00582	1019.17	91.46	308.15	0.00582	1014.89	93.14		
293.15	0.00806	1019.27	91.89	308.15	0.00806	1014.99	93.83		
293.15	0.00993	1019.34	92.37	308.15	0.00993	1015.06	94.26		
298.15	0.00000	1017.63		313.15	0.00000	1013.05			
298.15	0.00199	1017.72	90.78	313.15	0.00199	1013.13	93.45		
298.15	0.00409	1017.81	91.32	313.15	0.00409	1013.22	93.67		
298.15	0.00582	1017.88	91.85	313.15	0.00582	1013.28	94.19		
298.15	0.00806	1017.97	92.31	313.15	0.00806	1013.37	94.62		
298.15	0.00993	1018.04	92.73	313.15	0.00993	1013.44	95.23		
303.15	0.00000	1016.15							
303.15	0.00199	1016.23	91.53						
303.15	0.00409	1016.32	91.97						
303.15	0.00582	1016.39	92.53						
303.15	0.00806	1016.48	92.99						
303.15	0.00993	1016.55	93.59						

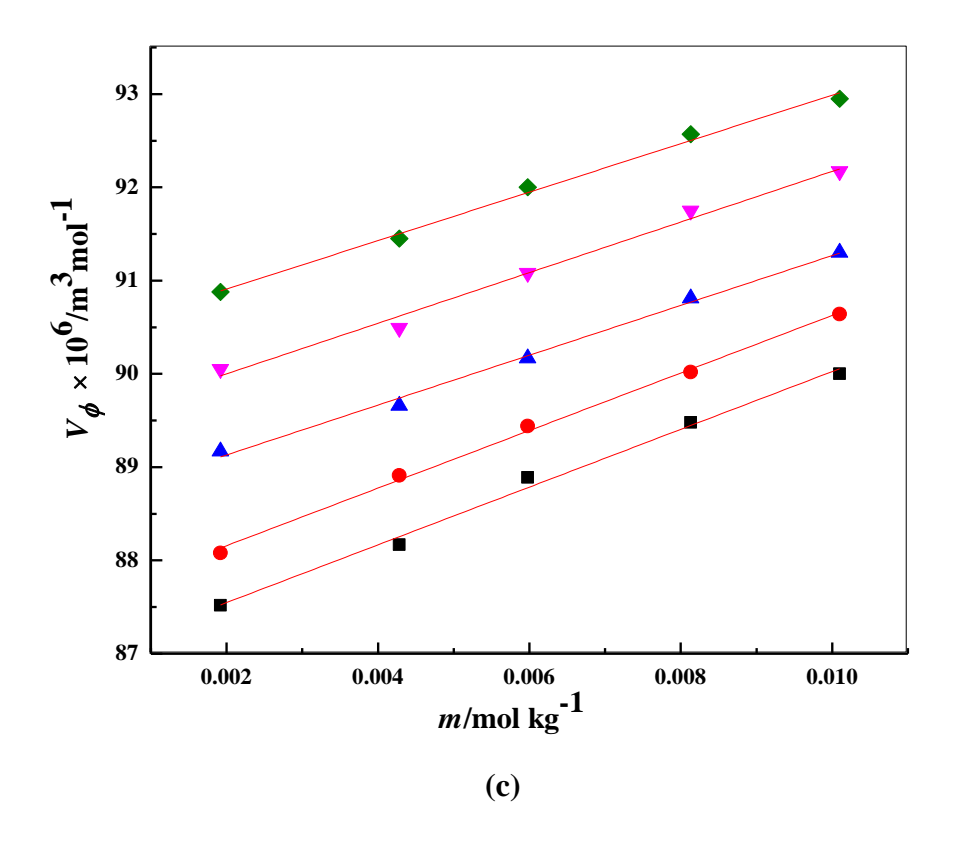
^am(mol kg⁻¹) symbolizes the molal composition of adenine in (water + D-glucose/D-maltose) solutions.

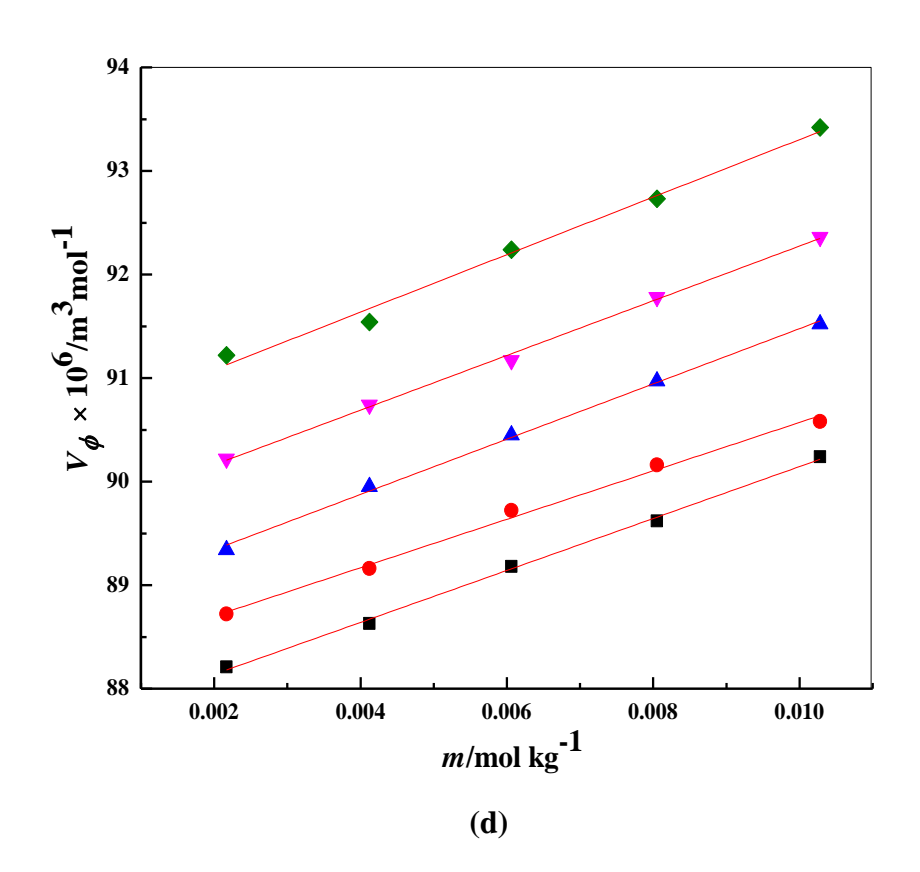
4.2.1.2 Limiting Apparent Molar Volume

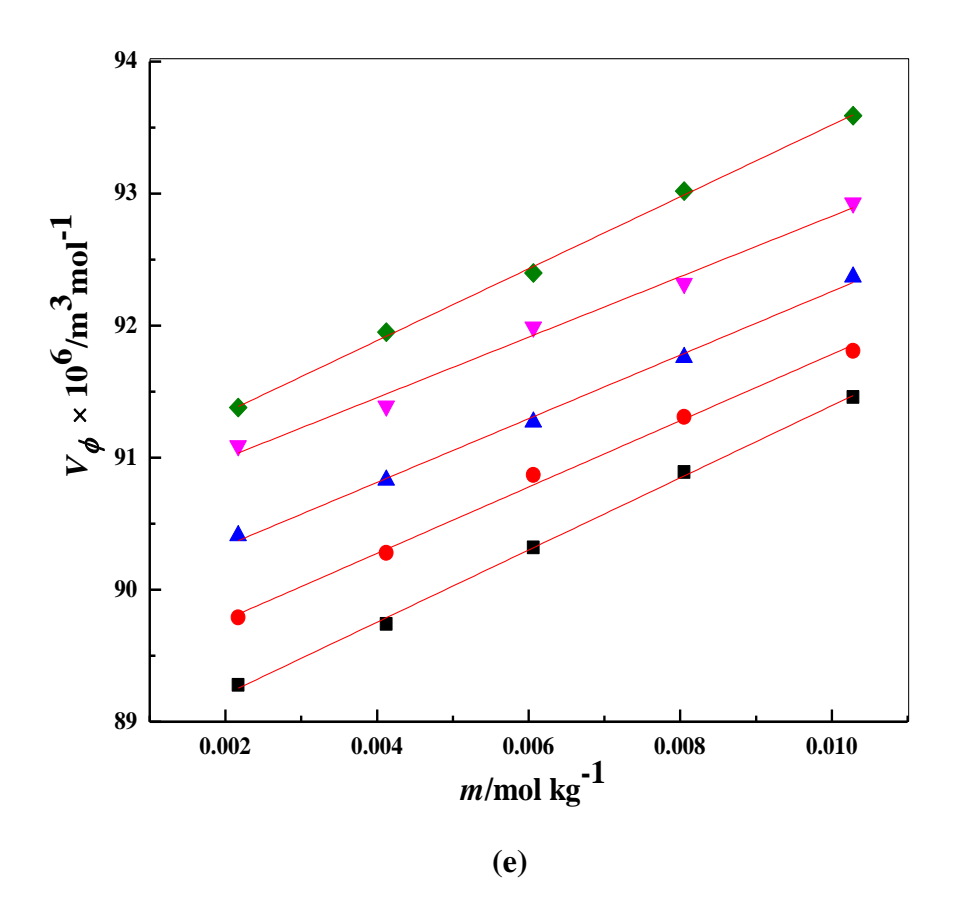
To determinate assorted interactions persisting amid adenine and saccharide solvent system, the Masson equation [11] i.e. (2.2) has been employed and the limiting apparent molar volumes have been scrutinized for the solution systems. As per the Masson equation, the plot of V_{ϕ} against m furnishes the intercept, limiting apparent molar volume (V^0_{ϕ}) which is a criterion of solute-solvent interactions existing in the solution systems. Figure 4.2.2 (a) – (g) portrays the plots of V_{ϕ} against m for all solution systems of adenine in water and aqueous D-glucose/D-maltose solvent system. The graphically inferred data of and along with their connected typical errors is documented in Table 4.2.2. Upon examination of Table 4.2.2, it can be analyzed that the positive V^0_{ϕ} values are progressing with the advancement in temperature forecasting the existence of enhanced solute-solvent interactions in the scrutinized systems.

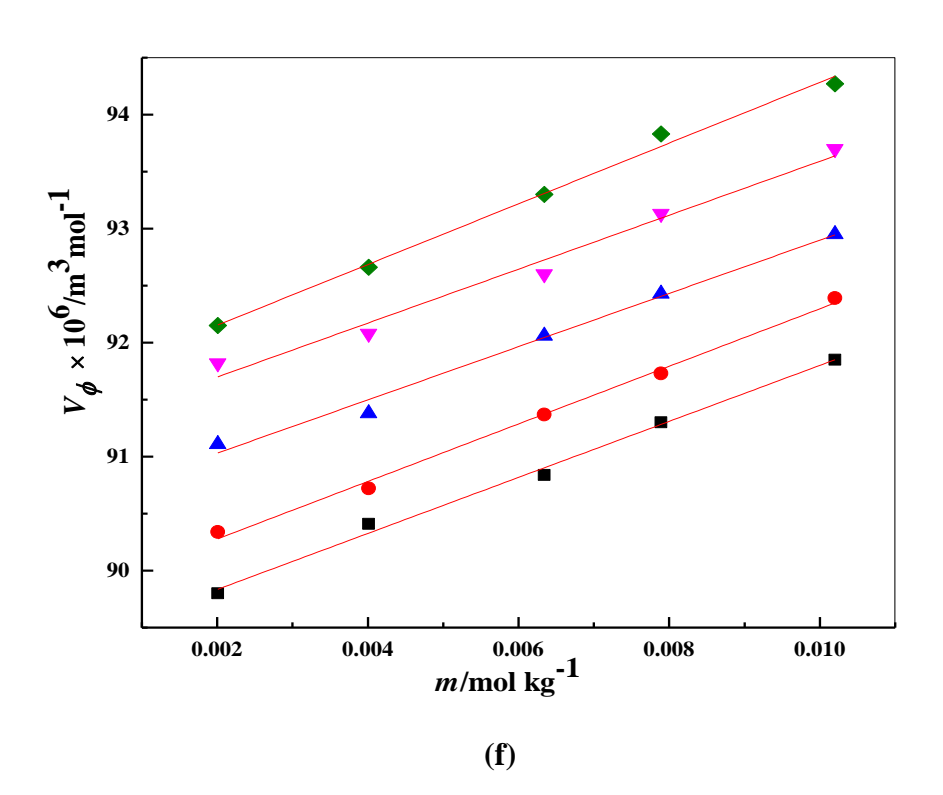












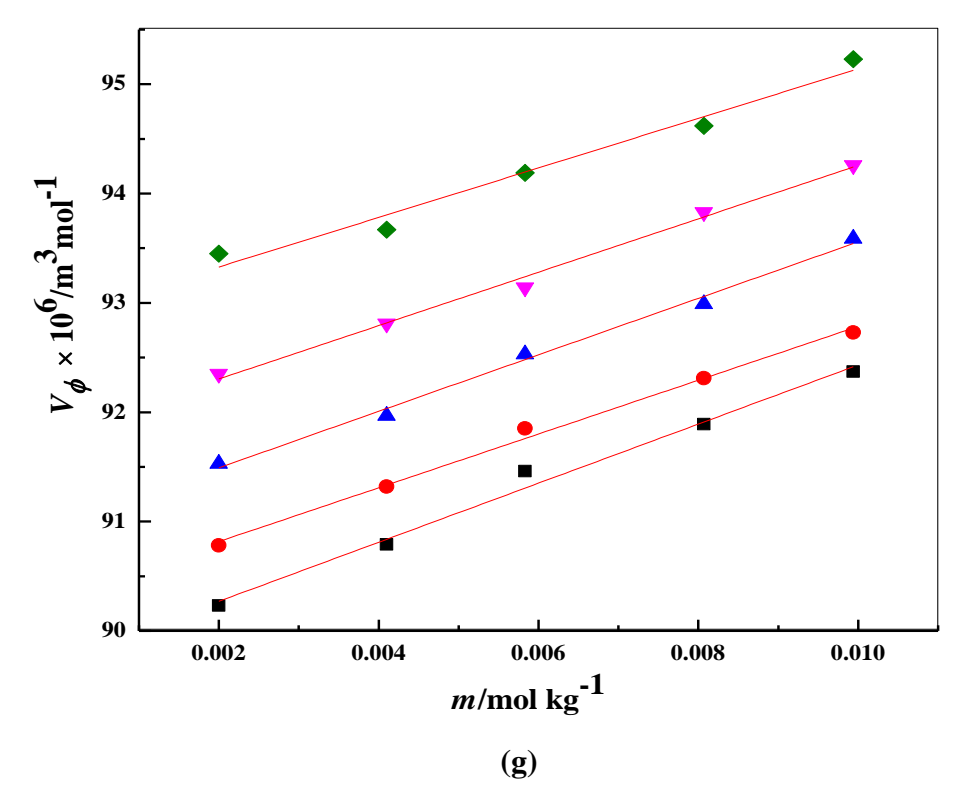


Figure 4.2.2: The graphs depicting change in $V_{\phi} \times 10^6/\text{m}^3 \text{ mol}^{-1}$ against *m*/mol kg⁻¹ for adenine in (a) water, (b) 0.04994 mol kg⁻¹ D-glucose, (c) 0.09939 mol kg⁻¹ D-glucose, (d) 0.15003 mol kg⁻¹ D-glucose, (e) 0.04992 mol kg⁻¹ D-maltose, (f) 0.09947 mol kg⁻¹ D-maltose, (g) 0.14947 mol kg⁻¹ D-maltose at discrete temperatures, ■ : 293.15 K, • : 298.15 K, • : 303.15 K, • : 308.15 K, • : 313.15 K.

The progression in the magnitude of V^0_{ϕ} with temperature might be owed to the lessening of H₂O from hydration shells of adenine molecules ie. the H₂O molecules get released and drive towards the interior of the solution, in courtesy directing towards proliferation in the volume of solution [12]. In acquisition, the enhancement in V^0_{ϕ} with molality of D-glucose/D-maltose solvent system is owed to the dehydration impact of D-glucose/D-maltose over hydrated adenine molecules in the solution [13].

4.2.1.3 Limiting Apparent Molar Volume of Transfer

For a more reasonable perspicuity of varied kinds of intermolecular interactions (solute-solute/solute-solvent) enduring in the studied systems, a decent information is acquired by limiting apparent molar volume of transfer $(\Delta_{tr}V^0_{\phi})$. This is because, at infinite

dilution, there are negligible interactions amid solute moieties. The relation (2.4) has been employed for the perseverance of $\Delta_{tr}V^0_{\phi}$ for adenine from water to aqueous D-glucose/D-maltose solvent system. The deduced data of $\Delta_{tr}V^0_{\phi}$, is reported in Table 4.2.2 which shows that the $\Delta_{tr}V^0_{\phi}$ is positive at each exploratory temperature and these values are advancing with advancement in molal concentration of D-glucose/D-maltose in the ternary systems. The upsurge in $\Delta_{tr}V^0_{\phi}$ with ascending molality of D-glucose/D-maltose solvent system is attributable to the reduction of shrinkage volume. For this rationale, the $\Delta_{tr}V^0_{\phi}$ values are positive and this compliance simply implies the dehydration influence of D-glucose/D-maltose over hydrated solute molecules in the solutions.

Table 4.2.2: Data of limiting molar volume, V^0_{ϕ} along with the S_v slopes as well as analogous transfer volumes $\Delta_{tr}V^0_{\phi}$ for adenine in water and aqueous D-glucose/D-maltose solutions at T/K = 293.15 - 313.15 and P = 0.1 MPa.

D 4			T(K)							
Property	293.15	293.15 298.15 303.15 30		308.15	313.15					
	Adenine + water									
$V^0_\phi imes 10^6/\mathrm{m}^3\mathrm{mol}^{-1}$	85.89(±0.05)	86.44(±0.04)	86.98(±0.08)	87.64(±0.16)	88.57(±0.06)					
$S_{\nu} \times 10^6 / \mathrm{m}^3 \mathrm{mol}^{-2} \mathrm{kg}$	271.54(±8.27)	268.35(±5.95)	277.91(±12.27)	286.16(±24.73)	282.55(±8.76)					
	Adenine +0.04994 mol/kg D-glucose									
$V^0_{\phi} imes 10^6/\mathrm{m}^3\mathrm{mol}^{-1}$	86.66(±0.06)	87.28(±0.11)	88.37(±0.05)	89.44(±0.07)	89.99(±0.03)					
$S_{\nu} \times 10^6 / \mathrm{m}^3 \mathrm{mol}^{-2} \mathrm{kg}$	241.68(±8.48)	257.31(±16.25)	210.70(±7.88)	197.56(±9.92)	207.82(±4.63)					
$\Delta_{tr}V^0_{\phi}\times 10^6/\mathrm{m}^3\mathrm{mol}^{-1}$	0.77	0.84	1.39	1.80	2.35					
	Ade	nine +0.09939 m	ol/kg D-glucose							
$V^0_\phi imes 10^6/\mathrm{m}^3\mathrm{mol}^{-1}$	86.93(±0.09)	87.54(±0.06)	88.59(±0.07)	89.46(±0.11)	90.39(±0.07)					
$S_{\nu} \times 10^6 / \text{m}^3 \text{mol}^{-2} \text{kg}$	309.58(±13.79)	308.53(±8.69)	267.17(±10.04)	303.01(±13.97)	259.96(±10.92)					
$\Delta_{tr}V^0_{\phi}\times 10^6/\mathrm{m}^3\mathrm{mol}^{-1}$	1.04	1.10	1.61	1.82	2.75					
	Ade	nine +0.15003 m	ol/kg D-glucose							
$V^0_\phi imes 10^6/\mathrm{m}^3\mathrm{mol}^{-1}$	87.64(±0.04)	88.23(±0.07)	88.81(±0.05)	89.63(±0.04)	90.52(±0.10)					
$S_{\nu} \times 10^6 / \mathrm{m}^3 \mathrm{mol}^{-2} \mathrm{kg}$	250.78(±6.33)	233.81(±9.86)	276.51(±12.66)	264.14(±6.51)	277.69(±15.37)					

$\Delta_{tr}V^0_{\phi} \times 10^6/\mathrm{m}^3\mathrm{mol}^{-1}$	1.75	1.79	1.83	1.99	2.88			
	Ade	nine +0.04992 n	nol/kg D-maltose	:				
$V^0_{\phi} \times 10^6 / \mathrm{m}^3 \mathrm{mol}^{-1}$	88.66(±0.04)	89.27(±0.06)	89.85(±0.05)	90.54(±0.09)	90.79(±0.04)			
$S_{\nu} \times 10^6/\text{m}^3\text{mol}^{-2}\text{kg}$	273.38(±5.61)	251.26(±8.78)	250.78(±4.47)	253.91(±12.59)	272.44(±5.90)			
$\Delta_{tr}V^0_{\phi} \times 10^6/\mathrm{m}^3\mathrm{mol}^{-1}$	2.77	2.83	2.87	2.90	3.15			
Adenine +0.09947 mol/kg D-maltose								
$V^0_{\phi} \times 10^6 / \mathrm{m}^3 \mathrm{mol}^{-1}$	89.34 (±0.07)	89.77(±0.06)	90.56(±0.09)	91.23(±0.13)	91.62(±0.08)			
$S_{\nu} \times 10^6/\text{m}^3\text{mol}^{-2}\text{kg}$	245.74(±9.88)	252.69(±9.35)	259.41(±12.82)	272.25(±8.72)	278.22(±13.97)			
$\Delta_{tr}V^0_{\phi} \times 10^6/\mathrm{m}^3\mathrm{mol}^{-1}$	3.45	3.53	3.58	3.59	3.98			
	Adei	nine + 0.14947 n	nol/kg D-maltose	2				
$V^0_{\phi} \times 10^6 / \mathrm{m}^3 \mathrm{mol}^{-1}$	89.73(±0.10)	90.32(±0.06)	90.97(±0.07)	91.81(±0.07)	92.87(±0.14)			
$S_{\nu} \times 10^6/\text{m}^3\text{mol}^{-2}\text{kg}$	270.28(±16.02)	245.98(±9.82)	273.76(±5.86)	249.95(±2.61)	296.12(±13.24)			
$\Delta_{tr}V^0_{\phi}\times 10^6/\mathrm{m}^3\mathrm{mol}^{-1}$	3.84	3.88	3.99	4.17	4.30			

Upon examination of $\Delta_{tr}V^0_{\phi}$ values, we speculated that the $\Delta_{tr}V^0_{\phi}$ values of adenine are lower for the solution systems of D-glucose as analogized to D-maltose. This may be owed to variations in the configurational attributes of the deemed saccharides. Since D-maltose is formulated of two D-glucose units, there occur efficient interactions of adenine with hydroxyl groups of D-maltose in comparison to monosaccharide (D-glucose).

As per Friedman and Krishnan's Cosphere overlap model [14], overlapping of hydration shells of charged/polar molecules results in volume proliferation while overlapping of hydration shells of uncharged/non-polar molecules results in volume lessening. In the Conducted examination, positive transfer values are acquired owing to interactions amid polar clusters of adenine and D-glucose/D-maltose moieties. In easy terms, overlapping of hydration shells declines the attractive forces amid H₂O and adenine that guides to augmentation in volume of solutions and it also amplifies with advancing concentration of D-glucose/D-maltose solvent system in the studied systems.

The potential interactions predominant in the investigated systems are conferred beneath:

- (i) Hydrophilic-hydrophilic interactions amid >C=N-, >C-N=, -NH₂ groups of adenine and >C=O, -OH, >C-O- groups of saccharide moieties.
- (ii) Hydrophobic-hydrophobic interactions amid the non-polar fragments of adenine and saccharide moieties.

In general, kind (i) interactions offer a positive assistance to transfer values whilst type (ii) interactions proffer a negative assistance to transfer values. Accordingly, it can be analyzed that kind (i) interactions are ushering in the explored systems.

4.2.1.4 Temperature Dependent Limiting Apparent Molar Volume

The limiting apparent molar volume relies on temperature as per the polynomial equation (2.7). In the conducted case, 303.15 K is taken as reference temperature. The speculated data of empirical constants for adenine in water and aqueous D-glucose/Dmaltose solvent system is documented in Table 4.2.3. Also, the first derivative of limiting apparent molar volume concerning temperature is referred to as limiting apparent molar expansibility, E^0_{ϕ} which is an influential parameter in enlightening multifarious interactions persisting in the scrutinized systems. It has been assessed by using expression (2.8). Table 4.2.4 demonstrates that positive E^0_{ϕ} values are lowering with elevation in temperature. The positive E^0_{ϕ} values in Table 4.2.4 display the caging effect ie. Intensification of the solvation spheres of the solute molecules upon divagation in the concentration of solvent media [15]. This signifies the presence of vital interactions amid adenine and solvent media. The drop in E^0_{ϕ} values with an increase in temperature for all the scrutinized mixtures illustrates the dehydration of hydrated solute moieties. In verity, for the accounting of the structure making/breaking demeanor of adenine in the composed solvent systems, a thermodynamic relation was allocated by Hepler [16], which is displayed in equation (2.10). In the present experimentation, sign of $(\partial E^0_{\phi}/\partial T)_P$ is negative for all the solution systems of adenine. This manifests the structure-breaking (chaotropic) behavior of adenine in water and aqueous D-glucose/D-maltose solvent system. Table 4.2.4 itemizes the enumerated data of $(\partial E^0_{\phi}/\partial T)_P$ for all the assessed solution systems.

Table 4.2.3: Deduced data of a, b and c constants corresponding to adenine in aqueous and $H_2O + D$ -glucose/D-maltose mixtures.

	$a \times 10^6$ (m ³ /mol ⁻¹)	$b \times 10^6$ (m ³ /mol/ K)	c ×10 ⁶ (m ³ /mol/ K ²)
Adenine + water	86.98(±0.04)	0.1312(±0.0039)	-0.00251(±0.00067)
Adenine +0.04994 mol/kg (D-glucose)	88.37(±0.15)	0.1764(±0.0140)	-0.00046(±0.00237)
Adenine +0.09939 mol/kg (D-glucose)	88.52(±0.08)	0.1768(±0.0074)	-0.00131(±0.00121)
Adenine +0.15003 mol/kg (D-glucose)	88.85(±0.03)	0.1432(±0.0019)	-0.00240(±0.00042)
Adenine +0.04992 mol/kg (D-maltose)	89.91(±0.07)	0.1106(±0.0069)	-0.00174(±0.00116)
Adenine +0.09947 mol/kg (D-maltose)	90.53(±0.10)	0.1204(±0.0092)	-0.00057(±0.00156)
Adenine + 0.14947 mol/kg (D-maltose)	90.98(±0.02)	0.1554(±0.0023)	-0.00323(±0.00039)

Table 4.2.4: Deduced data of apparent molar expansibility, E^0_{ϕ} and $(\partial E^0_{\phi}/\partial T)_P$, Hepler's constant for adenine in water and aqueous D-glucose/D-maltose solutions at T/K = 293.15 - 313.15 and P = 0.1 MPa.

		E^{c}	$\rho_{\phi} \times 10^6 (\mathrm{m}^3 / \mathrm{s})$	mol/ K)		$(\partial E^0 \phi / \partial T)_P$
Interpreted Systems	293.15 K	298.15 K	303.15 K	308.15 K	313.15 K	(m ³ /mol/ K ²)
Adenine + water	0.1814	0.1563	0.1312	0.1061	0.0810	-0.00502
Adenine + 0.04994 mol/kg (D-glucose)	0.1856	0.181	0.1764	0.1718	0.1672	-0.00092
Adenine + 0.09939 mol/kg (D-glucose)	0.2030	0.1899	0.1768	0.1637	0.1506	-0.00262
Adenine + 0.15003 mol/kg (D-glucose)	0.1912	0.1672	0.1432	0.1192	0.0952	-0.00480
Adenine + 0.04992 mol/kg (D-maltose)	0.1454	0.128	0.1106	0.0932	0.0758	-0.00348
Adenine + 0.09947 mol/kg (D-maltose)	0.1318	0.1261	0.1204	0.1147	0.1090	-0.00114
Adenine + 0.14947 mol/kg (D-maltose)	0.2200	0.1877	0.1554	0.1231	0.0908	-0.00646

4.2.1.5 Taste Behavior

For the analysis of the taste behavior of solute (adenine) in assorted aqueous saccharide media, a volumetric parameter i.e. apparent specific volume or apparent massic volume has been assessed. It is a paramount parameter that demonstrates the hydrological packing of solute molecules in the chosen solvent media. The formula (2.11) has been employed for the assessment of apparent specific volume. Herein, the reckoned ASV values for adenine in water and varied aqueous saccharide media are in the range $(0.64\text{-}0.70) \times 10^{-3} \text{ m}^3 \text{ kg}^{-1} \text{ mol}^{-1}$. The inferred ASV data specify that adenine has a sweet taste in water and anomalous concentrations of chosen saccharides. The deduced ASV data has been illustrated in Table 4.2.5, from where we can intimate that ASV of adenine advances with the proliferation in its molality as well as with the elevation in temperature. This in turn divulges that the sweetness of adenine enriches with an increase in its molality as well as with temperature.

Table 4.2.5: The deduced data of *ASV* for adenine in water and aqueous D-glucose/D-maltose solutions at T/K = 293.15 - 313.15 and P = 0.1 MPa.

T/K	am/mol kg ⁻¹	ASV	T/K	^a m/mol kg ⁻¹	ASV
		Ade	nine in water		
293.15	0.00000		308.15	0.00000	
293.15	0.00202	0.64	308.15	0.00202	0.65
293.15	0.00408	0.64	308.15	0.00408	0.66
293.15	0.00582	0.65	308.15	0.00582	0.66
293.15	0.00765	0.65	308.15	0.00765	0.67
293.15	0.00992	0.66	308.15	0.00992	0.67
298.15	0.00000	0.64	313.15	0.00000	
298.15	0.00202	0.65	313.15	0.00202	0.66
298.15	0.00408	0.65	313.15	0.00408	0.66
298.15	0.00582	0.65	313.15	0.00582	0.67
298.15	0.00765	0.66	313.15	0.00765	0.67
298.15	0.00992	0.64	313.15	0.00992	0.68
303.15	0.00000				
303.15	0.00202	0.65			
303.15	0.00408	0.65			
303.15	0.00582	0.66			
303.15	0.00765	0.66			
303.15	0.00992	0.66			

		Adenine in 0.0	04994 mol kg ⁻¹ D-gl	ucose	
293.15	0.00000		308.15	0.00000	
293.15	0.00193	0.64	308.15	0.00193	0.66
293.15	0.00413	0.65	308.15	0.00413	0.67
293.15	0.00650	0.65	308.15	0.00650	0.67
293.15	0.00797	0.66	308.15	0.00797	0.67
293.15	0.01000	0.66	308.15	0.01000	0.68
298.15	0.00000		313.15	0.00000	
298.15	0.00193	0.65	313.15	0.00193	0.67
298.15	0.00413	0.65	313.15	0.00413	0.67
298.15	0.00650	0.66	313.15	0.00650	0.68
298.15	0.00797	0.66	313.15	0.00797	0.68
298.15	0.01000	0.66	313.15	0.01000	0.68
303.15	0.00000				
303.15	0.00193	0.66			
303.15	0.00413	0.66			
303.15	0.00650	0.66			
303.15	0.00797	0.67			
303.15	0.01000	0.67			
		Adenine in 0.0)9939 mol kg ⁻¹ D-gl	ucose	
293.15	0.00000		308.15	0.00000	
293.15	0.00191	0.65	308.15	0.00191	0.67
293.15	0.00427	0.65	308.15	0.00427	0.67
293.15	0.00597	0.66	308.15	0.00597	0.67
293.15	0.00812	0.66	308.15	0.00812	0.68
293.15	0.01009	0.67	308.15	0.01009	0.68
298.15	0.00000		313.15	0.00000	
298.15	0.00191	0.65	313.15	0.00191	0.67
298.15	0.00427	0.66	313.15	0.00427	0.68
298.15	0.00597	0.66	313.15	0.00597	0.68
298.15	0.00812	0.67	313.15	0.00812	0.69
298.15	0.01009	0.67	313.15	0.01009	0.69
303.15	0.00000				
303.15	0.00191	0.66			
303.15	0.00427	0.66			
303.15	0.00597	0.67			
303.15	0.00812	0.67			
303.15	0.01009	0.68			

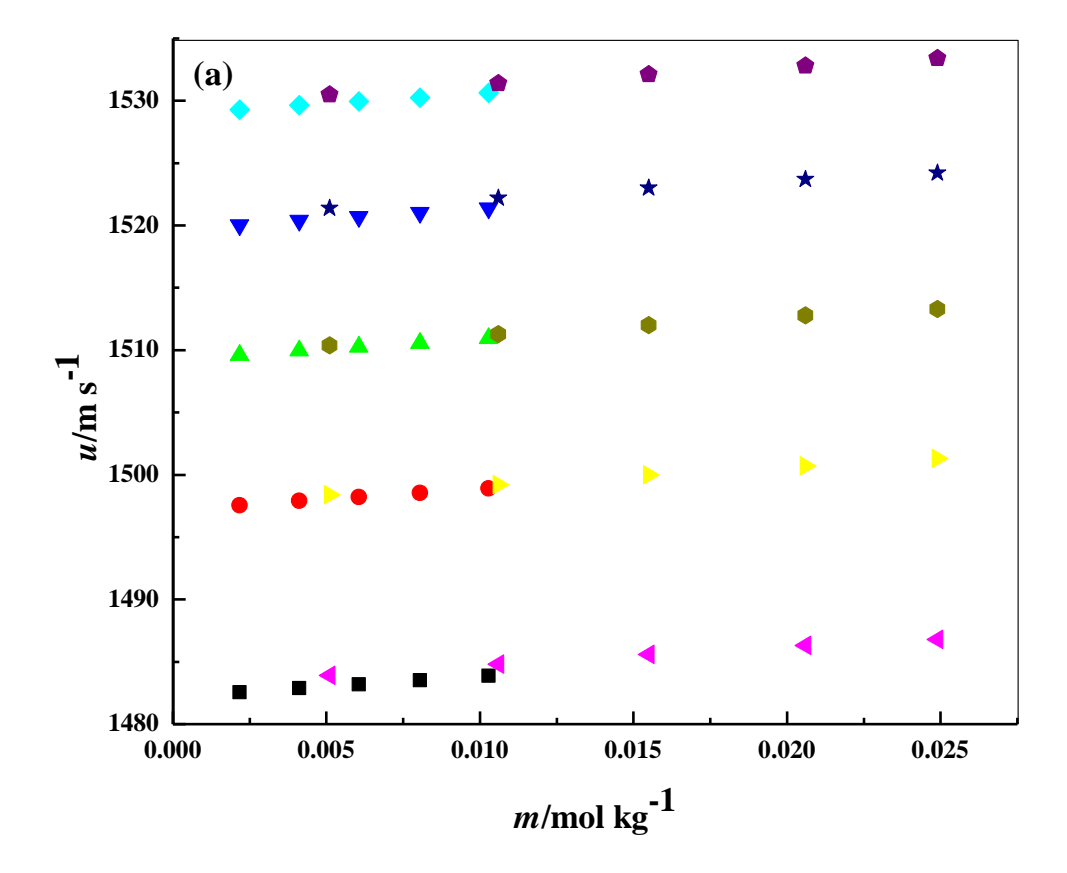
		Adenine in 0.1	15003 mol kg ⁻¹ D-gl	ucose	
293.15	0.00000		308.15	0.00000	
293.15	0.00216	0.65	308.15	0.00216	0.67
293.15	0.00411	0.66	308.15	0.00411	0.67
293.15	0.00605	0.66	308.15	0.00605	0.67
293.15	0.00804	0.66	308.15	0.00804	0.68
293.15	0.01027	0.67	308.15	0.01027	0.68
298.15	0.00000		313.15	0.00000	
298.15	0.00216	0.66	313.15	0.00216	0.68
298.15	0.00411	0.66	313.15	0.00411	0.68
298.15	0.00605	0.66	313.15	0.00605	0.68
298.15	0.00804	0.67	313.15	0.00804	0.69
298.15	0.01027	0.67	313.15	0.01027	0.69
303.15	0.00000				
303.15	0.00216	0.66			
303.15	0.00411	0.67			
303.15	0.00605	0.67			
303.15	0.00804	0.67			
303.15	0.01027	0.68			
		Adenine in 0.0)4992 mol kg ⁻¹ D-m	altose	
293.15	0.00000		308.15	0.00000	
293.15	0.00217	0.66	308.15	0.00217	0.67
293.15	0.00411	0.66	308.15	0.00411	0.68
293.15	0.00606	0.67	308.15	0.00606	0.68
293.15	0.00805	0.67	308.15	0.00805	0.68
293.15	0.01028	0.68	308.15	0.01028	0.69
298.15	0.00000		313.15	0.00000	
298.15	0.00217	0.66	313.15	0.00217	0.68
298.15	0.00411	0.67	313.15	0.00411	0.68
298.15	0.00606	0.67	313.15	0.00606	0.68
298.15	0.00805	0.68	313.15	0.00805	0.69
298.15	0.01028	0.68	313.15	0.01028	0.69
303.15	0.00000				
303.15	0.00217	0.67			
303.15	0.00411	0.67			
303.15	0.00606	0.68			
303.15	0.00805	0.68			
303.13					

		Adenine in 0.0	9947 mol kg ⁻¹ D-m	altose	
293.15	0.00000		308.15	0.00000	
293.15	0.00200	0.66	308.15	0.00200	0.68
293.15	0.00400	0.67	308.15	0.00400	0.68
293.15	0.00633	0.67	308.15	0.00633	0.69
293.15	0.00788	0.68	308.15	0.00788	0.69
293.15	0.01019	0.68	308.15	0.01019	0.69
298.15	0.00000		313.15	0.00000	
298.15	0.00200	0.67	313.15	0.00200	0.68
298.15	0.00400	0.67	313.15	0.00400	0.69
298.15	0.00633	0.68	313.15	0.00633	0.69
298.15	0.00788	0.68	313.15	0.00788	0.69
298.15	0.01019	0.68	313.15	0.01019	0.70
303.15	0.00000				
303.15	0.00200	0.67			
303.15	0.00400	0.68			
303.15	0.00633	0.68			
303.15	0.00788	0.68			
303.15	0.01019	0.69			
		Adenine in 0.1	4947 mol kg ⁻¹ D-m	altose	
293.15	0.00000		308.15	0.00000	
293.15	0.00199	0.67	308.15	0.00199	0.68
293.15	0.00409	0.67	308.15	0.00409	0.69
293.15	0.00582	0.68	308.15	0.00582	0.69
293.15	0.00806	0.68	308.15	0.00806	0.69
293.15	0.00993	0.68	308.15	0.00993	0.70
298.15	0.00000		313.15	0.00000	
298.15	0.00199	0.67	313.15	0.00199	0.69
298.15	0.00409	0.68	313.15	0.00409	0.69
298.15	0.00582	0.68	313.15	0.00582	0.70
298.15	0.00806	0.68	313.15	0.00806	0.70
298.15	0.00993	0.69	313.15	0.00993	0.70
303.15	0.00000				
303.15	0.00199	0.68			
303.15	0.00409	0.68			
303.15	0.00582	0.68			
303.15	0.00806	0.69			
303.15	0.00993	0.69			

 $^{^{}a}m$ (molkg⁻¹) symbolizes the molal composition of adenine in (water + D-glucose/D-maltose) solutions.

4.2.2 Speed of Sound Data

Experimentally gauged velocity of sound data concerning diverse concentrations of binary/ternary combinations at five discrete temperatures (T = 293.15 K to 313.15 K) is exemplified in Table 4.2.6. From this data, it can be observed that the velocity of sound increases with both higher temperature and greater adenine concentration. In upsurge, the acquired velocity of sound data related to adenine, D-glucose, and D-maltose in H₂O has been approximated with the available literature reports [1-3,6,7,9,13,15,17] and the comparison plots are being presented in Figures 4.2.3 (a), (b), (c). From comparative plots of assessment, it can be gathered that there triumphs first-class concurrence between the obtained data and literature essays. However, the small deviations in the plots could be attributed to instrumental variations, inconsistencies in the experimental procedure, and differences in the assessed uncertainties.



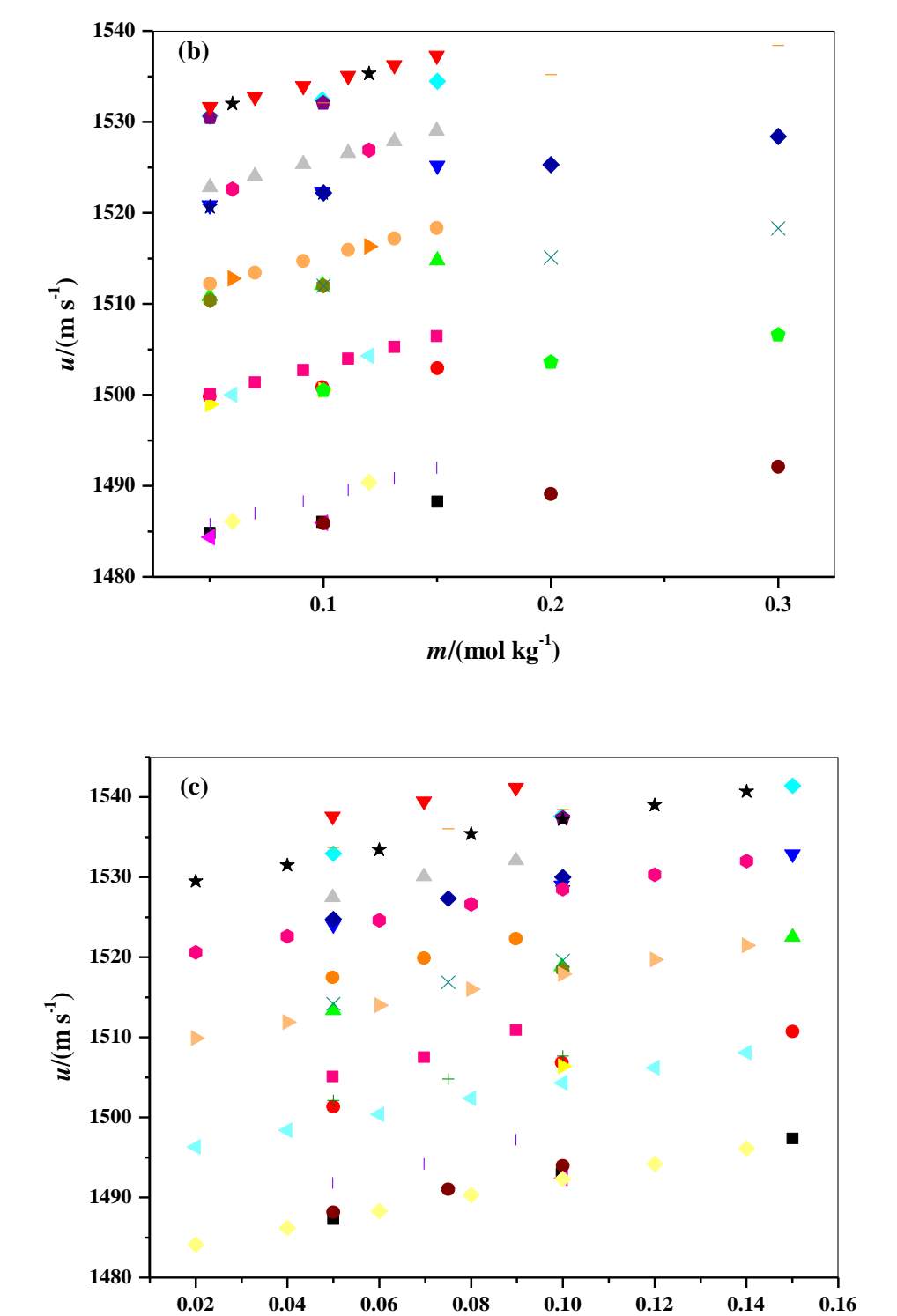


Figure 4.2.3: Graphs representing deviation in measured sound velocity data with the accessible reports at discrete temperatures.

 $m/(\text{mol kg}^{-1})$

- (a) For adenine + water at $T(K) = \blacksquare$: Conducted investigation on 293.15, \bullet : Conducted dataon 298.15, \blacktriangle : Conducted investigation on 303.15, \blacktriangledown Conducted investigation on 308.15, \bullet Conducted investigation on 313.15, \blacktriangleleft : Lit. [1] on 293.15, \blacktriangleright : Lit. [1] on 298.15, \bullet : Lit. [1] on 303.15.
- **(b)** D-Glucose + water at $T(K) = \blacksquare$: Conducted investigation on 293.15, : Conducted investigation on 298.15, ▲ : Conducted investigation on 303.15, ▼ : Conducted investigation on 308.15, : Lit. [2] on 293.15, ▶ : Lit. [2] on 298.15, : Lit. [2] on 303.15, ★ : Lit. [2] on 308.15, : Lit. [2] on 313.15, : Lit. [3] on 293.15, : Lit. [3] on 298.15, × : Lit. [3] on 303.15, ◆ : Lit. [3] on 308.15, □ : Lit. [17] on 308.15, □ : Lit. [17] on 308.15, : Lit. [6] on 303.15, : Lit. [6] on 303.15.
- (c) D-Maltose + water at $T(K) = \blacksquare$: Conducted investigation on 293.15, : Conducted investigation on 298.15, ▲ : Conducted investigation on 303.15, ▼ : Conducted investigation on 308.15, : Lit. [13] on 293.15, ► : Lit. [13] on 298.15, : Lit. [13] on 303.15, ★ : Lit. [13] on 308.15, : Lit. [13] on 313.15, : Lit. [15] on 293.15, + : Lit. [15] on 298.15, × : Lit. [15] on 303.15, : Lit. [15] on 303.15, □ : Lit. [15] on 303.15, □ : Lit. [15] on 303.15, □ : Lit. [15] on 303.15, : Lit. [15] on 303.15, □ :

4.2.2.1 Apparent Molar Isentropic Compression

Furthermore, the exploratory density and velocity of sound data were utilized for the estimation of apparent molar isentropic compression as per the equation (2.12). By the use of the Newton-Laplace relation, the adiabatic compressibilities have been inferred, as per the relations (2.13) and (2.14). Further, the figured data of $K_{\phi,s}$ has been itemized in Table 4.2.6. It can be analyzed via this Table 4.2.6 that $K_{\phi,s}$ values are negative for the examined combinations at all temperatures and molalities. This in turn demonstrates that the solvent molecules that are near adenine molecules in the solvation shells are slightly compressible in comparison to bulk solvent [18]. In proliferation, these $K_{\phi,s}$ values are advancing with an increase in temperature as well as concentration of adenine/aqueous saccharide media. The increase in temperature renders an elaboration in molecular pulsations which results in expansion in volume and adiabatic compressibility of solutions.

Table 4.2.6: Experimentally acquired sound velocities, u and calculated apparent molar isentropic compressions, $K_{\phi,s}$ for adenine in water and aqueous D-glucose/D-maltose solutions at T/K = 293.15 - 313.15 and P = 0.1 MPa.

T(K)	^a m(mol/kg)	u(m/s)	$K_{\phi,s} \times 10^{15} (\text{m}^3/\text{mol}^7/\text{Pa})$	T(K)	^a m(mol/kg)	<i>u</i> (m/s)	$K_{\phi,s} \times 10^{15} (\text{m}^3/\text{mol}^3/\text{Pa})$		
Adenine + water									
293.15	0.00000	1482.18		308.15	0.00000	1519.68			
293.15	0.00202	1482.54	-92.19	308.15	0.00202	1520.04	-84.73		
293.15	0.00408	1482.90	-90.81	308.15	0.00408	1520.40	-83.01		
293.15	0.00582	1483.20	-89.68	308.15	0.00582	1520.70	-82.15		
293.15	0.00765	1483.51	-88.33	308.15	0.00765	1521.01	-80.90		
293.15	0.00992	1483.89	-86.97	308.15	0.00992	1521.39	-79.51		
298.15	0.00000	1497.20		313.15	0.00000	1528.92			
298.15	0.00202	1497.56	-89.10	313.15	0.00202	1529.28	-82.62		
298.15	0.00408	1497.92	-87.76	313.15	0.00408	1529.64	-81.35		
298.15	0.00582	1498.22	-86.64	313.15	0.00582	1529.94	-80.33		
298.15	0.00765	1498.53	-85.43	313.15	0.00765	1530.25	-79.01		
298.15	0.00992	1498.91	-84.01	313.15	0.00992	1530.63	-77.70		
303.15	0.00000	1509.25							
303.15	0.00202	1509.61	-86.71						
303.15	0.00408	1509.97	-85.40						
303.15	0.00582	1510.27	-84.27						
303.15	0.00765	1510.58	-82.96						
303.15	0.00992	1510.96	-81.69						
		A	denine + 0.04994	mol/kg D	-glucose				
293.15	0.00000	1484.81		308.15	0.00000	1520.83			
293.15	0.00193	1485.16	-91.97	308.15	0.00193	1521.18	-83.74		
293.15	0.00413	1485.55	-90.39	308.15	0.00413	1521.57	-82.39		
293.15	0.00650	1485.97	-89.44	308.15	0.00650	1521.99	-81.45		
293.15	0.00797	1486.22	-88.22	308.15	0.00797	1522.24	-80.47		
293.15	0.01000	1486.56	-86.69	308.15	0.01000	1522.58	-79.08		
298.15	0.00000	1499.83		313.15	0.00000	1530.64			
298.15	0.00193	1500.18	-88.86	313.15	0.00193	1530.99	-81.45		
298.15	0.00413	1500.57	-87.14	313.15	0.00413	1531.38	-80.18		
298.15	0.00650	1500.99	-86.31	313.15	0.00650	1531.79	-78.95		
298.15	0.00797	1501.24	-85.10	313.15	0.00797	1532.04	-77.98		
298.15	0.01000	1501.58	-83.55	313.15	0.01000	1532.38	-76.67		

303.15	0.00000	1510.85					
303.15	0.00193	1511.20	-86.21				
303.15	0.00413	1511.59	-84.78				
303.15	0.00650	1512.01	-83.92				
303.15	0.00797	1512.26	-82.86				
303.15	0.01000	1512.60	-81.36				
		A	denine + 0.0	9939 mol/kg D-g	glucose		
293.15	0.00000	1486.03		308.15	0.00000	1522.33	
293.15	0.00191	1486.38	-90.70	308.15	0.00191	1522.68	-83.00
293.15	0.00427	1486.80	-89.77	308.15	0.00427	1523.10	-81.93
293.15	0.00597	1487.10	-88.44	308.15	0.00597	1523.40	-80.80
293.15	0.00812	1487.48	-87.39	308.15	0.00812	1523.78	-79.87
293.15	0.01009	1487.81	-85.61	308.15	0.01009	1524.11	-78.29
298.15	0.00000	1500.85		313.15	0.00000	1532.42	
298.15	0.00191	1501.20	-88.56	313.15	0.00191	1532.76	-80.03
298.15	0.00427	1501.62	-86.39	313.15	0.00427	1533.19	-79.15
298.15	0.00597	1501.92	-85.32	313.15	0.00597	1533.48	-77.79
298.15	0.00812	1502.30	-84.44	313.15	0.00812	1533.85	-76.51
298.15	0.01009	1502.64	-83.20	313.15	0.01009	1534.18	-75.26
303.15	0.00000	1512.07					
303.15	0.00191	1512.42	-85.85				
303.15	0.00427	1512.84	-84.01				
303.15	0.00597	1513.14	-82.99				
303.15	0.00812	1513.52	-82.06				
303.15	0.01009	1513.86	-80.97				
		A	denine + 0.1	5003 mol/kg D-g	glucose		
293.15	0.00000	1488.26		308.15	0.00000	1525.18	
293.15	0.00216	1488.66	-89.68	308.15	0.00216	1525.57	-81.16
293.15	0.00411	1489.01	-88.92	308.15	0.00411	1525.92	-80.24
293.15	0.00605	1489.35	-87.31	308.15	0.00605	1526.26	-79.07
293.15	0.00804	1489.70	-86.30	308.15	0.00804	1526.61	-78.19
293.15	0.01027	1490.08	-84.62	308.15	0.01027	1527.00	-77.17
298.15	0.00000	1502.94		313.15	0.00000	1534.46	
298.15	0.00216	1503.34	-87.15	313.15	0.00216	1534.85	-78.76
298.15	0.00411	1503.68	-85.63	313.15	0.00411	1535.20	-77.79
298.15	0.00605	1504.03	-84.42	313.15	0.00605	1535.53	-76.25

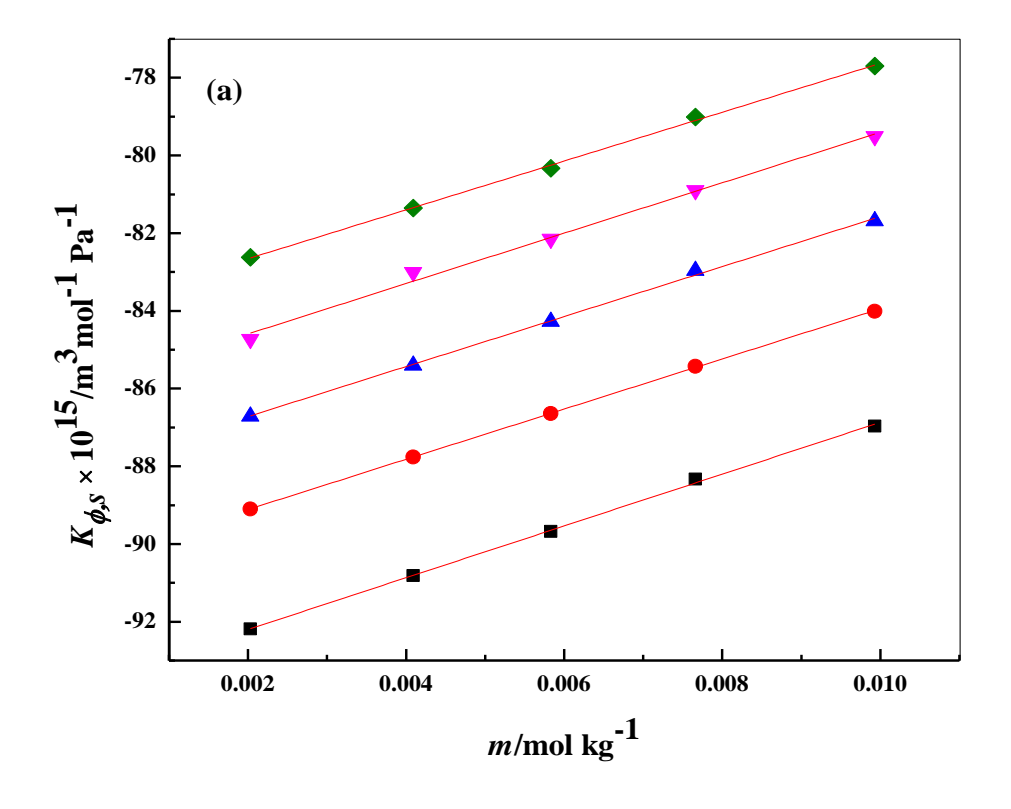
298.15	0.00804	1504.38	-83.43	313.15	0.00804	1535.88	-75.58
298.15	0.01027	1504.77	-82.36	313.15	0.01027	1536.26	-74.34
303.15	0.00000	1514.78					
303.15	0.00216	1515.17	-84.24				
303.15	0.00411	1515.52	-82.98				
303.15	0.00605	1515.87	-82.05				
303.15	0.00804	1516.22	-81.00				
303.15	0.01027	1516.60	-79.46				
		A	denine + 0.04	4992 mol/kg D-r	naltose		
293.15	0.00000	1487.32		308.15	0.00000	1524.10	
293.15	0.00217	1487.72	-90.66	308.15	0.00217	1524.50	-83.06
293.15	0.00411	1488.07	-89.24	308.15	0.00411	1524.85	-82.06
293.15	0.00606	1488.42	-88.38	308.15	0.00606	1525.20	-81.22
293.15	0.00805	1488.78	-87.66	308.15	0.00805	1525.55	-80.12
293.15	0.01028	1489.17	-86.35	308.15	0.01028	1525.94	-78.94
298.15	0.00000	1501.32		313.15	0.00000	1532.97	
298.15	0.00217	1501.72	-87.81	313.15	0.00217	1533.37	-80.64
298.15	0.00411	1502.07	-86.41	313.15	0.00411	1533.71	-79.70
298.15	0.00606	1502.42	-85.56	313.15	0.00606	1534.06	-78.81
298.15	0.00805	1502.77	-84.32	313.15	0.00805	1534.41	-77.71
298.15	0.01028	1503.16	-83.18	313.15	0.01028	1534.79	-76.18
303.15	0.00000	1513.37					
303.15	0.00217	1513.77	-85.48				
303.15	0.00411	1514.12	-84.30				
303.15	0.00606	1514.47	-83.38				
303.15	0.00805	1514.82	-82.13				
303.15	0.01028	1515.21	-80.92				
		A	denine + 0.09	9947 mol/kg D-r	naltose		
293.15	0.00000	1492.98		308.15	0.00000	1529.01	
293.15	0.00200	1493.36	-89.20	308.15	0.00200	1529.39	-82.56
293.15	0.00400	1493.73	-88.52	308.15	0.00400	1529.76	-81.52
293.15	0.00633	1494.16	-87.64	308.15	0.00633	1530.18	-80.02
293.15	0.00788	1494.44	-86.61	308.15	0.00788	1530.47	-79.38
293.15	0.01019	1494.85	-85.11	308.15	0.01019	1530.87	-77.78
298.15	0.00000	1506.82		313.15	0.00000	1537.62	
298.15	0.00200	1507.19	-86.95	313.15	0.00200	1537.99	-79.50

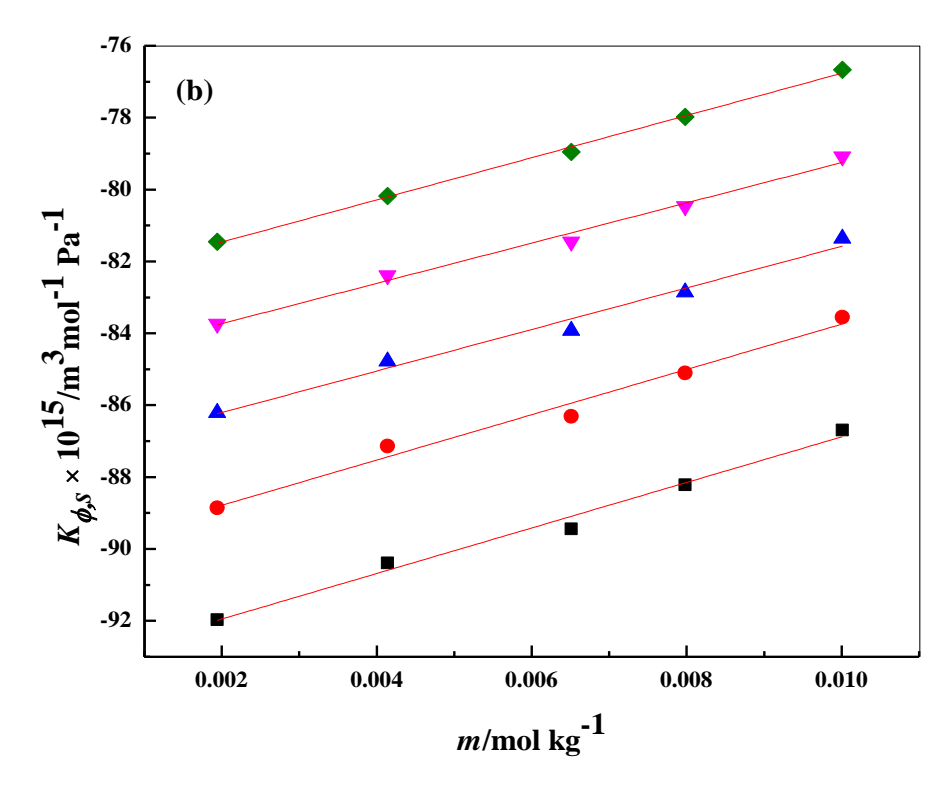
298.15	0.00400	1507.57	-85.95	313.15	0.00400	1538.36	-78.58
298.15	0.00633	1507.99	-84.55	313.15	0.00633	1538.78	-77.23
298.15	0.00788	1508.28	-83.77	313.15	0.00788	1539.05	-76.17
298.15	0.01019	1508.69	-82.67	313.15	0.01019	1539.46	-75.19
303.15	0.00000	1518.85					
303.15	0.00200	1519.23	-84.92				
303.15	0.00400	1519.60	-83.85				
303.15	0.00633	1520.03	-82.64				
303.15	0.00788	1520.31	-81.70				
303.15	0.01019	1520.71	-79.72				
		A	denine + 0.1	4947 mol/kg D-	maltose		
293.15	0.00000	1497.35		308.15	0.00000	1532.87	
293.15	0.00199	1497.73	-88.05	308.15	0.00199	1533.25	-80.82
293.15	0.00409	1498.13	-87.46	308.15	0.00409	1533.64	-79.97
293.15	0.00582	1498.45	-86.48	308.15	0.00582	1533.96	-78.74
293.15	0.00806	1498.87	-85.56	308.15	0.00806	1534.37	-77.63
293.15	0.00993	1499.21	-84.41	308.15	0.00993	1534.71	-76.75
298.15	0.00000	1510.74		313.15	0.00000	1541.41	
298.15	0.00199	1511.12	-85.81	313.15	0.00199	1541.78	-77.82
298.15	0.00409	1511.52	-84.83	313.15	0.00409	1542.17	-76.75
298.15	0.00582	1511.84	-83.67	313.15	0.00582	1542.49	-75.87
298.15	0.00806	1512.25	-82.68	313.15	0.00806	1542.89	-74.90
298.15	0.00993	1512.59	-81.60	313.15	0.00993	1543.23	-74.01
303.15	0.00000	1522.55					
303.15	0.00199	1522.93	-83.56				
303.15	0.00409	1523.33	-82.40				
303.15	0.00582	1523.65	-81.30				
303.15	0.00806	1524.06	-80.17				
303.15	0.00993	1524.39	-78.78				

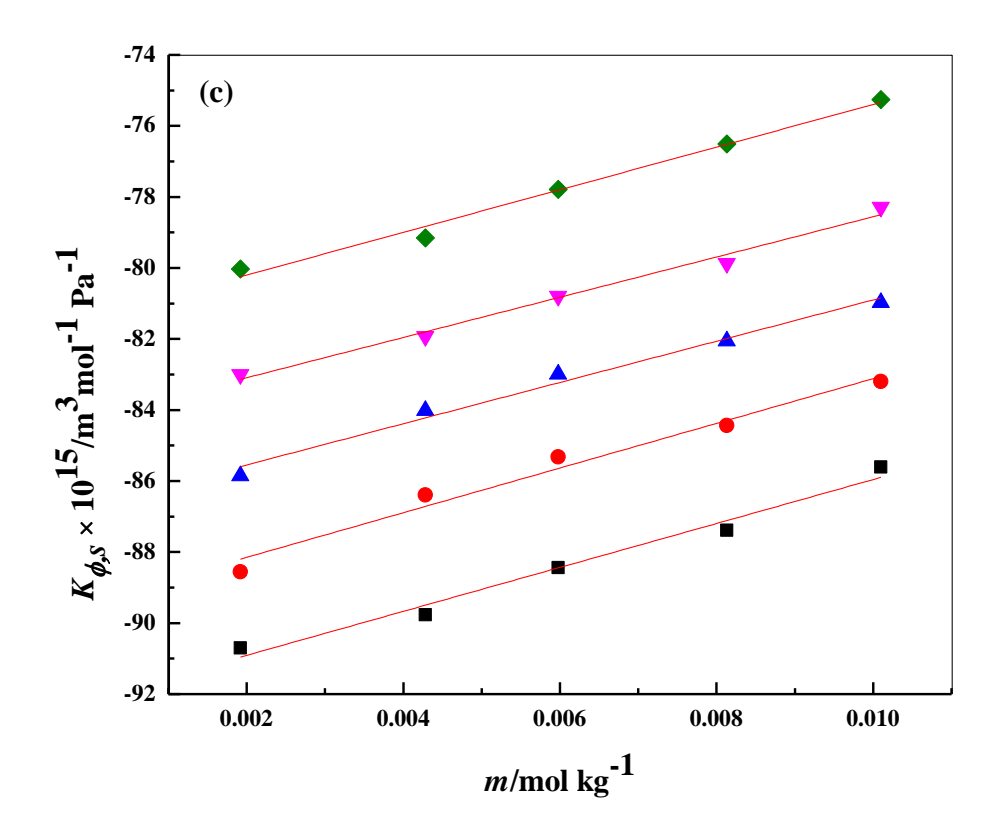
^am(mol/kg) symbolizes the molal composition of adenine in (water + D-glucose/D-maltose) solutions.

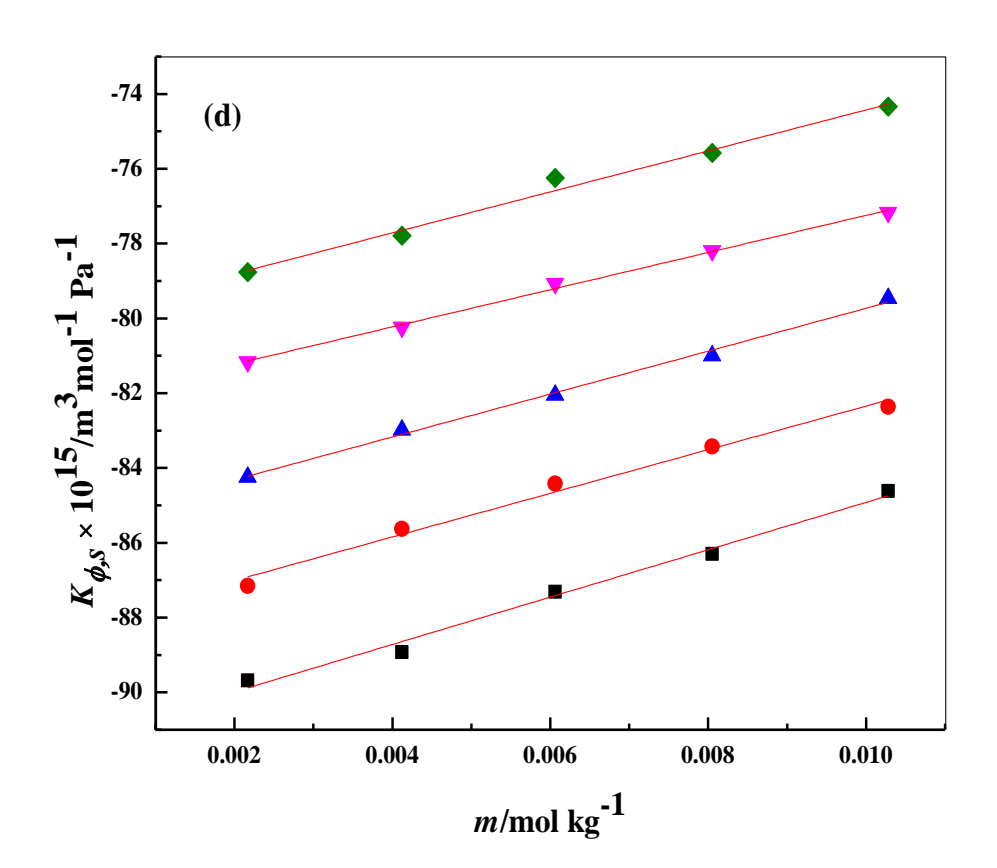
4.2.2.2 Limiting Apparent Molar Isentropic Compression

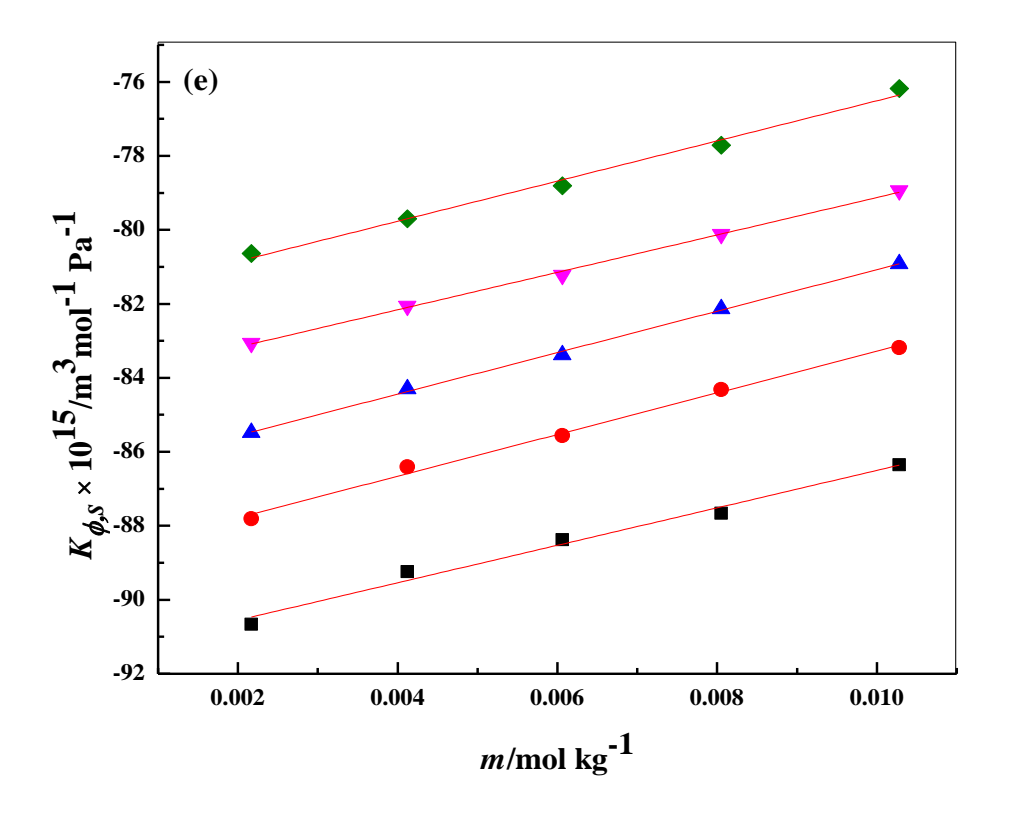
The limiting apparent molar isentropic compression $(K^0_{\phi,s})$ furnishes commendable data related to the extent of interactions acting in the explored systems. By creating the plots of $K_{\phi,s}$ against m, we obtain the intercept $(K^0_{\phi,s})$ and slope (S_k) as illustrated by equation (2.15).

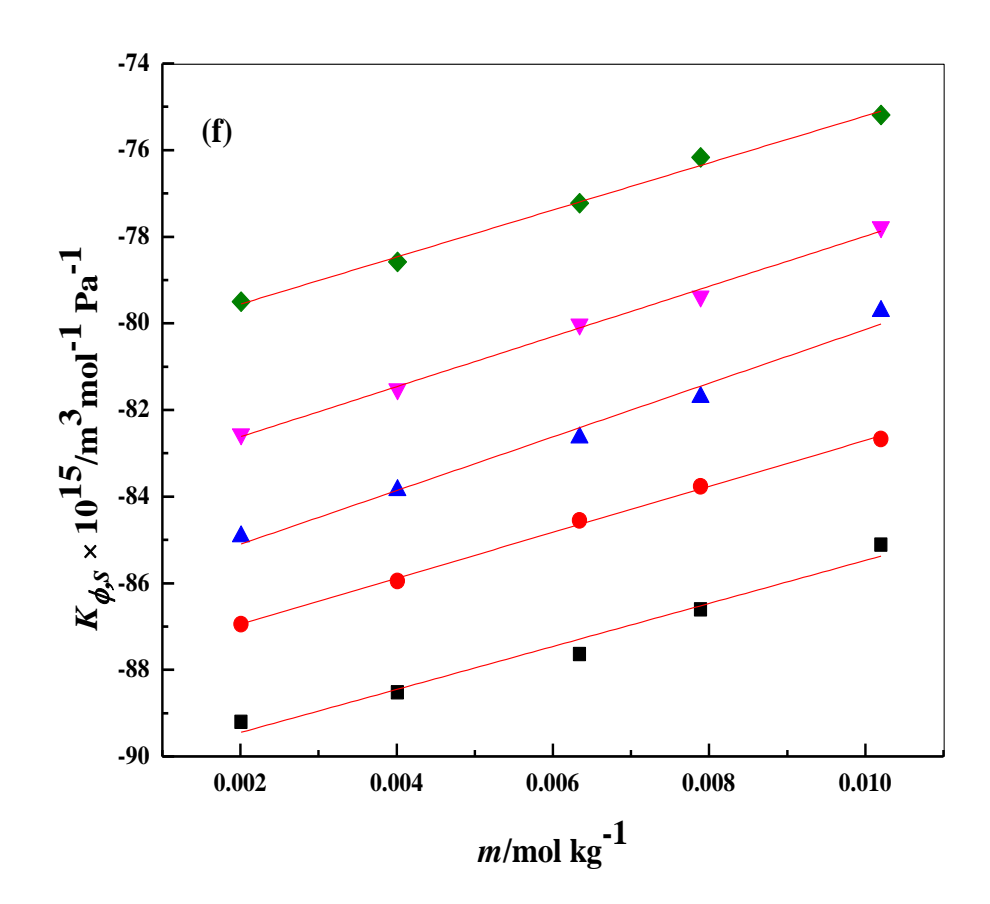












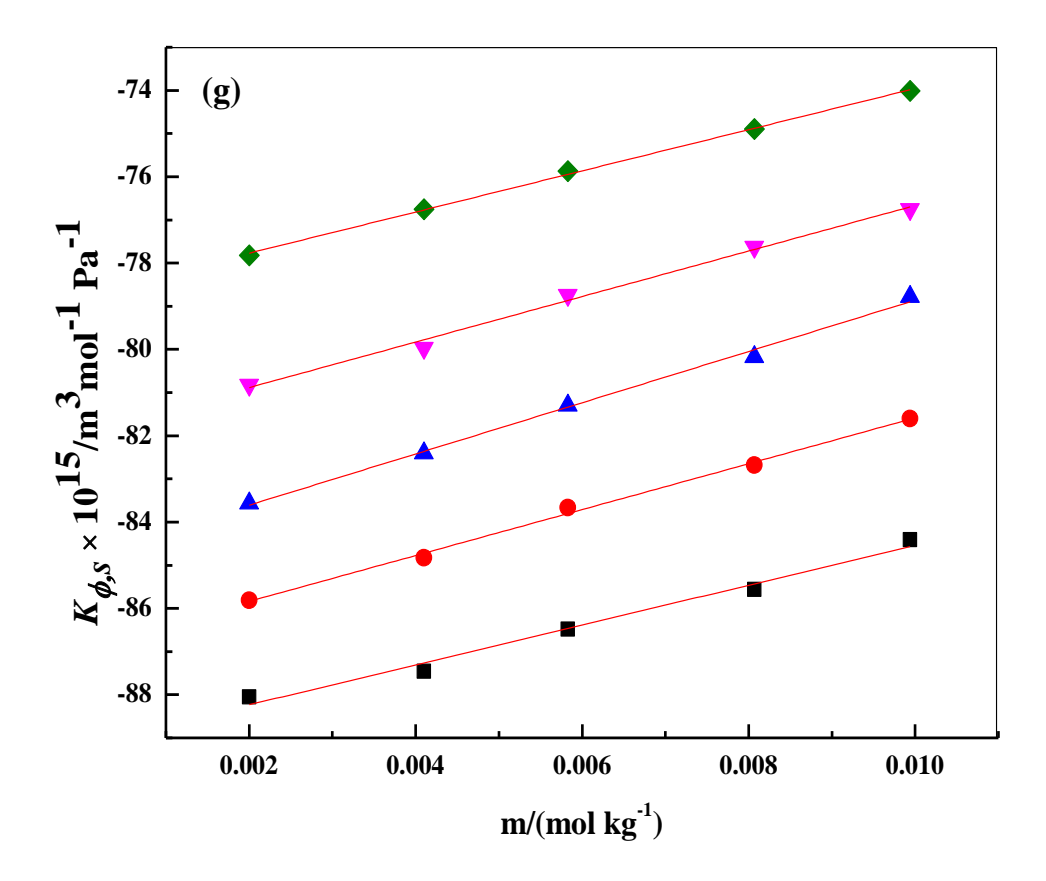


Figure 4.2.4: The graph depicting change in $K_{\phi,s} \times 10^{15}$ /m³ mol⁻¹ Pa⁻¹ against m/mol kg⁻¹ for adenine in (a) water, (b) 0.04994 mol kg⁻¹ D-glucose, (c) 0.09939 mol kg⁻¹ D-glucose, (d) 0.15003 mol kg⁻¹ D-glucose, (e) 0.04992 mol kg⁻¹ D-maltose, (f) 0.09947 mol kg⁻¹ D-maltose, (g) 0.14947 mol kg⁻¹ D-maltose at discrete temperatures, ■ : 293.15 K, •: 298.15 K, •: 303.15 K, •: 308.15 K, •: 313.15 K.

Figure 4.2.4 (a) – (g) displays the plots of $K_{\phi,s}$ against m for adenine in varying solvent media, while Table 4.2.7 demonstrates the received data of slopes and intercepts at varied temperatures. It can be decoded through Table 4.2.7 that there is a rise in $K^0_{\phi,s}$ values with an upsurge in temperature, in turn supplementing the compressibility of studied samples.

Higher values of $K^0_{\phi,s}$ in aqueous D-maltose than D-glucose media simply insinuates that the dehydration of hydrated adenine molecules is more in the case of aqueous D-maltose than aqueous D-glucose solvent system. Consequently, this reveals the presence of efficient interactions amid adenine and D-maltose in comparison to D-glucose.

4.2.2.3 Limiting Apparent Molar Isentropic Compression of Transfer

For adenine, the limiting apparent molar isentropic compression of transfer from water to aqueous D-glucose/D-maltose media has been fetched by the use of equation (2.16). The enumerated data of $\Delta_{tr}K^0_{\phi,s}$ is demonstrated in Table 4.2.7, from where it can be analyzed that these values are positive and are advancing with an increase in molality of D-glucose/D-maltose media which simply conveys the presence of enriched hydrophilic–hydrophilic interactions that are ushering over hydrophobic–hydrophobic interactions in the analyzed solutions.

Table 4.2.7: Data of apparent molar isentropic compression at very high dilution, $K^0_{\phi,s}$ along with S_k slopes, and corresponding transfer values $\Delta_{tr}K^0_{\phi,s}$ for adenine in water and aqueous D-glucose/D-maltose solutions at T/K = 293.15 - 313.15 and P = 0.1 MPa.

	T/K								
Property	293.15	298.15	303.15	308.15	313.15				
Adenine in water									
$K^{\theta}_{\phi,s} \times 10^{15} (\text{m}^3/\text{mol/Pa})$	-93.53(±0.07)	-90.40(±0.02)	-88.01(±0.09)	-85.89(±0.18)	-83.91(±0.08)				
$S_k \times 10^{15} (\text{m}^3 \text{kg/mol}^2/\text{Pa})$	666.37(±11.04)	645.65(±3.19)	643.38(±13.35)	648.39(±26.96)	628.40(±11.75)				
Adenine in 0.04994 mol kg ⁻¹ D-glucose									
$K^0_{\phi,s} \times 10^{15} (\text{m}^3/\text{mol/Pa})$	-93.22(±0.27)	-90.05(±0.32)	-87.36(±0.27)	-84.85(±0.21)	-82.64(±0.11)				
$S_k \times 10^{15} (\text{m}^3 \text{kg/mol}^2/\text{Pa})$	633.46(±40.79)	630.14(±47.00)	578.20(±40.61)	559.99(±31.02)	586.92(±15.82)				
$\Delta_{tr} K^0_{\phi,s} \times 10^{15} (\text{m}^3/\text{mol/Pa}) 0.32$		0.36	0.64	1.04	1.28				
	Adenii	ne in 0.09939 mo	l kg ⁻¹ D-glucose						
$K^0_{\phi,s} \times 10^{15} (\text{m}^3/\text{mol/Pa})$	-92.15(±0.33)	-89.41(±0.38)	-86.71(±0.27)	-84.22(±0.23)	-81.40(±0.24)				
$S_k \times 10^{15} (\text{m}^3 \text{kg/mol}^2/\text{Pa})$	618.89(±49.29)	628.89(±55.96)	580.72(±39.64)	566.55(±34.41)	560.23(±35.61)				
$\Delta_{tr}K^0_{\phi,s} \times 10^{15} (\text{m}^3/\text{mol/Pa})$	1.39	0.99	1.30	1.67	2.52				
Adenine in 0.15003 mol kg ⁻¹ D-glucose									
$K^{\theta}_{\phi,s} \times 10^{15} (\text{m}^3/\text{mol/Pa})$	-91.25(±0.25)	-88.18(±0.25)	-85.46(±0.14)	-82.22(±0.10)	-79.90(±0.23)				
$S_k \times 10^{15} (\text{m}^3 \text{kg/mol}^2/\text{Pa})$	633.09(±36.56)	583.19(±36.44)	573.47(±21.03)	497.24(±15.23)	547.72(±34.62)				
$\Delta_{tr}K^0_{\phi,s} \times 10^{15} (\text{m}^3/\text{mol/Pa})$	2.28	2.23	2.54	3.67	4.01				

Adenine in 0.04992 mol kg ⁻¹ D-maltose								
$K^0_{\phi,s} \times 10^{15} (\text{m}^3/\text{mol/Pa})$	-91.56(±0.23)	-88.91(±0.15)	-86.68(±0.08)	-84.18(±0.07)	-81.94(±0.19)			
$S_k \times 10^{15} (\mathrm{m}^3 \mathrm{kg/mol}^2/\mathrm{Pa})$	506.13(±33.59)	562.89(±21.78)	560.35(±11.47)	505.58(±10.93)	542.78(±27.50)			
$\Delta_{tr}K^0_{\phi,s} \times 10^{15} (\mathrm{m}^3/\mathrm{mol/Pa})$	1.97	1.49	1.33	1.71	1.98			
Adenine in 0.09947 mol kg ⁻¹ D-maltose								
$\overline{K^0_{\phi,s} \times 10^{15} (\text{m}^3/\text{mol/Pa})}$	-90.44(±0.31)	-88.01(±0.09)	-86.34(±0.29)	-83.78(±0.14)	-80.64(±0.15)			
$S_k \times 10^{15} (\text{m}^3 \text{kg/mol}^2/\text{Pa})$	496.69(±46.13)	530.39(±13.32)	619.72(±43.57)	579.14(±20.54)	543.20(±21.96)			
$\Delta_{tr}K^0_{\phi,s} \times 10^{15} (\mathrm{m}^3/\mathrm{mol/Pa})$	3.09	2.39	1.67	2.11	3.27			
	Adenir	ne in 0.14947 mo	l kg ⁻¹ D-maltose					
$\overline{K^0_{\phi,s} \times 10^{15} (\text{m}^3/\text{mol/Pa})}$	-89.16(±0.20)	-86.90(±0.11)	-84.79(±0.13)	-81.94(±0.15)	-78.72(±0.06)			
$S_k \times 10^{15} (\mathrm{m}^3 \mathrm{kg/mol}^2/\mathrm{Pa})$	461.57(±31.01)	531.51(±17.19)	593.24(±19.59)	527.11(±22.99)	476.80(±8.98)			
$\Delta_{tr}K^0_{\phi,s} \times 10^{15} (\mathrm{m}^3/\mathrm{mol/Pa})$) 4.38	3.50	3.21	3.95	5.19			

4.2.2.4 Hydration Number

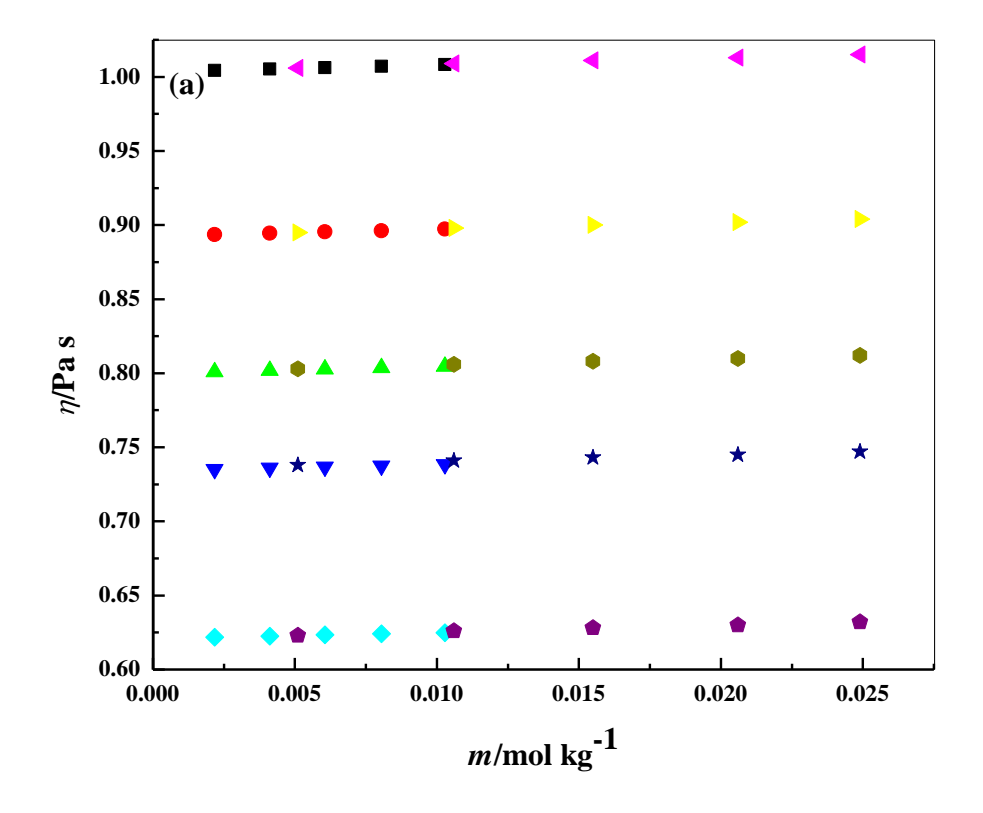
For the appraisal of the hydration number of considered solute (adenine) in water and (0.05, 0.10, and 0.15) mol kg⁻¹ D-glucose/D-maltose solvent media, two models can be engaged which were instructed by Millero *et al.* [19]. Out of the two offered models, one of the models has been employed for the perseverance of hydration number which is based on the data of limiting apparent molar isentropic compressibility. As per this model, the hydration number is communed to partial molar volume of bulk water ($V^0_{\phi,b}$) and isentropic compressibility of bulk water ($K^0_{\phi,s,b}$) via the expression (2.17). The figured data of hydration number for the examined mixtures is itemized in Table 4.2.8. Through Table 4.2.8, we can analyze that augmenting temperature, as well as saccharide concentration, renders a descent in hydration number. Consequently, it can be analyzed that both temperature as well as D-glucose/D-maltose have a dehydrating influence on hydrated adenine molecules. This trend displays the preponderance of influential interactions amid adenine and saccharide molecules, that result in lessening in electrostriction of H₂O around adenine molecules.

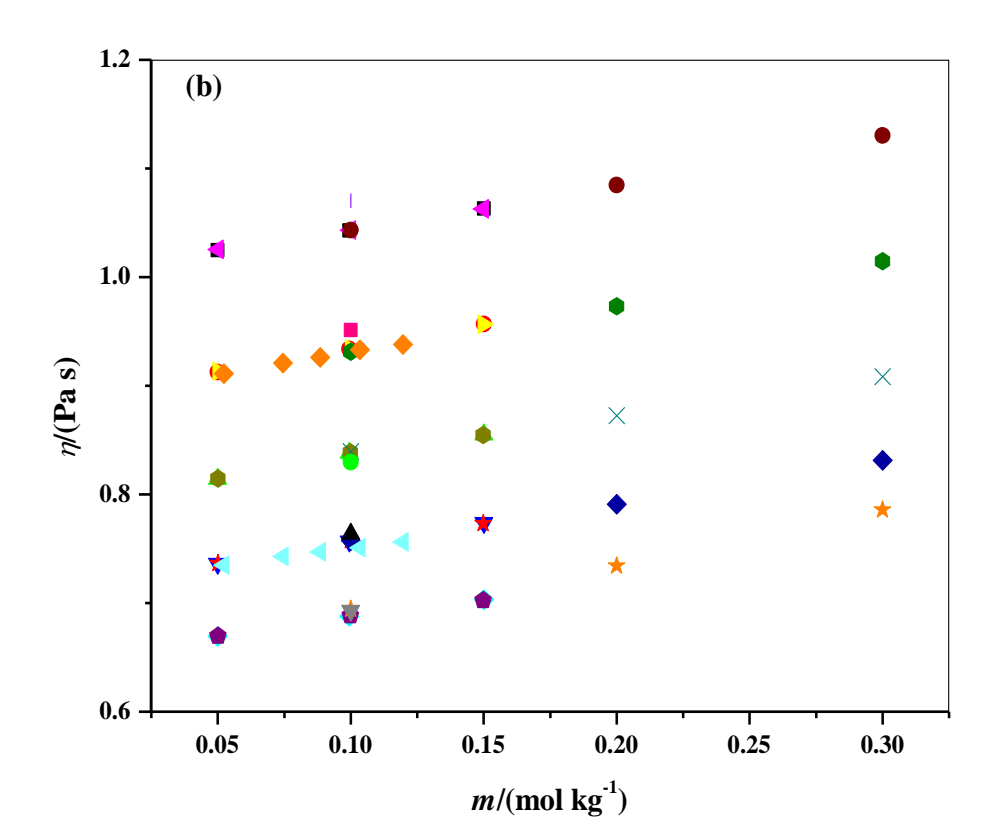
Table 4.2.8: Data of hydration number (n_H) for adenine in water and aqueous D-glucose/D-maltose solutions at T/K = 293.15 to 313.15 and P = 0.1 MPa.

		η_H		
293.15	298.15	303.15	308.15	313.15
11.55	11.16	10.86	10.60	10.36
11.51	11.12	10.78	10.47	10.20
11.38	11.04	10.70	10.40	10.05
11.26	10.89	10.55	10.15	9.86
11.30	10.98	10.70	10.39	10.12
11.16	10.86	10.66	10.34	9.96
11.01	10.73	10.47	10.12	9.72
	11.55 11.51 11.38 11.26 11.30 11.16	11.55 11.16 11.51 11.12 11.38 11.04 11.26 10.89 11.30 10.98 11.16 10.86	T/K 293.15 298.15 303.15 11.55 11.16 10.86 11.51 11.12 10.78 11.38 11.04 10.70 11.26 10.89 10.55 11.30 10.98 10.70 11.16 10.86 10.66	T/K 293.15 298.15 303.15 308.15 11.55 11.16 10.86 10.60 11.51 11.12 10.78 10.47 11.38 11.04 10.70 10.40 11.26 10.89 10.55 10.15 11.30 10.98 10.70 10.39 11.16 10.86 10.66 10.34

4.2.3 Viscosity Data

For the prepared stock solutions (0.05, 0.10 and 0.15) mol kg⁻¹ aqueous D-glucose/D-maltose media and assorted concentrations of adenine in water and contrasted aqueous D-glucose/D-maltose media, the dynamic viscosity has been gauged via the use of Lovis 2000 M/ME affixed to DSA 5000 M. The viscosity data has been documented in Table 4.2.9. In proliferation, the fetched viscosity data complementary to adenine, D-glucose, and D-maltose in water has been compared with the available literature reports [1-3,7,13,20-23] and the comparison plots have been presented in Fig's 4.2.5 (a), (b), (c). From drawn figures, it can be analyzed that there is a good agreement between obtained data and available literature. However, the slight deviations in the plots might be due to instrumental variations, disparities in the way of rendition of the experiment and divagations in the uncertainties being apprised. Moreover, viscosity of the solution is leagued to its molarity (mol dm⁻³) at every temperature as per the Jones-Dole expression (2.22) [24,25].





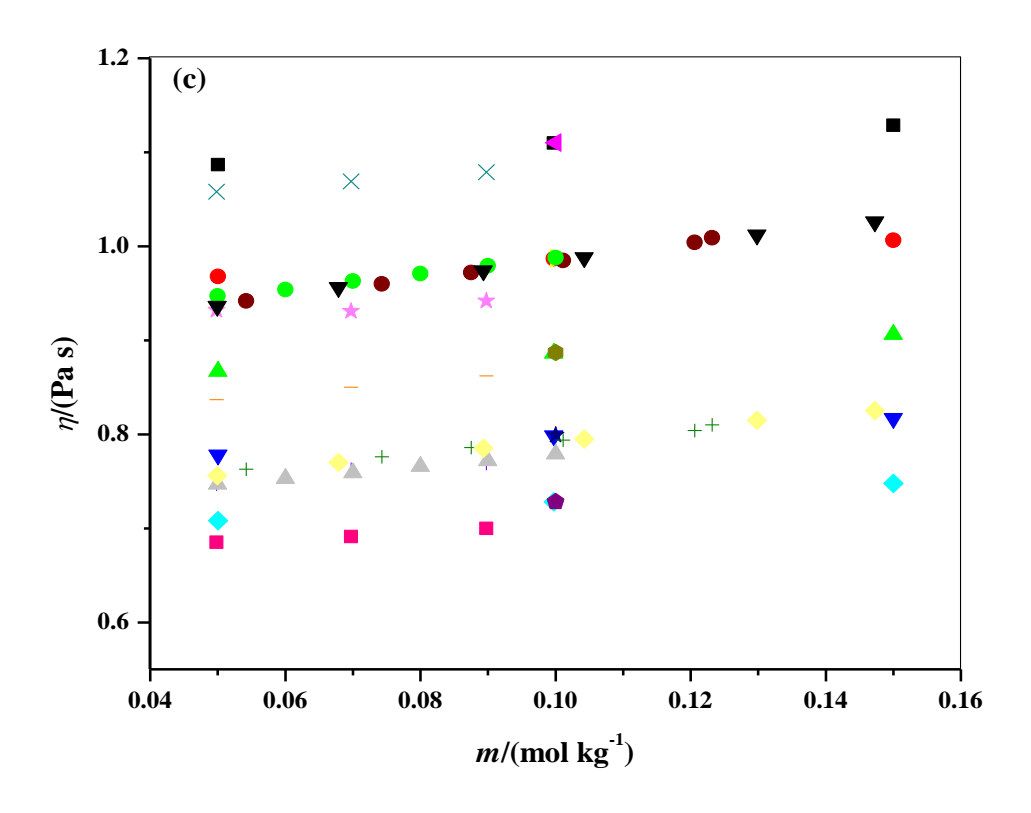


Figure 4.2.5: Graphs representing contrast of measured viscosity data with the accessible reports at discrete temperatures.

- (a) For adenine + water at $T(K) = \blacksquare$: Conducted investigation on 293.15, \bullet : Conducted investigation on 298.15, \blacktriangle : Conducted investigation on 303.15, \blacktriangledown Conducted investigation on 308.15, \blacklozenge Conducted investigation on 313.15, \blacktriangleleft : Lit. [1] on 293.15, \blacktriangleright : Lit. [1] on 303.15, \bigstar : Lit. [1] on 313.15.
- **(b)** D-Glucose + water at $T(K) = \blacksquare$: Conducted investigation on 293.15, : Conducted investigation on 298.15, ▲ : Conducted investigation on 303.15, ▼ : Conducted investigation on 308.15, : Lit. [2] on 293.15, : Lit. [2] on 303.15, ★ : Lit. [2] on 308.15, : Lit. [2] on 313.15, : Lit. [3] on 293.15, : Lit. [3] on 293.15, : Lit. [3] on 303.15, ★ : Lit. [3] on 303.15, : Lit. [20] on 303.15, : Lit. [20] on 293.15, : Lit. [20] on 303.15, : Lit. [21] on 308.15.
- (c) D-Maltose + water at $T(K) = \blacksquare$: Conducted investigation on 293.15, ●: Conducted investigation on 298.15, ▲: Conducted investigation on 303.15, ▼: Conducted investigation on 308.15, ♦: Conducted investigation on 313.15, ■: Lit. [13] on 293.15, ▷: Lit. [13] on 298.15, ●: Lit. [13] on 303.15, ★: Lit. [13] on 308.15, ♠: Lit. [13] on 313.15, ●: Lit. [21] on 298.15, +: Lit. [21] on 308.15, ×: Lit. [7] on 293.15, ★: Lit. [7] on 298.15, —: Lit. [7] on 303.15, □: Lit. [7] on 308.15, ○: Lit. [7] on 313.15 K, ○: Lit. [22] on 298.15, ♠: Lit. [22] on 308.15, ▼: Lit. [23] on 298.15, ○: Lit. [23] on 308.15.

Table 4.2.9: Experimentally acquired viscosities, η and calculated relative viscosities, η_r for adenine in water and aqueous D-glucose/D-maltose solutions at T/K = 293.15 - 313.15 and P = 0.1 MPa.

T/K	am/mol kg-1	$\eta \times 10^3/\text{Pa s}$	η_r	T/K	am/mol kg-1	$\eta \times 10^3/\text{Pa s}$	η_r
			Adenin	e in water			
293.15	0.00000	1.002		308.15	0.00000	0.733	
293.15	0.00202	1.004	1.0024	308.15	0.00202	0.735	1.0030
293.15	0.00408	1.005	1.0034	308.15	0.00408	0.736	1.0042
293.15	0.00582	1.006	1.0043	308.15	0.00582	0.737	1.0053
293.15	0.00765	1.007	1.0052	308.15	0.00765	0.738	1.0064
293.15	0.00992	1.008	1.0064	308.15	0.00992	0.739	1.0076
298.15	0.00000	0.891		313.15	0.00000	0.620	
298.15	0.00202	0.893	1.0026	313.15	0.00202	0.621	1.0032
298.15	0.00408	0.894	1.0036	313.15	0.00408	0.622	1.0044
298.15	0.00582	0.895	1.0046	313.15	0.00582	0.623	1.0056
298.15	0.00765	0.896	1.0056	313.15	0.00765	0.624	1.0068
298.15	0.00992	0.897	1.0068	313.15	0.00992	0.625	1.0081
303.15	0.00000	0.799					
303.15	0.00202	0.801	1.0027				
303.15	0.00408	0.802	1.0039				
303.15	0.00582	0.803	1.0049				
303.15	0.00765	0.804	1.0060				
303.15	0.00992	0.805	1.0073				
		Adeni	ne in 0.0499	94 mol kg ⁻¹ D-	glucose		
293.15	0.00000	1.025		308.15	0.00000	0.752	
293.15	0.00193	1.028	1.0033	308.15	0.00193	0.756	1.0046
293.15	0.00413	1.029	1.0044	308.15	0.00413	0.757	1.0061
293.15	0.00650	1.030	1.0055	308.15	0.00650	0.758	1.0076
293.15	0.00797	1.031	1.0064	308.15	0.00797	0.759	1.0085
293.15	0.01000	1.032	1.0074	308.15	0.01000	0.760	1.0097
298.15	0.00000	0.913		313.15	0.00000	0.649	
298.15	0.00193	0.916	1.0037	313.15	0.00193	0.653	1.0052
298.15	0.00413	0.917	1.0049	313.15	0.00413	0.654	1.0068
298.15	0.00650	0.918	1.0061	313.15	0.00650	0.655	1.0085
298.15	0.00797	0.919	1.0070	313.15	0.00797	0.656	1.0094

298.15	0.01000	0.920	1.0081	313.15	0.01000	0.657	1.0108
303.15	0.00000	0.814					
303.15	0.00193	0.818	1.0042				
303.15	0.00413	0.819	1.0055				
303.15	0.00650	0.820	1.0069				
303.15	0.00797	0.821	1.0079				
303.15	0.01000	0.822	1.0090				
		Ado	enine in 0.0993	39 mol kg ⁻¹ D-	glucose		
293.15	0.00000	1.043		308.15	0.00000	0.757	
293.15	0.00191	1.047	1.0043	308.15	0.00191	0.761	1.0057
293.15	0.00427	1.049	1.0055	308.15	0.00427	0.762	1.0071
293.15	0.00597	1.050	1.0063	308.15	0.00597	0.763	1.0085
293.15	0.00812	1.051	1.0075	308.15	0.00812	0.764	1.0096
293.15	0.01009	1.052	1.0085	308.15	0.01009	0.765	1.0110
298.15	0.00000	0.934		313.15	0.00000	0.688	
298.15	0.00191	0.938	1.0047	313.15	0.00191	0.692	1.0061
298.15	0.00427	0.939	1.0059	313.15	0.00427	0.693	1.0078
298.15	0.00597	0.940	1.0070	313.15	0.00597	0.694	1.0090
298.15	0.00812	0.941	1.0081	313.15	0.00812	0.695	1.0106
298.15	0.01009	0.942	1.0092	313.15	0.01009	0.696	1.0119
303.15	0.00000	0.838					
303.15	0.00191	0.843	1.0052				
303.15	0.00427	0.844	1.0066				
303.15	0.00597	0.845	1.0077				
303.15	0.00812	0.846	1.0089				
303.15	0.01009	0.847	1.0103				
		Ado	enine in 0.1500	03 mol kg ⁻¹ D-	glucose		
293.15	0.00000	1.063		308.15	0.00000	0.774	
293.15	0.00216	1.069	1.0053	308.15	0.00216	0.779	1.0067
293.15	0.00411	1.070	1.0063	308.15	0.00411	0.780	1.0080
293.15	0.00605	1.071	1.0073	308.15	0.00605	0.781	1.0094
293.15	0.00804	1.072	1.0084	308.15	0.00804	0.782	1.0107
293.15	0.01027	1.073	1.0095	308.15	0.01027	0.783	1.0120
298.15	0.00000	0.957		313.15	0.00000	0.703	

298.15	0.00216	0.962	1.0057	313.15	0.00216	0.708	1.0071
298.15	0.00411	0.963	1.0068	313.15	0.00411	0.709	1.0087
298.15	0.00605	0.965	1.0079	313.15	0.00605	0.710	1.0101
298.15	0.00804	0.966	1.0091	313.15	0.00804	0.711	1.0114
298.15	0.01027	0.967	1.0102	313.15	0.01027	0.713	1.0131
303.15	0.00216	0.860	1.0062				
303.15	0.00411	0.861	1.0074				
303.15	0.00605	0.863	1.0086				
303.15	0.00804	0.864	1.0099				
303.15	0.01027	0.865	1.0113				
		Ade	enine in 0.0499	2 mol kg ⁻¹ D-	maltose		
293.15	0.00000	1.087		308.15	0.00000	0.778	
293.15	0.00217	1.091	1.0042	308.15	0.00217	0.783	1.0056
293.15	0.00411	1.093	1.0053	308.15	0.00411	0.784	1.0071
293.15	0.00606	1.094	1.0063	308.15	0.00606	0.785	1.0085
293.15	0.00805	1.095	1.0073	308.15	0.00805	0.786	1.0096
293.15	0.01028	1.096	1.0084	308.15	0.01028	0.787	1.0110
298.15	0.00000	0.968		313.15	0.00000	0.708	
298.15	0.00217	0.972	1.0047	313.15	0.00217	0.713	1.0063
298.15	0.00411	0.973	1.0058	313.15	0.00411	0.714	1.0076
298.15	0.00606	0.974	1.0069	313.15	0.00606	0.715	1.0092
298.15	0.00805	0.975	1.0080	313.15	0.00805	0.716	1.0106
298.15	0.01028	0.977	1.0092	313.15	0.01028	0.717	1.0120
303.15	0.00000	0.867					
303.15	0.00217	0.872	1.0052				
303.15	0.00411	0.873	1.0065				
303.15	0.00606	0.874	1.0076				
303.15	0.00805	0.875	1.0088				
303.15	0.01028	0.876	1.0103				
		Ade	enine in 0.0994	7 mol kg ⁻¹ D-	maltose		
293.15	0.00000	1.110		308.15	0.00000	0.798	
293.15	0.00200	1.116	1.0051	308.15	0.00200	0.804	1.0065
293.15	0.00400	1.117	1.0062	308.15	0.00400	0.805	1.0080
293.15	0.00633	1.118	1.0074	308.15	0.00633	0.806	1.0095

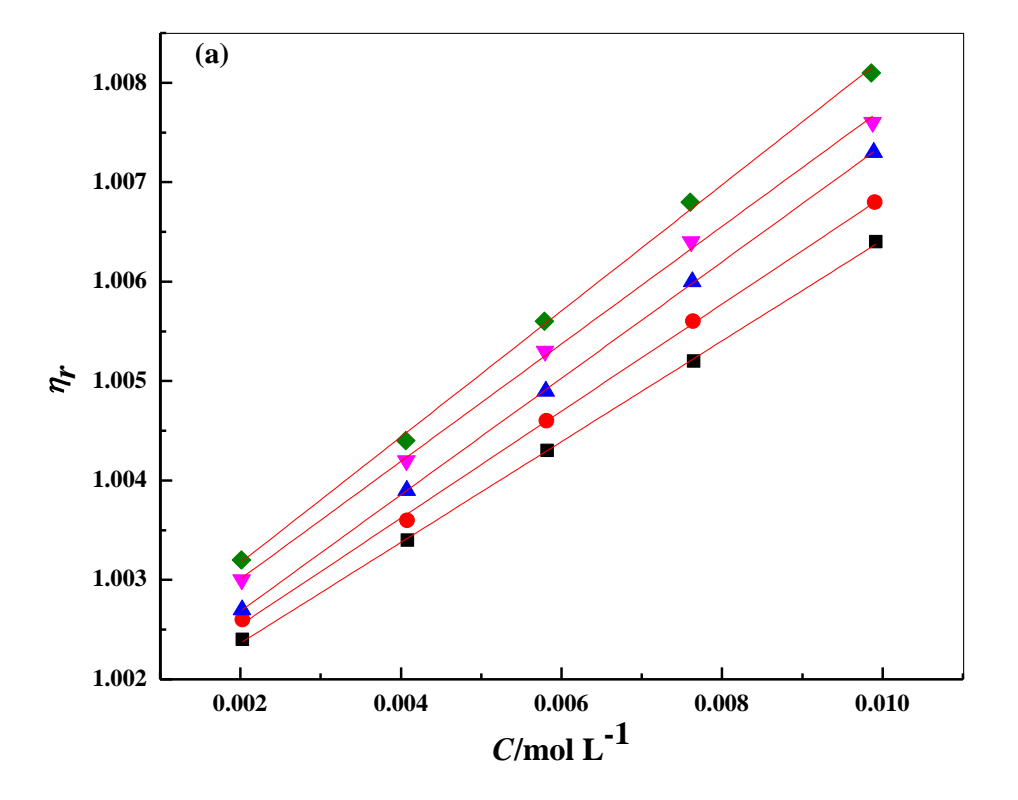
293.15	0.00788	1.119	1.0083	308.15	0.00788	0.807	1.0106
293.15	0.01019	1.120	1.0094	308.15	0.01019	0.808	1.0120
298.15	0.00000	0.987		313.15	0.00000	0.728	
298.15	0.00200	0.992	1.0056	313.15	0.00200	0.733	1.0071
298.15	0.00400	0.993	1.0067	313.15	0.00400	0.734	1.0086
298.15	0.00633	0.995	1.0081	313.15	0.00633	0.736	1.0105
298.15	0.00788	0.996	1.0090	313.15	0.00788	0.737	1.0115
298.15	0.01019	0.997	1.0102	313.15	0.01019	0.738	1.0130
303.15	0.00000	0.886					
303.15	0.00200	0.892	1.0061				
303.15	0.00400	0.893	1.0073				
303.15	0.00633	0.894	1.0089				
303.15	0.00788	0.895	1.0099				
303.15	0.01019	0.896	1.0112				
		Ade	nine in 0.1494	7 mol kg ⁻¹ D-	maltose		
293.15	0.00000	1.129		308.15	0.00000	0.817	
293.15	0.00199	1.135	1.0058	308.15	0.00199	0.823	1.0075
293.15	0.00409	1.137	1.0072	308.15	0.00409	0.824	1.0089
293.15	0.00582	1.138	1.0081	308.15	0.00582	0.825	1.0103
293.15	0.00806	1.139	1.0092	308.15	0.00806	0.826	1.0116
293.15	0.00993	1.140	1.0102	308.15	0.00993	0.828	1.0130
298.15	0.00000	1.006		313.15	0.00000	0.748	
298.15	0.00199	1.013	1.0064	313.15	0.00199	0.754	1.0080
298.15	0.00409	1.014	1.0077	313.15	0.00409	0.755	1.0098
298.15	0.00582	1.015	1.0087	313.15	0.00582	0.756	1.0111
298.15	0.00806	s1.016	1.0099	313.15	0.00806	0.757	1.0126
298.15	0.00993	1.018	1.0111	313.15	0.00993	0.758	1.0140
303.15	0.00000	0.906					
803.15	0.00199	0.913	1.0069				
303.15	0.00409	0.914	1.0083				
303.15	0.00582	0.915	1.0095				
303.15	0.00806	0.916	1.0109				
303.15	0.00993	0.917	1.0120				

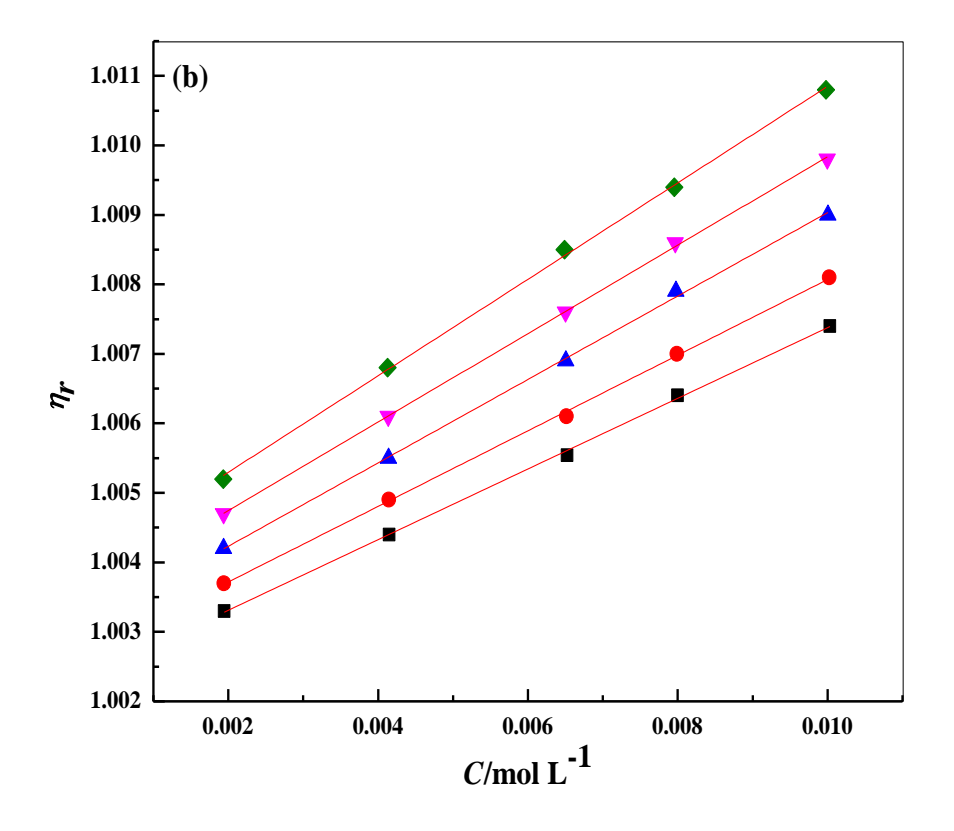
^am(mol kg⁻¹) symbolizes the molal composition of adenine in (water + D-glucose/D-maltose) solutions.

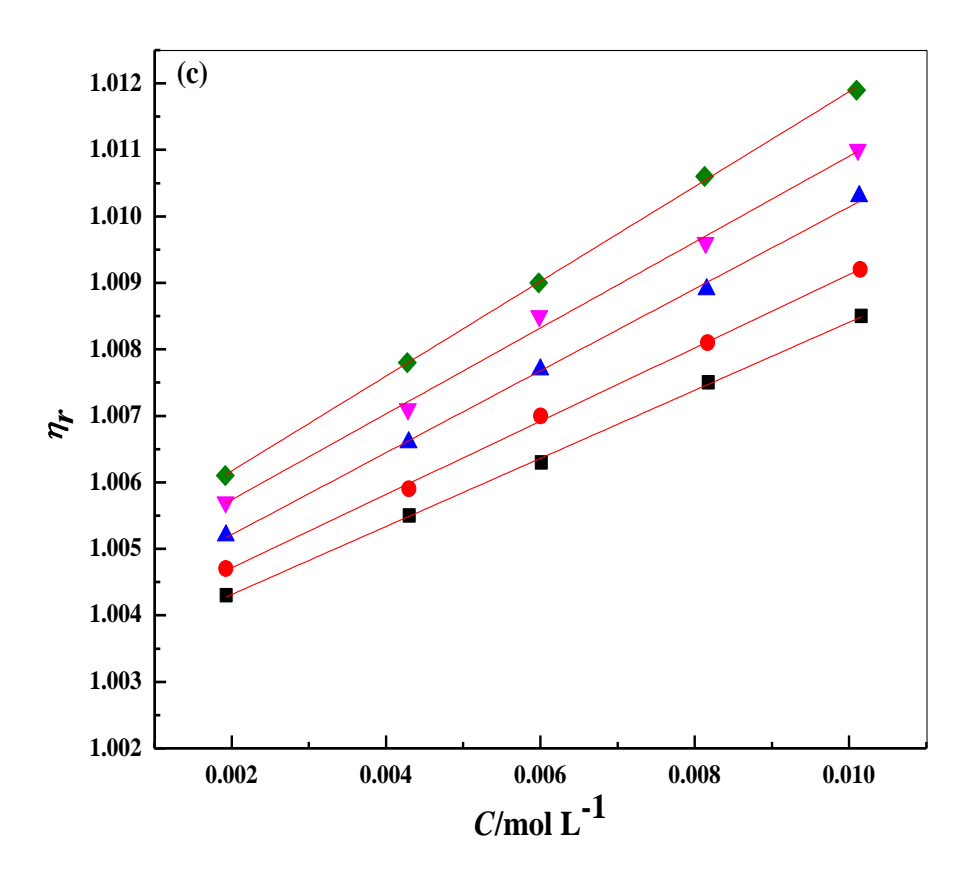
4.2.3.1 Jones-Dole B-coefficient

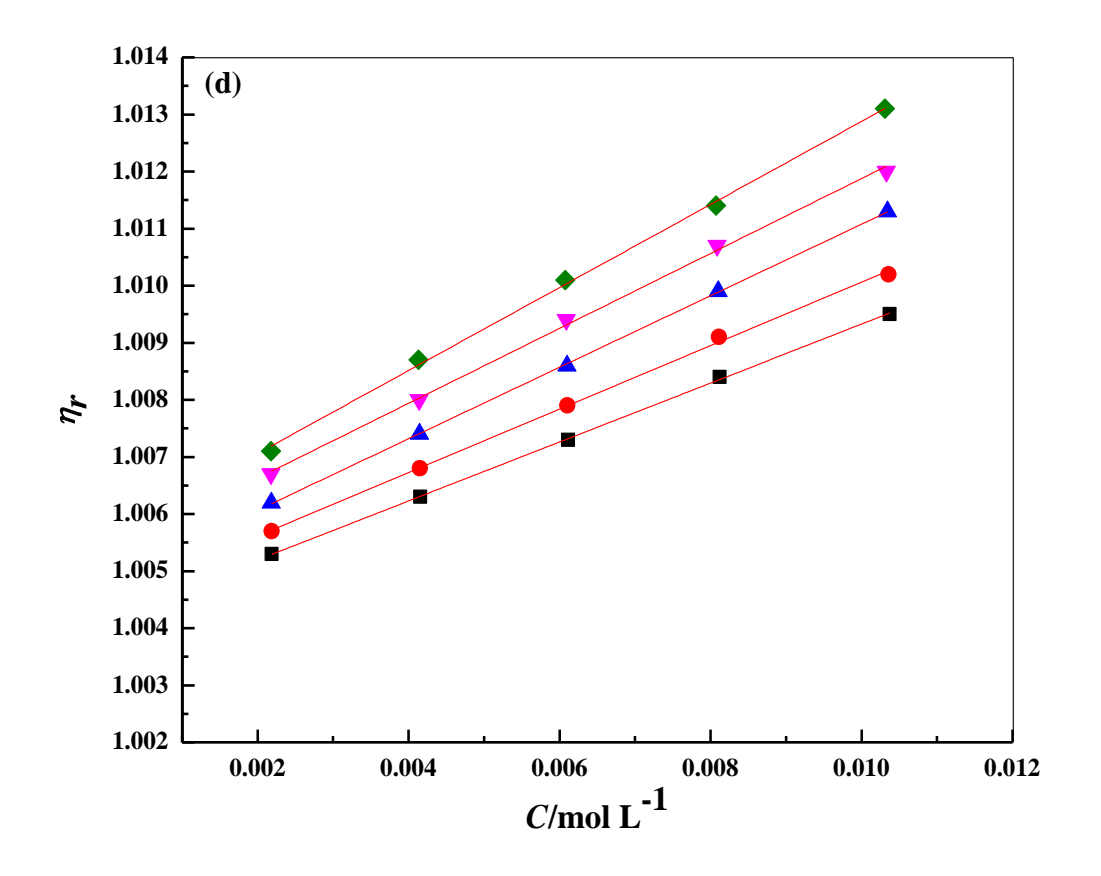
Furthermore, the *B*-coefficient is usually exemplified for the use of structure making/structure breaking demeanor of solutes [26]. Furthermore, via the sign of dB/dT, we can categorize the solutes as structure breakers/makers. Those solutes which have positive sign of dB/dT values are exemplified as structure breakers whereas the solutes harboring negative sign of dB/dT values are embodied as structure makers. Consequently, *B*-coefficient furnishes paramount information communed to the understanding of solvation behavior of a solute along with the structure of solvent in the adjoining layers of solvated solute molecules [27].

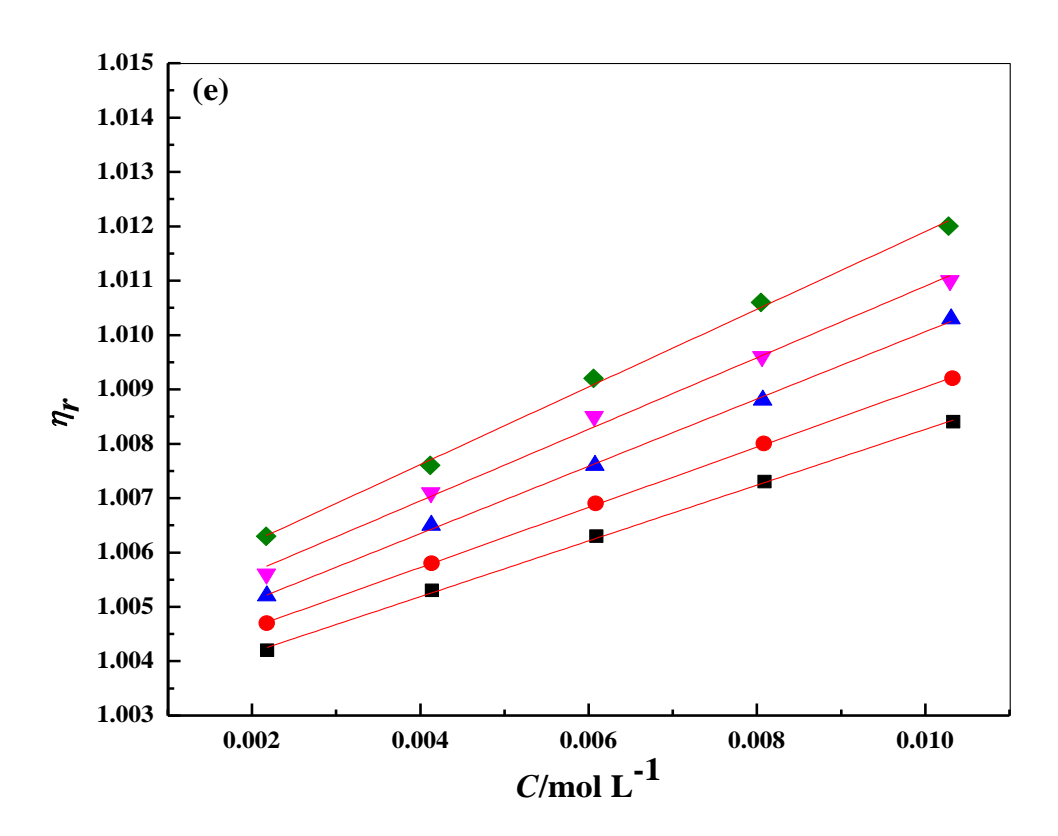
In the Conducted study, the solute (adenine) is non-ionic, so the graph of η_r -1 versus C furnishes the viscosity B-coefficient. The graphs of η_r versus C for all the scrutinized solution systems of adenine are portrayed in Figure 4.2.6 (a) - (g) and the graphically received viscosity B-coefficient values are apprised in Table 4.2.10. Through the graphically demarcated data (Table 4.2.10), we analyzed that B-coefficient values are augmenting with temperature for all the solution systems of adenine.

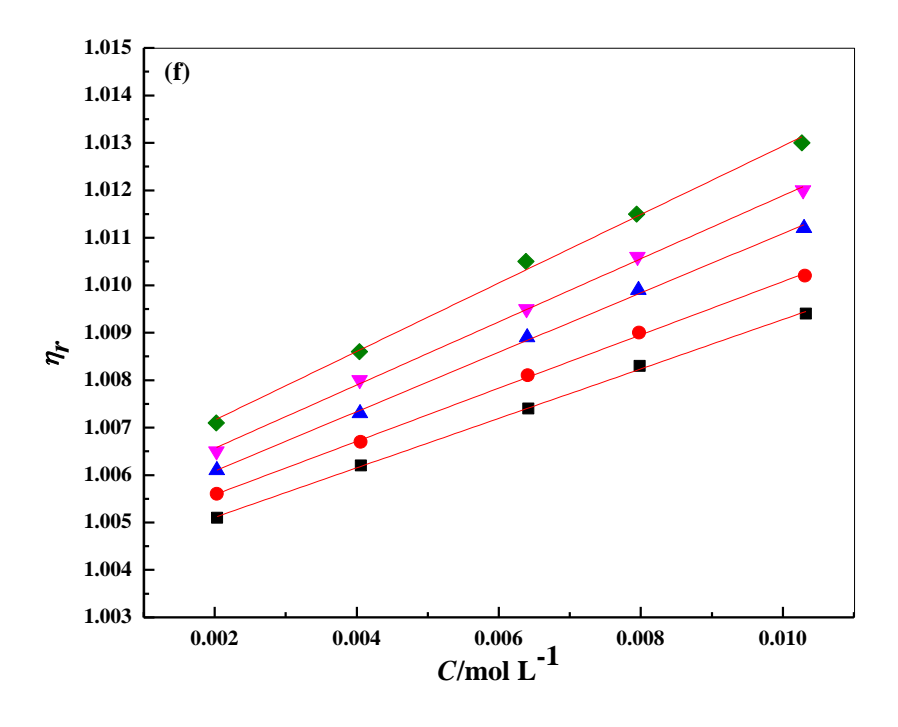












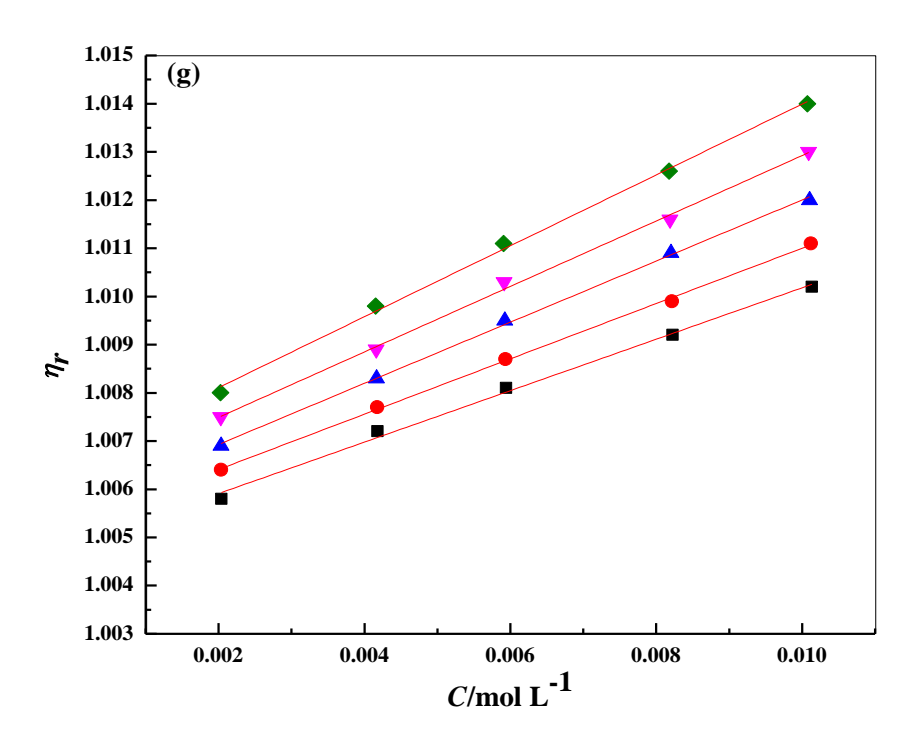


Figure 4.2.6: The graph depicting change in η_r against C(mol/L) for adenine in (a) water, (b) 0.04994 mol/kg D-glucose, (c) 0.09939 mol/kg D-glucose, (d) 0.15003 mol/kg D-glucose, (e) 0.04992 mol/kg D-maltose, (f) 0.09947 mol/kg D-maltose, (g) 0.14947 mol/kg D-maltose at discrete temperatures, ■: 293.15 K, ●: 298.15 K, ▲: 303.15 K, ▼: 308.15 K, ♦: 313.15 K.

4.2.3.2 *Jones–Dole B-coefficient of Transfer*

For adenine, the Jones Dole *B*-coefficient of transfer has been obtained via subtraction of *B*-coefficient values in H₂O from *B*-coefficient values in aqueous D-glucose/D-maltose media as per the relation (2.24). The deduced $\Delta_{tr}B$ values for all the investigated systems are exemplified in the Table 4.2.10. Its investigation displays that $\Delta_{tr}B$ data augment with the rise in the concentration of aqueous D-glucose/D-maltose media. Therefore, revealing the sovereignty of dipole-dipole interactions amid adenine and saccharide molecules. Furthermore, upon examination of $\Delta_{tr}B$ values, we concluded that these values are descending for the solution systems of D-glucose as analogized to D-maltose. This might conceivably be owed to the verity of more hydroxyl groups in D-maltose (dimer of D-glucose) in comparison to D-glucose. That's why there emerge efficient interactions of adenine with D-maltose in comparison to D-glucose. Moreover, from the alluded positive values of d*B*/d*T* data, we encountered that adenine functions as structure breaker in water and in different molalities of saccharide solvent systems. The computed data of d*B*/d*T* is listed in Table 4.2.11.

Table 4.2.10: Deduced data of viscosity *B* coefficients and corresponding transfer values $\Delta_{tr}B$ for adenine in water and aqueous D-glucose/D-maltose solutions at T/K = 293.15 - 313.15 and P = 0.1 MPa.

Properties			T(K)		
Properties	293.15	298.15 303.15		308.15	313.15
		Adenine	+ water		
$B \times 10^3 (\text{m}^3/\text{mol})$	0.506(±0.004)	0.538(±0.007)	0.585(±0.002)	0.591(±0.0116)	0.633(±0.012)
	Ad	enine + 0.04994	mol/kg D-glucos	se	
$B \times 10^3 (\text{m}^3/\text{mol})$	0.508(±0.008)	0.544(±0.008)	0.600(±0.009)	0.636(±0.006)	0.694(±0.010)
$\Delta_{tr}B \times 10^3 (\text{m}^3/\text{mol})$	0.002	0.006	0.015	0.045	0.060
	Ad	enine + 0.09939	mol/kg D-glucos	se	
$B \times 10^3 (\text{m}^3/\text{mol})$	0.512(±0.007)	0.551(±0.010)	0.616(±0.012)	0.646(±0.022)	0.713(±0.007)
$\Delta_{tr}B \times 10^3 (\text{m}^3/\text{mol})$	0.005	0.013	0.031	0.055	0.079
	Ad	enine + 0.15003	mol/kg D-glucos	se	
$B \times 10^3 (\text{m}^3/\text{mol})$	0.516(±0.005)	0.556(±0.009)	0.626(±0.004)	0.656(±0.014)	0.727(±0.015)

$\Delta_{tr}B \times 10^3 (\mathrm{m}^3/\mathrm{mol})$	$_{r}B \times 10^{3} (\text{m}^{3}/\text{mol}) 0.009$		0.041	0.066	0.094
	Ado	enine + 0.04992	mol/kg D-malto	se	
$B \times 10^3 (\text{m}^3/\text{mol})$	0.513(±0.008)	0.553(±0.004)	0.619(±0.010)	0.658(±0.024)	0.714(±0.018)
$\Delta_{tr}B\times 10^3 (\text{m}^3/\text{mol})^1$	0.006	0.015	0.033	0.067	0.081
	Ado	enine + 0.09947	mol/kg D-malto	se	
$B \times 10^3 (\text{m}^3/\text{mol})$	0.521(±0.008)	0.561(±0.009)	0.626(±0.013)	0.665(±0.014)	0.721(±0.021)
$\Delta_{tr}B \times 10^3 (\text{m}^3/\text{mol})$	0.014	0.023	0.040	0.074	0.088
	Ado	enine + 0.14947	mol/kg D-malto	se	
$B \times 10^3 (\text{m}^3/\text{mol})$	0.534(±0.019)	0.574(±0.009)	0.634(±0.011)	0.679(±0.017)	0.735(±0.020)
$\Delta_{tr}B \times 10^3 (\text{m}^3/\text{mol})$	0.027	0.036	0.049	0.088	0.102

Table 4.2.11: Deduced data of dB/dT for adenine in water and aqueous D-glucose/D-maltose solutions at T/K = 293.15 - 313.15 and P = 0.1 MPa.

Systems	dB/dT	
Adenine + water	0.00614(±0.00062)	
Adenine + 0.04994 mol/kg D-glucose	0.00928(±0.00041)	
Adenine + 0.09939 mol/kg D-glucose	0.00994(±0.00063)	
Adenine + 0.15003 mol/kg D-glucose	0.01044(±0.00070)	
Adenine + 0.04992 mol/kg D-maltose	$0.01004(\pm0.00099)$	
Adenine + 0.09947 mol/kg D-maltose	0.01008(±0.00042)	
Adenine + 0.14947 mol/kg D-maltose	0.01014(±0.00033)	

4.2.4 Thermodynamic Properties of Viscous Motion

By the usage of activated complex theory presented by Eyring *et al.* [28], the Gibb's free energy of activation per mole of solute (chemical potential) has been demarcated for the inspected solute (adenine) in water and assorted concentrations of D-glucose/D-maltose media. As per this theory, in one molar solution, the solvent molecules are escorted by a shift, as an influence of which they either incorporate strongly or weakly with solute molecules in the solution. Hence, the chemical potential of the solvent has been figured at

eclectic temperatures via the relation (2.25). Likewise, the chemical potential of solute (adenine) has been summed utilizing a thermodynamic relation (2.27) given by Feakin's *et al.* [29]. Essentially, $\Delta\mu^0_2$ is a criterion of divergence in chemical potential of solute in the immediacy of selected solvent system as well as additional free energy differences appearing as a consequence of vibrations of solute molecules. In the Conducted examination, the anticipated data of $\Delta\mu^0_1$ and $\Delta\mu^0_2$ is positive for all the studied systems of adenine in contrasting aqueous solvent media at all the investigational temperatures. In addition, the $\Delta\mu^0_2$ values are rising with the upsurge in temperature for all explored systems of adenine. As per model of Feakin's *et al.*, the positive as well as advancing values of $\Delta\mu^0_2$ designate that innovation of transition state is feeble for adenine in the chosen solvent systems at all investigational temperatures. Likewise, the evaluation of entropy and enthalpy of activation has been accomplished for all the desired mixtures via the use of equations (2.28) and (2.29).

Table 4.2.12: Data of chemical potential, entropy and enthalpy of activation for adenine in water and aqueous D-glucose/D-maltose solutions at T/K = 293.15 - 313.15 and P = 0.1 MPa.

T/K	$\Delta \mu^{\theta}_{I}/\mathrm{kJ}\;\mathrm{mol}^{-1}$	$\Delta\mu^0$ ₂ /kJ mol ⁻¹	T∆S ⁰ 2/kJ mol ⁻¹	ΔH ⁰ ₂ /kJ mol ⁻¹				
		Adenine in wa	ter					
293.15	9.30	86.87	325.81	412.68				
298.15	9.17	92.43	331.36	423.79				
303.15	9.06	100.22	336.92	437.14				
308.15	8.99	102.44	342.48	444.92				
313.15	8.70	109.65	348.03	457.68				
Adenine in 0.04994 mol kg ⁻¹ D-glucose								
293.15	9.36	86.95	459.54	546.49				
298.15	9.24	93.07	467.38	560.45				
303.15	9.11	102.13	475.22	577.35				
308.15	9.06	108.73	483.06	591.79				
313.15	8.82	118.31	490.89	609.20				
		Adenine in 0.09939 mol	kg ⁻¹ D-glucose					
293.15	9.42	87.19	485.28	572.47				
298.15	9.30	93.69	493.56	587.25				
303.15	9.19	103.98	501.83	605.81				

308.15	9.09	109.60	510.11	619.71
313.15	8.99	120.62	518.39	639.01
		Adenine in 0.15003 me	ol kg ⁻¹ D-glucose	
293.15	9.47	87.47	502.99	590.46
298.15	9.38	94.12	511.57	605.69
303.15	9.25	104.96	520.14	625.10
308.15	9.16	110.59	528.72	639.31
313.15	9.06	122.13	537.30	659.43
		Adenine in 0.04992 mo	ol kg ⁻¹ D-maltose	
293.15	9.52	87.57	490.15	577.72
298.15	9.40	94.21	498.51	592.72
303.15	9.28	104.55	506.87	611.42
308.15	9.16	111.39	515.23	626.62
313.15	9.07	120.78	523.59	644.37
		Adenine in 0.09947 mo	ol kg ⁻¹ D-maltose	
293.15	9.60	87.92	485.22	573.14
298.15	9.47	94.47	493.50	587.97
303.15	9.36	104.62	501.77	606.39
308.15	9.25	111.47	510.05	621.52
313.15	9.17	120.80	518.33	639.13
		Adenine in 0.14947 mo	ol kg ⁻¹ D-maltose	
293.15	9.66	88.87	485.16	574.03
298.15	9.55	95.37	493.44	588.81
303.15	9.45	104.75	501.71	606.46
308.15	9.34	112.38	509.99	622.37
313.15	9.27	121.74	518.26	640.00

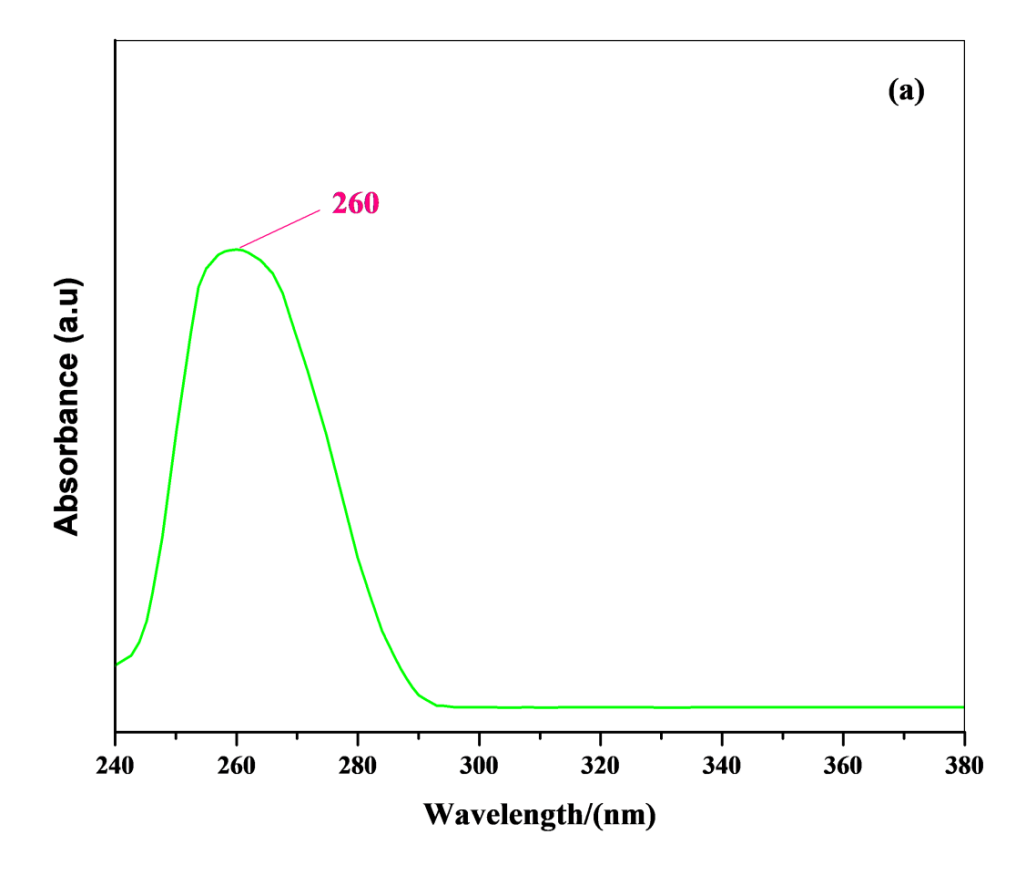
4.2.5 UV Absorption Studies

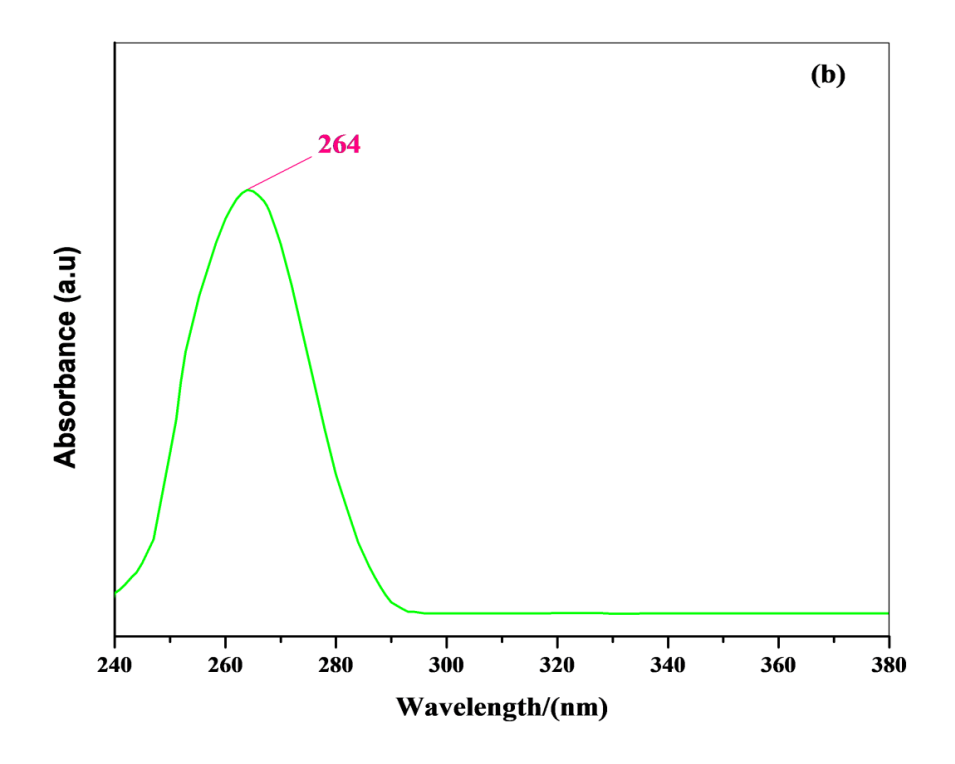
A UV-visible spectrophotometer (LAMBDA 1050+) was used to record the absorption spectra of adenine in water as well as 0.15 mol/kg D-glucose and D-maltose solutions By keeping the wavelength in the (200-400 nm) range and utilising quartz cuvettes with a 1 cm path length, the UV spectra of all the produced samples were inferred.

The acquired absorbances versus wavelength charts are given in Figure 4.3.6. In this Figure, (a) indicates that the absorption band of adenine in water emerges at 260 nm,

whereas (b) shows that the absorption band of adenine in 0.15 mol/kg aqueous D-glucose appears at 264 nm. Also, in Figure 4.3.6 (c) i.e. for adenine in 0.15 mol/kg aqueous D-maltose, the absorption band appears at 266 nm. As a result, the bathochromic shift in absorption maxima of adenine from 260 nm (in water) to 264 nm (in 0.15 mol/kg aqueous D-glucose) takes place. In addition, bathochromic shift of the absorption maxima of adenine from 260 nm (in water) to 266 nm (0.15 mol/kg aqueous D-maltose) occurs.

This shows that adenine has significant hydrophilic-hydrophilic interactions with aqueous D-glucose and D-maltose solutions, which stabilize the excited state upto a bigger degree than the ground state. As a result, energy divergence in the ground state and the excited state dwindle, causing the absorption band to shift toward advanced wavelengths. Therefore, amplification of varied hydrophilic-hydrophilic synergies among the considered systems is clearly demonstrated via the UV-vis spectra measurements of adenine in H₂O besides in implicated H₂O mixtures comprising D-glucose and D-maltose.





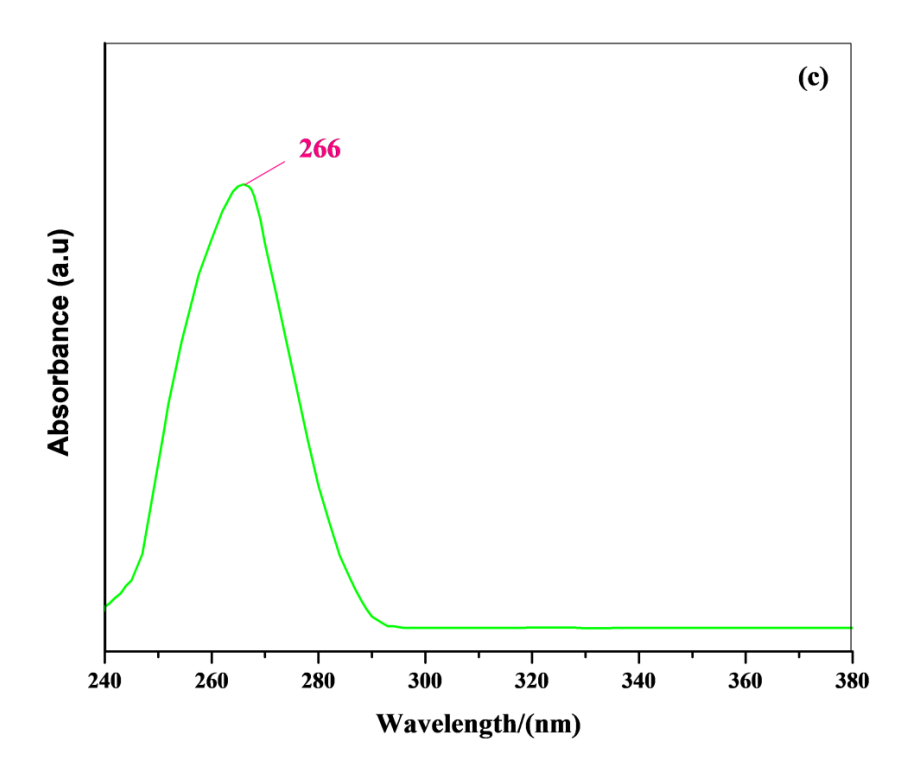


Figure 4.2.7: Plots of absorbance versus wavelength for discrete systems of implication: (a) adenine + H₂O; (b) adenine + 0.15 mol/kg D-glucose; (c) adenine + 0.15 mol/kg D-maltose.

REFERENCES

- 1. Rajput, P., Richu, Sharma, T., & Kumar, A. (2021). Temperature dependent physicochemical investigations of some nucleic acid bases (uracil, thymine and adenine) in aqueous inositol solutions. *Journal of Molecular Liquids*, 326, 115210.
- Sharmhal, A., Singh, H., Richu, Fatma, I., Sharma, P. K., Sharma, S., Kumar, A., & Kumar, A. (2023). Influence of carbohydrates on the volumetric, acoustic and viscometric properties of thymine in aqueous solutions at different temperatures. *Journal of Molecular Liquids*, 385, 122264.
- 3. Rani, R., Kumar, A., & Bamezai, R. K. (2017). Effect of glucose/lactose on the solution thermodynamics of thiamine hydrochloride in aqueous solutions at different temperatures. *Journal of Molecular Liquids*, 240, 642-655.
- 4. Chauhan, S., & Kumar, K. (2014). Effect of glycine on aqueous solution behavior of saccharides at different temperatures: volumetric and ultrasonic studies. *Journal of Molecular Liquids*, 194, 212-226.
- 5. Seitz, J. C., Schulte, M. D., Hall, A. S., & Rhett, G. W. (2019). Volumetric properties of dilute (D-glucose + H₂O) solutions at temperatures from (293.15 to 433.15) K and pressures from (0.10 to 50.00) MPa. *The Journal of Chemical Thermodynamics*, 128, 372-382.
- 6. Jain, A., & Zodape, S. P. (2023). Investigation of molecular interactions of 1-ethyl-3-methylimidazolium diethyl phosphate in water and aqueous D-glucose solutions through thermodynamic and compressibility parameters. *Journal of Chemical & Engineering Data*, 68, 1899-1910.
- 7. Sharma, T., Rani, R., Kumar, A., & Bamezai, R. K. (2019). Apparent molar (volumetric/compressibility) and transport properties of D-maltose-1-butyl-3-methylimidazolium hexafluorophosphate—water ternary systems at different temperatures. *Journal of Solution Chemistry*, 48, 658-675.

- 8. Khanlarzadeh, K., & Iloukhani, H. (2018). Thermo-acoustical and volumetric studies on interionic interactions of L-histidine in aqueous maltose solutions at different temperatures. *Journal of Molecular Liquids*, 271, 421-428.
- 9. Sharma, P., Sharma, S., & Sharma, M. (2022). Effect of trisodium citrate dihydrate on thermophysical properties of saccharides in aqueous media at different temperatures: Volumetric and acoustic properties. *Chemical Thermodynamics and Thermal Analysis*, 6, 100051.
- 10. Chauhan, S., & Kumar, K. (2014). Partial molar volumes and isentropic compressibilities of some saccharides in aqueous solutions of leucine at different temperatures. *Journal of Chemical & Engineering Data*, 59, 1375-1384.
- 11. Masson, D. O. (1929). XXVIII. Solute molecular volumes in relation to solvation and ionization. *The London, Edinburgh, and Dublin Philosophical Magazine and Journal of Science*, 8, 218-235.
- 12. Sharma, T., Kumar, A., Shah, S. S., & Bamezai, R. K. (2020). Analysis of interactions between streptomycin sulphate and aqueous food acids (L-ascorbic acid and citric acid): Physico-chemical and spectroscopic insights. *The Journal of Chemical Thermodynamics*, 151, 106207.
- 13. Richu, Kumar, A. (2020). Apparent molar volume, isentropic compressibilities, viscosity B-coefficients and activation parameters of thiamine hydrochloride in aqueous solutions of saccharides at different temperatures. *The Journal of Chemical Thermodynamics*, 150, 106228.
- 14. Friedman, H. L., & Krishnan, C. V. (1973). Studies of hydrophobic bonding in aqueous alcohols: enthalpy measurements and model calculations. *Journal of Solution Chemistry*, 2, 119-140.
- Sharma, R., Chauhan, S., Thakur, N., & Kumar, K. (2024). Volumetric, compressibility and viscometric studies on intermolecular interactions of NaC and NaDC with Emtricitabine and Lamivudine in aqueous medium at (298.15–313.15)
 K. Journal of Molecular Liquids, 407, 125233.

- 16. Hepler, L. G. (1969). Thermal expansion and structure in water and aqueous solutions. *Canadian Journal of Chemistry*, 47, 4613-4617.
- 17. Singh, V., Chhotaray, P. K., Islam, N., & Gardas, R. L. (2016). Implicit and explicit solvent models to understand the D-(+)-glucose solvation in aqueous protic ionic liquid solution: Volumetric and computational approach. *The Journal of Chemical Thermodynamics*, 103, 7-16.
- 18. Bandral, A., Majid, Q., & Kumar, A. (2021). Investigations on volumetric, compressibility and viscometric properties of L-ascorbic acid and thiamine hydrochloride in aqueous 1-ethyl-3-methylimidazolium hydrogen sulfate solutions at different temperatures. *Journal of Molecular Liquids*, 339, 116833.
- 19. Millero, F. J. (1971). Molal volumes of electrolytes. *Chemical Reviews*, 71, 147-176.
- 20. Kumar, A., Rani, R., Sharma, T., & Bamezai, R. K. (2019). Effect of concentration and temperature variations on interactions in (L-serine/L-valine+ aqueous glucose/sucrose/lactose) systems: Viscometric and activation parametric study. *Indian Journal of Pure & Applied Physics (IJPAP)*, 57, 225-235.
- 21. Banipal, P. K., Kaur, K., Mithu, V. S., & Banipal, T. S. (2016). Rheological and time domain 1H NMR relaxation studies of some polyhydroxy solutes in presence of 1-glycine. *The Journal of Chemical Thermodynamics*, 100, 29-43.
- 22. Oroian, M., Ropciuc, S., Amariei, S., & Gutt, G. (2015). Correlations between density, viscosity, surface tension and ultrasonic velocity of different mono-and disaccharides. *Journal of Molecular Liquids*, 207, 145-151.
- 23. Banipal, P. K., Arti, S., & Banipal, T. S. (2015). Influence of NH₄Br on solvation behavior of polyhydroxy solutes in aqueous solutions at different temperatures and atmospheric pressure. *Journal of Chemical & Engineering Data*, 60, 1023-1047.

- 24. Jones, G., & Dole, M. (1929). The viscosity of aqueous solutions of strong electrolytes with special Reference to barium chloride. *Journal of the American Chemical Society*, *51*, 2950-2964.
- 25. Beri, A., Kant, R., & Banipal, T. S. (2024). Physicochemical, calorimetry and spectroscopic properties of l-methionine and l-cysteine in presence of sodium based food preservatives. *Brazilian Journal of Chemical Engineering*, 41(4), 1305-1316.
- 26. Pradhan, R. K., Sahoo, L., & Singh, S. (2024). Volumetric and viscometric properties of L-glutamic acid in aqueous L-arabinose and D-xylose solutions between the temperature range of (293.15–313.15) K at atmospheric pressure. *The Journal of Chemical Thermodynamics*, 189, 107193.
- 27. Pattnaik, S. S., Dalai, B., Nanda, B. B., Nanda, B., & Pradhan, M. (2023). Studies on the interference of citrate salts on the ion–solvent interactions of ionic liquid with water at different temperatures through volumetric, viscometric, and acoustic methods. *Journal of Molecular Liquids*, 383, 122053.
- 28. Glasstone S., Laidler K. J., Erying H. (1941). Theory of Rate Processes, McGraw Hill, New York, 477.
- 29. Feakins, D., Waghorne, W. E., & Lawrence, K. G. (1986). The viscosity and structure of solutions. Part 1.—A new theory of the Jones–Dole B-coefficient and the related activation parameters: application to aqueous solutions. *Journal of the Chemical Society, Faraday Transactions 1: Physical Chemistry in Condensed Phases*, 82, 563-568.

CHAPTER 4.3

Studies on Various Thermophysical Parameters of Cytosine in (Water + D-Xylose/D-Lactose) Solutions at Distinct Compositions and Temperatures

Journal of Molecular Liquids, 2025, 430, 127621

(Impact factor: 5.2)

Studies on Various Thermophysical Parameters of Cytosine in (Water + D-Xylose/D-Lactose) Solutions at Distinct Compositions and Temperatures

In this chapter, thermophysical parameters of cytosine in H_2O and (0.05 - 0.15)mol/kg of (H₂O + D-xylose/D-lactose) solutions are investigated at varied empirical temperatures (ranging from 293.15 K to 313.15 K) and ambient pressure (0.1 MPa). The experimentally determined physical properties such as density, velocity of sound, and viscosity have been utilized for the estimation of several parameters such as apparent molar volume (V_{ϕ}) , limiting apparent molar volume (V_{ϕ}^{0}) , hydration number (n_{H}) , limiting apparent molar expansivity (E^0_{ϕ}) , Hepler's constant $(\partial E^0_{\phi}/\partial T)_P$, apparent specific volume (ASV), apparent molar isentropic compression $(K_{\phi,s})$, limiting apparent molar isentropic compression $(K^0_{\phi,s})$, viscosity B-coefficients, transfer parameters and thermodynamic parameters of viscous flow $(\Delta \mu^0_1, \Delta \mu^0_2, T\Delta S^0_2)$ and ΔH^0_2 . Additionally, the Co-sphere overlap model has been utilized for the analysis of assorted probable interactions operating in the prepared systems. The received outcomes forecast that in all solution systems, the solute-solvent interactions are progressing with rising temperatures and concentrations of saccharides. Furthermore, the structure breaking proclivity of cytosine has been scrutinized via the abstraction of Hepler's constant data and positive values of dB/dT data for all the explored systems. Moreover, the inferred apparent specific volumes state that cytosine is sweet in taste in aqueous media while sweet-bitter in taste in peculiar concentrations of Dxylose/D-lactose media.

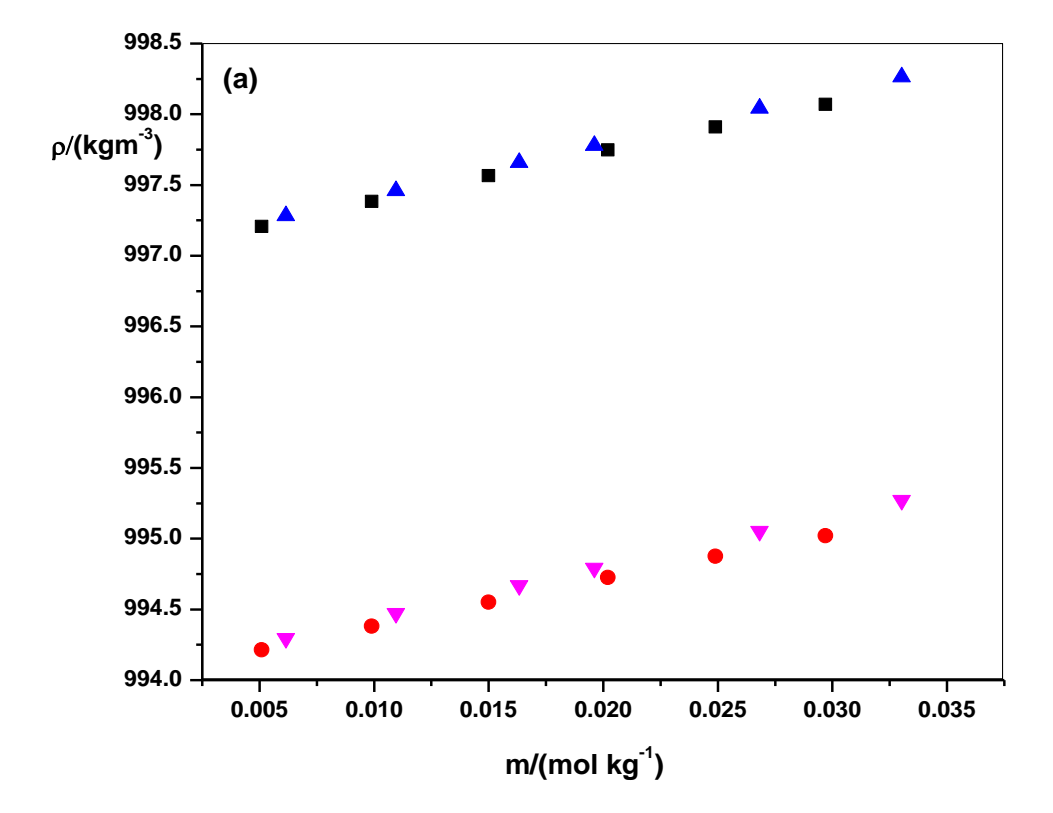
4.3.1 Volumetric Properties

Through the usage of Density and Speed of sound analyzer (DSA 5000 M) [1], the physical properties like density and speed of sound have been acquired at five dissimilar temperatures (293.15 K to 313.15 K) for (0.005 - 0.030) mol kg⁻¹ cytosine in H₂O and (0.05, 0.10) as well as 0.15 mol kg⁻¹ D-xylose/D-lactose media. The assessed density values corresponding to diversifying mixtures are exemplified inside Table 4.3.1.

The introspection of Table 4.3.1 indicates the augmentation in density values with succession in molal concentration of cytosine as well as D-xylose/D-lactose solvent media, whereas with intensifying temperature, density decreases.

Further, the acquired data of density corresponding to cytosine, D-xylose and D-lactose in water is compared with literature [2-6] and the comparison graphs are shown in Figure's 4.3.1 (a), (b), (c).

A fine conformity among measured data and literature can be inferred through these comparison graphs. Though, the minor deviations in graphs are attributed to instrumental disparities, variation in the manner of recital of experimentation and discrepancies in the uncertainties that are accounted.



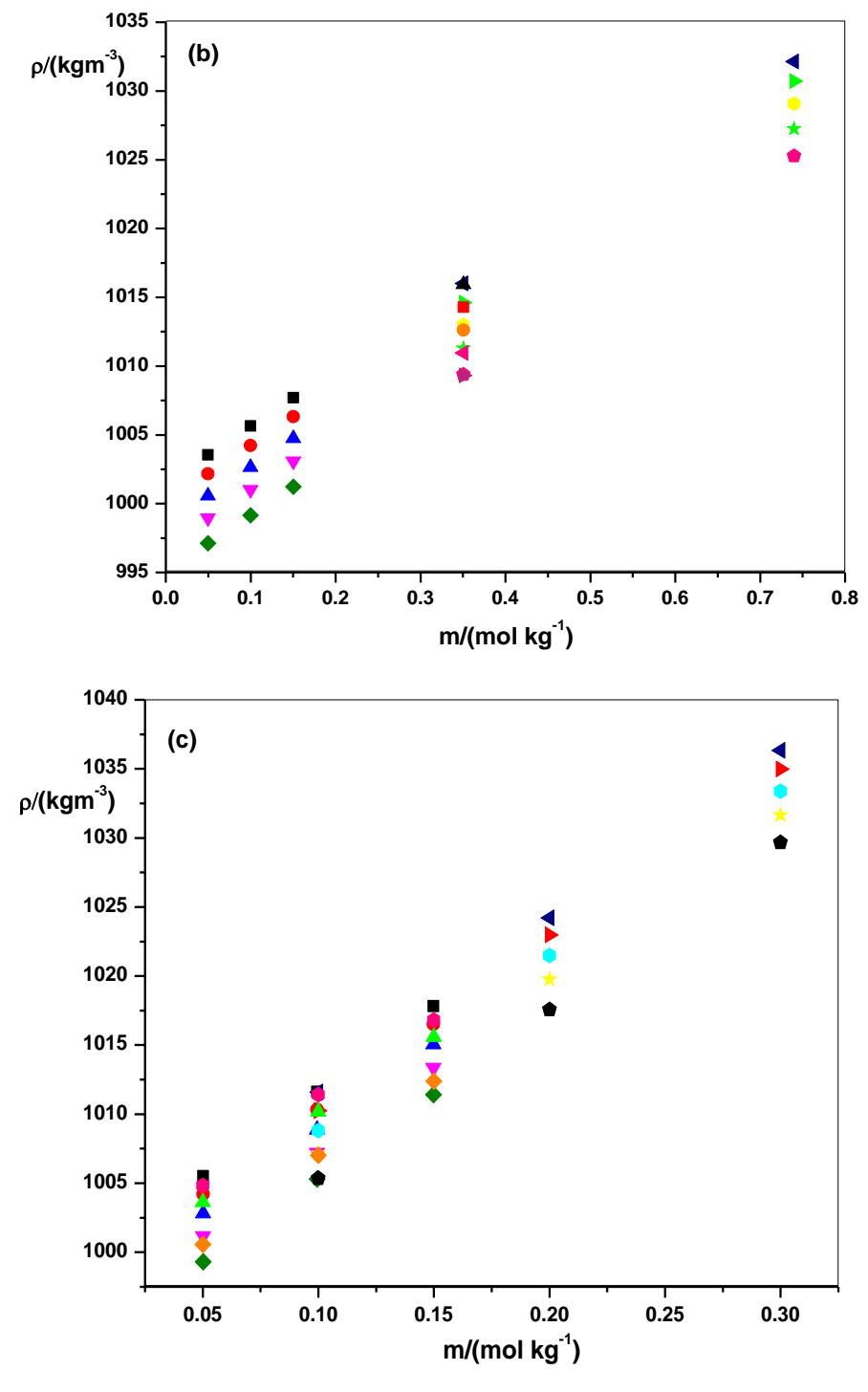


Figure 4.3.1: Graphs insinuating contrast of measured density data with the accessible reports at discrete temperatures.

(a) For cytosine in water at T/K, \blacksquare : Conducted investigation on 298.15, \bullet : Conducted investigation on 308.15, \blacktriangle : Lit. [2] on 298.15, \blacktriangledown : Lit. [2] on 308.15.

- (b) D-Xylose in water at *T/*K, ■: Conducted investigation on 293.15, ●: Conducted investigation on 298.15, ▲: Conducted investigation on 303.15, ▼ Conducted investigation on 308.15, ▼ Conducted investigation on 313.15, ▼: Lit. [3] on 293.15, ►: Lit. [3] on 298.15, ●: Lit. [3] on 303.15, ★: Lit. [3] on 308.15, ♠: Lit. [4] on 293.15, ■: Lit. [4] on 298.15, ●: Lit. [4] on 303.15, ▼: Lit. [4] on 308.15, ►: Lit. [4] on 313.15.
- (c) D-Lactose in water at *T/K*, ■: Conducted investigation on 293.15, ●: Conducted investigation on 298.15, ▲: Conducted investigation on 303.15, ▼: Conducted investigation on 308.15, ♦ Conducted investigation on 313.15, ■: Lit. [5] on 293.15, ▶: Lit. [5] on 298.15, •: Lit. [5] on 303.15, ★: Lit. [6] on 293.15, ▲: Lit. [6] on 298.15, ♦: Lit. [6] on 308.15.

4.3.1.1 Apparent Molar Volume

Through the utilization of acquired ρ data as well as equation (2.1), the apparent molar volume for assorted mixtures are evaluated and listed in Table 4.3.1. Examination of V_{ϕ} data indicates that there is succession in V_{ϕ} with rising molality of cytosine and also with the temperature.

Further, the enhancement in V_{ϕ} with increasing concentrations of cytosine might be accredited to rise in vander Waals volume of cytosine in studied mixtures [7].

In addition, for better perception of the interactions among cytosine as well as D-xylose/D-lactose solvent media, the partial or limiting molar volumes (V^0_{ϕ}) can be computed at different temperatures and concentrations [8].

Table 4.3.1: Experimentally acquired densities, ρ and calculated apparent molar volumes, V_{ϕ} for cytosine in water and aqueous D-xylose/D-lactose solutions at T/K = 293.15 - 313.15 and P = 0.1 MPa.

			ρ/(kg m	-3)			V_{ϕ} >	< 10 ⁶ /(m ²	³ mol ⁻¹)	
<i>m</i> /(mol kg ⁻¹)					T(K)					
	293.15	298.15	303.15	308.15	313.15	293.15	298.15	303.15	308.15	313.15
	Cytosine + water									
0.0000	998.24	997.02	995.64	994.03	992.21					
0.0051	998.43	997.21	995.83	994.22	992.39	73.11	73.96	74.98	75.84	76.90
0.0099	998.61	997.38	996.00	994.38	992.55	73.56	74.25	75.39	76.27	77.27
0.0150	998.80	997.57	996.17	994.55	992.72	73.99	74.70	75.84	76.78	77.67
0.0202	998.98	997.75	996.35	994.73	992.89	74.43	75.05	76.38	77.09	77.98

0.0249	999.14	997.91	996.50	994.88	993.04	74.84	75.43	76.76	77.48	78.37
0.0297	999.30	998.07	996.66	995.02	993.19	75.23	75.84	77.03	78.09	78.65
Cytosine + 0.0497 mol/kg D-xylose										
0.0000	1003.54	1002.16	1000.57	998.96	997.12					
0.0051	1003.72	1002.34	1000.74	999.13	997.28	75.26	76.29	77.34	78.39	79.66
0.0100	1003.89	1002.50	1000.90	999.28	997.43	75.73	76.58	77.85	78.92	80.02
0.0152	1004.07	1002.68	1001.07	999.44	997.59	76.18	76.95	78.21	79.27	80.42
0.0199	1004.23	1002.82	1001.22	999.59	997.73	76.48	77.59	78.56	79.54	80.74
0.0250	1004.39	1002.99	1001.37	999.74	997.87	76.84	77.94	79.01	79.93	81.07
0.0298	1004.54	1003.13	1001.51	999.88	998.00	77.24	78.41	79.39	80.37	81.51
Cytosine + 0.0998 mol/kg D-xylose										
0.0000	1005.64	1004.23	1002.66	1001.02	999.16					
0.0052	1005.82	1004.40	1002.82	1001.18	999.31	77.00	78.77	79.80	81.04	83.06
0.0100	1005.97	1004.55	1002.97	1001.32	999.44	77.62	78.98	80.14	81.42	83.32
0.0149	1006.13	1004.70	1003.12	1001.46	999.57	78.05	79.32	80.33	81.55	83.60
0.0200	1006.28	1004.86	1003.27	1001.60	999.70	78.59	79.45	80.62	81.85	84.00
0.0247	1006.43	1005.00	1003.40	1001.74	999.82	78.95	79.86	80.94	82.04	84.21
0.0299	1006.58	1005.15	1003.55	1001.88	999.95	79.35	80.05	81.23	82.38	84.53
Cytosine + 0.1504 mol/kg D-xylose										
0.0000	1007.71	1006.32	1004.75	1003.09	1001.22					
0.0051	1007.87	1006.47	1004.90	1003.23	1001.36	79.73	80.96	81.82	82.88	84.16
0.0101	1008.02	1006.62	1005.04	1003.37	1001.49	80.00	81.24	82.11	83.08	84.47
0.0151	1008.17	1006.76	1005.18	1003.51	1001.62	80.34	81.66	82.46	83.21	84.64
0.0199	1008.31	1006.89	1005.31	1003.64	1001.74	80.71	81.87	82.65	83.39	84.85
0.0251	1008.46	1007.03	1005.45	1003.77	1001.87	80.96	82.37	82.85	83.66	85.00
0.0299	1008.59	1007.16	1005.58	1003.89	1001.99	81.16	82.59	83.08	83.97	85.21
			Cyto	osine + 0.0	502 mol/k	g D-lact	tose			
0.0000	1005.51	1004.22	1002.82	1001.17	999.32					
0.0053	1005.69	1004.40	1002.99	1001.33	999.47	76.14	77.50	79.07	80.09	81.50
0.0102	1005.86	1004.56	1003.14	1001.48	999.61	76.53	77.94	79.57	80.43	81.99
0.0153	1006.03	1004.72	1003.29	1001.63	999.76	76.97	78.38	79.94	80.68	82.34
0.0201	1006.18	1004.87	1003.43	1001.77	999.89	77.57	78.61	80.31	81.09	82.63
0.0247	1006.32	1005.01	1003.57	1001.90	1000.01	77.99	79.02	80.61	81.51	82.94
0.0298	1006.47	1005.16	1003.71	1002.04	1000.15	78.39	79.48	80.88	81.67	83.22
Cytosine +0.0995 mol/kg D-lactose										
0.0000	1011.61	1010.32	1008.89	1007.21	1005.30					
0.0054	1011.79	1010.49	1009.05	1007.37	1005.45	77.96	79.29	80.63	82.00	83.75
0.0100	1011.94	1010.63	1009.19	1007.50	1005.57	78.24	79.67	81.02	82.39	83.97

0.0152	1012.10	1010.79	1009.34	1007.64	1005.71	78.61	79.96	81.39	82.71	84.25
0.0192	1012.22	1010.90	1009.45	1007.74	1005.81	78.94	80.27	81.68	83.15	84.60
0.0249	1012.39	1011.07	1009.60	1007.89	1005.95	79.35	80.59	81.97	83.45	84.91
0.0300	1012.54	1011.21	1009.73	1008.02	1006.07	79.69	80.93	82.54	83.69	85.22
Cytosine + 0.1498 mol/kg D-lactose										
0.0000	1017.83	1016.53	1015.06	1013.37	1011.42					
0.0051	1017.98	1016.68	1015.20	1013.50	1011.55	80.75	81.58	82.61	83.85	85.30
0.0101	1018.13	1016.81	1015.33	1013.63	1011.67	81.03	81.96	82.91	84.35	85.72
0.0150	1018.26	1016.95	1015.46	1013.75	1011.79	81.38	82.23	83.28	84.67	85.96
0.0200	1018.40	1017.08	1015.59	1013.87	1011.90	81.69	82.73	83.54	85.00	86.29
0.0250	1018.53	1017.20	1015.71	1013.99	1012.01	82.03	83.26	84.01	85.24	86.65
0.0298	1018.65	1017.31	1015.83	1014.10	1012.12	82.53	83.83	84.28	85.69	86.92

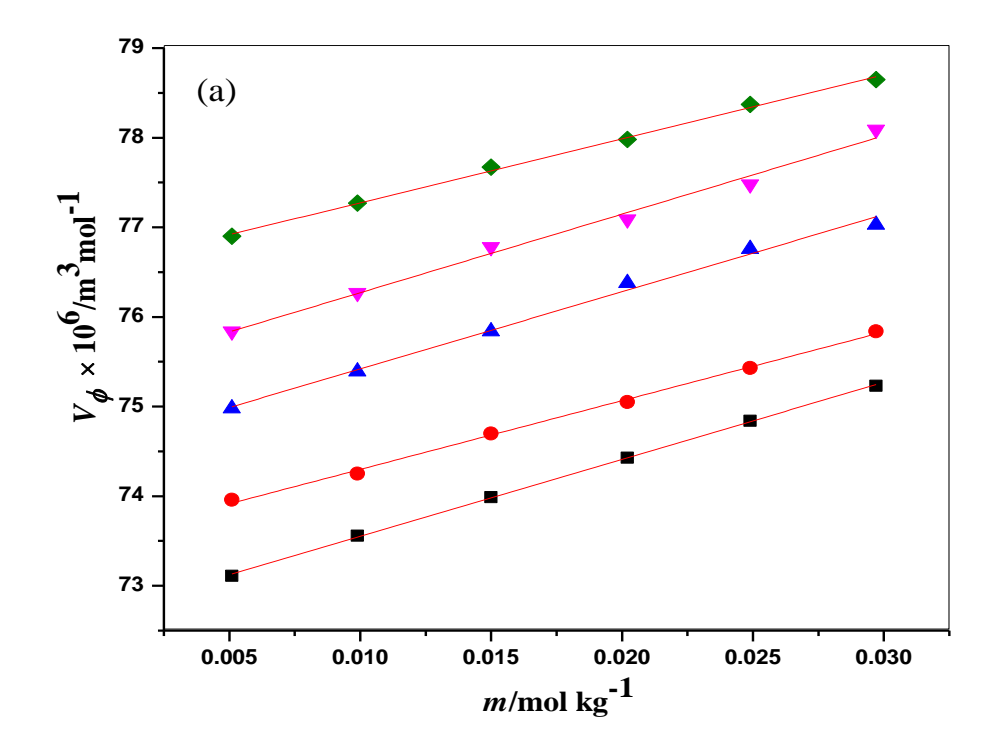
m(mol/kg) stands for the assessed molality for assorted solutions pertaining to cytosine in (water + D-xylose/D-lactose).

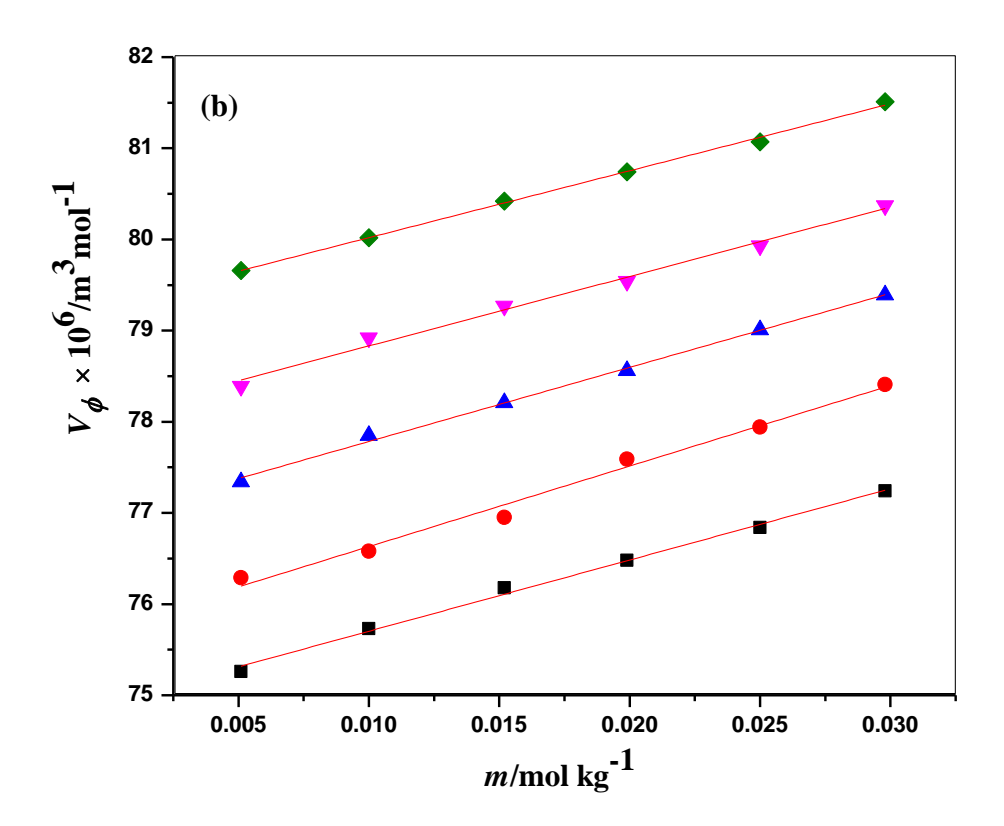
4.3.1.2 Limiting Apparent Molar Volume

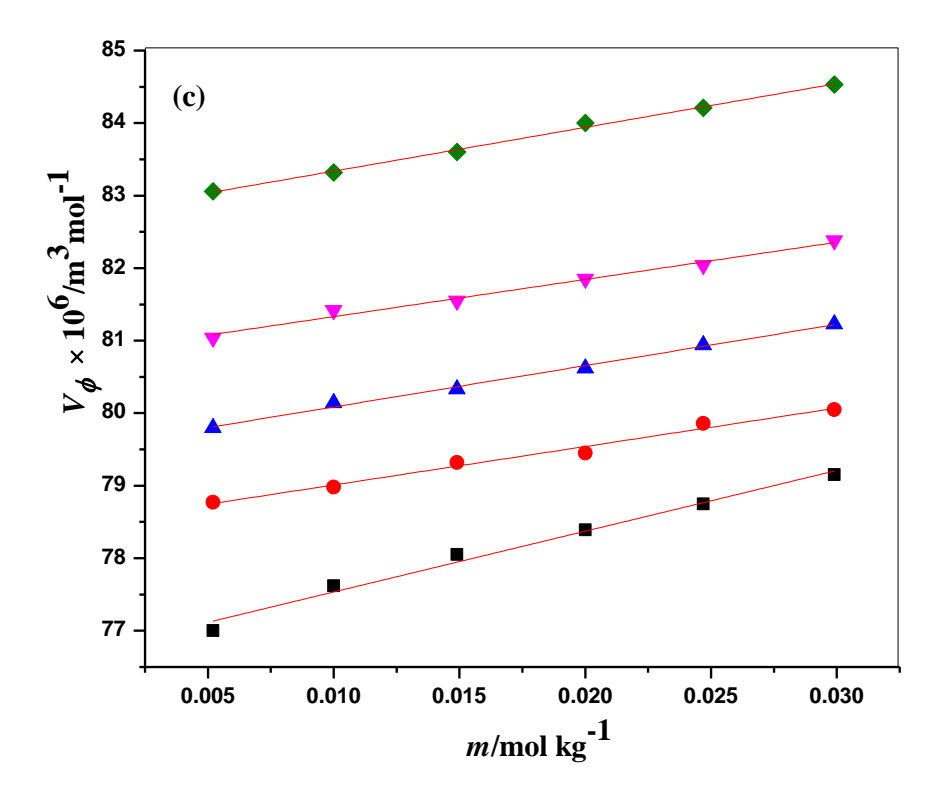
To determinate assorted interactions persisting amid cytosine and saccharide solvent system, the Masson equation [9] i.e. (2.2) is employed and V^0_{ϕ} data are deduced for considered mixtures. As per the Masson equation, the plot of V_{ϕ} against m furnishes the intercept, limiting apparent molar volume (V_{ϕ}^{o}) which is a criterion of solute-solvent interactions existing in the solution systems [10]. For all the solution samples of cytosine in H₂O as well as H₂O + D-xylose/D-lactose solutions, the graphs of V_{ϕ} against m have been shown in Figures 4.3.2 (a) – (g).

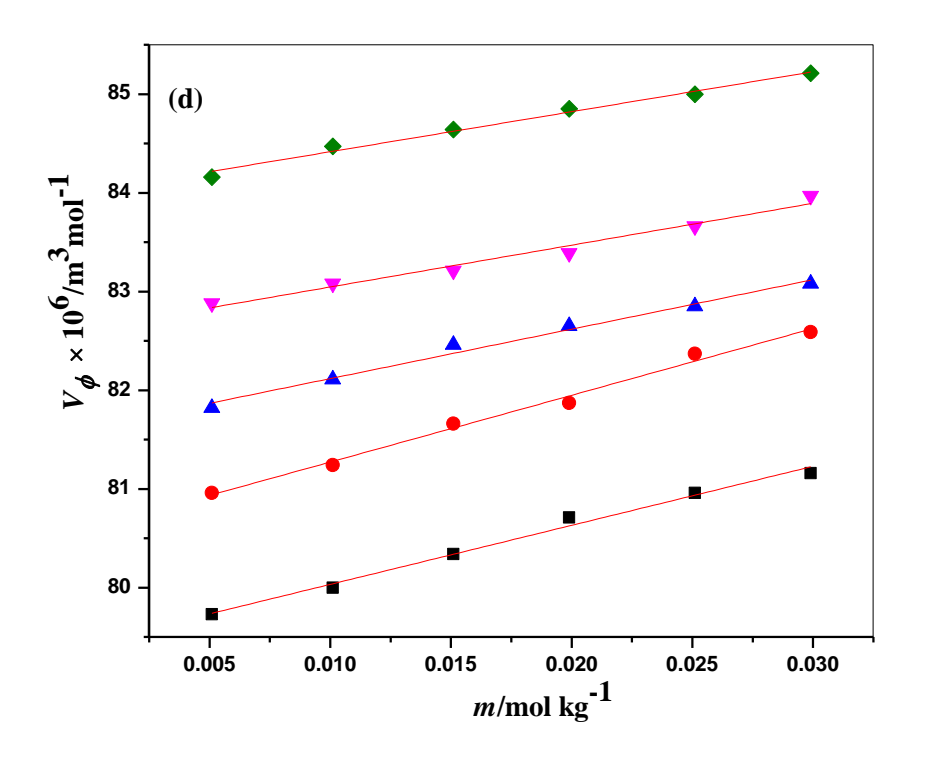
The graphical data for V^0_{ϕ} and S_{ν} together with their consequent standard inaccuracies is presented in the Table 4.3.2. The examination of Table 4.3.2 reveal that the V^0_{ϕ} values which are assessed are all positive as well as rising along with succession in temperature values, in sequence infers the occurrence of better solute/solvent synergies in examined mixtures.

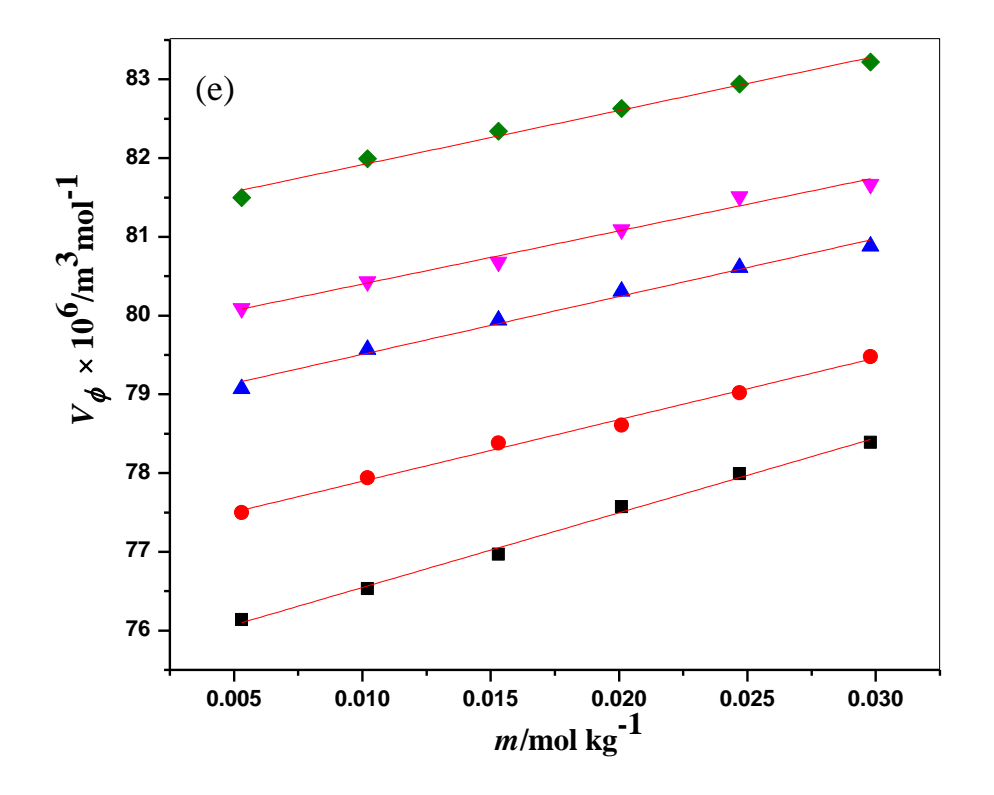
The succession in V^0_{ϕ} with temperature might be allocated to attenuation in the electrostriction of H₂O surrounding the cytosine molecules [11]. Moreover, the augmentation in V^0_{ϕ} with molality of D-xylose/D-lactose media is attributed to dehydration effect of D-xylose/D-lactose above hydrated cytosine in the mixtures [12].

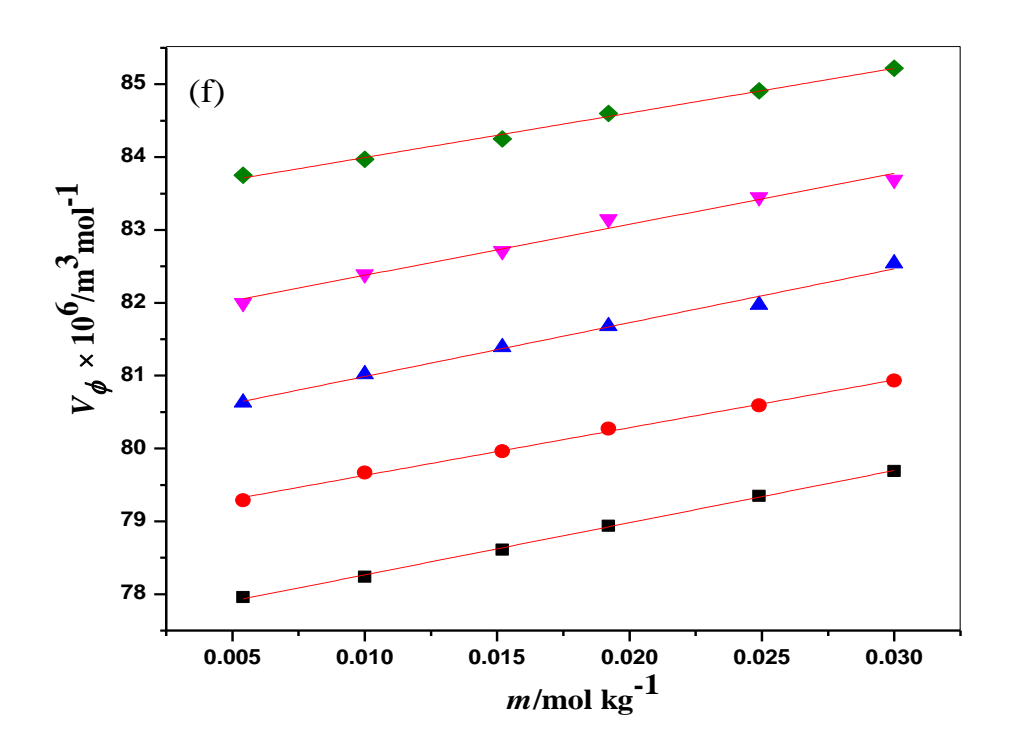












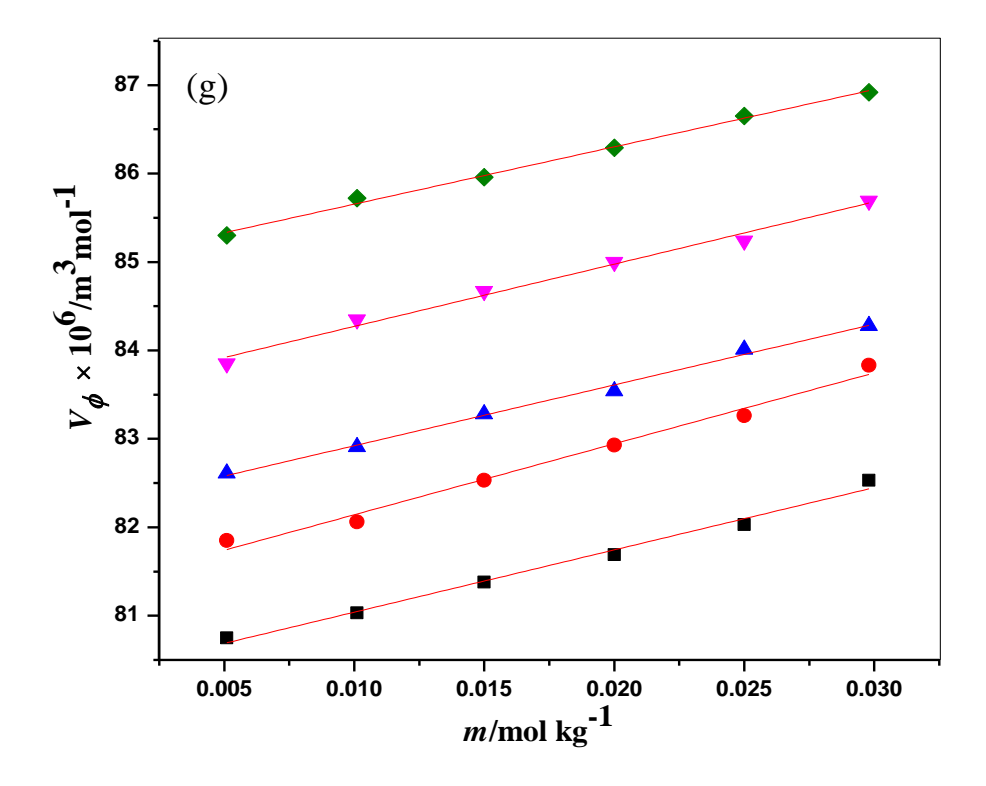


Figure 4.3.2: The analysed graphs depicting change in $V_{\phi} \times 10^6 (\text{m}^3/\text{mol})$ against m(mol/kg) for diverse systems (a) cytosine + H₂O, (b) cytosine + 0.05 mol/kg D-xylose, (c) cytosine + 0.10 mol/kg D-xylose, (d) cytosine + 0.15 mol/kg D-xylose, (e) cytosine + 0.05 mol/kg D-lactose, (f) cytosine + 0.10 mol/kg D-lactose, (g) cytosine + 0.15 mol/kg D-lactose at several T(K). \blacksquare : 293.15, \bullet : 303.15, \checkmark : 308.15, \diamond : 313.15.

4.3.1.3 Limiting Apparent Molar Volume of Transfer

To have a good imminent of different kind of synergies prevailing in mixtures, a commendable information is manifested via the transfer volumes [13]. Basically at infinite dilution, there occurs a very little interaction amid solute particles. Thus, the relation (2.4) has been employed for the inference of $\Delta_{tr}V^0_{\phi}$ for cytosine from water to aqueous D-xylose/D-lactose media. The deduced data of $\Delta_{tr}V^0_{\phi}$, is reported in Table 4.3.2 which shows that the $\Delta_{tr}V^0_{\phi}$ is positive at each exploratory temperature and these values are advancing with advancement in molal concentration of D-xylose/D-lactose in the ternary systems.

Table 4.3.2: Data of limiting apparent molar volume, V^0_{ϕ} together with slopes, S_v and associated transfer values $\Delta_{tr}V^0_{\phi}$ for cytosine in H₂O and aqueous D-xylose/D-lactose media at T/K = 293.15 - 313.15 and P = 0.1 MPa.

Duananty	$T(\mathbf{K})$										
Property	293.15	298.15	303.15	308.15	313.15						
Cytosine + water											
${V^0_{\phi} \times 10^6 (\mathrm{m}^3/\mathrm{mol})}$	72.69(±0.01)	73.53(±0.03)	74.56(±0.06)	75.39(±0.08)	76.56(±0.03)						
$S_{\nu} \times 10^6 (\mathrm{m}^3/\mathrm{mol})$	85.91(±0.78)	76.72(±1.77)	86.11(±3.26)	87.62(±4.08)	71.36(±1.63)						
Cytosine + 0.04970 mol/kg D-xylose											
$V^0_{\phi} \times 10^6 (\mathrm{m}^3/\mathrm{mol})$	74.92(±0.05)	75.78(±0.09)	76.97(±0.04)	78.07(±0.06)	79.28(±0.03)						
$S_{\nu} \times 10^{-6} (\mathrm{m}^3 \mathrm{kg/mol}^2)$	78.14(±2.49)	88.37(±4.77)	81.29(±2.07)	76.21(±3.35)	73.43(±1.58)						
$\Delta_{tr}V^0_{\phi} \times 10^6 (\mathrm{m}^3/\mathrm{mol})$	2.23	2.25 2.41		2.68	2.72						
Cytosine + 0.09980 mol/kg D-xylose											
${V^0_{\phi} \times 10^6 (\mathrm{m}^3/\mathrm{mol})}$	76.69(±0.08)	78.48(±0.06)	79.52(±0.04)	80.82(±0.06)	82.73(±0.03)						
$S_{\nu} \times 10^{6} (\mathrm{m}^{3}\mathrm{kg/mol}^{2})$	94.23(±4.26)	53.05(±3.16)	56.96(±1.87)	51.31(±2.85)	60.36(±1.77)						
$\Delta_{tr}V^0_{\phi} \times 10^6 (\mathrm{m}^3/\mathrm{mol})$	4.00	4.95	4.96	5.43	6.17						
Cytosine+ 0.15040 mol/kg D-xylose											
$\overline{V^0_{\phi} \times 10^6 (\mathrm{m}^3/\mathrm{mol})}$	79.43(±0.05)	80.59(±0.06)	81.63(±0.05)	82.62(±0.06)	84.01(±0.04)						
$S_{\nu} \times 10^{6} (\mathrm{m}^{3}\mathrm{kg/mol^{2}})$	59.83(±2.78)	67.65(±2.99)	50.11(±2.79)	42.40(±3.25)	40.55(±2.17)						
$\Delta_{tr}V^0_{\phi} \times 10^6 (\mathrm{m}^3/\mathrm{mol})$	6.74	7.06	7.07	7.23	7.45						
Cytosine + 0.05020 mol/kg D-lactose											
$V^{\theta_{\phi}} \times 10^6 (\mathrm{m}^3/\mathrm{mol})$	75.59(±0.06)	77.11(±0.06)	78.77(±0.07)	79.72(±0.07)	81.23(±0.07)						
$S_{\nu} \times 10^{6} (\mathrm{m}^{3}\mathrm{kg/mol^{2}})$	94.98(±3.19)	78.31(±2.91)	73.44(±3.76)	67.53(±3.85)	68.76(±3.43)						
$\Delta_{tr} V^0_{\phi} \times 10^6 (\mathrm{m}^3/\mathrm{mol})$	2.90	3.58	4.21	4.33	4.67						
Cytosine + 0.09950 mol/kg D-lactose											
$V^{\theta_{\phi}} \times 10^6 (\mathrm{m}^3/\mathrm{mol})$	77.55(±0.02)	78.97(±0.03)	80.25(±0.07)	81.68(±0.08)	83.38(±0.04)						
$S_{\nu} \times 10^{6} (\mathrm{m}^{3}\mathrm{kg/mol^{2}})$	71.67(±1.24)	65.53(±1.71)	73.90(±3.57)	69.98(±4.16)	61.19(±2.14)						
$\Delta_{tr}V^0_{\phi} \times 10^6 (\mathrm{m}^3/\mathrm{mol})$	4.86	5.44	5.69	6.29	6.82						

Cytosine + 0.14980 mol/kg D-lactose								
$V^0_\phi \times 10^6 (\mathrm{m}^3/\mathrm{mol})$	80.33(±0.07)	81.34(±0.09)	82.43(±0.04)	83.57(±0.07)	85.01(±0.04)			
$S_{\nu} \times 10^{6} (\mathrm{m}^3 \mathrm{kg/mol}^2)$	70.46(±3.41)	80.21(±4.57)	68.76(±2.32)	70.43(±3.58)	64.79(±1.90)			
$\Delta_{tr}V^0_{\phi}\times 10^6(\mathrm{m}^3/\mathrm{mol})$	7.64	7.81	7.87	8.18	8.45			

The augmentation in $\Delta_{tr}V^0_{\phi}$ with intensifying molality of D-xylose/D-lactose is due to reduction in shrinkage volume of cytosine [14]. Therefore, the $\Delta_{tr}V^0_{\phi}$ data is positive which simply specify the dehydration effect by D-xylose/D-lactose over the hydrated cytosine molecules in the mixtures [15]. Further, the $\Delta_{tr}V^0_{\phi}$ values for cytosine are found to be lower for D-xylose in comparison to D-lactose. This might be owing to disparity in configurational features of considered saccharides. As indicated by Friedman and Krishnan's model [16], overlapping by hydration spheres for polar moieties cause expansion in volumes whereas that of non-polar moieties results in the reduction of volume of mixtures. Herein, the positive transfer values are acquired on account of synergies existing amid polar moieties of cytosine and D-xylose/D-lactose moieties.

The plausible interactions established in the considered mixtures are discussed as under:

- (i) Hydrophilic type interactions among >C=N-, >C-N<, >C=O and -NH₂ groups of cytosine and, >C-O-, >C=O, -OH groups in saccharide molecules.
- (ii) Hydrophobic type interactions among hydrocarbon fragments in cytosine as well as saccharide molecules.

On the whole, type (i) offer positive part to transfer volumes whereas type (ii) offer negative part to transfer volumes. As a result, type (i) interactions are principal in examined mixtures.

Additionally, disparity in configurational features of D-xylose and D-lactose is a potential reason for differences in their interaction dynamics. D-Xylose has a five-carbon backbone and contains an aldehydic functional group. This makes it a smaller, simpler sugar. In contrast, D-Lactose is formed by the condensation of one D-galactose molecule and one D-glucose molecule. These two units are joined by a β-1,4-glycosidic linkage. This

larger, more complex structure with the glycosidic bond is a key difference from the monosaccharide D-xylose.

The significant structural differences, particularly the size and complexity, directly impact how these saccharides interact with other molecules in a solution. Table 4.3.2 mentions that the differences in $\Delta_{tr}V^0_{\phi}$ values for cytosine in the two solutions may be attributed to differences in the saccharides configurational features. D-lactose has more hydroxyl (-OH) groups than D-xylose, which increases its capacity for hydrogen bonding and hydrophilic interactions with cytosine. The larger, more complex surface area of D-lactose, with its greater number of hydroxyl groups, would likely result in a different balance and intensity of these interactions compared to the simpler D-xylose.

4.3.1.4 Temperature Reliance of the Limiting Molar Volume

It can be attained that at dilution (infinite), the apparent molar volumes are reliant upon temperature as per polynomial expression [17] (2.7). In the conducted study, 303.15 K has been considered as the reference. The data of empirical constants of cytosine in H₂O as well as aqueous D-xylose/D-lactose media is reported in Table 4.3.3. Additionally, first derivative in the limiting apparent molar volumes w.r.t temperature is computed as well [18], which is known as limiting apparent molar expansibility, E^0_{ϕ} . It is a considerable parameter in explicating assorted interactions existing in the studied mixtures [19] and can be determined through expression (2.8). The construed data of limiting apparent or partial molar expansibility is presented in Table 4.3.4. Through this table, it is noticeable that E^0_{ϕ} data are all positive and decreasing along rising temperature. The E^0_{ϕ} values are positive because of caging effect [20]. These merely signify the subsistence of well-built interactions amid cytosine and D-xylose/D-lactose molecules. For all investigated mixtures, the decrease in E^0_{ϕ} values with elevation in temperature display dehydration on hydrated solute molecules. Actually, for assessment of chaotropic or kosmotropic behavior of cytosine in prepared solvent mixtures, a thermodynamic expression presented by Hepler [21], ie equation (2.10) is used. Here, the sign of $(\partial E^0_{\phi}/\partial T)_P$ is observed to be negative for cytosine (in Table 4.3.4) which indicate chaotropic behavior of cytosine in aqua and aqueous D-xylose/D-lactose solvent media.

Table 4.3.3: Deduced constraints (a, b, c) for cytosine in H₂O as well as aqueous D-xylose/D-lactose mixtures.

Studied Mixtures	a × 10 ⁶ (m ³ /mol)	b × 10 ⁶ (m ³ /mol /K)	c ×10 ⁶ (m ³ /mol /K ²)
Cytosine + water	74.48(±0.06)	0.1920(±0.0054)	-0.00131 (±0.0009)
Cytosine + 0.04970 mol/kg D-xylose	76.92(±0.05)	0.2202(±0.0045)	-0.00174(±0.0007)
Cytosine + 0.09980 mol/kg D-xylose	79.57(±0.21)	$0.2884(\pm0.0195)$	-0.00143(±0.00331)
Cytosine + 0.15040 mol/kg D-xylose	81.59(±0.08)	$0.2238(\pm0.0076)$	-0.00117(±0.00129)
Cytosine + 0.05020 mol/kg D-lactose	$78.59(\pm0.14)$	0.2778(±0.01297)	-0.00209(±0.00216)
Cytosine + 0.09950 mol/kg D-lactose	80.26(±0.06)	$0.2874(\pm0.0059)$	-0.00203(±0.00090)
Cytosine + 0.14980 mol/kg D-lactose	82.41(±0.04)	0.2318(±0.0034)	-0.00260(±0.00058)

Table 4.3.4: Deduced data of apparent molar expansibility at dilution (infinite), E^0_{ϕ} besides Hepler's constant, $(\partial E^0_{\phi}/\partial T)_P$ for cytosine in H₂O and H₂O + D-xylose/D-lactose mixtures.

(mal /laa)		$(\partial E^0 \phi / \partial T)_P$				
m (mol/kg)	293.15 K	298.15 K	303.15 K	308.15 K	313.15 K	$(m^3/mol/K^2)$
Cytosine + water	0.2182	0.2051	0.1920	0.1789	0.1658	-0.00262
Cytosine + 0.04970 mol/kg D-xylose	0.2550	0.2376	0.2202	0.2028	0.1854	-0.00348
Cytosine + 0.09980 mol/kg D-xylose	0.3170	0.3027	0.2884	0.2741	0.2598	-0.00286
Cytosine + 0.15040 mol/kg D-xylose	0.2472	0.2355	0.2238	0.2121	0.2004	-0.00234
Cytosine + 0.05020 mol/kg D-lactose	0.3196	0.2987	0.2778	0.2569	0.2360	-0.00418
Cytosine + 0.09950 mol/kg D-lactose	0.3280	0.3077	0.2874	0.2671	0.2468	-0.00406
Cytosine + 0.14980 mol/kg D-lactose	0.2838	0.2578	0.2318	0.2058	0.1798	-0.00520

4.3.1.5 Taste Behavior

For the assessment of taste savour of cytosine in water and assorted saccharide media, parameter specifically apparent massic volume (apparent specific volume) had been assessed. This consideration expresses the hydrological packaging of cytosine moieties D-xylose/D-lactose media [22]. Relation (2.11) can be implicated for assessment of *ASV* values. Basically, these values depend on the molar mass and apparent molar volumes of solute particles [23].

In conducted work, the ASV (in Table 4.3.5) for cytosine in aqueous media and aqueous D-xylose/D-lactose media falls in array $(0.66\text{-}0.78) \times 10^{-3} \text{ m}^3 \text{ kg}^{-1} \text{ mol}^{-1}$. The assessed ASV data clearly demonstrates the sweet taste of cytosine in H_2O and sweet-bitter taste in peculiar concentrations of D-xylose/D-lactose media. From Table 4.3.5, it can be analyzed that the ASV of cytosine advances with augmentation in its molal concentrations or temperatures. Thus, it can be premediated that the sweetness of cytosine enhances with amplification in its concentration and with temperature.

Table 4.3.5: The deduced data of ASV for cytosine in water and aqueous D-xylose/D-lactose solutions at T/K = 293.15 - 313.15 and P = 0.1 MPa.

m(mol/kg)			<i>T</i> (K)		
	293.15	298.15	303.15	308.15	313.15
		Cytosine + wat	ter		
0.00000					
0.00510	0.66	0.67	0.67	0.68	0.69
0.00990	0.66	0.67	0.68	0.69	0.70
0.01500	0.67	0.67	0.68	0.69	0.70
0.02020	0.67	0.68	0.69	0.69	0.70
0.02490	0.67	0.68	0.69	0.70	0.71
0.02970	0.68	0.68	0.69	0.70	0.71
	Cytosine	e+ 0.04970 mol/l	kg D-xylose		
0.00000					
0.00510	0.68	0.69	0.70	0.71	0.72
0.01000	0.68	0.69	0.70	0.71	0.72
0.01520	0.69	0.69	0.70	0.71	0.72
0.01990	0.69	0.70	0.71	0.72	0.73
0.02500	0.69	0.70	0.71	0.72	0.73
0.02980	0.70	0.71	0.71	0.72	0.73
	Cytosine	e + 0.09980 mol/	kg D-xylose		
0.00000					
0.00520	0.69	0.71	0.72	0.73	0.75
0.01000	0.70	0.71	0.72	0.73	0.75
0.01490	0.70	0.71	0.72	0.73	0.75
0.02000	0.71	0.72	0.73	0.74	0.76

0.02470	0.71	0.72	0.73	0.74	0.76						
0.02990	0.71	0.72	0.73	0.74	0.76						
	Cytosin	ne + 0.15040 mo	l/kg D-xylose								
0.00000											
0.00510	0.72	0.73	0.74	0.75	0.76						
0.01010	0.72	0.73	0.74	0.75	0.76						
0.01510	0.72	0.73	0.74	0.75	0.76						
0.01990	0.73	0.74	0.74	0.75	0.76						
0.02510	0.73	0.74	0.75	0.75	0.77						
0.02990	0.73	0.74	0.75	0.76	0.77						
Cytosine + 0.05020 mol/kg D-lactose											
0.00000											
0.00530	0.69	0.70	0.71	0.72	0.73						
0.01020	0.69	0.70	0.72	0.72	0.74						
0.01530	0.69	0.71	0.72	0.73	0.74						
0.02010	0.70	0.71	0.72	0.73	0.74						
0.02470	0.70	0.71	0.73	0.73	0.75						
0.02980	0.71	0.72	0.73	0.74	0.75						
	Cytosin	e + 0.09950 mol	/kg D-lactose								
0.00000											
0.00540	0.70	0.71	0.73	0.74	0.75						
0.01000	0.70	0.72	0.73	0.74	0.76						
0.01520	0.71	0.72	0.73	0.74	0.76						
0.01920	0.71	0.72	0.74	0.75	0.76						
0.02490	0.71	0.73	0.74	0.75	0.76						
0.03000	0.72	0.73	0.74	0.75	0.77						
	Cytosin	e + 0.14980 mol	/kg D-lactose								
0.00000											
0.00510	0.73	0.73	0.74	0.75	0.77						
0.01010	0.73	0.74	0.75	0.76	0.77						
0.01500	0.73	0.74	0.75	0.76	0.77						
0.02000	0.74	0.74	0.75	0.77	0.78						
0.02500	0.74	0.75	0.76	0.77	0.78						
0.02980	0.74	0.75	0.76	0.77	0.78						

4.3.2 Speed of Sound Data

The experimentally acquired sound velocity of D-lactose [5] in the aqueous media is referred with the available data (literature) and depicted in Figure 4.3.3 (a).

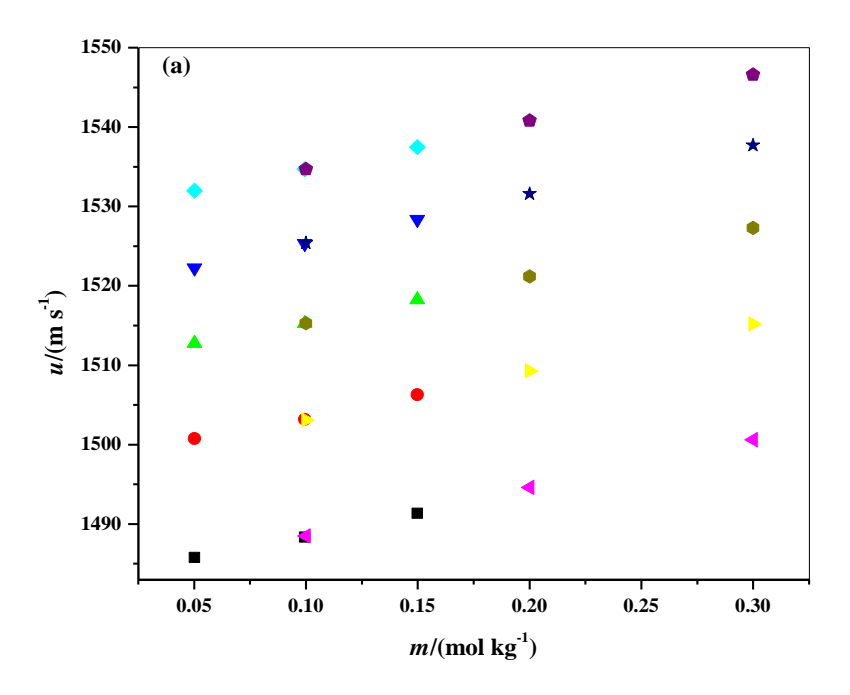


Figure 4.3.3: Graph representing deviation in measured sound velocity data with the accessible reports at discrete temperatures for D-lactose in water. ■ : Conducted investigation on 293.15 K, ● : Conducted investigation on 298.15 K, ▲ : Conducted investigation on 303.15 K, ▼: Conducted investigation on 308.15 K, ● : Lit. [5] on 293.15 K, ▷ : Lit. [5] on 298.15 K, ● : Lit. [5] on 303.15 K, ★ : Lit. [5] on 308.15 K, ♠ : Lit. [5] on 313.15 K.

These Figures further demonstrate the strong concordance between published data and empirically determined sound velocities. Moreover, Table 4.3.6 enlists the empirical estimates of the solute's or cytosine's ultrasonic velocity, in both H_2O as well as binary D-xylose/D-lactose aqueous medium at T/(K) = 293.15 to 313.15. It might be deduced via this data table that sound speed enhances in the midst of increasing temperatures or molal concentrations.

4.3.2.1 Apparent Molar Isentropic Compressions

Exploratory density and velocity of sound data were utilized for the estimation of apparent molar isentropic compression as per the equation (2.12). By the use of the

Newton-Laplace relation, the adiabatic compressibilities have been inferred, as per the relations (2.13) and (2.14). The $K_{\phi,s}$ values of cytosine in H₂O and H₂O + D-xylose/D-lactose media have been displayed in Table 4.3.6. Furthermore, $K_{\phi,s}$ data are established as negative at molalities and temperature values, and their magnitude decreases as molal composition of D-xylose/D-lactose rises. The compressibility of H₂O molecules is indicated through the negative $K_{\phi,s}$ data, that also suggest that presence of cytosine molecules have a stronger ordering influence on D-xylose/D-lactose molecules [24–26].

Table 4.3.6: Experimentally acquired sound velocities, u and calculated apparent molar isentropic compressions, $K_{\phi,s}$ for cytosine in H₂O and H₂O + D-xylose/D-lactose mixtures at several temperatures (K).

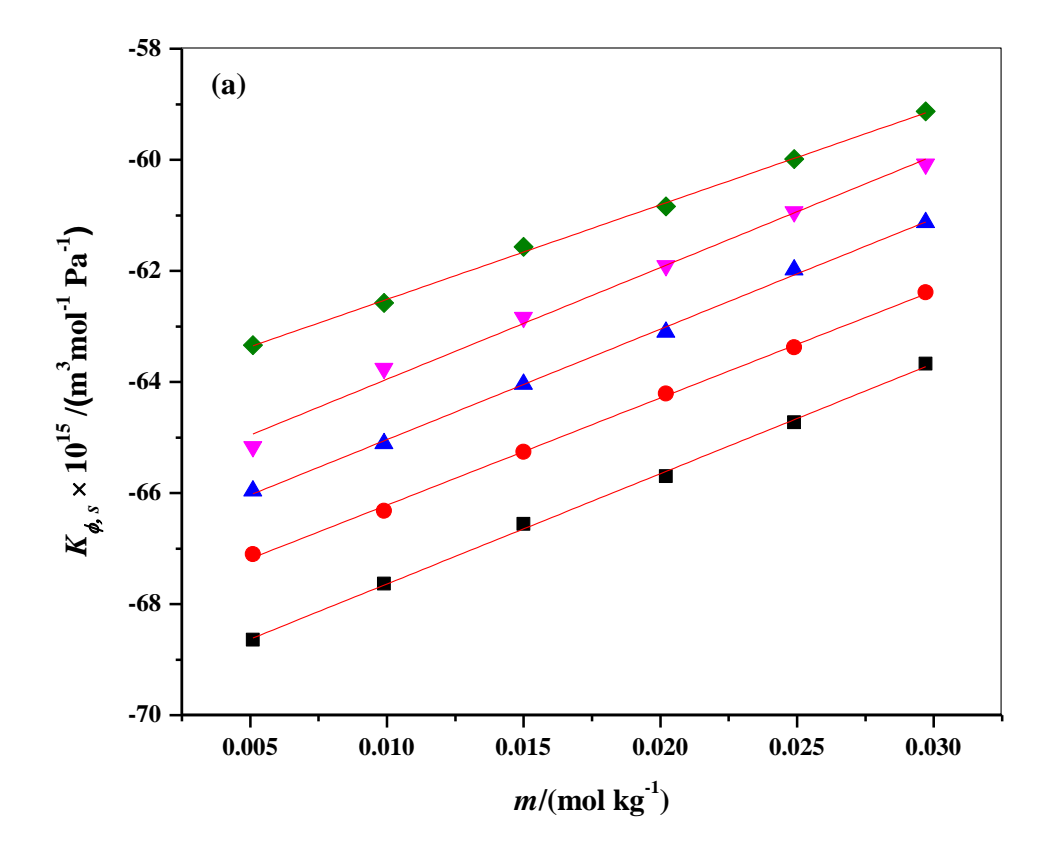
			u(m/s))		$K_{\phi,s} \times 1$	$0^{15} (m^3 / 10^{15})$	mol /Pa))	
m(mol/kg)										
	293.15	298.15	303.15	308.15	313.15	293.15	298.15	303.15	308.15	313.15
				Cytosi	ne + water					
0.0000	1482.12	1497.21	1508.72	1519.35	1528.52					
0.0051	1482.82	1497.92	1509.44	1520.08	1529.25	-68.64	-67.10	-65.96	-65.17	-63.33
0.0099	1483.47	1498.58	1510.11	1520.75	1529.93	-67.63	-66.32	-65.11	-63.76	-62.58
0.0150	1484.15	1499.27	1510.81	1521.46	1530.64	-66.56	-65.26	-64.04	-62.84	-61.57
0.0202	1484.84	1499.96	1511.52	1522.17	1531.36	-65.70	-64.21	-63.10	-61.91	-60.84
0.0249	1485.45	1500.58	1512.14	1522.80	1532.00	-64.73	-63.38	-61.98	-60.94	-59.99
0.0297	1486.06	1501.20	1512.77	1523.45	1532.64	-63.67	-62.39	-61.13	-60.08	-59.13
			Cytos	sine+ 0.04	97 mol/kg I)-xylose				
0.0000	1484.67	1498.89	1511.22	1521.68	1530.89					
0.0051	1485.39	1499.62	1511.97	1522.43	1531.62	-67.63	-66.07	-65.64	-63.90	-63.01
0.0100	1486.07	1500.31	1512.67	1523.15	1532.30	-66.44	-65.09	-64.30	-63.37	-62.26
0.0152	1486.78	1501.04	1513.40	1523.89	1533.01	-65.28	-64.39	-63.03	-62.12	-61.26
0.0199	1487.41	1501.69	1514.06	1524.55	1533.72	-64.29	-63.36	-62.27	-61.18	-60.25
0.0250	1488.10	1502.38	1514.76	1525.26	1534.35	-63.62	-62.35	-61.20	-60.23	-59.23
0.0298	1488.73	1503.02	1515.41	1525.92	1534.98	-62.64	-61.31	-60.26	-59.29	-58.26
			Cytos	ine + 0.09	98 mol/kg I	D-xylose				
0.0000	1487.69	1501.55	1513.59	1524.13	1533.33					
0.0052	1488.43	1502.31	1514.37	1524.91	1534.13	-66.56	-65.35	-64.76	-63.21	-62.07
0.0100	1489.12	1503.01	1515.07	1525.63	1534.86	-65.69	-64.54	-63.28	-62.17	-61.33
0.0149	1489.80	1503.71	1515.78	1526.34	1535.59	-64.42	-63.59	-62.50	-61.08	-60.33

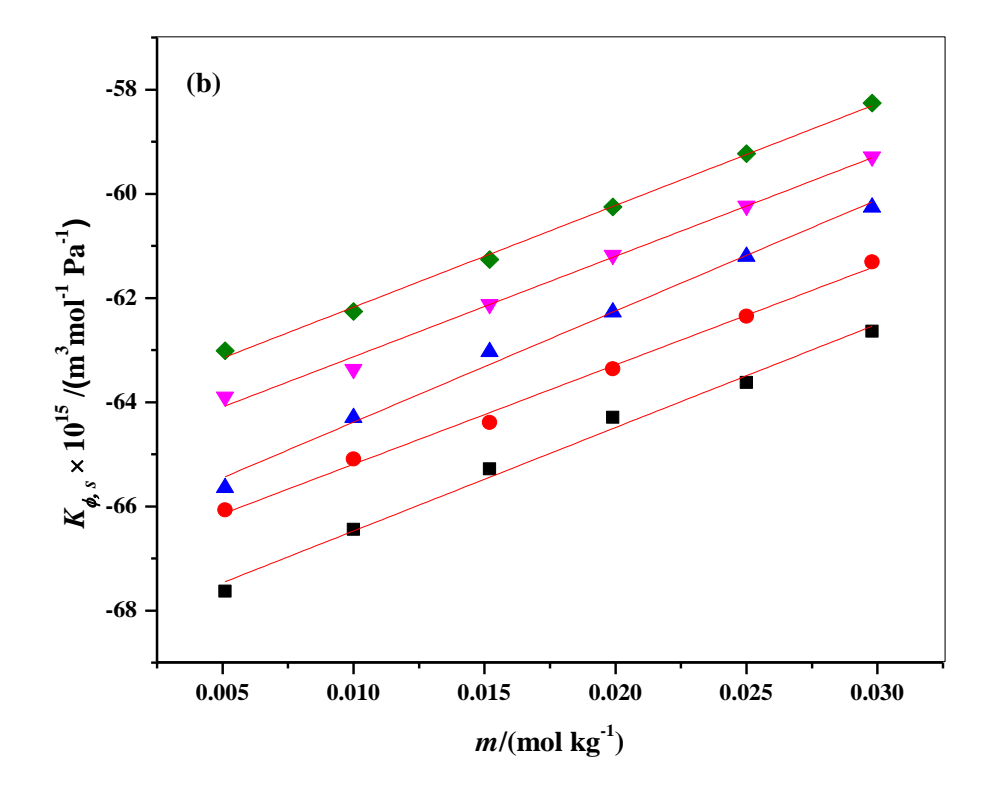
0.0200	1490.51	1504.42	1516.50	1527.07	1536.34	-63.54	-62.58	-61.36	-60.04	-59.29		
0.0247	1491.15	1505.07	1517.15	1527.74	1537.01	-62.63	-61.60	-60.25	-59.37	-58.25		
0.0299	1491.84	1505.76	1517.86	1528.46	1537.75	-61.46	-60.40	-59.22	-58.29	-57.30		
	Cytosine + 0.1504 mol/kg D-xylose											
0.0000	1490.15	1503.96	1515.90	1526.37	1535.47							
0.0051	1490.90	1504.73	1516.67	1527.16	1536.26	-65.49	-64.63	-63.18	-62.50	-61.53		
0.0101	1491.62	1505.46	1517.42	1527.91	1537.03	-64.31	-63.25	-62.27	-61.43	-60.48		
0.0151	1492.33	1506.19	1518.16	1528.65	1537.78	-63.26	-62.36	-61.45	-60.46	-59.49		
0.0199	1493.01	1506.87	1518.85	1529.35	1538.48	-62.51	-61.30	-60.44	-59.57	-58.32		
0.0251	1493.72	1507.61	1519.59	1530.09	1539.23	-61.36	-60.35	-59.53	-58.45	-57.36		
0.0299	1494.36	1508.27	1520.24	1530.76	1539.91	-60.30	-59.39	-58.25	-57.38	-56.43		
			Cytos	sine+ 0.05	02 mol/kg I)-lactose						
0.0000	1485.77	1500.73	1512.78	1522.24	1531.98							
0.0053	1486.52	1501.50	1513.57	1523.03	1532.78	-66.47	-65.58	-64.95	-63.06	-61.94		
0.0102	1487.21	1502.20	1514.28	1523.75	1533.51	-65.88	-64.46	-63.32	-62.15	-60.95		
0.0153	1487.91	1502.92	1515.01	1524.49	1534.26	-64.65	-63.46	-62.20	-61.34	-60.07		
0.0201	1488.57	1503.58	1515.69	1525.17	1534.95	-63.73	-62.43	-61.29	-60.22	-59.09		
0.0247	1489.19	1504.21	1516.33	1525.82	1535.60	-62.81	-61.51	-60.39	-59.36	-58.12		
0.0298	1489.86	1504.89	1517.03	1526.51	1536.31	-61.69	-60.31	-59.48	-58.25	-57.16		
			Cytos	ine + 0.09	95 mol/kg l	D-lactose						
0.0000	1488.34	1503.18	1515.27	1525.34	1534.69							
0.0054	1489.11	1503.97	1516.08	1526.16	1535.52	-63.91	-63.05	-62.59	-61.40	-60.04		
0.0100	1489.76	1504.64	1516.76	1526.85	1536.22	-63.27	-62.51	-61.66	-60.56	-59.43		
0.0152	1490.49	1505.38	1517.52	1527.61	1536.99	-62.57	-61.49	-60.75	-59.32	-58.24		
0.0192	1491.03	1505.93	1518.08	1528.19	1537.58	-61.45	-60.31	-59.52	-58.41	-57.48		
0.0249	1491.81	1506.72	1518.87	1529.00	1538.40	-60.60	-59.38	-58.23	-57.32	-56.35		
0.0300	1492.48	1507.41	1519.60	1529.71	1539.12	-59.46	-58.38	-57.56	-56.35	-55.33		
			Cytos	ine + 0.14	98 mol/kg l	D-lactose						
0.0000	1491.34	1506.29	1518.24	1528.35	1537.48							
0.0051	1492.09	1507.05	1519.02	1529.14	1538.28	-62.42	-61.44	-60.95	-59.94	-58.93		
0.0101	1492.81	1507.79	1519.77	1529.90	1539.05	-61.26	-60.34	-59.85	-58.69	-57.78		
0.0150	1493.51	1508.50	1520.49	1530.63	1539.79	-60.40	-59.40	-58.68	-57.58	-56.77		
0.0200	1494.21	1509.22	1521.21	1531.37	1540.53	-59.41	-58.46	-57.58	-56.72	-55.65		
0.0250	1494.90	1509.93	1521.93	1532.09	1541.27	-58.44	-57.45	-56.65	-55.73	-54.84		
0.0298	1495.55	1510.60	1522.60	1532.78	1541.95	-57.32	-56.38	-55.68	-54.81	-53.72		

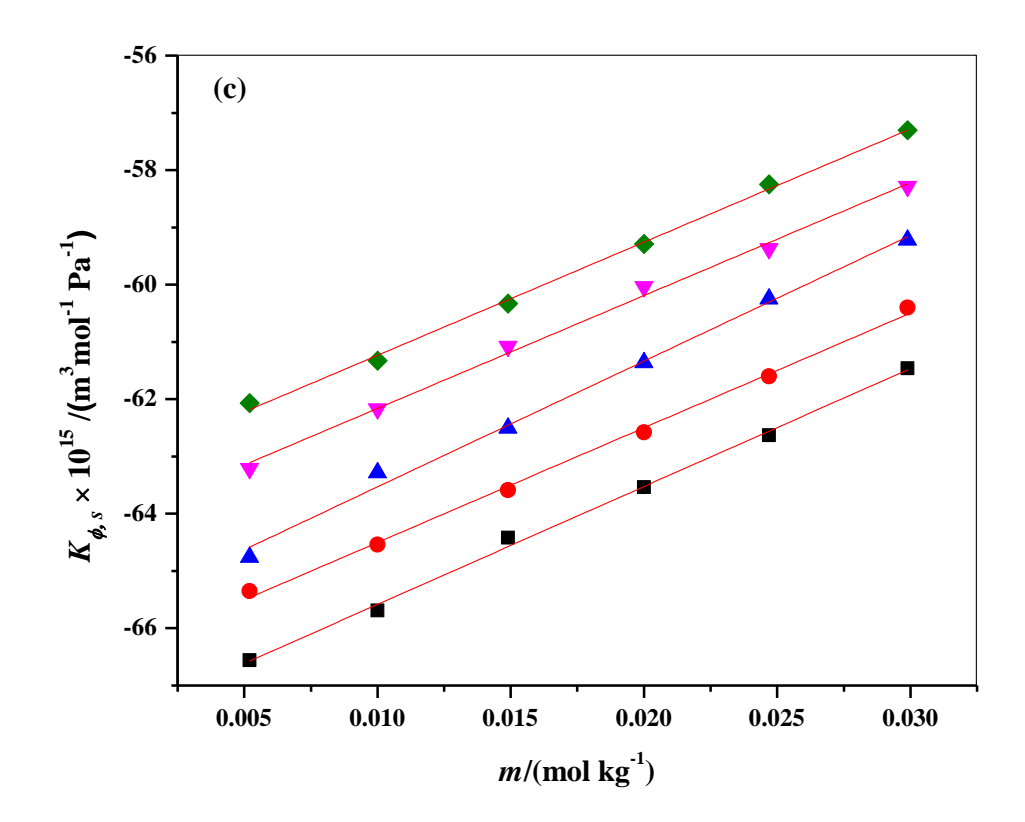
m(mol/kg) stands for the concentration in molality for assorted solutions pertaining to cytosine in (water + D-xylose/D-lactose).

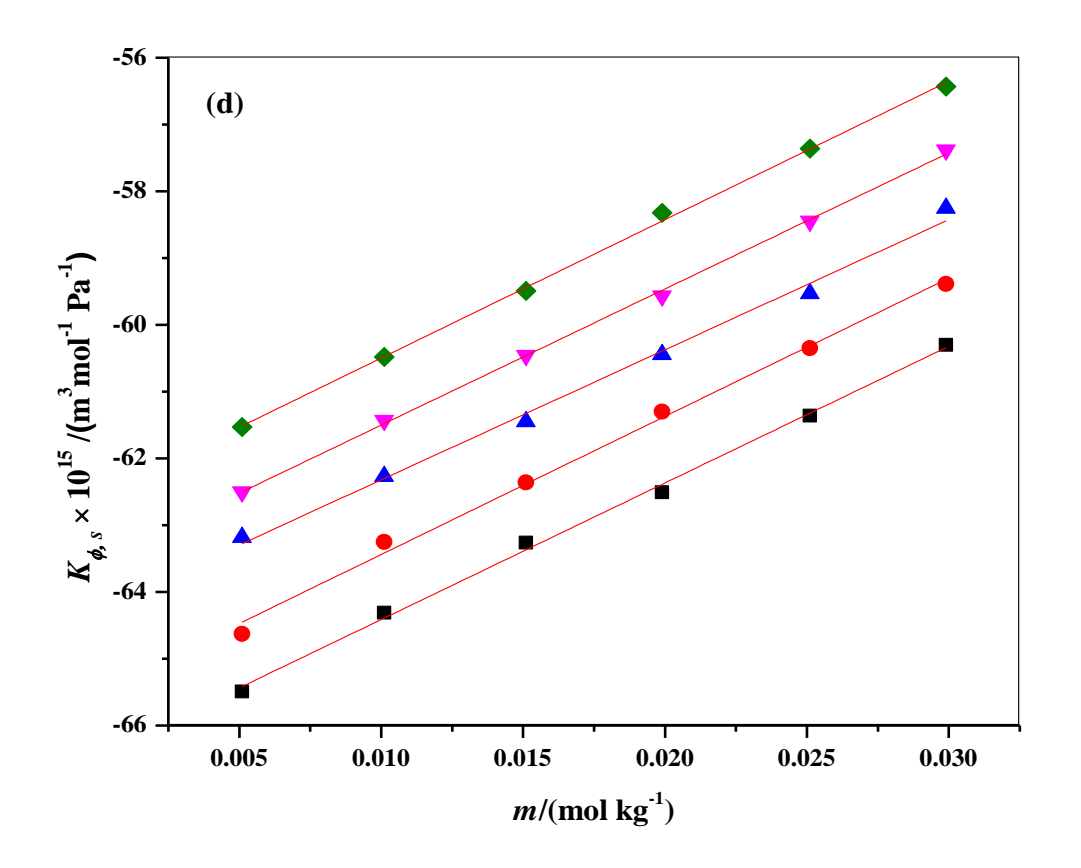
4.3.2.2 Limiting Apparent Molar Isentropic Compressions

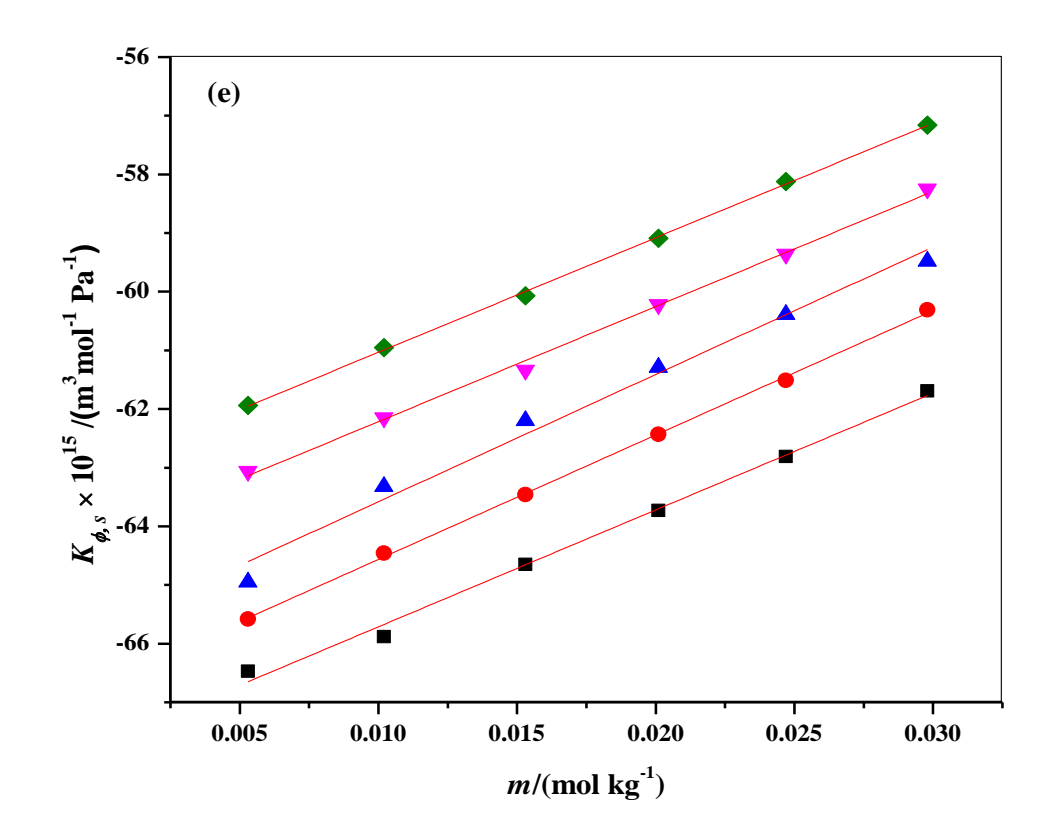
Another parameter, $K^0_{\phi,s}$ or limiting apparent molar isentropic compressions, measures interactions amid the solute in addition to cosolute and can be deliberated by least squares fitting Eqn. (2.15). The $K^0_{\phi,s}$ values foe cytosine in aqua as well as D-xylose along with D-lactose solutions are enlisted in the Table 4.3.7. Table 4.3.7 infers that as temperature rises, the $K^0_{\phi,s}$ values of cytosine grow less negative, which can be explained by considering various models [27,28]. These simulations suggest that water undergoes electrostriction around solute molecules, rendering the molecules more compressible than bulk water with an open structure. Additionally, plots of $K_{\phi,s}$ for cytosine in H₂O as well as aqueous D-xylose and D-lactose solutions against molal concentrations, m are shown in Figure 4.3.4 (a) to (g).

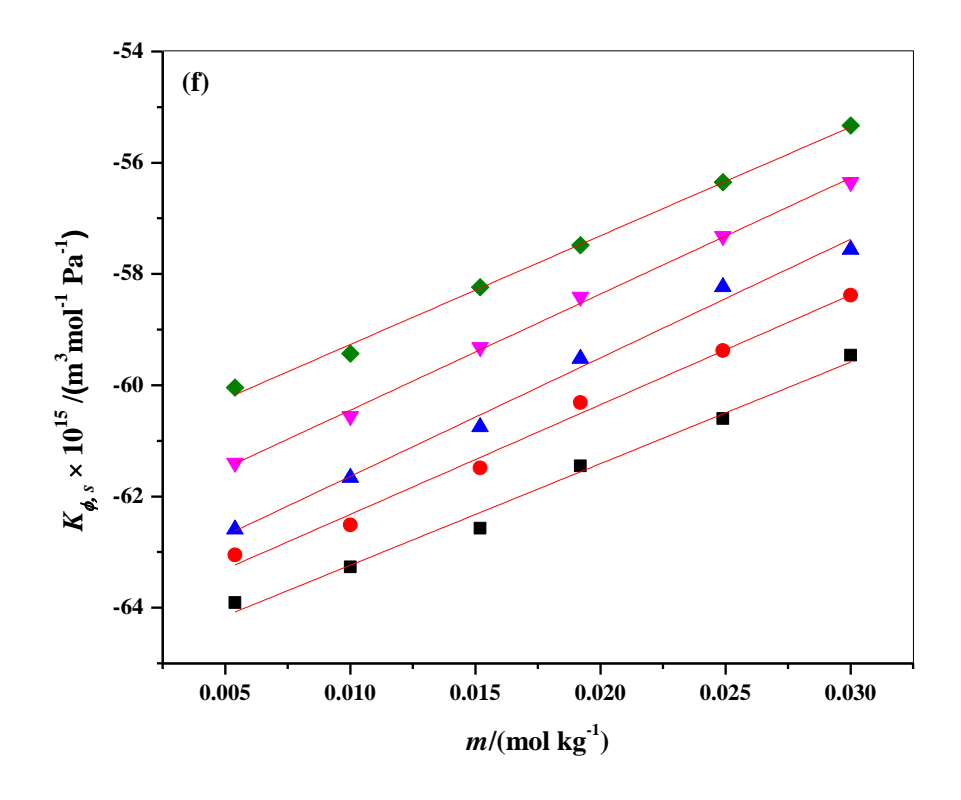












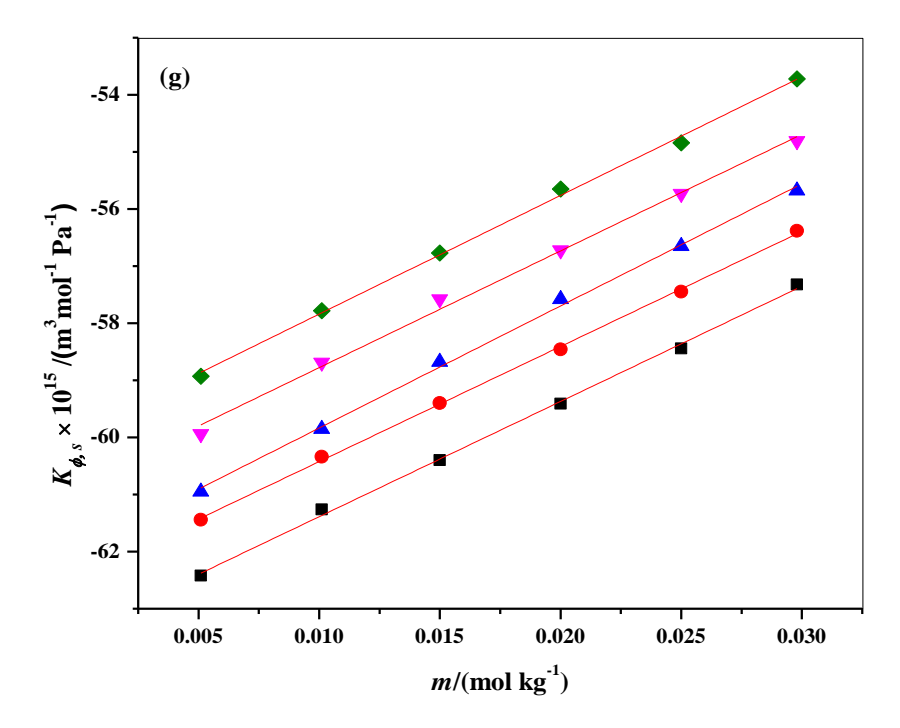


Figure 4.3.4: Graphs of $K_{\phi,s} \times 10^{15} (\text{m}^3 / \text{mol/Pa})$ against m(mol/kg) for several systems (a) cytosine + H₂O, (b) cytosine + 0.05 mol/kg D-xylose, (c) cytosine + 0.10 mol/kg D-xylose, (d) cytosine + 0.15 mol/kg D-xylose, (e) cytosine + 0.05 mol/kg D-lactose, (f) cytosine + 0.10 mol/kg D-lactose, (g) cytosine + 0.15 mol/kg D-lactose at varying T/(K), \blacksquare : 293.15, \bullet : 303.15, \checkmark : 308.15, \diamond : 313.15.

4.3.2.3 Limiting Apparent Molar Isentropic Compression of Transfer

For cytosine, the limiting apparent molar isentropic compression of transfer from water to aqueous D-xylose and D-lactose media has been fetched by the use of equation (2.16). Table 4.3.7 gives the values for $\Delta_{tr}K^0_{\phi,s}$. The positive transfer results show that interactions of the hydrophilic kind are preferred over those of the hydrophobic type. Additionally, the positive transfer values become stronger as the cosolute concentration rises. As such, the outcomes of acoustic analyses are more consistent with the findings of volumetric studies.

Table 4.3.7: Obtained partial molar isentropic compressions, $K^0_{\phi,s}$ together with slope, S_k besides calculated transfer partial molar isentropic compression, $\Delta_{tr}K^0_{\phi,s}$ for cytosine in pure H₂O as well as aqueous D-xylose and D-lactose solutions.

Inferred parameter	$T(\mathbf{K})$										
imerreu parameter	293.15	298.15	303.15	308.15	313.15						
Cytosine + water											
$K^0_{\phi,s} \times 10^{15} (\text{m}^3/\text{mol/Pa})$	-69.62(±0.07)	-68.15(±0.06)	-67.03(±0.07)	-65.96(±0.16)	-64.22(±0.06)						
$S_k \times 10^{15} (\mathrm{m}^3 \mathrm{kg/mol}^2/\mathrm{Pa})$	198.59(±3.60)	193.00(±2.92)	199.05(±3.64)	201.11(±8.32)	170.44(±3.07)						
Cytosine + 0.0497 mol/kg D-xylose											
$K^{\theta}_{\phi,s} \times 10^{15} (\text{m}^3/\text{mol/Pa})$	-68.46(±0.17)	-67.10(±0.12)	-66.52(±0.16)	-65.06(±0.14)	-64.13(±0.09)						
$S_k \times 10^{15} (\mathrm{m}^3 \mathrm{kg/mol}^2/\mathrm{Pa})$	198.64(±8.82)	190.71(±6.12)	213.51(±8.42)	192.92(±7.26)	195.40(±4.51)						
$\Delta_{tr}K^0_{\phi,s} \times 10^{15} (\mathrm{m}^3/\mathrm{mol/Pa})$	1.66	1.05	0.51	0.90	0.09						
	Cytosi	ne + 0.0998 m	ol/kg D-xylose								
$K^{\theta}_{\phi,s} \times 10^{15} (\text{m}^3/\text{mol/Pa})$	-67.64(±0.10)	-66.51(±0.09)	-65.73(±0.15)	-64.13(±0.11)	-63.21(±0.09)						
$S_k \times 10^{15} (\mathrm{m}^3 \mathrm{kg/mol}^2/\mathrm{Pa})$	205.92(±4.94)	200.30(±4.90)	219.53(±7.76)	197.12(±5.95)	197.64(±4.42)						
$\Delta_{tr}K^0_{\phi,s} \times 10^{15} (\mathrm{m}^3/\mathrm{mol/Pa})$	1.98	1.64	1.30	1.83	1.01						
	Cytosi	ne + 0.1504 mo	ol/kg D-xylose								
$K^{\theta}_{\phi,s} \times 10^{15} (\text{m}^3/\text{mol/Pa})$	-66.46(±0.10)	-65.51(±0.13)	-64.27(±0.14)	-63.54(±0.06)	-62.57(±0.07)						
$S_k \times 10^{15} (\text{m}^3 \text{kg/mol}^2/\text{Pa})$	204.58(±4.96)	206.89(±6.57)	194.87(±7.13)	203.87(±2.95)	207.28(±3.56)						

$\Delta_{tr}K^0_{\phi,s} \times 10^{15} (\text{m}^3/\text{mol/Pa})$	3.16	2.64	2.76	2.42	1.65						
	Cytosine + 0.0502 mol/kg D-lactose										
$\overline{K^0_{\phi,s} \times 10^{15} (\text{m}^3/\text{mol/Pa})}$	-67.70(±0.14)	-66.68(±0.05)	-65.75(±0.25)	-64.18(±0.10)	-62.99(±0.05)						
$S_k \times 10^{15} (\mathrm{m}^3 \mathrm{kg/mol}^2/\mathrm{Pa})$	199.25(±7.04)	212.14(±2.64)	217.05(±12.74)	196.31(±4.97)	195.31(±2.44)						
$\Delta_{tr}K^0_{\phi,s} \times 10^{15} (\mathrm{m}^3/\mathrm{mol/Pa})$	1.92	1.46	1.28	1.78	1.23						
	Cytosi	ne + 0.0995 mo	l/kg D-lactose								
$\overline{K^0_{\phi,s} \times 10^{15} (\text{m}^3/\text{mol/Pa})}$	-65.06(±0.18)	-64.30(±0.18)	-63.77(±0.19)	-62.54(±0.09)	-61.22(±0.10)						
$S_k \times 10^{15} (\mathrm{m}^3 \mathrm{kg/mol}^2/\mathrm{Pa})$	182.60(±9.20)	197.26(±9.24)	213.15(±9.82)	208.77(±4.52)	195.54(±5.08)						
$\Delta_{tr}K^0_{\phi,s} \times 10^{15} (\mathrm{m}^3/\mathrm{mol/Pa})$	4.56	3.85	3.26	3.43	2.99						
	Cytosi	ne + 0.1498 mo	l/kg D-lactose								
$\overline{K^0_{\phi,s} \times 10^{15} (\text{m}^3/\text{mol/Pa})}$	-63.41(±0.08)	-62.44(±0.05)	-61.97(±0.09)	-60.82(±0.12)	-59.92(±0.09)						
$S_k \times 10^{15} (\mathrm{m}^3 \mathrm{kg/mol}^2/\mathrm{Pa})$	201.77(±3.97)	201.54(±2.76)	213.93(±4.42)	204.34(±6.30)	207.78(±4.45)						
$\Delta_{tr}K^0_{\phi,s} \times 10^{15} (\mathrm{m}^3/\mathrm{mol/Pa})$	6.22	5.71	5.05	5.14	4.30						

4.3.2.4 *Hydration Number*

In order to determine the extent of hydration of cytosine molecules with sugar moieties, the hydration number, (n_H) is computed. Many techniques can be used to determine it. In present work, the implicated apparent molar compressibilities at very very high dilution in electrostriction has also been implicated to get the hydration number i.e. Eqn. (2.20), given by Millero and coworkers [29]. These n_H data for cytosine + water, cytosine + water + D-xylose/D-lactose mixtures is summarized in Table 4.3.8.

As temperature and cosolute concentration increase, this table shows that the n_H values decreases, suggesting an amplification of interactions among cytosine and saccharides molecules. The dehydration effect on solute (cytosine) caused by D-xylose and D-lactose moieties [30], in which D-xylose and D-lactose molecules replace water particles with increasing concentrations, possibly explain it.

Table 4.3.8: Hydration number (nH) for cytosine in H₂O and water +D-xylose/D-lactose implicated mixtures at assorted temperatures.

			η_H		
System					
	293.15	298.15	303.15	308.15	313.15
Cytosine + water	8.59	8.41	8.27	8.14	7.93
Cytosine + 0.04970 mol/kg D-xylose	8.45	8.28	8.21	8.03	7.92
Cytosine + 0.09980 mol/kg D-xylose	8.35	8.21	8.11	7.92	7.80
Cytosine + 0.15040 mol/kg D-xylose	8.20	8.09	7.93	7.84	7.72
Cytosine + 0.05020 mol/kg D-lactose	8.36	8.23	8.12	7.92	7.78
Cytosine + 0.09950 mol/kg D-lactose	8.03	7.94	7.87	7.72	7.56
Cytosine + 0.14980 mol/kg D-lactose	7.83	7.71	7.65	7.51	7.40

4.3.3 Viscosity Data

As viscosity η , is dependent on effective bonding amid solute-solvent entities, thus this physical property of solutions can be utilised in explaining the interactions amongst solute (cytosine) and solvents (aqueous D-xylose and D-lactose). Table 4.3.9 illustrates the viscosity values of cytosine in H_2O as well as water + D-xylose/D-lactose. Given that viscosity and molar mass are co-related, the cosolute having more molecular mass will move slowly, increasing the viscosity value; in this regard, D-lactose moieties have a higher viscosity values than the D-xylose molecules. Additionally, comparison graphs of the dynamic viscosity values of D-lactose [5] in an aqueous media with the available literature are shown in Figure 4.3.5 (a). This Figure demonstrates the improved congruence between data obtained through experiments and data from the literature. Nonetheless, changes in the experimental mode of performance and variances in the instruments themselves could be the cause of observed variations in cytosine comparison plots.

Moreover, Table 4.3.9 demonstrates that although solution viscosity reduces with temperature, it increases with molal concentration of cytosine. This may be due to the reason that stronger interactions amongst solute and cosolute moieties result in an augmentation in the frictional acceptance towards the molecular motions. Additionally, as temperature rises, the solution mixture's enlarged molecular movements cause the viscosity to decrease.

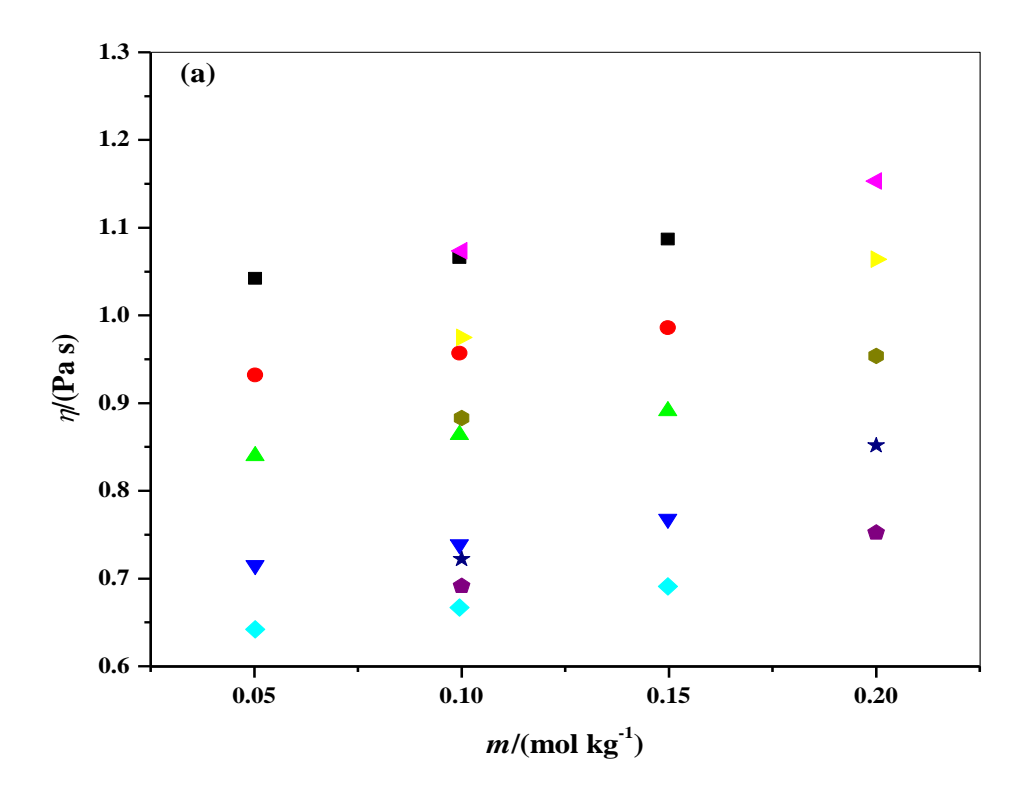


Figure 4.3.5: Graph representing comparison of measured viscosity data with the accessible reports at discrete T(K) for D-lactose in water. ■ : Conducted investigation on 293.15, • : Conducted investigation on 298.15, • : Conducted investigation on 303.15, • : Conducted investigation on 303.15, • : Lit. [5] on 293.15, • : Lit. [5] on 303.15, • : Lit. [5] on 303.15.

Table 4.3.9: Experimentally determined viscosities, η , and computed η_r values for cytosine in H₂O and H₂O + D-xylose/D-lactose media at diverse temperatures (K).

			$\eta \times 10^{\circ}$	³ (Pa s)				η_r		
m(mol/kg)						T(K)				
	293.15	298.15	303.15	308.15	313.15	293.15	298.15	303.15	308.15	313.15
		Cytosine + water								
0.0000	1.002	0.890	0.799	0.683	0.603					
0.0051	1.004	0.892	0.802	0.685	0.605	1.0020	1.0022	1.0025	1.0029	1.0033
0.0099	1.005	0.893	0.803	0.686	0.606	1.0030	1.0034	1.0037	1.0044	1.0050
0.0150	1.006	0.894	0.804	0.687	0.607	1.0040	1.0045	1.0050	1.0059	1.0066
0.0202	1.007	0.895	0.805	0.688	0.608	1.0050	1.0056	1.0062	1.0073	1.0083
0.0249	1.008	0.896	0.806	0.689	0.609	1.0060	1.0067	1.0075	1.0088	1.0099

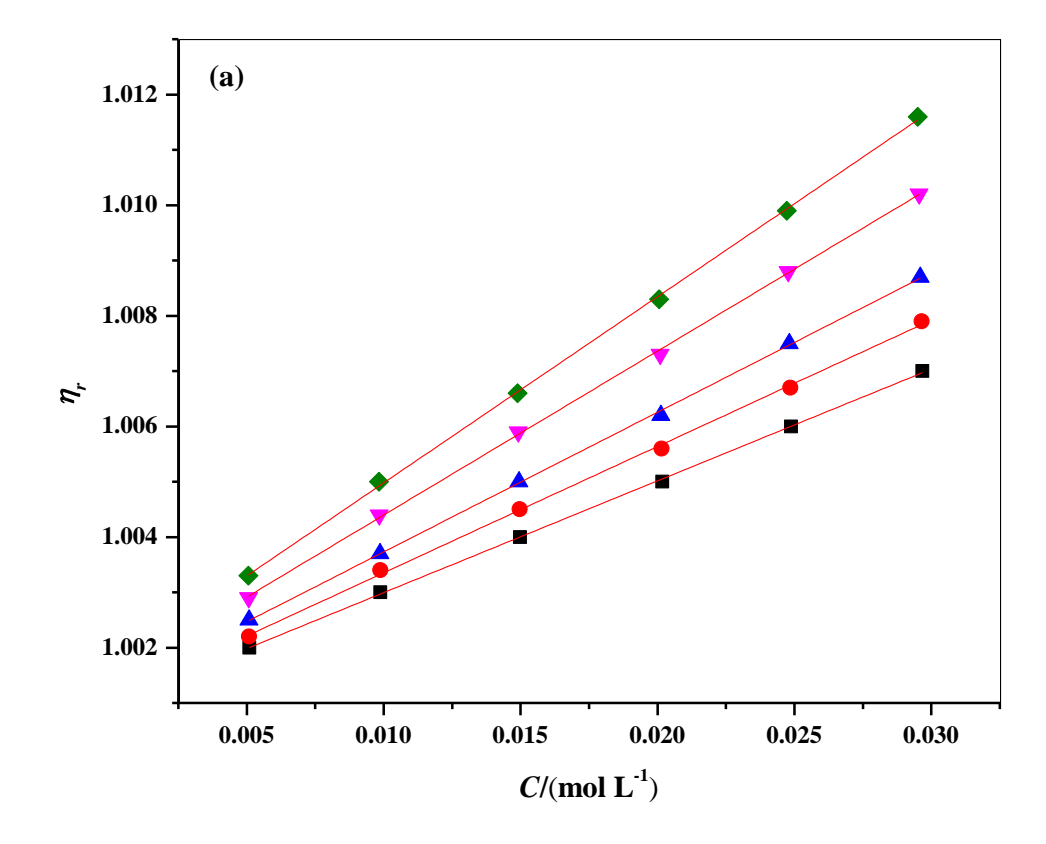
0.0297	1.009	0.897	0.807	0.690	0.610	1.0070	1.0079	1.0087	1.0102	1.0116
			Cy	tosine +	0.0497 n	nol/kg D-	xylose			
0.0000	1.021	0.911	0.821	0.691	0.620					
0.0051	1.024	0.914	0.824	0.694	0.623	1.0029	1.0033	1.0036	1.0043	1.0048
0.0100	1.026	0.916	0.826	0.696	0.625	1.0049	1.0055	1.0061	1.0072	1.0081
0.0152	1.029	0.919	0.829	0.699	0.628	1.0078	1.0087	1.0097	1.0116	1.0129
0.0199	1.031	0.921	0.831	0.701	0.630	1.0098	1.0110	1.0122	1.0145	1.0161
0.0250	1.034	0.924	0.834	0.704	0.633	1.0127	1.0143	1.0158	1.0188	1.0210
0.0298	1.036	0.926	0.837	0.706	0.635	1.0147	1.0165	1.0195	1.0217	1.0242
			Су	tosine +	0.0998 m	ol/kg D-	xylose			
0.0000	1.035	0.925	0.833	0.709	0.636					
0.0052	1.039	0.929	0.837	0.713	0.640	1.0039	1.0043	1.0048	1.0056	1.0063
0.0100	1.041	0.931	0.839	0.715	0.642	1.0058	1.0065	1.0072	1.0085	1.0094
0.0149	1.044	0.934	0.842	0.718	0.645	1.0087	1.0097	1.0108	1.0127	1.0141
0.0200	1.046	0.936	0.845	0.720	0.647	1.0106	1.0119	1.0144	1.0155	1.0173
0.0247	1.049	0.939	0.848	0.723	0.650	1.0135	1.0151	1.0180	1.0197	1.0220
0.0299	1.052	0.942	0.850	0.726	0.653	1.0164	1.0184	1.0204	1.0240	1.0267
			Су	tosine +	0.1504 n	nol/kg D-	xylose			
0.0000	1.047	0.936	0.845	0.720	0.648					
0.0051	1.052	0.941	0.850	0.725	0.653	1.0048	1.0053	1.0059	1.0069	1.0077
0.0101	1.055	0.944	0.853	0.728	0.656	1.0076	1.0085	1.0095	1.0111	1.0123
0.0151	1.058	0.947	0.856	0.731	0.659	1.0105	1.0117	1.0130	1.0153	1.017
0.0199	1.060	0.949	0.859	0.733	0.661	1.0124	1.0139	1.0166	1.0181	1.0201
0.0251	1.063	0.952	0.862	0.736	0.664	1.0153	1.0171	1.0201	1.0222	1.0247
0.0299	1.066	0.955	0.864	0.739	0.667	1.0181	1.0203	1.0224	1.0264	1.0293
			Су	tosine +	0.0502 m	ol/kg D-	lactose			
0.0000	1.041	0.931	0.840	0.714	0.641					
0.0053	1.045	0.935	0.844	0.718	0.645	1.0038	1.0043	1.0048	1.0056	1.0062
0.0102	1.048	0.938	0.847	0.721	0.648	1.0067	1.0075	1.0083	1.0098	1.0109
0.0153	1.051	0.941	0.850	0.724	0.651	1.0096	1.0107	1.0119	1.0140	1.0156
0.0201	1.054	0.944	0.853	0.726	0.653	1.0125	1.0130	1.0155	1.0168	1.0187

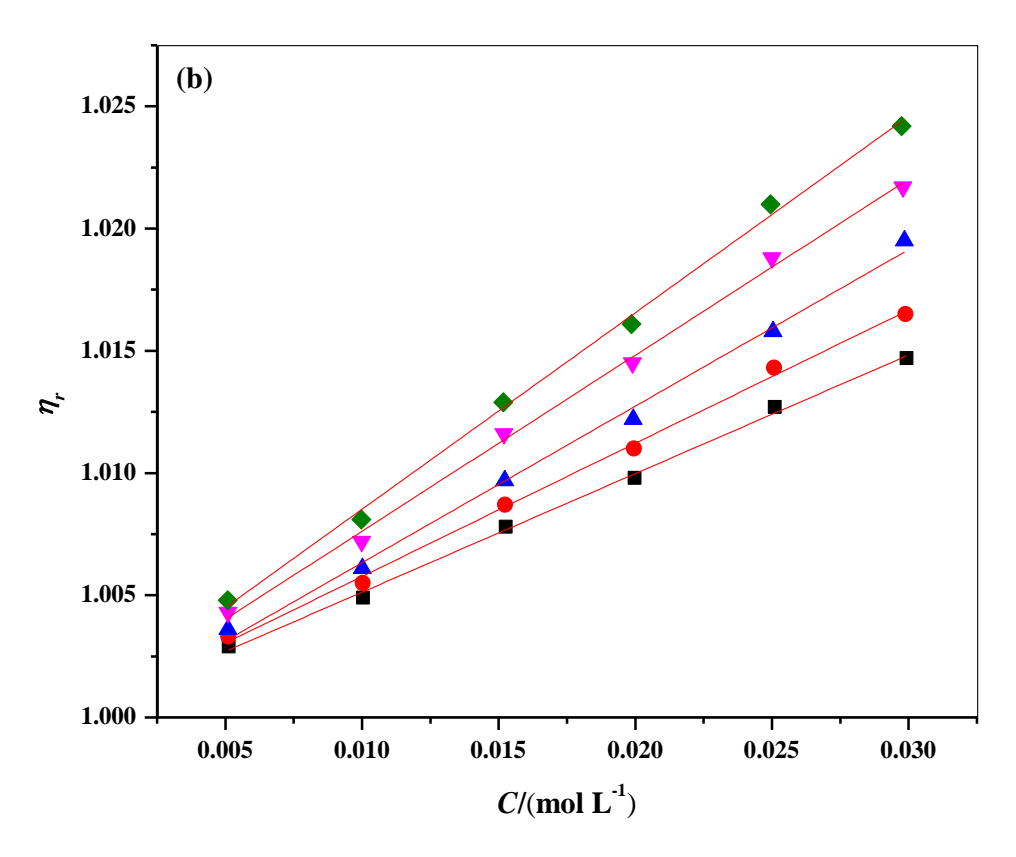
0.0247	1.057	0.947	0.856	0.729	0.656	1.0154	1.0172	1.0190	1.0210	1.0234
0.0298	1.060	0.950	0.859	0.732	0.659	1.0182	1.0204	1.0226	1.0252	1.0281
Cytosine + 0.0995 mol/kg D-lactose										
0.0000	1.066	0.957	0.864	0.739	0.670					
0.0054	1.071	0.962	0.869	0.744	0.675	1.0047	1.0052	1.0058	1.0068	1.0075
0.0100	1.074	0.965	0.872	0.747	0.678	1.0075	1.0084	1.0093	1.0108	1.0119
0.0152	1.077	0.968	0.875	0.750	0.681	1.0103	1.0115	1.0127	1.0149	1.0164
0.0192	1.080	0.971	0.878	0.752	0.683	1.0131	1.0146	1.0162	1.0176	1.0194
0.0249	1.084	0.975	0.882	0.756	0.687	1.0169	1.0188	1.0208	1.0230	1.0254
0.0300	1.087	0.978	0.885	0.759	0.630	1.0197	1.0219	1.0243	1.0271	1.0298
			Су	tosine +	0.1498 m	ol/kg D-l	lactose			
0.0000	1.086	0.984	0.886	0.767	0.690					
0.0051	1.092	0.990	0.892	0.773	0.696	1.0055	1.0061	1.0068	1.0078	1.0087
0.0101	1.095	0.993	0.895	0.776	0.699	1.0083	1.0091	1.0102	1.0117	1.0130
0.0150	1.099	0.997	0.899	0.780	0.703	1.0120	1.0132	1.0147	1.0169	1.0188
0.0200	1.102	0.100	0.902	0.783	0.706	1.0147	1.0163	1.0181	1.0209	1.0232
0.0250	1.106	1.004	0.906	0.786	0.709	1.0184	1.0203	1.0226	1.0248	1.0275
0.0298	1.109	1.007	0.909	0.789	0.712	1.0212	1.0234	1.0260	1.0287	1.0319

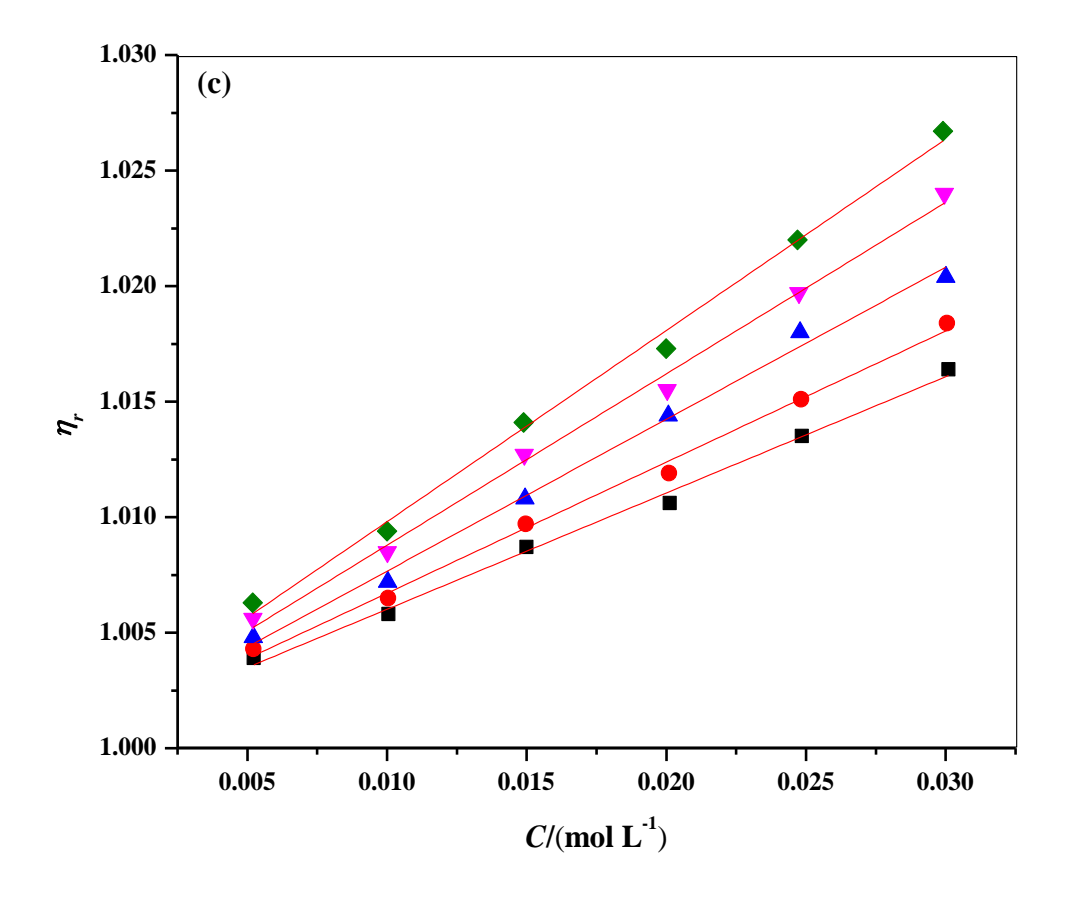
m(mol/kg) stands for the assessed molality for assorted solutions pertaining to cytosine in (water + D-xylose/D-lactose).

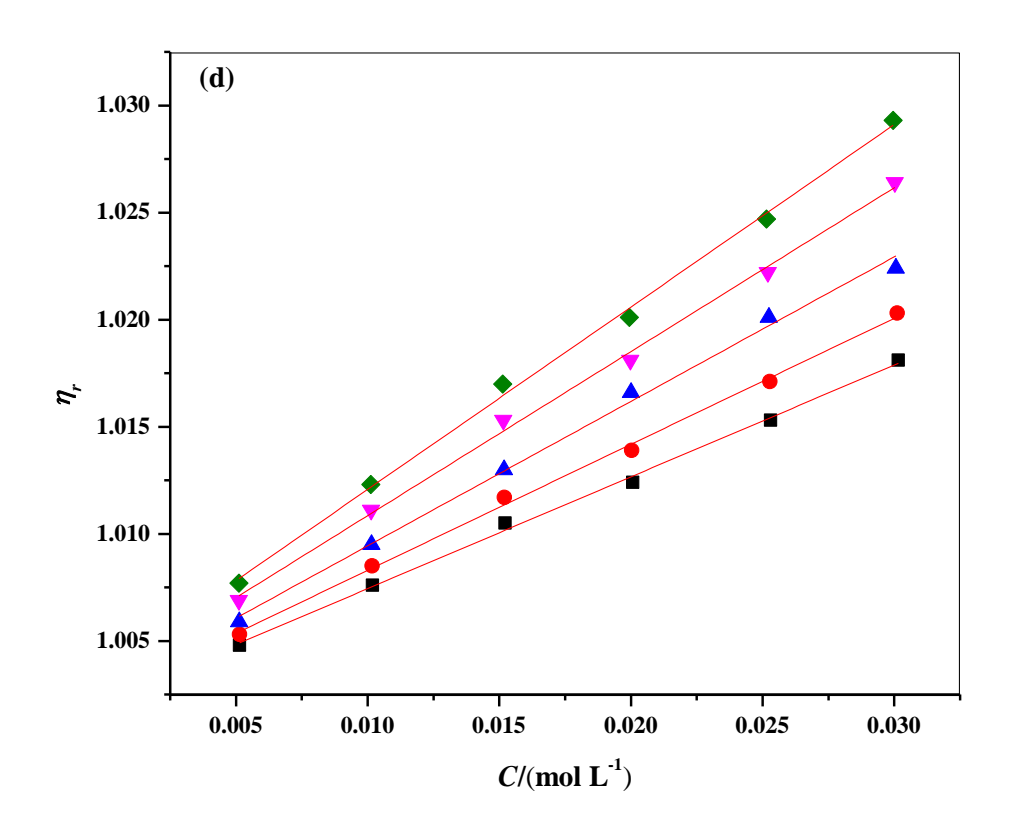
4.3.3.1 Viscosity coefficient

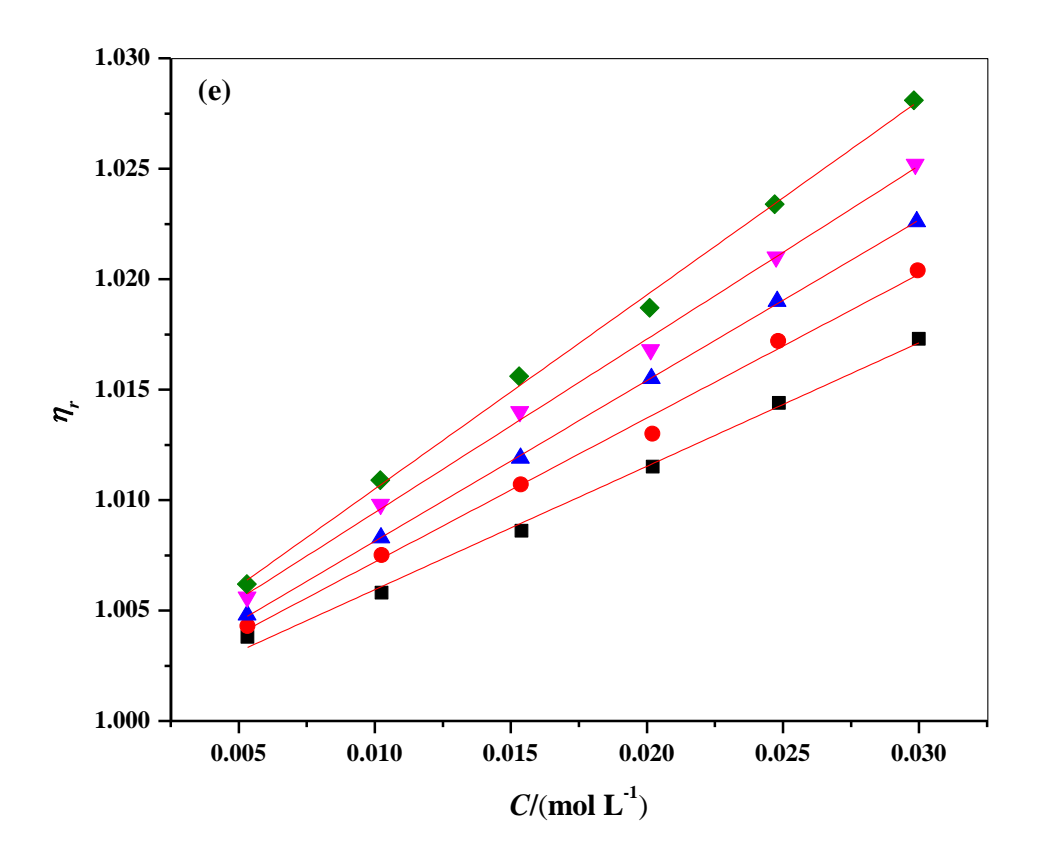
Also, the empirical viscosities of all the prepared sample solutions are related to the consequent molalities in harmony with Jones-Dole Eqn. (2.23) [31,32]. Figure 4.3.6 [(a)-(g)] signifies the graphs of η_r (relative viscosity) versus molarity, C of cytosine in binary and ternary systems. Further, Table 4.3.10 displays the stated data of B-coefficients together with corresponding standard deviations. In the selected systems, this increase in the B-coefficient indicates the intensification of solute-cosolute synergies with temperature. Also, a greater number of hydrophilic sites in D-lactose molecules might be liable for the advanced B-coefficient values pertaining to cytosine in aqueous D-lactose compared to aqueous D-xylose solutions. As a result, the data acquired by analysing viscosity coefficients agrees better with the volumetric and acoustic data.

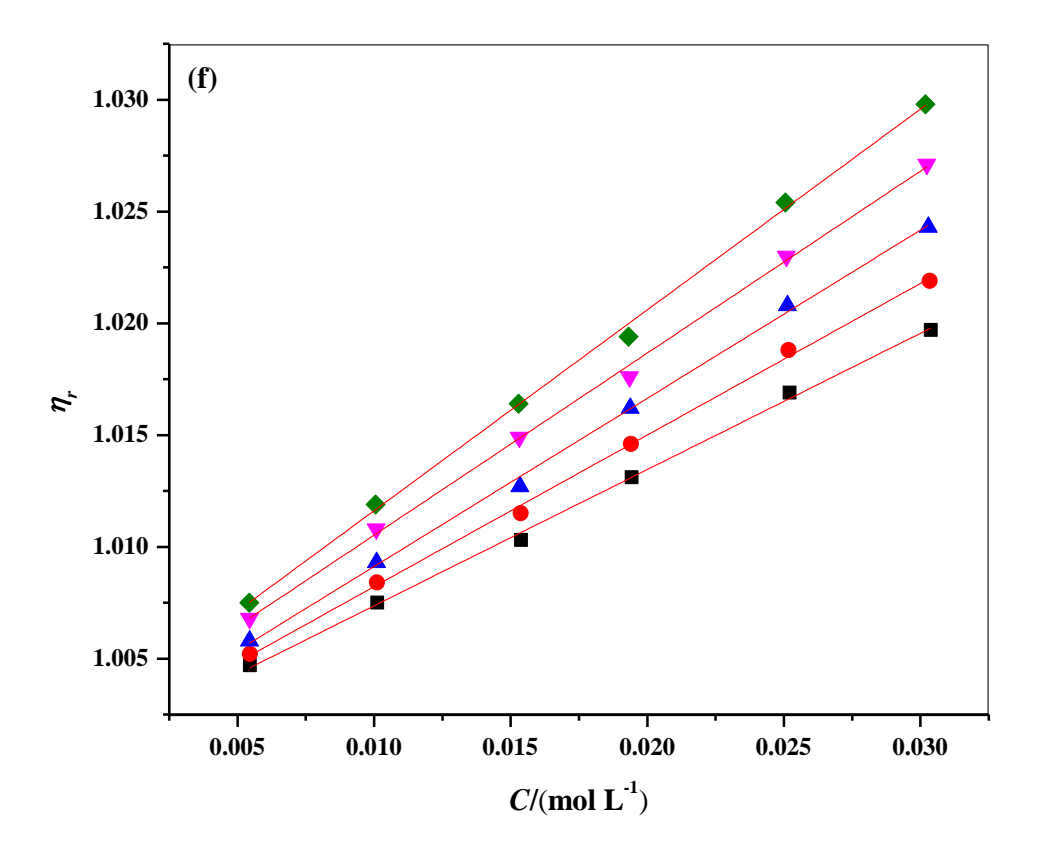












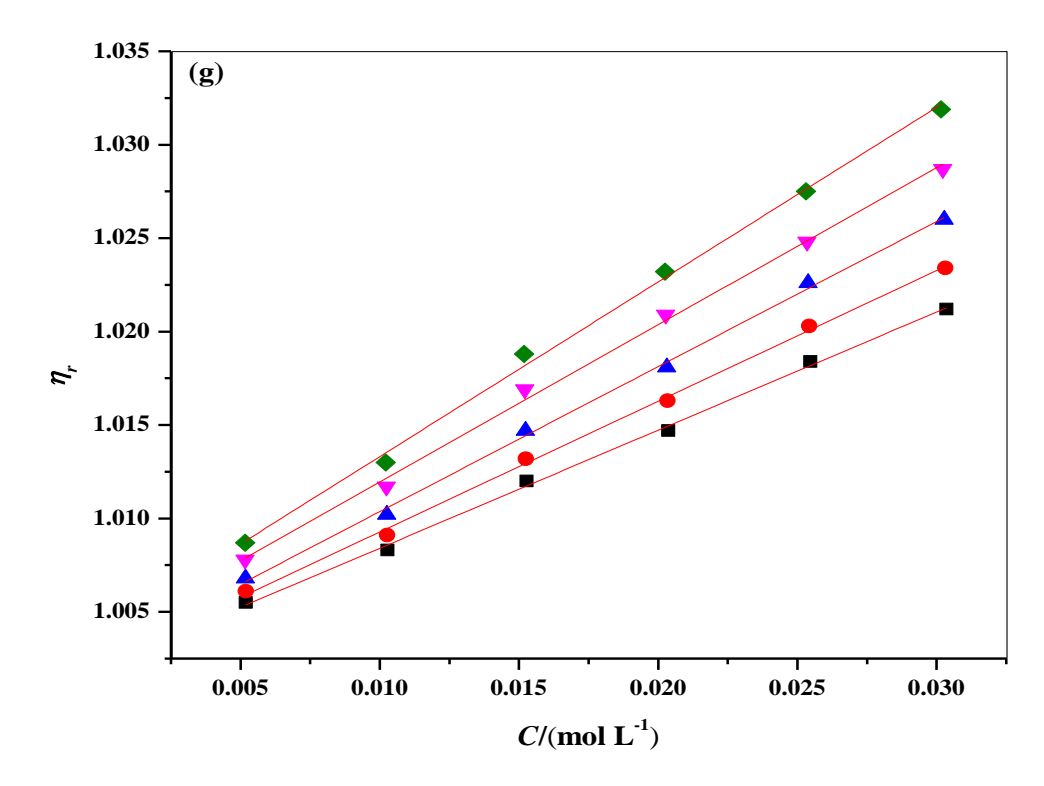


Figure 4.3.6: Graphs of $η_r$ against concentration, $C/(\text{mol L}^{-1})$ for diverse mixtures (a) cytosine + H₂O, (b) cytosine + 0.05 mol/kg D-xylose, (c) cytosine + 0.10 mol/kg D-xylose, (d) cytosine + 0.15 mol/kg D-xylose, (e) cytosine + 0.05 mol/kg D-lactose, (f) cytosine + 0.10 mol/kg D-lactose, (g) cytosine + 0.15 mol/kg D-lactose at discrete temperatures, ■ : 293.15 K, ● : 298.15 K, ▲ : 303.15 K, ▼ : 308.15 K, ♠ : 313.15 K.

Table 4.3.10: Deduced data of dB/dT for cytosine in H₂O and water + D-xylose/D-lactose mixtures at assorted temperatures.

System	dB/dT values
Cytosine + water	0.0067
Cytosine + 0.04970 mol/kg D-xylose	0.0162
Cytosine + 0.09980 mol/kg D-xylose	0.0165
Cytosine + 0.15040 mol/kg D-xylose	0.0167
Cytosine + 0.05020 mol/kg D-lactose	0.0154
Cytosine + 0.09950 mol/kg D-lactose	0.0143
Cytosine + 0.14980 mol/kg D-lactose	0.0150

Furthermore, via the sign of dB/dT, we can categorize the solutes as structure breakers/makers. Those solutes which have positive sign of dB/dT values are exemplified as structure breakers whereas the solutes harboring negative sign of dB/dT values are

embodied as structure makers [33,34]. Table 4.3.11 represents the evaluated dB/dT values in which the positive sign of cytosine in H₂O as well as aqueous D-xylose and D-lactose solutions reveal its structure-breaking ability. As a result, dB/dT results are supporting the information haggard from Hepler's constant analysis, presented in Table 4.3.4.

4.3.3.2 Viscosity B-coefficient of Transfer

For cytosine, the Jones–Dole *B*-coefficient of transfer has been obtained via subtraction of *B*-coefficient values in H₂O from *B*-coefficient values in aqueous D-xylose/D-lactose solutions as per the relation (2.24). The deduced $\Delta_{tr}B$ values for all the investigated systems are exemplified in Table 4.3.10. The investigation of Table 4.3.10 displays that $\Delta_{tr}B$ values augment with the rise in the concentration of aqueous D-xylose/D-lactose media. Hence, revealing the sovereignty of dipole-dipole interactions amid cytosine and saccharide molecules [35-37].

Table 4.3.11: Deduced data of graphically manifested B coefficients as well as corresponding transfer values $\Delta_{tr}B$ for cytosine in H₂O and water + D-xylose/D-lactose mixtures.

Graphical property	T(K)				
	293.15	298.15	303.15	308.15	313.15
		Cytosine +	water		
$B \times 10^3 (\text{m}^3/\text{mol})$	0.202(±0.002)	0.228(±0.003)	0.252(±0.002)	0.296(±0.003)	0.336(±0.003)
	Cyto	sine + 0.0497 m	ol/kg D-xylose		
$B \times 10^3 (\text{m}^3/\text{mol})$	0.485(±0.003)	0.545(±0.002)	0.640(±0.004)	0.720(±0.003)	0.804(±0.004)
$\Delta_{tr}B \times 10^3 (\text{m}^3/\text{mol})$	0.283	0.317	0.388	0.424	0.467
	Cyto	sine + 0.0998 m	ol/kg D-xylose		
$B \times 10^3 (\text{m}^3/\text{mol})$	0.503(±0.017)	0.567(±0.018)	0.657(±0.023)	0.742(±0.024)	0.828(±0.027)
$\Delta_{tr}B \times 10^3 (\text{m}^3/\text{mol})$	0.301	0.339	0.405	0.446	0.492
	Cyto	sine + 0.1504 m	ol/kg D-xylose		
$B \times 10^3 (\text{m}^3/\text{mol})$	0.522(±0.012)	0.588(±0.013)	0.675(±0.020)	0.766(±0.019)	0.852(±0.020)
$\Delta_{tr}B \times 10^3 (\text{m}^3/\text{mol})$	0.320	0.360	0.422	0.469	0.515

-					
	Cyto	sine + 0.0502 m	ol/kg D-lactose		
$B \times 10^3 (\text{m}^3/\text{mol})$	0.559(±0.017)	0.651(±0.023)	0.727(±0.004)	0.785(±0.019)	0.879(±0.021)
$\Delta_{tr}B \times 10^3 (\mathrm{m}^3/\mathrm{mol})$	0.357	0.423	0.475	0.489	0.542
	Cytosine + 0.0995 mol/kg D-lactose				
$B \times 10^3 (\text{m}^3/\text{mol})$	0.609(±0.011)	0.678(±0.012)	0.752(±0.013)	0.814(±0.015)	0.898(±0.016)
$\Delta_{tr}B \times 10^3 (\mathrm{m}^3/\mathrm{mol})$	0.407	0.450	0.500	0.518	0.562
	Cyto	osine+ 0.1498 mo	ol/kg D-lactose		
$B \times 10^3 (\text{m}^3/\text{mol})$	0.632(±0.013)	0.699(±0.014)	0.776(±0.015)	0.841(±0.020)	0.935(±0.022)
$\Delta_{tr}B \times 10^3 (\text{m}^3/\text{mol})$	0.430	0.471	0.524	0.545	0.598

4.3.4 Thermodynamic Properties of Viscous Motion

By utilising activated complex theory of Eyring and coworkers [38], the chemical potential or in other words, the Gibb's free energy of activation per mole for solute is demarcated for cytosine in H₂O and assorted molalities of D-xylose/D-lactose media. Consequently, chemical potential of D-xylose/D-lactose are figured at eclectic temperature values via expression (2.25). Likewise, chemical potential of cytosine is summed utilizing thermodynamic expression (2.27), by Feakin's *et al.* [39]. Essentially, $\Delta \mu^{0}_{2}$ gives criterion for divergence in the chemical potential of solute particles in immediacy of selected solvent system as well as additional free energy differences appearing as a consequence of vibrations of solute molecules. In the Conducted examination, the anticipated data of $\Delta \mu^{0}_{1}$ and $\Delta \mu^{0}_{2}$ is positive for all the studied systems of cytosine in contrasting aqueous solvent media at all the investigational temperatures [40].

In addition, the $\Delta\mu^0_2$ values are rising with the upsurge in temperature for all explored systems of cytosine. As per model of Feakin's theory, positive in addition to advancing $\Delta\mu^0_2$ values demonstrates the innovation of the transition state is feeble for cytosine in xylose as well as D-lactose at diverse temperatures. Likewise, the inference of entropy as well as enthalpy of activation is accomplished for all desired solution systems by employing eqns. (2.28) and (2.29). Besides, ΔH^0_2 data are encountered to have a superior magnitude than $T\Delta S^0_2$ (in Table the 4.3.12) thus exemplifying the preponderance of cogent interactions among cytosine and prepared D-xylose/D-lactose media in ground state

Table 4.3.12: Data of chemical potential, entropy and enthalpy of activation for cytosine in water and aqueous D-xylose/D-lactose media at T = 293.15 K - 313.15 K.

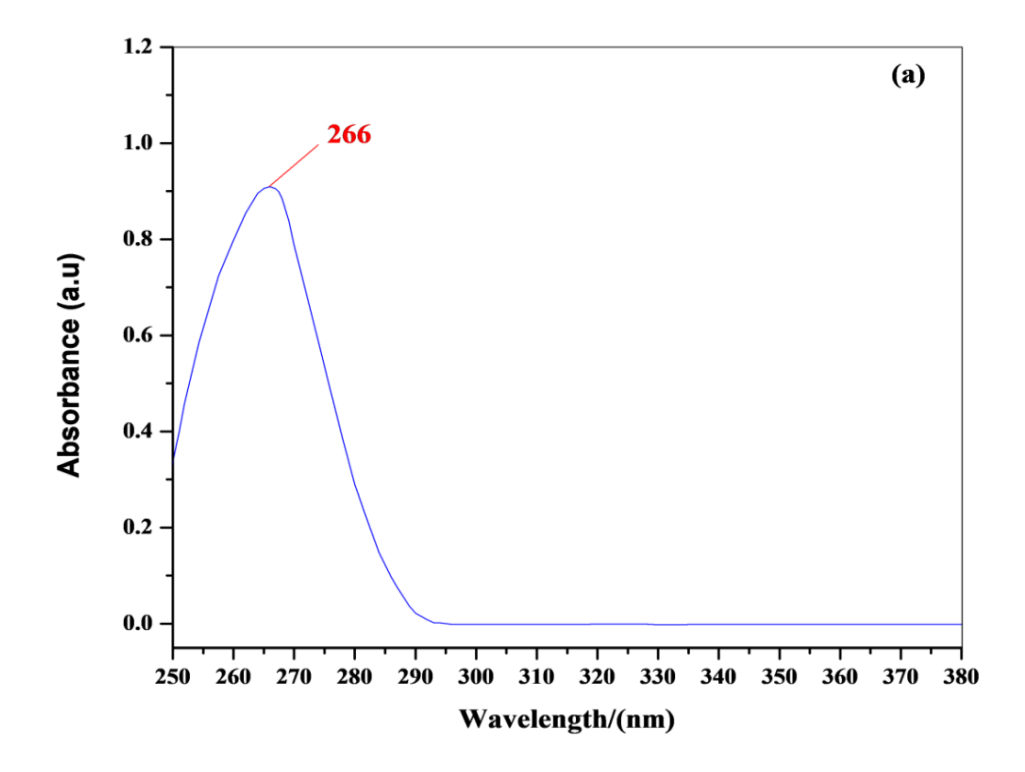
			T(K)		
Deduced property	293.15	298.15	303.15	308.15	313.15
		Cytosine	+ water		
$\Delta \mu^{\theta_I}$ (kJ/mol)	9.30	9.17	9.06	8.81	8.63
$\Delta \mu^{\theta_2}$ (kJ/mol)	44.01	48.14	52.13	58.85	65.30
$T\Delta S^{\theta_2}(\mathbf{kJ/mol})$	312.44	317.77	323.10	328.43	333.76
ΔH^{0}_{2} (kJ/mol)	356.45	365.91	375.23	387.28	399.06
	Cyto	sine + 0.04970	mol/kg D-xylo	ose	
$\Delta \mu^{\theta}_{I}$ (kJ/mol)	9.34	9.22	9.12	8.83	8.70
$\Delta \mu^{\theta_2}$ (kJ/mol)	82.53	91.87	106.44	119.02	132.63
$T\Delta S^{\theta}_{2}\left(\mathbf{kJ/mol}\right)$	746.65	759.39	772.12	784.86	797.59
ΔH^{0}_{2} (kJ/mol)	829.18	851.26	878.56	903.88	930.22
	Cyto	sine + 0.09980	mol/kg D-xylo	ose	
$\Delta \mu^{\theta_I}$ (kJ/mol)	9.39	9.27	9.17	8.91	8.78
$\Delta \mu^{\theta}_{2} (kJ/mol)$	84.88	94.95	108.77	122.05	136.10
$T\Delta S^{\theta}_{2}$ (kJ/mol)	759.49	772.45	785.40	798.36	811.31
ΔH^{0}_{2} (kJ/mol)	844.37	867.40	894.17	920.41	947.41
	Cyto	sine + 0.15040	mol/kg D-xylo	ose	
$\Delta \mu^{\theta_I}$ (kJ/mol)	9.43	9.27	9.17	8.91	8.78
$\Delta \mu^{\theta_2}$ (kJ/mol)	87.44	94.95	108.77	122.05	82.30
$T\Delta S^{\theta_2}(\mathbf{kJ/mol})$	766.18	772.45	785.40	798.36	429.43
ΔH^0_2 (kJ/mol)	844.37	867.40	894.17	920.41	511.74
	Cytos	sine + 0.05020	mol/kg D-lact	ose	
$\Delta \mu^{\theta_I}$ (kJ/mol)	9.43	9.29	9.14	9.02	8.91
$\Delta \mu^{\theta_2}$ (kJ/mol)	54.17	60.45	66.41	73.88	81.76
$T\Delta S^{\theta}_{2}\left(\mathbf{kJ/mol}\right)$	348.17	354.11	360.05	365.99	371.93
ΔH^{0}_{2} (kJ/mol)	402.34	141.59	426.47	439.87	453.69
	Cytos	sine + 0.09950	mol/kg D-lact	ose	
$\Delta \mu^{\theta_I}$ (kJ/mol)	9.55	9.43	9.28	9.16	9.05
$\Delta \mu^{\theta_2}$ (kJ/mol)	54.07	60.64	67.51	73.91	81.66
$T\Delta S^{\theta_2}(\mathbf{kJ/mol})$	347.57	353.50	359.42	365.35	371.28
$\Delta H^{\theta_2}(\text{kJ/mol})$	401.64	414.13	426.93	439.32	452.94

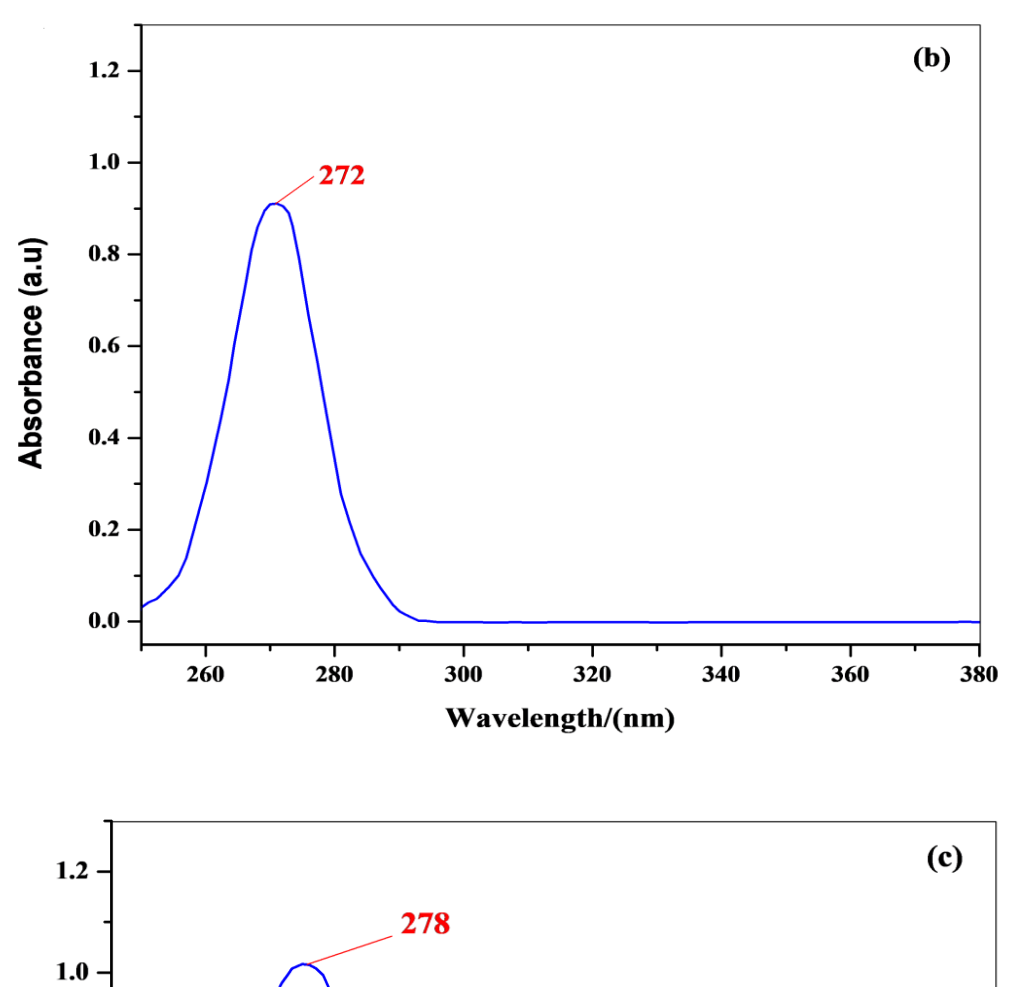
Cytosine + 0.14980 mol/kg D-lactose					
$\Delta \mu^{\theta_I}(kJ/mol)$	9.68	9.56	9.42	9.30	9.18
$\Delta\mu^{\theta_2}$ (kJ/mol)	54.19	60.86	67.31	73.95	81.41
$T\Delta S^{\theta}_{2}$ (kJ/mol)	341.58	347.40	353.23	359.06	364.88
ΔH^{0}_{2} (kJ/mol)	395.77	408.26	420.54	433.01	446.29

4.3.5 UV Absorption Studies

A UV-visible spectrophotometer (LAMBDA 1050+) was used to record the absorptions corresponding to cytosine in water besides 0.15 mol/kg of water + D-xylose and D-lactose solutions. By maintaining the range of wavelength from 200 nm to 400 nm and utilising quartz cuvettes with a 1 cm path length, the UV spectra of all the produced samples were inferred.

The acquired absorbances versus wavelength charts are demonstrated in Figure 4.3.6. In this Figure 4.3.6 (a) indicates that the absorption band of cytosine in water emerges at 266 nm, whereas (b) shows that the absorption band of cytosine in 0.15 mol/kg aqueous D-xylose appears at 272 nm. Also, in Figure 4.3.6 (c) i.e. for cytosine in 0.15 mol/kg aqueous D-lactose, the absorption band appears at 278 nm.





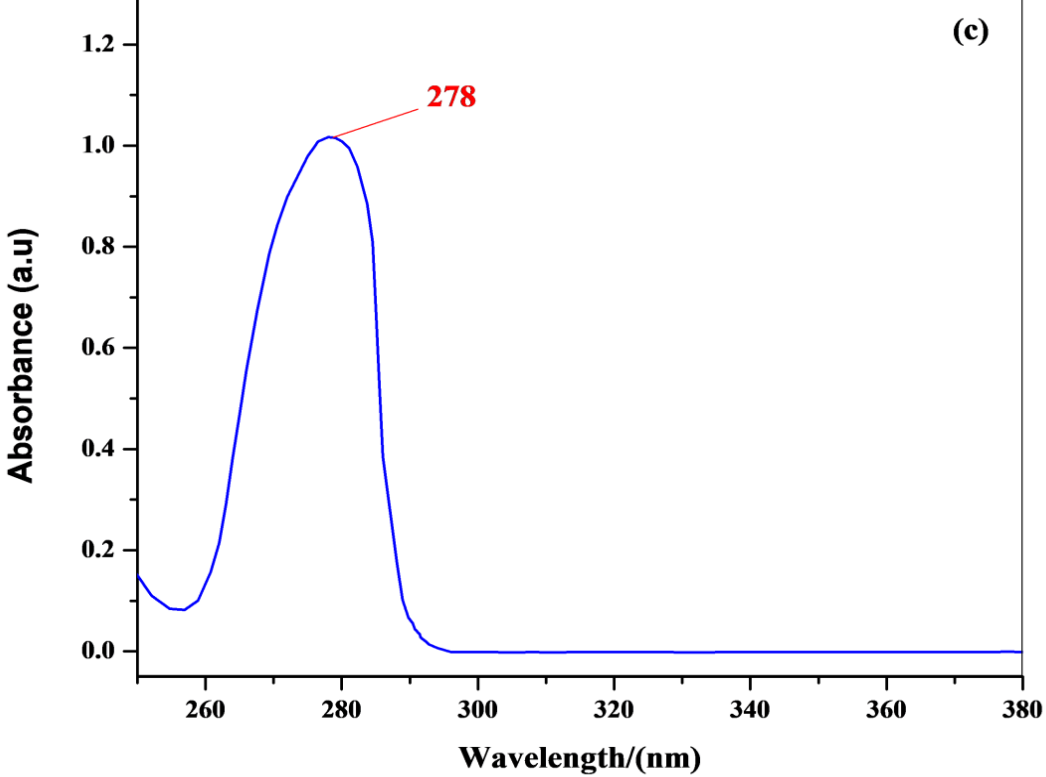


Figure 4.3.7: Plots of absorbance versus wavelength for peculiar systems (a) cytosine + H₂O, (b) cytosine + 0.15 mol/kg D-xylose and (c) cytosine + 0.15 mol/kg D-lactose.

As a result, the bathochromic shift in absorption maxima of cytosine from 266 nm (in water) to 272 nm (in 0.15 mol/kg aqueous D-xylose) takes place. In addition, bathochromic shift of the absorption maxima of cytosine from 266 nm (in water) to 278 nm (0.15 mol/kg aqueous D-lactose) occurs. This shows that cytosine has significant hydrophilic-hydrophilic interactions with aqueous D-xylose and D-lactose solutions, stabilizing the agitated state supplementary to the ground state. It results in the decrease of energy difference linking the ground as well as excited states, and thus band moves in the direction of the longer wavelength. Thus, the amplification in hydrophilic-hydrophilic interactions amid the systems under incorporation is clearly demonstrated by the measurement of the UV-vis spectra of cytosine in water and $H_2O + D$ -xylose/D-lactose media.

REFERENCES

- 1. Richu, Kumar, A. (2020). Apparent molar volume, isentropic compressibilities, viscosity *B*-coefficients and activation parameters of thiamine hydrochloride in aqueous solutions of saccharides at different temperatures. *The Journal of Chemical Thermodynamics*, 150, 106228.
- 2. Banipal, T. S., Kaur, N., & Banipal, P. K. (2015). Volumetric studies on nucleic acid bases and nucleosides in aqueous guanidine hydrochloride solutions at T = (288.15 to 318.15) K and at atmospheric pressure. *The Journal of Chemical Thermodynamics*, 82, 12-24.
- 3. Nain, A. K. (2020). Study on the interactions of drug isoniazid in aqueous-D-xylose/L-arabinose solutions at different temperatures using volumetric, acoustic and viscometric approaches. *Journal of Molecular Liquids*, 298, 112086.
- 4. Nain, A. K., & Lather, M. (2015). Study of solute–solute and solute–solvent interactions of L-serine in D-D-xylose/L-arabinose + water solutions using volumetric, ultrasonic and viscometric methods at different temperatures. *Physics and Chemistry of Liquids*, *53*, 599-618.
- 5. Rani, R., Kumar, A., & Bamezai, R. K. (2017). Effect of glucose/D-lactose on the solution thermodynamics of thiamine hydrochloride in aqueous solutions at different temperatures. *Journal of Molecular Liquids*, 240, 642-655.
- 6. Majdan-Cegincara, R., Zafarani-Moattar, M. T., Shekaari, H., & Ghaffari, F. (2018). Effect of fruit and milk sugars on solute–solvent interactions of diphenhydramine-hydrochloride drug in aqueous solutions in viewpoint of volumetric and transport properties. The Journal of Chemical Thermodynamics, 119, 44-60.
- 7. Richu, & Kumar, A. (2021). A comprehensive study on molecular interactions of L-ascorbic acid/nicotinic acid in aqueous [BMIm] Br at varying temperatures and compositions: spectroscopic and thermodynamic insights. *Journal of Chemical & Engineering Data*, 66, 3859-3880.

- 8. Richu, Bandral, A., Majid, Q., & Kumar, A. (2021). Investigations on volumetric, compressibility and viscometric properties of L-ascorbic acid and thiamine hydrochloride in aqueous 1-ethyl-3-methylimidazolium hydrogen sulfate solutions at different temperatures. *Journal of Molecular Liquids*, 339, 116833.
- 9. Sharmhal, A., Singh, H., Richu, Fatma, I., Sharma, P. K., Sharma, S., Kumar, A., & Kumar, A. (2023). Influence of carbohydrates on the volumetric, acoustic and viscometric properties of thymine in aqueous solutions at different temperatures. *Journal of Molecular Liquids*, 385, 122264.
- 10. Majid, Q., Richu, & Kumar, A. (2021). Effect of choline chloride and urea based deep eutectic solvent on the physicochemical properties of salicylic acid and salicylamide at T = (288.15 to 313.15) K. *Journal of Molecular Liquids*, 334, 116500.
- 11. Rajput, P., Singh, H., Bandral, A., Richu, Majid, Q., & Kumar, A. (2022). Explorations on thermophysical properties of nitrogenous bases (uracil/thymine) in aqueous L-histidine solutions at various temperatures. *Journal of Molecular Liquids*, 367, 120548.
- 12. Singh, H., Richu, Bandral, A., Majid, Q., & Kumar, A. (2023). Investigation of molecular interactions of streptomycin sulphate with aqueous L-aspartic acid through volumetric, ultrasonic and viscometric approach. *Journal of Molecular Liquids*, 382, 121885.
- Devi, S., Kumar, M., Sawhney, N., Syal, U., Sharma, A. K., & Sharma, M. (2021).
 Volumetric, acoustic and viscometric studies of L-histidine and L-serine in aqueous levofloxacin solutions at different temperatures and concentrations. *The Journal of Chemical Thermodynamics*, 154, 106321.
- Syal, U., Devi, S., Sharma, C., Kumar, M., Sawhney, N., Sharma, A. K., & Sharma,
 M. (2021). Physicochemical studies of L-valine and L-isoleucine in aqueous solutions of [Emim][HSO₄] at different temperatures. *Journal of Molecular Liquids*, 344, 117821.

- 15. Devi, S., Syal, U., Sharma, C., Kumar, M., Sawhney, N., Sharma, A. K., & Sharma, M. (2022). Volumetric, acoustic and viscometric studies of trilithium and triammonium citrate in aqueous solutions of [Emim][HSO₄] at different temperatures. *Journal of Molecular Liquids*, *354*, 118842.
- 16. Friedman, H. L., & Krishnan, C. V. (1973). Studies of hydrophobic bonding in aqueous alcohols: Enthalpy measurements and model calculations. *Journal of Solution Chemistry*, 2, 119-140.
- 17. Sharma, T., Kumar, A., Shah, S. S., & Bamezai, R. K. (2020). Analysis of interactions between streptomycin sulphate and aqueous food acids (L-ascorbic acid and citric acid): Physico-chemical and spectroscopic insights. *The Journal of Chemical Thermodynamics*, 151, 106207.
- 18. Kumar, D., Shah, S. S., Sharma, T., Singh, D., & Bamezai, R. K. (2022). Experimental assessment of physicochemical properties of L-phenylalanine and L-arginine in (water + 1-butyl-3-methylimidazolium bromide/tributylmethylammonium chloride) solutions at various temperatures. *Chemical Thermodynamics and Thermal Analysis*, 8, 100090.
- 19. Singh, M., Singh, J., Sharma, S., Sharma, S., & Sharma, M. (2023). Molecular interaction studies of an antidepressant drug with imidazolium-based ionic liquids in an aqueous system: A volumetric, acoustic, and viscometric approach. *Journal of Chemical & Engineering Data*, 68, 1834-1855.
- 20. Rani, R., Kumar, A., Sharma, T., Sharma, T., & Bamezai, R. K. (2019). Volumetric, acoustic and transport properties of ternary solutions of L-serine and L-arginine in aqueous solutions of thiamine hydrochloride at different temperatures. *The Journal of Chemical Thermodynamics*, 135, 260-277.
- 21. Hepler, L. G. (1969). Thermal expansion and structure in water and aqueous solutions. *Canadian Journal of Chemistry*, 47, 4613-4617.
- 22. Kumar, A., Rani, R., Saini, B., & Bamezai, R. K. (2017). Volumetric, compressibility, taste behavior and viscometric studies of methionine with some

- saccharides in aqueous medium at different temperatures. *Journal of Solution Chemistry*, 46, 931-956.
- 23. Kumar, A., Rani, R., Saini, B., & Bamezai, R. K. (2017). Thermophysical properties and taste behavior of L-serine/L-valine in aqueous glucose, sucrose and D-lactose solutions at different temperatures. *Journal of Molecular Liquids*, 241, 237-245.
- 24. Singh, H., Majid, Q., Richu, Singh, M., Kang, T. S., & Kumar, A. (2023). Explorations on solute–solvent interactions of tripotassium citrate and sodium benzoate in aqueous 1-ethyl-3-methylimidazolium ethyl sulfate solutions: Physicochemical, spectroscopic, and computational approaches. *Journal of Chemical & Engineering Data*, 68, 2563-2584.
- 25. Ghaffari, F., Shekaari, H., & Mousavi, F. (2025). Thermodynamic and Transport Properties of Lithium Bromide in Aqueous Solutions of Protic Ionic Liquids Based on 2-Hydroxyethylammonium Propionate at Different Temperatures. *Journal of Chemical & Engineering Data*, 70, 878-889.
- 26. Kumar, H., Singla, M., & Jindal, R. (2014). Investigations on solute–solvent interactions of amino acids in aqueous solutions of sodium dihydrogen phosphate at different temperatures. *Monatshefte für Chemie-Chemical Monthly*, 145, 1063-1082.
- 27. Frank, H. S., & Evans, M. W. (1945). Free volume and entropy in condensed systems III. Entropy in binary liquid mixtures; partial molal entropy in dilute solutions; structure and thermodynamics in aqueous electrolytes. *The Journal of Chemical Physics*, 13, 507-532.
- 28. Kirkwood, J. G. (1939). Theoretical studies upon dipolar ions. *Chemical Reviews*, 24, 233-251.
- 29. Millero, F. J., Lo Surdo, A., & Shin, C. (1978). The apparent molal volumes and adiabatic compressibilities of aqueous amino acids at 25. degree. C. *The Journal of Physical Chemistry*, 82, 784-792.

- 30. Sharma, S. K., Singh, G., Kumar, H., & Kataria, R. (2016). Effect of N-acetylglycine on volumetric and acoustic behaviour of aqueous tetrabutylammonium iodide solutions at different temperatures. *The Journal of Chemical Thermodynamics*, 96, 143-152.
- 31. Zhao, Z., Sun, Z., Lv, W., Sun, C., & Zhang, Z. (2024). Preparation of graphene/carbon nanotube-cellulose composites assisted by ionic liquids: A review. *International Journal of Biological Macromolecules*, 276, 133927.
- 32. Jones, G., & Dole, M. (1929). The viscosity of aqueous solutions of strong electrolytes with special reference to barium chloride. *Journal of the American Chemical Society*, *51*, 2950-2964.
- 33. Pradhan, R. K., & Singh, S. (2024). Exploring the effects of saccharides on the solvation behaviour of L-citrulline in aqueous medium: Volumetric, transition state theory, transfer parameters and spectroscopic approach. *Food Chemistry*, 452, 139554.
- 34. Sawhney, N., Kumar, M., Sharma, A. K., & Sharma, M. (2020). molecular interactions of non-steroid anti-inflammatory drug dolonex in aqueous solutions of L-alanine/L-valine at different temperatures: Viscometric approach. *Russian Journal of Physical Chemistry A*, *94*, 756-761.
- 35. Sharmhal, A., Richu, Singh, H., Sharma, P. K., Kumar, A., & Kumar, A. (2024). Physicochemical investigations on molecular interactions of adenine with aqueous D-glucose/D-maltose solvent media at varying temperatures and compositions. *The Journal of Chemical Thermodynamics*, 201, 107399.
- 36. Dhal, K., Singh, S., & Talukdar, M. (2022). Elucidation of molecular interactions of aspartic acid with aqueous potassium sorbate and sodium benzoate: Volumetric, viscometric and FTIR spectroscopic investigation. *Journal of Molecular Liquids*, 352, 118659.
- 37. Rajput, P., Singh, H., & Kumar, A. (2022). Volumetric, ultrasonic and viscometric behavior of nucleosides (uridine and cytidine) in aqueous L-ascorbic acid solutions

- at different temperatures. The Journal of Chemical Thermodynamics, 171, 106805.
- 38. Glasstone, S., Laidler, K. J., & Eyring, H. (1941). The theory of rate processes: the kinetics of chemical reactions, viscosity, diffusion and electrochemical phenomena. *McGraw-Hill Book Company*.
- 39. Feakins, D., Waghorne, W. E., & Lawrence, K. G. (1986). The viscosity and structure of solutions. Part 1.—A new theory of the Jones–Dole *B*-coefficient and the related activation parameters: application to aqueous solutions. *Journal of the Chemical Society, Faraday Transactions 1: Physical Chemistry in Condensed Phases*, 82, 563-568.
- 40. Sharma, T., Singh, H., Bamezai, R. K., & Kumar, A. (2022). Analysing the molecular interactions of ternary (D-lactose + water + tributylmethylammonium chloride) solutions at different temperatures via physicochemical methods. *Journal of Molecular Liquids*, 349, 118412.

CHAPTER 5 SUMMARY AND CONCLUSIONS

5 Summary

The complete summary and conclusions of volumetric, acoustic and viscometric analysis of nucleic acids in aqueous saccharides are included in this chapter.

5.1 Chapter 1

All the biological systems in this world are comprised of several lifeless substances that are existing in their cells in a very obscure but highly organized form, these are called biomolecules. Biomolecules encompass both large macromolecules and small molecules. Examples of macromolecules include proteins, nucleic acids, lipids, and carbohydrates, while small biomolecules include primary metabolites, natural products, and secondary metabolites. Most of the biological molecules are organic composites and only four elements: C, O, H and N make up 96% of the living body's weight. Various processes like morphogenesis, energy creation, hormonal activity, synthesis of plasma membranes, the transmission of biogenetic material etc. in the living systems are brought out by the biomolecules. So these are the substances that construct up the trunk of life in this world. Nucleic acids are vital biomolecules accountable for storing and passing on genetic information in all living beings. The two foremost kinds of nucleic acid bases are (i) RNA and (ii) DNA. These polymer groups are comprised of repeating units called as nucleotides, having a nitrogenous base, phosphate group, and pentose sugar.

Nucleic acids are assorted in nature having a dissimilar range of charged, polar and non-polar groups. DNA's double helical constitution is being equilibrated via the forces prevalent in it. It is well acknowledged that hydrogen bonding and stacking interactions amid purine/pyrimidine bases proffer noteworthy assistance to the conformational solidity of nucleic acids. Carbohydrates are referred to as hydrates of carbon that are sparingly solvable in organic solvents (except certain polysaccharides) and solvable in water. These are extensively allocated in plants as well as animals and normalize miscellaneous natal phenoms akin to signaling, cell transience transduction, provocative processes, cellular associations and stabilization of aboriginal compliance of proteins. Owing to charisma of –OH i.e. hydroxyl moieties in the saccharides, these attain attributes of hydration which is

of foremost applicability for the execution of glycolipids as well as glycoproteins in molecular recognition.

A comprehension of the forces that administer the conformational stability of polynucleotides is obligatory for the prophecy of the behavior of nucleic acids in mixtures. The formation of helices in nucleic acid strands is driven by the interactions of their nitrogenous bases. An understanding of the chemistry is unfeasible exclusive of an operational acquaintance of its elemental parts. Further, thermophysical examinations recreate a substantial part for apprehending the pinnacle as well as configurations of molecular relations which arise in water and furnish useful clues for construing varieties of interactions ubiquitous in assorted biochemical and physiological phenoms. The intermolecular forces operational amid moieties of solution play a key part in percepting the thermodynamic properties of mixtures. These forces (attractive/repulsive) are vital to discern the properties and constitution of liquids, gases, solids and stoutly cause the demeanour of a molecule in the environs of a different molecule. Consequently, an amalgamation of volumetric, ultrasonic and rheological studies is very valuable for the illumination of solute-solvent or solute-solute synergies. For that reason, learning of thermophysical characteristics of basic components of nucleic acids may possibly throw illumination on the nature of the interactions which preside over the conformational strength of nucleic acids in charisma of assorted carbohydrates. In addition, effect of assorted carbohydrates on the aqueous mixtures of the studied solutes at diverse temperatures as well as molalities has been streamlined in terms of diverse connections happening in the mixtures.

Thermophysical characteristics like V_{ϕ} , E^{0}_{ϕ} and $K_{\phi,s}$ besides transport properties have been employed to study different sorts of ionic and molecular interactions existing in the solution systems. In this study, both solute/solute along with solute/solvent interactions of nitrogeneous bases in aqua along with mixed aqueous systems of carbohydrates have been examined via volumetric, compressibility and viscometric approach.

5.2 Chapter 2

This chapter starts with the detailed literature review for the systems of study. It focuses on the examination of densimetric, ultrasonic, and rheological effects of mixtures (liquids). For divergent moieties comprising the solution either in equivalent phase or manifold phase, the synergies present amid them are of enormous apprehension in mixtures (binary/ternary). The thermodynamic examination plays a crucial part for percepting the nature as well as level of molecular aggregation that take place in these mixtures. The characteristics of the mixtures (mainly liquids) depend upon its bordering constitution that is in twist reliant on the forces prevalent amid the moieties and their structural types as well as size of molecules. As soon as the concentration of a mixture modifies, then there is amendment in the narrow constitution of molecules that consequences in modification of thermodynamic properties of that combination. Consequently, on mixing two moieties, the properties of untainted moieties are surpassed by radically vital partial molar quantities. For this reason, it is significant to comprehend these properties with the purpose of envisaging the diverse interactions in attendance amongst the assorted components of solution. Furthermore, the alterations taking place in thermodynamic quantities commencing unmixed to mixed state can further be scrutinized to surmise about the structural alterations taking place in former even as shifting to afterward state. Volumetric properties are deemed as a perceptive means in premeditating the assorted interactions widespread in the solution. The investigational density values are in turn applied to analyze noteworthy parameters at diverse temperatures along with concentrations of solvent as well as solute that facilitates to illuminate the interactions accessible in the mixtures. Also, ultrasonic techniques are highly beneficial and versatile as they can effectively analyze residual stress, hardness, microstructure, and other properties. Parameters acquired via speed of sound, such as compressibility, are sensitive indicators that can quickly provide information about molecular interactions when partial molar volume is unable to yield conclusive result. Further, studying the viscous behavior of molecules in a solution is crucial for understanding transport processes. Research suggests that the viscometric property is a perceptive tool for identifying the type of molecular exchanges prevalent among the solutions. Viscosity, which can be observed in the liquid and gaseous states of matter, reveals the underlying microscopic interactions among the material's molecules.

The relationship between the solution's viscosity and solute concentration has shed light on important interactions taking place in the solution and its structure. Thus, the prophecy of intermolecular interactions in assorted solvent systems is solitary owing to the realistic relevance of assorted solvent systems. Hence, it is vital to examine and scrutinize the density, viscosity, sound speed along with their allied parameters for getting acquaintance of varied plausible synergies and their applications in diverse fields.

5.3 Chapter 3

This chapter deals with the instrumental features, the materials and the method employed for performing the research work. The compounds utilized for experimenting were of analytical reagent category and used as received. These compounds include thymine, adenine, cytosine, saccharides (D-xylose, D-glucose, D-maltose, sucrose and D-lactose). Before experimentation, the apparatus such as beakers, glass rods, volumetric flasks and watch glasses, etc were thoroughly cleaned using freshly prepared chromic acid and triply distilled water. An electrical balance (Mettler Toledo, ML204) having an uncertainty of ± 0.1 mg had been used for the explicit measurement of the weight of chemical compounds.

The saccharide stock solutions, as well as aqueous solutions of nitrogeneous bases, were prepared utilizing triply distilled degassed water. The uncertainties in the molal concentration of samples were examined to be $\pm 58 \times 10^{-4}$ mol/kg. Additionally, explicit assurance of densimetric values along with velocities of sound for all prepared mixtures was done through the Anton Paar DSA 5000 M. Also, accuracy of this device is ± 0.005 kg/m³ allocated to density and ± 0.5 m/s allocated to velocity of sound, consequently. Moreover, viscosity of samples was done through the micro viscometer attached to DSA. Further, the measured values of viscosity are correct upto $\pm 0.5\%$. Collected experimental data was plied to evaluate densimetric, ultrasonic along with rheological characteristics to arrive at logical conclusion.

5.4 Chapter **4.1**

One of the popular topics in science right now is the molecular modelling of the biomolecules combining experimental and theoretical data. This chapter deals with the physical-chemical analysis of thymine, a nitrogenous base, in aqua along with aqua glucose/sucrose media solutions at temperatures interval (293.15 K to 313.15) K. Physical properties (sound velocity, density and viscosity) that were deducted through experimentation were used to calculate a number of volumetric, acoustic, and transport characteristics, such as apparent molar volume (V_{ϕ}) , limiting apparent molar volume (V^{0}_{ϕ}) , hydration number (n_{H}) , limiting apparent molar expansivity (E^{0}_{ϕ}) , Hepler's constant $(\partial E^{0}_{\phi}/\partial T)_{P}$, apparent molar isentropic compression $(K_{\phi,s})$, limiting apparent molar isentropic compression $(K_{\phi,s})$, viscosity *B*-coefficients, transfer characteristics of solutions $(\Delta_{tr}V^{0}_{\phi}, \Delta_{tr}K^{0}_{\phi,s})$ and $(\Delta_{tr}B)$, hydration number (n_{H}) , and thermodynamic parameters of viscous motion $(\Delta\mu^{0}_{1}, \Delta\mu^{0}_{2}, T\Delta S^{0}_{2})$ and (ΔH^{0}_{2}) . Further, the enhancement in apparent molar volume, $(\Delta_{tr}V^{0})$ with escalating concentration can be accredited to rise in solute's vander Waals volume.

Apparent molar isentropic compression $(K_{\phi,s})$ was endowed to progress with temperature and molal concentration of saccharides. This increase in $K_{\phi,s}$ with ascending temperature and concentration (molal) of saccharides on account of increase in compressibility of bulk water. Moreover, the chaotropic character of thymine in aqueous media and aqueous saccharide solution media has been ascertained by applying the Hepler's thermodynamic relation and via dB/dT data.

Lastly, a number of inter-molecular connections prevalent in the structures under consideration have also been accessed using the overlap model of co-sphere. In the overlap model, hydrophilic interactions are dominant and widespread in the prepared systems. Outcomes received from study of assorted thermophysical properties forecast that in all solution systems, the solute-solvent interactions are advancing with intensifying temperatures and concentrations of saccharides. Ultimately, UV spectral analysis validated that strong dipole amid dipole synergies remain present pertaining to the peculiar systems under investigation.

5.5 Chapter **4.2**

In this chapter, the physicochemical characteristics (mainly volumetric, compressibility and rheological properties) of a nitrogenous base (adenine) have been

investigated in water and aqueous (0.05, 0.10 and 0.15) mol kg⁻¹ D-glucose/D-maltose solvent media at 293.15 K to 313.15 K and 0.1 MPa (investigational pressure). The experimentally determined physical properties for instance, density, sound velocity as well as viscosity have been implicated for the estimation of numerous parameters particularly apparent molar volume (V_{ϕ}), hydration number (n_H), limiting apparent molar volume (V_{ϕ}), Hepler's constant (2c), expansivity parameters (E_{ϕ}^0), ASV, compressibility of solution systems ($K_{\phi,s}$), viscosity B-coefficients, transfer parameters ($\Delta_{tr}V_{\phi}^0$, $\Delta_{tr}K_{\phi,s}^0$ and $\Delta_{tr}B$), and thermodynamic parameters of viscous surge ($\Delta\mu^0_I$, $\Delta\mu^0_I$, $\Delta\mu^0_I$, $\Delta\mu^0_I$). Further, the enhancement in apparent molar volume, V_{ϕ} with rising concentration can be attributed to the increasing vander Waals volume for solute. Apparent molar isentropic compression ($K_{\phi,s}$) was endowed to progress with temperature and concentration (molal) of saccharides. This increase in $K_{\phi,s}$ with the temperature and molality of saccharides is due to increase in compressibility of bulk water.

In addition, the Co-sphere overlap model has been implicated for the analysis of assorted feasible interactions effective in the primed systems. The received outcomes forecast that in all solution systems, the solute-solvent interactions are progressing with rising temperatures and concentrations of saccharides.

Furthermore, the structure breaking proclivity of adenine has been scrutinized via the abstraction of Hepler's constant data and positive values of dB/dT data for all the explored systems. Moreover, the inferred apparent specific volume data specify that adenine has a sweet taste in water and distinct concentrations of selected saccharides.

5.5 Chapter **4.3**

In this chapter, thermophysical properties of cytosine in aqua (0.05 - 0.15) mol kg⁻¹ D-xylose/D-lactose solutions have been investigated at discrete temperatures (293.15 to 313.15) K and experimental pressure (0.1 MPa). The experimentally determined physical properties such as density, velocity of sound, and viscosity have been utilized for the estimation of several parameters such as apparent molar volume (V_{ϕ}) , limiting apparent molar volume (V_{ϕ}) , hydration number (n_H) , limiting apparent molar expansivity (E_{ϕ}^0) , Hepler's constant $(\partial E_{\phi}^0)/\partial T)_P$, apparent specific volume (ASV), apparent molar isentropic

compression ($K_{\phi,s}$), limiting apparent molar isentropic compression ($K^0_{\phi,s}$), viscosity B-coefficients, transfer parameters and thermodynamic parameters of viscous flow ($\Delta\mu^0_I$, $\Delta\mu^0_2$, $T\Delta S^0_2$ and ΔH^0_2). Apparent molar isentropic compression ($K_{\phi,s}$) was endowed to progress with temperature and concentration (molal) of saccharides. This increase in $K_{\phi,s}$ with rising temperature and molalities of saccharides is for the reason of increase in compressibility of bulk water. Additionally, the Co-sphere overlap model has been utilized for the analysis of assorted probable interactions operating in the prepared systems. The received outcomes forecast that in all solution systems, the solute-solvent interactions are progressing with rising temperatures and concentrations of saccharides. Furthermore, the structure breaking proclivity of cytosine has been scrutinized via the abstraction of Hepler's constant data and positive values of dB/dT data for all the explored systems. Moreover, the inferred apparent specific volume data specify that cytosine has sweet taste in water and sweet-bitter taste in peculiar concentrations of D-xylose/D-lactose media.

5.7 Conclusions

This chapter has provided a detailed investigation into the volumetric, acoustic, and viscometric properties of nucleobases in aqueous saccharide media, offering valuable insights into solute—solvent interactions, molecular association, and structural effects induced by saccharides. The study highlights the crucial role of saccharide cosolvents in modulating the physicochemical behavior of biologically important molecules like nucleobases, which are the fundamental units of nucleic acids.

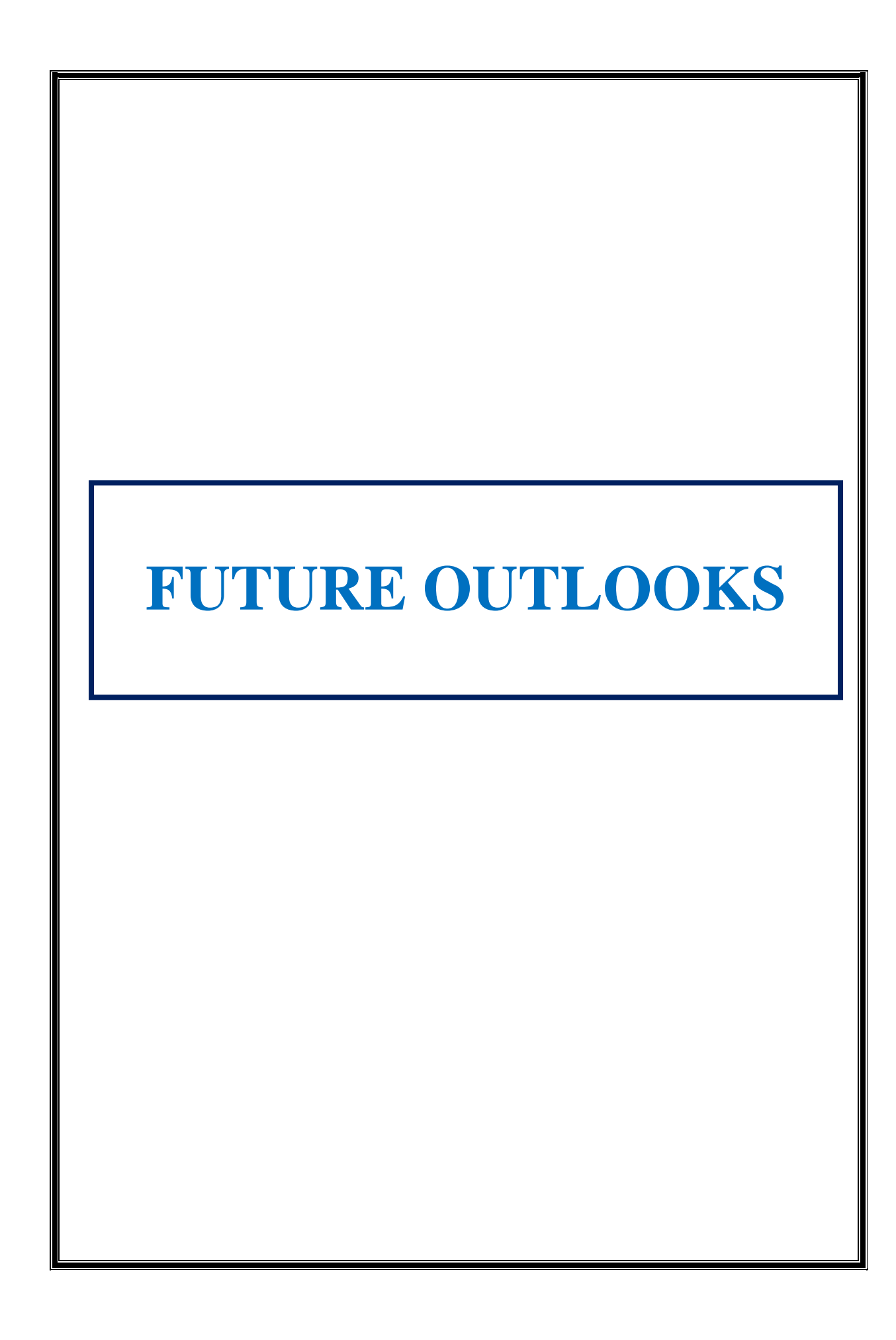
The findings hold notable implications in biotechnology, particularly in the design and optimization of biomolecular environments. For instance, the ability of saccharides to influence the solvation dynamics and stability of nucleobases can be directly applied in DNA/RNA preservation, gene therapy vectors, biocompatible drug delivery systems, and stabilization of nucleic acid-based biosensors. Such insights may also assist in the formulation of cryoprotectants and therapeutic media that enhance the longevity and efficacy of nucleic acid-based products.

Furthermore, this work contributes to a better understanding of solute-cosolvent interactions, which is essential for developing synthetic biological systems, enzymatic

reaction buffers, and nucleic acid storage media. These applications underscore the real-world relevance of the study in advancing molecular biotechnology and pharmaceutical formulations.

For future studies, it is proposed that exploring a broader range of nucleobases and saccharide types, including oligosaccharides and sugar alcohols, across varying temperature and pH conditions could provide a more comprehensive understanding of interaction patterns. Additionally, integrating spectroscopic techniques (e.g., NMR, FTIR) and molecular dynamics simulations may yield deeper insights into the interaction mechanisms at the molecular level. A comparative study involving ionic liquids or deep eutectic solvents alongside saccharide media may also uncover novel solvation environments for nucleobases.

In conclusion, this chapter provides a strong, structured closure reaffirming the significance of the study. It not only enhances our physicochemical understanding of nucleobases in biocompatible solvents but also lays the groundwork for future innovations in biotechnology and pharmaceutical sciences.



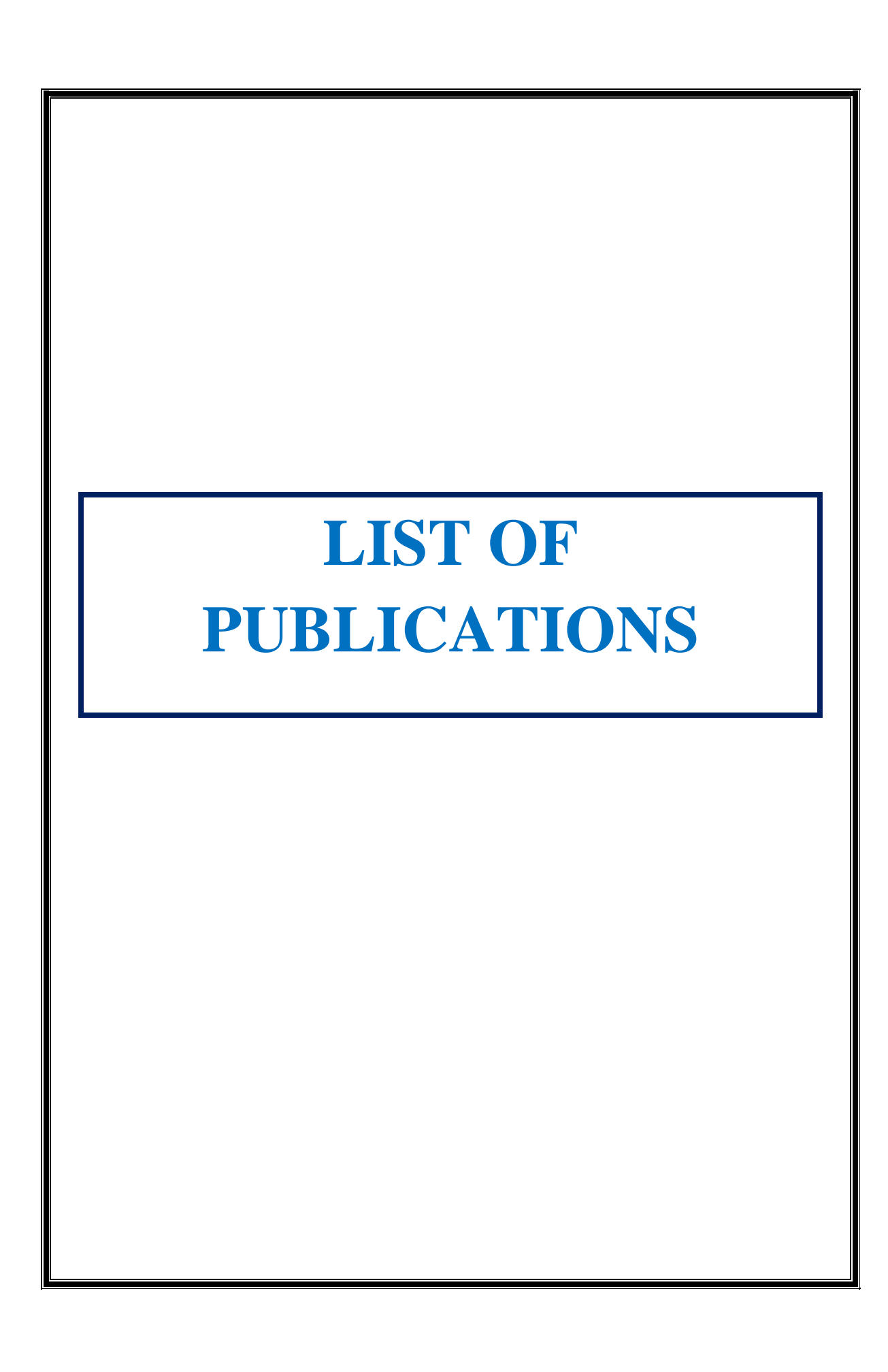
The intricate world of biomolecular interactions within aqueous solutions forms the foundation of numerous industrial and commercial applications. Specifically, the study of nucleic acid bases, the fundamental building blocks of DNA and RNA, in the presence of saccharides, versatile carbohydrates crucial for both biological and industrial processes, offers profound insights. Employing thermodynamic, ultrasonic, and transport studies to unravel these interactions is not merely an academic endeavor but a strategic imperative with significant commercial and industrial relevance.

The pharmaceutical sector stands as a primary beneficiary of these investigations. The burgeoning field of nucleic acid-based therapeutics, encompassing gene therapies, antisense oligonucleotides and siRNA, holds immense promise for treating a wide array of diseases. However, the inherent instability, poor solubility, and limited cellular uptake of these molecules pose significant challenges. Saccharides, with their biocompatibility and stabilizing properties, emerge as crucial excipients and delivery agents. Thermodynamic studies, which quantify the energy changes associated with molecular interactions, elucidate the strength of binding between nucleic acid bases and saccharides, enabling the optimization of formulations for enhanced stability and bioavailability. Ultrasonic studies, which probe the structural and dynamic properties of solutions, reveal the influence of saccharides on the hydration and conformational stability of nucleic acid bases, providing crucial insights into their behavior in complex environments. Transport studies, which track the movement of these molecules, are pivotal for designing controlled-release systems and improving cellular uptake, ensuring targeted and efficient drug delivery. Ultimately, these studies translate into more effective and reliable nucleic acid-based therapies, driving innovation and improving patient outcomes.

Furthermore, the biotechnology industry relies heavily on understanding these molecular interactions. Bioprocessing, which encompasses the production of biological products using living organisms or enzymes, often involves nucleic acids and saccharides. For instance, in gene synthesis, PCR, and protein production, the transport properties of nucleic acids in saccharide solutions are critical for optimizing purification processes and maximizing yields. Ultrasonic studies can provide insights into the aggregation behavior of nucleic acids in these solutions, informing the development of more efficient separation

techniques. Moreover, by understanding how saccharides affect the interactions between nucleic acid probes and target sequences, researchers can improve the performance of diagnostic tests, leading to earlier and more accurate disease detection.

The food industry also stands to gain significantly from these studies. Saccharides are ubiquitous in food products, serving as sweeteners, preservatives, and stabilizers. Understanding how they interact with nucleic acid components of food can lead to improved food preservation techniques and enhanced shelf life. In conclusion, the thermodynamic, ultrasonic, and transport studies of nucleic acid bases in aqueous saccharide solutions are not merely academic exercises, but critical investigations with farreaching commercial and industrial implications. By continuing to invest in this research, we can unlock the full potential of these molecular interactions and create a more sustainable and prosperous future.



- A. Sharmhal, H. Singh, Richu, I. Fatma, P. K. Sharma, S. Sharma, A. Kumar and A. Kumar, "Influence of carbohydrates on the volumetric, acoustic and viscometric properties of thymine in aqueous solutions at different temperatures" Journal of Molecular Liquids, 2023, 385, Article No. 122264, DOI: 10.1016/j.molliq. 2023.122264, ISSN: 0167-7322 (Print) 1873-3166 (Online), Peer Reviewed, Abstracted, Indexed, Impact factor: 5.2.
- 2. A. Sharmhal, Richu, H. Singh, P. K. Sharma, A. Kumar and A. Kumar, "Physicochemical investigations on molecular interactions of adenine with aqueous D-glucose/D-maltose solvent media at varying temperatures and compositions" Journal of Chemical Thermodynamics, 2024, 201, Article No. 107399, DOI: 10.1016/j.jct.2024.107399, ISSN: 0021-9614 (Print) 1096-3626 (Online), Peer Reviewed, Abstracted, Indexed, Impact factor: 2.2.
- 3. A. Sharmhal, H. Singh, Richu, Umeshwari, P. K. Sharma, A. Kumar and A. Kumar, "Temperature-dependent volumetric, ultrasonic and viscometric properties of cytosine in water and aqueous D-xylose/D-lactose solutions" Journal of Molecular Liquids, 2025, 430, Article No. 127621, DOI: 10.1016/j.molliq. 2025.127621, ISSN: 0167-7322 (Print) 1873-3166 (Online), Peer Reviewed, Abstracted, Indexed, Impact factor: 5.2.
- Richu, A. Sharmhal, A. Kumar and A. Kumar, "Insights into the applications and prospects of ionic liquids towards the chemistry of biomolecules" Journal of Molecular Liquids, 2022, 368A, Article No. 120580, DOI: 10.1016/j.molliq.2022. 120580, ISSN: 0167-7322 (Print) 1873-3166 (Online), Peer Reviewed, Abstracted, Indexed, Impact factor: 5.2.
- P. Rajput, H. Singh, Richu, A. Bandral, Umeshwari, A. Sharmhal, Q. Majid and A. Kumar, "Analysis on solution properties of uracil/uridine in aqueous and binary aqueous pyridoxine hydrochloride media at varied temperatures and compositions: A physicochemical and UV spectral study" Journal of Molecular Liquids, 2025, 436, Article No. 128231, ISSN: 0167-7322 (Print) 1873-3166 (Online), Peer Reviewed, Abstracted, Indexed, Impact factor: 5.2.

6. I. Fatma, H. Assad, V. Sharma, P. K. Sharma, A. Sharmhal, R. C. Thakur and A. Kumar, "Interaction Behavior of N-Lauroyl Sarcosine Sodium Salt (NLSS) and Benzethonium Chloride (BC) in Aqueous Human Serum Albumin (HSA) at Different Temperatures: A Volumetric and Acoustic Study" Journal of Chemical & Engineering Data, 2022, 67(11), 3385-3399, DOI: 10.1021/acs.jced.2c00489, ISSN: 0021-9568 (Print) 1520-5134 (Online), Peer Reviewed, Abstracted, Indexed, Impact factor: 2.1.



- 1. Presented paper titled, "Elucidation of molecular interactions among thymine and aqueous sugar solutions at different temperatures" in 4th International Conference on "Recent Advances in Fundamental and Applied Sciences" (RAFAS 2023) held on March 24-25, 2023, organized by School of Chemical Engineering and Physical Sciences, Lovely Faculty of Technology and Sciences, Lovely Professional University, Punjab.
- 2. Presented paper titled, "Physicochemical properties of thymine in aqueous saccharides at varying temperatures and compositions" in 4th International Conference on "Multidisciplinary Academic Research and Innovation (ICMARI-2023)" held on December 9-10, 2023, jointly organized by Amiruddaula Islamia Degree College, Lucknow and Aryabhat Institute of Academics and Research, Lucknow.
- 3. Presented paper titled, "Thermophysical measurements of adenine in aqueous glucose/maltose solvent systems at discrete temperatures" in 5th International Conference on "Recent Advances in Fundamental and Applied Sciences" (RAFAS-2024) held on 19th-20th April, 2024, organized by School of Chemical Engineering and Physical Sciences, Lovely Professional University, Punjab.
- 4. Presented paper titled, "Volumetric and compressibility investigations of adenine in aqueous D-glucose/D-maltose solutions in the temperature range (293.15 to 313.15) K" in International Conference on "Emerging Trends in Multidisciplinary Research" (ICETMR-2025) held on 20th-21th August, 2025, organized by Govt. Gandhi Memorial Science College, Jammu, J&K.